Searching for Novel Neural Inducing Signals

Irene Marta De Almeida

Submitted in partial fulfillment of the requirements for the degree of Doctor of Philosophy in the Department of Cell and Developmental Biology

University College London, 2011

I, Irene Marta De Almeida, confirm that the work presented in this thesis is my own. Where information has been derived from other sources, I confirm that this has been indicated in the thesis.

To James, for who you are and what we are;

To Tomaz, my most amazing experiment, for all the joy you bring to my life!

Para a minha Mãe, por tudo o que sempre foste e continuas a ser, e por muito mais;

In memory of my Father and Sandy.

Acknowledgements

The first leg of this journey is coming to the end. And I have met, made friendships, learnt and developed with so many along the way:

First and foremost I offer my sincerest gratitude to Professor Claudio Stern, my supervisor. Claudio has supported me throughout my stay in his lab: his rigorous and often critical approach, although not always welcome, has helped me to mature as a scientist and to think ideas clearly. Thank you for trusting me and allowing me the space to work in my own way.

Thank you Professor António Coutinho for investing in me in the beginning of this journey. I will forever admire your vision, generosity, wisdom and knowledge. And thank you to the "family Gulbenkian" and PGDBMs. We shared intensive learning, dreams, expectations, scientific discussions and the excitement of planning each of our journeys.

And I cannot forget all my "voyage companions", students, post-docs and scientists. Together we shared experiences, ideas and plain crazy talk. And we worked and played, and did mad O/N time courses, nurturing, culturing, manipulating and learning with our embryos. May our paths cross again...

And cheers to the next trip!

Abstract

Searching for Novel Neural Inducing Signals

Irene Marta De Almeida

Neural induction marks the beginning of vertebrate nervous system formation, consisting of an interaction between the organizer, which emits inducing signals, and the ectoderm, which responds by giving rise to the neural plate.

In the present study we explored the role of FGF signals, Wnt inhibition and BMP inhibition in chick neural induction. Contrasting with previous work, in vivo studies in the extraembryonic ectoderm revealed that FGF signals, even together with inhibition of Wnts and BMPs are not capable of causing the surrounding cells to acquire a neural character. Inhibition of BMPs can, however, extend the border of the neural plate.

To uncover possible missing factors secreted by the organizer, a screen to isolate cDNAs encoding for secreted proteins was carried out. 442 clones were obtained and, after blast analyses, 137 were selected to be put through an *in situ* hybridization screen, narrowing down the number of candidate molecules to 23. Of these, and based on their expression in the node and/or anterior primitive streak, 3 were studied further, including cloning, molecular characterization and functional analysis in the context of neural induction in the chick embryo.

Fibulin2 belongs to the Fibulin family of extracellular matrix proteins. Our results suggest that is not directly involved in neural induction.

Calreticulin is largely present in the endoplasmic reticulum, and widely studied as an intracellular calcium regulator. We report that it can be secreted and acts like a BMP inhibitor, extending the border of the neural plate and rescuing the effect of BMP overexpression. It cannot, however, induce neural character in the competent extraembryonic ectoderm.

Nhbr90 seems not to be translated but act as a RNA. It is the first molecule identified with the ability of inducing the neural marker Sox2 in the extraembryonic ectoderm.

The work presented emphasises the complexity of the neural induction process and that we are only beginning to understand how the molecular players interact to form an early neural plate.

Table of Contents

List of Figures

List of Tables

Chapter 1

General Introduction

Neural Induction – and the organizer

Induction was defined by Gurdon as the "interaction between one (inducing) tissue and another (responding) tissue as a result of which the responding tissue undergoes a change in its direction of differentiation" (Gurdon, 1987).

Neural induction marks the beginning of the vertebrate nervous system formation and results from an interaction between the organizer (a population of cells emitting signals) and the ectoderm (the induced tissue), which responds by giving rise to neural tissue.

Through the seminal work of Hilde Mangold, it was found that the dorsal blastopore lip of the gastrulating *Triturus* (newt) embryo "exerts an organizing effect on its environment in such a way that, following its transplantation to an indifferent region of another embryo, it there causes the formation of a secondary embryo" (Gerhart, 2001; Spemann and Mangold, 1924). This secondary embryo, fused to the host at the ventral midline, had two complete heads, two hearts, two of each of the main dorsal structures (the notochord, neural tube and somites) and one gut. Very crucially, and because Mangold used differently pigmented species of newts as grafts and as hosts, early lineage tracing experiments were possible and revealed that, while the notochord of the secondary axis was derived from the progeny of the graft, the nervous system (with the exception of the floor plate) was derived from the host. This clearly demonstrates that there is an instruction from the graft on cells, causing the latter to change their fate and become neural instead of epidermal: a small region of the dorsal mesoderm can initiate the formation of an entire nervous system. Furthermore, close examination revealed that the secondary axis was patterned anterior-posterioly and dorso-ventrally. Because the dorsal lip of the blastopore is able to both induce and organize a fully patterned secondary axis, it was named the organizer.

Spemman and Mangold's work marked the onset of the field of neural induction and many groups started to study the organizer and the molecular nature of its signals.

The organizer in other species

Soon the functional equivalent of the amphibian organizer was found in other species. The dorsal tip of the primitive streak, Hensen's node, was put forward as the organizer centre in the chick (Hunt, 1929) and later shown to have, in fact, neural inducing ability (Waddington, 1930; Waddington, 1933a; Waddington, 1933b; Waddington, 1934; Waddington and Schmidt, 1933b). Hensen's node was found to induce a secondary axis both in the prospective epidermis (the avian non neural ectoderm of the area *pellucida*) and in the extraembryonic ectoderm of the area *opaca* (Cuevas and Llorca, 1974; Dias and Schoenwolf, 1990; Gallera, 1970a).

Equivalent regions were soon described in other vertebrate classes: Hensen's node in the duck (Waddington, 1930; Waddington, 1932), rabbit (Waddington, 1934; Waddington, 1936; Waddington, 1937) and mouse (Beddington, 1994) and the embryonic shield in the fish (Oppenheimer, 1936).

Many grafting experiments demonstrated that the organizer induces neural tissue when transplanted ectopically, not only within the same species but also across vertebrate classes. To name some examples, chick Hensen's node grafts can induce neural tissue in *Xenopus* (Kintner and Dodd, 1991), rabbit (Waddington, 1934) and zebrafish (Hatta and Takahashi, 1996). Rabbit nodes can induce neural tissue in both chick and duck (Waddington, 1936; Waddington, 1937); the mouse or rabbit node act as organizers in *Xenopus* (Blum et al., 1992) and in chick (Knoetgen et al., 2000). These amazing experiments do not provide any clue to the organizer's molecular nature, but as a whole, are a clearly indication that, whatever the signals, whatever the mechanism, neural induction is conserved across species.

The organizer neural inducing ability and the competence of the responding tissue

The idea of competence was first introduced by Waddington (Waddington, 1932) and was later defined as "the physiological state of a tissue which permits it to react in a morphogenetically specific way to a determinative stimuli" (Holtfreter, 1955).

1. The chick as a system to study neural induction

Organizer grafting experiments in the chick have revealed that both the extraembryonic epiblast of the area *opaca* and non-embryonic ectoderm of the area *pellucida* of the gastrulating embryo are competent to respond by giving rise to secondary axis (Dias and Schoenwolf, 1990; Gallera, 1972; Gallera and Ivanov, 1964). In the present study, the epiblast of anterior inner third of the area *opaca* (just laterally to the host node) is used for most experiments because it represents a comparatively neutral environment in which to study neural induction: the epiblast of the area *opaca* does not contribute to any embryonic tissues and only gives rise to extra-embryonic membranes but, crucially, it is able to respond to neural inducing signals. The secondary axes formed in the area *opaca* remain separate from the host axis, so that a cellular contribution from the host can be ruled out (Hornbruch et al., 1979). Because of the relatively large distance from the host embryo, it is very unlikely that the induced neural structures will be influenced by signals from the host embryo (Dias and Schoenwolf, 1990; Shieh, 1963; Storey et al., 1992; Tsung et al., 1965).

2. The inducing ability of the node and neural competence of the epiblast: changes over time

Node grafting experiments (reviewed by (**Gallera**, 1971; Nieuwkoop, 1985) suggest that the developmental age and orientation of the grafted Hensen's node, the age of the host epiblast and the position of the graft all influence whether and to what extent new axes are induced and how their patterning is affected. By transplanting nodes into host embryos of different developmental stages, Storey and colleagues (Storey et al., 1992) identified the time frame during which neural inducing signals are present in Hensen's node and the stage by which the epiblast loses its competence to respond to neural inducing signals. Furthermore, the age of a transplanted Hensen's node determines the

extent to which new neural structures are induced and the regions of the nervous system that form: young Hensen's nodes (stages 2 to 4) induce both anterior and posterior central nervous system (CNS), while older nodes (stages 5 to 6) have a reduced inducing ability and progressively generate more posterior structures (Dias and Schoenwolf, 1990; Gallera, 1970b; Storey et al., 1992; Streit et al., 1997b; Tsung et al., 1965; Vakaet, 1965).

As mentioned above, not only the age of the node, but also the age of the epiblast affect the extent to which posterior CNS is formed. While young epiblasts, up to stage $3^+/4$ can be induced to form a fully patterned, anterior to posterior, secondary axis, the competence of the host embryo to respond to neural inducing signals decreases substantially after stage 4 (Storey et al., 1992), disappearing completely by stage 6 (Gallera, 1971a; Gallera and Ivanov, 1964; Woodside, 1937). It is interesting to note that the competence of the epiblast to respond to neural inducing signals starts to decrease from stage 4, which coincides with the time at which inducing signals begin to decrease in the node. Finally, it also appears that, while the contribution to the induced secondary axis by a younger node is minimal (notochord and part of the floorplate), older nodes have a greater tendency to differentiate into neural structures, rather than exerting an induction on the neighboring tissues (Dias and Schoenwolf, 1990; Gallera, 1970b; Gallera and Ivanov, 1964).

3. L5^{220}: A marker for neural competence

Neural competence in the chick seems to be closely correlated with the expression of the carbohydrate epitope L5^{220} (Roberts et al., 1991; Streit et al., 1995; Streit et al., 1996; Streit and Stern, 1997a). Its expression begins in a broad domain that resembles the region that appears to be competent to neural inducing signals (Gallera, 1970b). At stages $3^+/4$, L5^{220} is expressed in a broad domain around the node and extending to the lateral and anterior inner third part of the area *opaca*. The posterior part of both the embryonic and extraembryonic regions lack L5^{220} expression (Streit et al., 1997b). At stage 5, when the area *opaca* has lost its neural competence, L5^{220} is absent from this region and is only present in the presumptive neural plate (Roberts et al., 1991; Streit et al., 1997b; Streit et al., 1995). Apart from L5^{220} expression, two further experiments support its relation to neural competence. First, the chick organizer is not able to induce neural tissue when grafted together with cells secreting L5 antibody (Roberts et al., 1991). Second, Streit and colleagues (Streit et al., 1997b) demonstrated that Hepatocyte Growth Factor/Scatter Factor (HGF/SF) can maintain L5^{220} expression in the anterior *area opaca* to at least stage 5 and that this also prolongs competence to respond to neural inducing signals: a grafted node is able to induce neural character in a stage 5 host that had previously received a

graft of hepatocyte growth factor/scatter factor (HGF/SF) (Stern et al., 1990) secreting cells (Streit et al., 1997b). This establishes L5^{220} as a marker for competence and indicates that L5^{220} might also be involved in the response of the epiblast to Hensen's node signals, a concept that is supported by the fact that antibodies to the L5^{220} epitope inhibit this response (Roberts et al., 1991).

The long search for the chemical nature of organizer signals

Although much headway was made in understanding neural induction, with the identification of the organizer across several species and vertebrate classes and, to some extent, the timing of neural induction, the identity of the inducing signal (or signals) remained elusive for many decades.

An early finding was that neural induction could be initiated by a variety of tissues, ranging from the extract of a fish swim bladder to guinea pig bone marrow (for review see (Grunz, 1997)). Tiedemann demonstrated that the phenol phase of an extract of an 11-day chick embryo was able to neuralize animal caps, and was the first to speculate that proteins were the likely candidates for the inducing signal (Tiedemann, 1956a; Tiedemann, 1956b). Soon after, Saxén (Saxén and Toivonen, 1962) and later Toivonen (Toivonen and Wartiovaara, 1976) separated organizers from juxtaposed animal caps by using filters that excluded cell–cell contact. Their results showed that neuralization could still occur in the absence of direct cell–cell contact, indicating that the signals were diffusible.

The default model of neural induction: BMPs and their inhibitors

A number of experiments performed in *Xenopus* involving dissociated single cells from blastula animal caps indicated that neural fate might be the default in the amphibian (Godsave and Slack, 1989; Grunz and Tacke, 1989; Sato and Sargent, 1989). Immersion of

the animal cap in media depleted of calcium and magnesium causes it to dissociate into single cells. When the ions are immediately added back, the cells re-associate. Upon further culture these re-aggregates differentiate into epidermis, similar to the intact cap. However, if the re-association is delayed, the re-aggregate acquires a neural character (Born et al., 1989; Godsave and Slack, 1989; Grunz and Tacke, 1989; Saint-Jeannet et al., 1990; Sato and Sargent, 1989). These results suggested that intact blastula animal caps had some kind of activity that maintains non-neural character, and that this activity is diluted by dissociation. These experiments first suggested that during *Xenopus* early development, some factor intrinsic to the animal cap (that is lost during dissociation in the animal cap assays, inhibits neural differentiation (Godsave and Slack, 1989; Grunz and Tacke, 1989).

It was only with the onset of molecular biology that the nature and the mechanism of the signals responsible for neural induction started to be elucidated. The main breakthrough on the molecular nature of neural induction happened almost by chance. Hemmati-Brivanlou, while studying the role of activin, a member of the Transforming Growth Factor-β (TGF-β) family, realized that the caps, upon injection of a truncated activin receptor, become neural, instead of epidermal (Hemmati-Brivanlou and Melton, 1994b). The RNA encoding the truncated activin receptor lacks the transducing, cytoplasmic domain, but had intact the extracellular and transmembrane domains, acting as a dominant negative (although ligand binding could occur, it was unable to elicit a response) (Hemmati-Brivanlou and Melton, 1992). Perhaps activin, or another member of the TGF-β family, inhibits neural fate.

Around the same time, Smith and Harland (Smith and Harland, 1992) isolated *noggin*, a secreted molecule able to rescue dorsal development in *Xenopus* embryos that had been ventralized by UV radiation of the vegetal pole. *Noggin* was found to be expressed first in the dorsal mesoderm and later in the notochord of the embryo. This initial study was only concerned with dorsalizing activity of Noggin on the mesoderm, but a subsequent study suggested *noggin* as a neural inducer. When *Xenopus* animal caps are incubated in a solution contained purified Noggin protein (Lamb et al., 1993), the caps produce neural tissue without expressing mesodermal markers.

The next neural inducer to be identified was *follistatin*, a known activin inhibitor (Hemmati-Brivanlou et al., 1994a), also able to induce neural, but not mesodermal, markers in animal caps. Since *follistatin* is an inhibitor of TGF-β signalling this suggested that a TGF-β may be an endogenous inhibitor of neural fate. The first candidate was

activin, because of the similar effects of follistatin and injection of a truncated activin receptor (see above) (Hemmati-Brivanlou and Melton, 1994b). As it turned out, neither follistatin nor the construct used by Hemmati-Brivanlou and Merton are specific activin inhibitors, but also antagonise other members of the TGF-β family (Hemmati-Brivanlou and Melton, 1994b).

BMP2 and *BMP4*, members of the TGF-β superfamily, are both expressed in the ventral part of the embryo (Dale et al., 1992; Jones et al., 1992). *BMP4* is expressed in the non-neural ectoderm, consistent with it being an epidermal inducer. Moreover, when BMP4 is added to dissociated animal cap cells, neural induction is prevented, regardless of how long re-association is delayed (Wilson and Hemmati-Brivanlou, 1995). Moreover, overexpression of *BMP4* RNA on the dorsal side of the embryo reduces neural ectoderm and also dorsal mesoderm and expands the expression of epidermal markers (Dale et al., 1992; Jones et al., 1992).

Soon after, genetic analyses in *Drosophila* lead to the isolation of *decapentaplegic* (*dpp*), which is homologous to the vertebrate genes *BMP2* and *BMP4* (Holley et al., 1995). In the fly, eliminating *dpp* converts the epidermal cells into neuroectoderm; conversely, overexpression of *dpp* changes the fate of neuroectodermal cells to epidermis (Biehs et al., 1996). Further studies in *Drosophila* led to the isolation of *short gastrulation* (*sog*), an antagonist of *dpp* (Holley et al., 1995). *Chordin* is the vertebrate homologue of *sog*. In *Xenopus*, *Chordin* is expressed in the organizer and later in the prechordal mesoderm and notochord, all structures capable of neural induction (Sasai et al., 1994).

By now it was starting to emerge that members of the TGF-β family act as neural inhibitors and that the neural inducers discovered so far, *noggin*, *follistatin* and *chordin*, act by inhibiting TGF signals. Indeed, it was soon demonstrated that *chordin*, *noggin*, and *follistatin* all bind to BMP4 and BMP2 (Iemura et al., 1998; Piccolo et al., 1996; Zimmerman et al., 1996). Ingenious genetic analysis in *Drosophila*, where *chordin* or *noggin* is ectopically expressed in various *Drosophila* mutants defective in components of the BMP pathway, allowed the site of action of these proteins to be placed upstream of the receptor, in the extracellular matrix (Holley et al., 1995; Holley et al., 1996b). Subsequently, other extracellular, secreted antagonists of BMP activity were found, such as *Cerberus*, *Gremlin*, and *Xnr-3*, all of which induce neural markers in *Xenopus* animal cap assays (Bouwmeester et al., 1996; Hsu, 1998; Smith et al., 1995).

Further support for the idea that BMP inhibition is responsible for neural induction came from inhibiting the intracellular components of the BMP signal-transduction pathway. As well as the truncated activin receptors, acting as dominant negative forms of the endogenous BMP receptor, negative forms of Smad molecules were also shown to promote neural differentiation in animal cap experiments (Bhushan et al., 1998; Liu et al., 1998). Inhibitory versions of the transcription factors that form the nuclear response to BMP were also shown to neuralize *Xenopus* animal caps (Onichtchouk et al., 1998; Trindade et al., 1999).

The data so far indicated that the inhibitory signal of neural induction was a member of the TGF-β family, more precisely BMP4 (or BMP2) and that neural inducers might inhibit these to allow the default, neural fate. That the inhibitory substance was BMP4 was also suggested by the finding that BMP4 is an effective inhibitor of neural fate while promoting epidermal differentiation, even in dissociated cells (Hawley et al., 1995; Wilson and Hemmati-Brivanlou, 1995).

To summarise the findings so far:

1. Dissociation of animal caps of gastrulating *Xenopus* embryos results in the formation of neural tissue;
2. Missexpression of dominant negative forms of the "activin" receptor not only blocks mesoderm formation, but also induces neural tissue (Hemmati-Brivanlou and Melton, 1992; Hemmati-Brivanlou and Melton, 1994b). The activin dominant negative receptor used by Hemmati-Brivanlou was later found to inhibit other members of the TGF-β family.
3. Other neural inducing molecules, such as *follistatin* (Hemmati-Brivanlou et al., 1994a), *noggin* (Lamb et al., 1993; Smith and Harland, 1992; Smith et al., 1993) and *chordin* (Sasai et al., 1995; Sasai et al., 1994) were discovered and are all expressed in the organizer and can induce neural tissue when ectopically expressed. These bind and antagonise BMP signalling (Fainsod et al., 1997; Piccolo et al., 1996; Zimmerman et al., 1996).

These observations led to the notion that neural induction may not be due to an instructive signal, but rather to inhibition of an endogenous inhibitor of neural fate, which is also an inducer of epidermis. Thus, the neural state may be an intrinsic, or default, property of cells in the animal cap. This is the "Default Model" of neural induction. The neural antagonist and epidermal inducer would be a member of the BMP family and the neural inducers, all expressed in the organizer, would bind to and inhibit

the BMP signals, allowing the surrounding ectoderm to pursue its intrinsic neural fate.

Challenging the Default Model

However, it soon became apparent that the patterns of expression of BMPs and their antagonists in the chick embryo, when compared to the timing of neural induction (see above) do not easily fit with the predictions of the Default Model. The next sections address some key findings surrounding neural induction by the node in amniote embryos, mainly the chick.

1. Is the node absolutely necessary for Neural Induction?

The role of the organizer and how fundamental it for neural induction to occur has been questioned. In the chick, neural induction can take place even after the node is surgically ablated (Waddington, 1932). This result was initially interpreted as showing that the Hensen's node, though sufficient for neural induction, is not required. However, this view was abandoned when subsequent studies showed that after ablation, the node quickly regenerates into a new, functional organizer (Grabowski, 1956; Joubin and Stern, 1999; Psychoyos and Stern, 1996; Schoenwolf and Yuan, 1995; Yuan and Schoenwolf, 1998; Yuan and Schoenwolf, 1999). On the other hand, genetic ablation of both the node and notochord in the mouse, and in the fish, seems to have little effect on the induction of neural tissue (Gritsman et al., 1999; Klingensmith et al., 1999).

Studies in the fish, and using the mutant *one-eyed-pinhead* (*oep*), where the embryonic shield and dorsal mesoderm do not form, showed that some *chordin* is still expressed and some neural-inducing activity still persists (Gritsman et al., 2000; Gritsman et al., 1999). Also, in the zebrafish *chordino* mutants, some nervous system still develops (Schulte-Merker et al., 1997).

Comparable results were obtained in the mouse. In the *HNF-3β* mutant (Ang and Rossant, 1994; Chen et al., 1994b; Weinstein et al., 1994) the node and axial mesoderm are absent, and do not express organizer markers, including *chordin* and *noggin*. However, the rostral streak, from which the node derives, is still capable of neural induction

(Klingensmith et al., 1999). Moreover, embryos mutated for either *follistatin* (Matzuk et al., 1995c), *noggin* (McMahon et al., 1998) or *Cer1* (*Cerberus related-1*) (Simpson et al., 1999) develop a normal sized neural plate. Even in the *chordin:noggin* double mutants, although lacking the forebrain, still develop a relatively normal posterior nervous system, indicating that some neural induction did take place (Bachiller et al., 2000).

Another explanation for why node ablation still results in neural tissue formation could relate to the finding that neural induction in vertebrates begins even before the appearance of a morphologically distinct organizer. For example, explants of prospective neural ectoderm express neural markers even if isolated before the beginning of gastrulation (Darnell et al., 1999; Streit et al., 2000a; Wilson et al., 2000). Also in *Xenopus*, it now seems that neural induction is initiated during the late blastula stages of development (Faure et al., 2000; Hemmati-Brivanlou and Thomsen, 1995). This conclusion was a result of studies in which the downregulation of the expression of components of the BMP pathway was used as the time point for when neural induction was taking place (Faure et al., 2000; Hemmati-Brivanlou and Thomsen, 1995).

2. Is BMP Inhibition Sufficient for Neural Induction?

Experiments performed in the chick started to question the idea of BMP inhibition mediating neural induction. The expression patterns of the BMP inhibitors *noggin*, *follistatin*, and *chordin* (Connolly et al., 1997; Connolly et al., 1995; Streit et al., 1998) do not correlate well with the spatio-temporal patterns of inducing ability of the node or responses of the epiblast.

Streit and colleagues showed that neural tissue could not be induced by either *chordin* or *noggin* expressing cells when placed in the competent epiblast of the extraembryonic area *opaca* (Streit et al., 1998). Moreover cells expressing BMP2 or BMP7 failed to inhibit neural plate formation (Streit et al., 1998). However, in chick pre-gastrula epiblast explants, fated to become neural ectoderm, and cultured for 40 hours, BMP4 induces expression of epidermal markers (Wilson et al., 2000). The mostly likely explanation for the difference in the results may reside in the timing in the experimental set-up as a more recent study (Linker and Stern, 2004), revealed that BMP overexpression in the chick does indeed inhibit *Sox2* expression but only at a later stage of neural plate formation.

Mouse double mutants for *noggin:chordin* still have neural tissue (Bachiller et al., 2000), whereas null mutants of *BMP2* (Zhang and Bradley, 1996), *BMP4* (Winnier et al., 1995), or *BMP7* (Wawersik et al., 1999) do not have a massively expanded neural plate. However, the possibility remains of some functional redundancy between different BMPs and different antagonists, with one compensating for the loss of another (Dudley and Robertson, 1997); And other inhibitors of BMP signalling may also account for some aspects of neural induction (Munoz-Sanjuan and Brivanlou, 2002; Scott et al., 2001; von Bubnoff and Cho, 2001).

On the other hand, there is evidence suggesting an important conserved role for BMP inhibition, together with Nodal inhibition, in establishing the neural tissue in the mouse embryo. Importantly, recent work found that loss of the BMP receptor *Alk3* (Di-Gregorio et al., 2007) or of *Nodal* (Camus et al., 2006) each result in a dramatic and precocious conversion of almost the entire epiblast into anterior neural tissue that expresses *Otx2* and *Sox1* as well as markers of anterior forebrain such as *Six3*, *Dlx5*, and *Hesx1*. These results have been interpreted as indicating that Nodal and BMP signalling are required before gastrulation to prevent the entire embryo becoming neuralised and to maintain a pluripotent epiblast that can also form epidermis, mesoderm, and endoderm.

In the chick there is other evidence supporting the idea that BMP inhibition accompanies neural induction in the embryo. This comes from experiments in which the level of phosphorylated Smad1, Smad5 and Smad8 (intracellular regulators of BMP signalling) was assessed. By using antibodies that recognize activated forms of the above Smads, it was shown that there is no BMP activity in the forming neural plate (Faure et al., 2002). It now appears that BMP inhibition is a late step in the neural induction process: BMP inhibition has a function of stabilizing and reinforcing neural cell fates, and that other molecules will be the primary neural inducers (Streit and Stern, 1999). In support of this, Linker and Stern (Linker and Stern, 2004) showed that BMP can inhibit the maintenance of neural marker expression at late gastrulation/early neurulation stages but does not affect the onset of expression of these markers.

3. BMP inhibition at the border of the neural plate

Experiments in the chick first raised the possibility that not all of the ectoderm, as the default model predicts, but only cells close to the neural/epidermal border are sensitive

to BMP and its antagonists (Streit et al., 1998; Streit and Stern, 1999; Streit and Stern, 1999a). The prospective neural plate, delimited by the border, is not inhibited by *BMP4* or *BMP7* and the non-neural ectoderm outside the border is not induced by *chordin* or *noggin*. However, when BMP-4 is misexpressed, by means of pellets of expressing cells, at the edge of the prospective neural plate, the domain of expression of the early neural marker *Sox3* becomes narrower. This narrowing of the neural plate is further supported by the lateral shift of *msx1*, a border marker. Conversely, downregulation of BMP signals, at the border, using BMP antagonists, leads to a widening of the neural plate (Linker and Stern, 2004; Streit et al., 1998; Streit and Stern, 1999a).

In *Xenopus*, the reason by which animal caps are so easily neuralized by misexpression of BMP antagonists, might reside on the fact that they contain some neural plate and/or border cells. In fact, Linker and colleagues (Linker et al., 2009), through systematic fate mapping of animal caps of a wide range of sizes, revealed that even the smallest caps contribute cells to the anterior neural plate itself in as many as 60% of cases, and nearly all caps contribute to the prospective placodal domain at the border of the anterior neural plate. Furthermore, isolated animal caps express both anterior neural (*Otx2*) and border (*XAG1/XCG1*) markers (Knecht et al., 1995; Lamb and Harland, 1995; Lamb et al., 1993). Although these data are consistent with previous fate maps made at the 16 cell stage (Moody, 1987a) and at the 32 cell stage (Dale and Slack, 1987b; Moody, 1987b), Linker's results (Linker et al., 2009) provide the first demonstration that virtually all animal caps excised at stage 8 contain cells fated to became neural plate border.

In *Xenopus BMP2* and *BMP4* are expressed ubiquitously in the entire ectoderm before gastrulation, and then cleared from the prospective neural plate at the time when the organizer appears (Fainsod et al., 1994). On the other hand, in the chick embryo, neither *BMP2*, *BMP4* or *BMP7* is expressed in the future neural plate at the early primitive stage (Streit et al., 1998). However, by early neurulation, the expression of *BMPs* in both Chick and *Xenopus* becomes strongly localized to the border of the neural plate. This seems to mean that, even though the expression patterns differ at the early stages, they converge just after the appearance of the neural plate, suggesting that a role for BMP at the border is important and has been conserved in evolution.

The role of other players and signaling molecules in neural induction

This section will provide a short overview on some molecular players and signalling molecules currently studied in relation with neural induction.

1. Fibroblast Growth Factors (FGFs) in neural induction

FGF, a mesodermal inducer (Isaacs et al., 1994; Slack, 1994a; Slack, 1994b; Slack and Isaacs, 1994) has been reported to have direct neural inducing ability in several species. In ascidians, several lines of evidence indicate that FGF signalling initiates the formation of the nervous system (Bertrand et al., 2003; Hudson et al., 2003; Hudson and Lemaire, 2001; Kim and Nishida, 2001), suggesting an ancient role for this family of signalling molecules in neural induction. In *Xenopus*, FGF can induce neuralization of animal cap cells that have undergone brief dissociation (Kengaku and Okamoto, 1993). Furthermore, in animal cap experiments, blocking FGF signalling with dominant negative FGF receptor prevents induction of neural markers by BMP antagonists *noggin* (Launay et al., 1996) and *chordin* (Sasai et al., 1996). An alternative view suggests that FGF signalling provides the ectoderm with competence to become defined as neural, by analogy to the observations (Cornell et al., 1995) that FGF contributes to define the competence of the ectoderm to respond to mesoderm induction by TGF-β signals in *Xenopus*.

FGF may induce neural tissue by a mechanism independent of BMP inhibition. Experiments in *Xenopus* with *Smad10*, a Co-Smad, component of the BMP signalling pathway, revealed that it induces neural tissue within the animal cap (LeSueur et al., 2002). More surprisingly, by removing Smad10 protein using antisense oligonucleotides, neural tissue is never formed in the affected embryos and, using co-injection studies, the authors found that Smad10 cannot inhibit the BMP pathway, indicating some other mechanism for its function. The authors further identify one site in the Smad10 protein that becomes phosphorylated and activated as a result of FGF signalling (LeSueur et al., 2002).

In the chick embryo, the role of FGF in neural induction has received considerable attention. Storey and colleagues (Storey et al., 1998) provided the first comprehensive study examining the role of FGF signalling in the induction of neural tissue in the amniote embryo. Using chick embryos, the authors showed that FGFs, which are expressed in the node and anterior primitive streak, induce a subset of genes associated

with the laying down of the posterior nervous system. FGF can also maintain and/or induce the expression of the early neural marker *L5* in the extraembryonic epiblast and may, therefore, maintain the competence of this tissue to respond to other neural inducing signals (Streit et al., 1997b; Streit et al., 1995; Streit and Stern, 1997a).

A few years later, Streit and co-workers (Streit et al., 2000a) reported that the gene *Early Response to Neural Induction* (*ERNI*) starts to be expressed very early in the pre-streak epiblast. *ERNI* is induced by a grafted node in as quickly as 1 hour, and this is mimicked by FGF8. The induction of ERNI by the node can be inhibited by the FGF receptor antagonist SU5402 or by a chimaeric secreted FGF receptor construct *in vivo*. The same treatment also abolished induction of *Sox3* and *Sox2* by the node, strongly suggesting an absolute requirement for FGF signalling not only in the early stages of neural induction but also for later marker expression (Streit et al., 2000a). During normal development, *ERNI* is expressed in a large domain of the pre-streak stage epiblast – at this stage, the underlying hypoblast expresses FGF8. These observations first suggested that the earliest neural inducing signals may arise early, from the hypoblast (Streit et al., 2000a). At the same time, another study, also using SU5402, also showed that neural differentiation is blocked in chick epiblast explants obtained from the central region of pre-streak stage chick embryos (Wilson et al., 2000). In the chick FGF8 induces, amongst other markers, the early neural marker *Sox3* but not *Sox2*, a later, more definitive neural plate marker (de Almeida et al., 2008; Linker et al., 2009; Linker and Stern, 2004; Pinho et al., 2011; Streit and Stern, 1999a). This, together with the ability quickly and robustly to induce *ERNI* (Streit et al., 2000a) suggests that FGF signals initiate the process of neural induction, but additional signals are further required for the establishment of a fully committed neural plate.

Despite some initial controversy, it is now generally accepted that FGF signalling is absolutely required for neural induction to take place not only in *Xenopus* (Delaune et al., 2005; Hardcastle et al., 2000; Launay et al., 1996; Linker and Stern, 2004; Pera et al., 2003; Sasai et al., 1996; Strong et al., 2000; Xu et al., 1997) and chick (Linker and Stern, 2004; Streit et al., 2000c; Wilson et al., 2000), but also in zebrafish (Kudoh et al., 2004) and ascidians (Bertrand et al., 2003; Hudson et al., 2003; Hudson and Lemaire, 2001; Kim and Nishida, 2001).

There is also strong evidence for interactions between FGF and BMP signaling. It was proposed that FGF signaling aids the clearance of BMP activity from the neural plate, and

downstream effectors of the FGF pathway have been shown to inhibit the nuclear accumulation of the R-Smad/Co-Smad complex (Kretzschmar et al., 1997a; Kretzschmar et al., 1999; Kretzschmar et al., 1997b).

An important effector of BMP signals is the transcription factor Smad1, which becomes phosphorylated at three conserved carboxy-terminal serine residues upon activation by the BMP receptor (BMPR) serine/threonine kinase (Massague and Chen, 2000). It has further been shown (Kretzschmar et al., 1997b) that Smad1 also undergoes phosphorylation by MAPK in the central linker region. Whereas phosphorylation by BMPR promotes nuclear translocation and transcriptional activity of Smad1, phosphorylation by MAPK in the linker region has the opposite effect, causing cytoplasmic localization and inhibition of transcriptional activity (Kretzschmar et al., 1997b; Massague and Chen, 2000).

A conclusive study, performed in *Xenopus*, has clearly demonstrated that FGF8, through the MAPK cascade, causes phosphorylation in the linker region of Smad1, acting as an effective inhibitor of BMP signals (Pera et al., 2003). This has been proposed to be an explanation for the requirement of FGF signalling in *Xenopus* neural induction (Pera et al., 2003). However this does not account for all the findings implicating FGF, because some of its actions appear independent of BMP inhibition (see (de Almeida et al., 2008; Linker et al., 2009; Linker and Stern, 2004).

2. Wnts in neural induction

The role of the *Wnt* family has been investigated in the context of neural induction. In chick explant experiments, *Wnt* overexpression induces epidermal markers in epiblast from the prospective neural domain of pre-streak embryos (Wilson et al., 2001). Conversely, in presumptive epidermal tissue from the same stage, Wnt inhibition induces neural markers. In the same study it was shown that at a certain concentration of *Wnt* inhibitors, below the level required for neural induction in the epidermal epiblast explants, a combination of BMP inhibition and FGF could induce neural ectoderm. The authors' proposed mechanism is that *Wnt* signalling causes an upregulation of *BMP* expression and, therefore, induces the epidermal fate (Wilson and Edlund, 2001; Wilson et al., 2001). Contradicting this view are results from *Xenopus*, suggesting that expression of *Wnts* downregulates that of *BMPs* (Baker et al., 1999; Gomez-Skarmeta et al., 2001). However also in *Xenopus*, Delaune and colleagues (Delaune et al., 2005) obtained evidence supporting the view of Wilson *et al.* (Wilson et al., 2001).

Results in chick embryos *in vivo*, however, do not easily fit with the model of Wilson *et al.* (Wilson et al., 2001). Inhibition of Wnt signals, even together with FGFs and BMP inhibition do not induce the neural marker *Sox2* in the competent epiblast of the extraembryonic area *opaca* (de Almeida et al., 2008; Linker et al., 2009; Linker and Stern, 2004b, this study). There are many possible reasons for the differences between these results but among them is the fact that explants are cultured in medium containing the supplement N2, which contains insulin, a factor that acts through the MAPK pathway common to FGFs. Moreover, there is evidence implicating insulin or insulin-like growth factor (IGF) in neural induction in *Xenopus* (Pera et al., 2003)

It was also proposed that Wnt signalling can modulate the strength of the transduced BMP signal via activation of the calmodulin/Ca^{2+} pathway (Scherer and Graff, 2000; Zimmerman et al., 1998). This may explain why BMP inhibition cannot induce neural tissue in epidermal epiblast explants. If the level of inhibition of BMP signalling is not complete, the sensitized transduction pathway can still receive an input, resulting in epidermal cell fates. If, however, Wnt signalling is also inhibited, reception is desensitized and when combined with BMP inhibition, can lead to neural cell fates. In agreement with this view, it is interesting to note that two naturally occurring inhibitors of Wnt signalling, *FrzB* and *Sfrp-2*, are expressed in the chick presumptive neural plate at around the stages that neural induction is taking place (Ladher et al., 2000).

3. Calcium in neural induction

Most information regarding Ca^{2+} signalling during neural induction comes from studies in amphibians. As early as 1974, it was suggested that Ca^{2+} is important in triggering neuralization in *Rana pipiens* ectoderm (Barth and Barth, 1974a; Barth and Barth, 1974b). More recently, the dissociation of animal caps in Ca^{2+} and Mg^{2+}-free medium has been shown to direct the cells toward a neural fate (Grunz and Tacke, 1989; Saint-Jeannet et al., 1989; Saint-Jeannet et al., 1993). Frequently, the explanation given for this neuralization by dissociation phenomenon is that the epidermal inductors (BMPs) are being diluted from their receptors. This theory was taken as fact for many years because it was reported that when BMP4 is added at a high concentration during dissociation, the expression of neural markers is totally abolished (Wilson et al., 1997). Recently, it has been shown that cell dissociation induced a sustained activation of the Ras/MAPK pathway, which causes the phosphorylation of Smad1 at sites that inhibit the activity of this transcription factor. This demonstrates that BMP ligands continue to signal in

dissociated cells (Kuroda et al., 2005). In addition, it has been shown that the dissociation of animal caps in Ca^{2+}-free medium triggers an increase in $[Ca^{2+}]_i$ and that this increase is due to an efflux of Ca^{2+} from internal stores resulting from the inversion of the gradient of concentration in Ca^{2+} between intra- and extracellular compartments (Leclerc et al., 2001). To distinguish whether, during cell dissociation, the increase in $[Ca^{2+}]_i$ is a cause or a consequence of neural induction, animal cap cells were loaded with the Ca^{2+} chelator BAPTA: under these conditions, the neuralization by dissociation is blocked (i.e., the neural marker *NCAM* is not expressed) (Leclerc et al., 2001). This demonstrates that, at least in animal caps, a Ca^{2+}-dependent signal is necessary to trigger neuralization of the ectoderm and to inhibit epidermal determination.

Many more studies have suggested that calcium fluxes (Leclerc et al., 1997; Leclerc et al., 1999; Leclerc et al., 2003; Leclerc et al., 2000; Leclerc et al., 2008; Lee et al., 2009; Moreau et al., 1994; Moreau et al., 2008) or associated Protein Kinase C signalling (Otte and Moon, 1992; Otte et al., 1989) may play a role in the specification of the embryonic nervous system in *Xenopus*. But how these fluxes are regulated and how they relate to the neural induction cascade are only now starting to become understood. In a recent study (Papanayotou et al., submitted), *Calfacilitin*, a novel transmembrane protein was identified and characterized as a regulator of calcium signalling and as a new player in neural induction. It is a calcium channel facilitator that increases calcium flux by generating a larger window current and slowing the inactivation of the L-type $Ca_v1.2$ channel. It is required early, downstream of initial FGF signals, to induce *Geminin*, and defines an essential step for the later acquisition of *Sox2* expression and neural plate formation. The authors demonstrate that *Calfacilitin* acts by modulating intracellular Ca^{2+} levels, providing a long-sought mechanism for how L-type calcium channels are involved in neural induction.

5. Insulin-Like Growth Factor (IGF) in neural induction

It has been shown that the insulin-like growth factor (IGF) family can play a role in neural induction. Experiments performed in *Xenopus* show that animal caps are neuralized by IGFs (Pera et al., 2001; Van Obberghen et al., 2001). The necessity for IGF signalling has also been shown using a truncated IGF receptor. In these embryos, neural induction mediated by *noggin* is inhibited. The authors propose that the IGF pathway may act downstream of BMP inhibition during neural induction, and that as well as a passive role for BMP inhibition, neural induction may not be a default as previously thought. Instead, it may also require an active signal, induced as a result of BMP

inhibition (Pera et al., 2001). As mentioned above, these findings may be relevant to the interpretation of the chick explant results (Wilson et al., 2000; Wilson et al., 2001) since these are cultured in the presence of medium supplement N2, a major component of which is insulin.

6. Retinoic acid (RA) and Notch in neural induction

Retinoic acid (RA) and Notch are signalling molecules which, although they have attracted considerable attention in neural development, have not been studied extensively in the earlier process of neural induction.

RA is a signalling molecule widely studied as involved in neuronal patterning, neural differentiation and axonal outgrowth. As a patterning factor, it contributes to both the anteroposterior and dorsoventral patterning of the neural plate and neural tube. In the anteroposterior axis of the neural plate, RA, along with Wnts and FGFs, is specifically responsible for the organization of the posterior hindbrain and the anterior spinal cord (Liu et al., 2001; Maden, 2002; Melton et al., 2004). In the absence of RA signalling, the posterior hindbrain is missing and the anterior spinal cord is abnormal (Maden et al., 1996; Wilson et al., 2004). As RA is synthesized in the posterior mesoderm and the RA catabolizing enzyme CYP26C1 is expressed in the anterior mesoderm, a gradient of RA that is able to pattern the overlying presumptive hindbrain of the neural plate is generated (Reijntjes et al., 2004; Wilson et al., 2004).

Despite an early report in the chick embryo that ectopic RA can induce neural tissue, and that the response differs between left and right sides of the embryo (Chen et al., 1992; Chen and Solursh, 1992), this has barely been studied further. It is relevant to note that, in cultured NT2/D1 carcinoma cells, RA can activate *Sox3*. The authors further identify a novel positive regulatory element within the Sox3 promoter responsible for this RA-dependent activation of *Sox3* (Nikcevic et al., 2008).

Another study, this time performed in chick embryos, explored the role of the hypoblast in neural induction (Albazerchi and Stern, 2007), showing that it plays a role in establishing an initial "pre-neural/ pre-prosencephalic" territory in the epiblast. The signals involved include a combination of FGF and RA signalling, perhaps together with Wnt and BMP antagonists. This induction is transient, but can be stabilized by RA and continued Wnt and BMP inhibition. However, a definitive neural state requires additional factors remaining to be identified. Interestingly, FGF and RA, generally

considered as caudalizing factors, are shown in Albazerchi's study to play a role in the induction of a transient "pre-neural/pre-forebrain" state (Albazerchi and Stern, 2007).

And finally, a recent study demonstrated an interaction between BMP signaling and RA/RA receptor (RAR) pathway (Sheng et al., 2010). The authors show that RA represses the duration of BMP signals by reducing the level of phosphorylated Smad1 (pSmad1). Through its nuclear receptor-mediated transcription, RA enhances the interaction between pSmad1 and its ubiqitin E3 ligases, promoting pSmad1 ubiquitination and subsequent proteasomal degradation (Sheng et al., 2010).

Notch has been extensively studied on neurogenesis in *Drosophila* embryos. In the absence of *Notch*, the embryo forms too many neuroblasts at the expense of the hypodermal cell layer (Artavanis-Tsakonas, 1988; Campos-Ortega, 1988). Even though *Notch* appears to play a role in deciding the fate of neural/hypodermal cells, it is expressed ubiquitously in early embryos in the neurogenic region (Hartley et al., 1987; Kidd et al., 1989).

The *Xenopus* homolog of *Notch*, *Xotch*, is very similar to *Drosophila Notch* in structure and shares some similar features in its developmental expression (Coffman et al., 1990). A study in which *Xotch* was truncated by a deletion in its extracellular domain, *XotchΔE*, shed some light on its function in *Xenopus* (Coffman et al., 1993). Broad overexpression causes the loss of dorsal structures and the expansion and disorganization of the brain, whereas injections of *XotchΔE* into a single blastomere induce neural and mesodermal hypertrophy in the descendants of the injected cell. *XotchΔE* further inhibits the early expression of epidermal and neural crest markers and yet enhances and extends the response of animal caps to mesodermal and neural induction. The authors suggest that *Notch* might be working on delaying differentiation and leaving undetermined cells competent to respond to later inductive signals (Coffman et al., 1993). A more recent study, also performed in *Xenopus*, has suggested that Notch signalling modulates the nuclear localization of carboxy-terminal-phosphorylated Smad2 and controls the competence of ectodermal cells for *activin* (Abe et al., 2005). Further studies will be needed to access if Notch signalling can also crosstalk with other TGF-β family members.

The requirement for more players upstream of BMP signals

In the chick embryo, BMP inhibitors alone (or in combinations) are unable to induce *Sox2*, a late, stable neural marker, unless mesoderm is also induced (de Almeida et al., 2008; Linker et al., 2009; Linker and Stern, 2004; Streit et al., 1998) A graft of Hensen's node into the inner third of the area *opaca* induces the pre-neural marker *Sox3* within 3 hours. However, if the graft is removed before 12 hours, the induced expression is lost and no neural plate develops (Streit et al., 1998). However, expression of *Sox3* can be maintained if *Chordin* expressing cells are added following the removal of the node at 5 hours, but not earlier (Streit et al., 1998). These results suggest the requirement for other signals upstream of BMP inhibition to initiate neural induction.

To identify the molecular events taking place in the first 5 hours of induction by the node, a differential screen was performed between area *opaca* epiblast cells that had been exposed to a graft of Hensen's node for 5 hours and control cells from the contralateral side of the same embryo. The expression of about 10 genes was found to differ between the two conditions; these have now been characterized functionally and their regulation by secreted factors investigated. All the isolated genes are expressed in the prospective neural plate and are induced by a node graft in the area *opaca* within 5 hours. When it comes to the regulation of the genes isolated, it was revealed that a significant subset can be induced by FGF8: *ERNI* (Streit et al., 2000a), *Churchill* (Sheng et al., 2003), *Calfacilitin* (Papanayotou *et al*, submitted), *Dad1*, *polyubiquitin* (*UbII*) and *ferritin heavy chain* (*Fth*) (Gibson et al., 2010) and *Asterix* (Pinho et al., 2011). However, another subset is not regulated by FGF: *Obelix* and *TrkC* (Pinho et al., 2011). These genes are also not regulated by BMP antagonits or by other factors previously implicated in neural induction.

These results indicate that FGF is the major, but not the only, signal involved in the early steps of neural induction, and that other signals remain to be identified. Examination of the timing of induction of all of these response genes after a node graft revealed that they are expressed as three distinct temporal waves, or "epochs" (Pinho et al., 2011): genes induced within 3 hours of a node graft (*ERNI*, *Sox3*, *Calfacilitin* and *Geminin*) are normally expressed in the epiblast of pre-primitive-streak stage embryos; genes induced within 5 hours of a node graft (*Churchill*, *UbII*, *Dad1*, *Fth*, *TrkC*, *Asterix* and *Obelix*) are normally expressed in the prospective neural plate from the late primitive streak stage; a third wave of expressed genes comprises those induced after about 12 hours of a node graft such as *Sox2* and *BERT* (Papanayotou et al., 2008). In normal development, these genes

start to be expressed in the very early neural plate when the axial mesoderm starts to form, at stage 4+/5. Apart from *TrkC* and *Obelix* (Pinho et al, 2011) from the first two waves, *BERT* (Papanayotou et al., 2008) is also not regulated by FGFs. These results suggest that at least one, and probably more, signals from the node remain unidentified. This conclusion is further supported by the observation that neither FGF together with BMP antagonists, nor exposure to Hensen's node for 5 hours followed by BMP antagonists, is sufficient to induce expression of *Sox2* or the formation of a neural plate.

The search for neural inducing signals from the node

The conclusions from the previous sections suggest that it is now critically important to identify the missing signals involved in neural induction. This is the aim of the work reported in the present thesis.

Here, we start by reassessing the role of BMP inhibition during neural induction in the chick embryo. We find that BMP inhibition, even together with FGF and Wnt signals, is unable to induce neural markers in competent epibast of the area *opaca;* and the only region capable to respond to BMP inhibition is the border of the neural plate (see also (Streit et al., 1998; Streit and Stern, 1999a).

Next, we used a technique to isolate putative secreted factors (Jacobs et al., 1997) to look for novel factors expressed in the chick Hensen's node at stages 3+- 4. A genetic screen was carried out, resulting in the isolation of 137 sequences, which were studied by *in situ* hybridisation; 22 were found to have defined expression patterns.

Based on their time and pattern of expression three genes were chosen and further studied. Their full-length cDNAs were cloned and characterized in the context of neural induction.

Fibulin2, a previously described extracellular protein, did not display any activity in neural induction assays: Fibulin2 misexpression does not induce the neural markers *Sox3* or *Sox2* and a combination of FGF8 and *Fibulin2* is unable to induce *Sox2* in the competent epiblast of the area *opaca*.

Calreticulin, a previously well characterized endoplasmic reticulum protein, was cloned and studied in connection with neural induction. It is unable to induce neural markers in

the area *opaca* but can extend the border of the neural plate when ectopically expressed by electroporation. This activity resembles that of BMP antagonists.

Nhbr90, a previously undescribed 2Kb sequence, seems not to encode a protein, but may function as a long non-coding RNA. It is expressed early in development in the hypoblast and later in the node. Surprinsigly, *nhbr90* is able to induce both *Sox3* and *Sox2* in the extraembryonic epiblast of the area *opaca*.

Chapter 2

General Methods

This chapter is dedicated to material and methods commonly used throughout the work presented in this manuscript. Specific methodologies will be introduced at the beginning of each subsequent chapter, as appropriate.

Chick embryology

Fertile hens' eggs (White Leghorn: SPAFAS, U.S.A.; Henry Stewart &Co., UK) were incubated at 38ºC to the desired stages. For electroporation and grafts embryos were cultured using a modified New Culture Method (Stern and Ireland, 1981).

Electroporation

Chick embryos at stage 3^{+} were placed in an acrylic chamber with Pt cathode embedded in the bottom, exposed to the saline through a 1.5mm window. The embryo was positioned over the window (dorsal side up) and the DNA (pCAβ-IRES-GFP construct) was applied between the dorsal side of the embryo and an adjustable anode (Pt or Cu wire). Three 50 ms pulses of 5-6 volts were applied with a TSS10 pulse generator (Intracel). Embryos were then placed in New culture (Stern and Ireland, 1981) and grown to the desired stages.

FGF beads

Heparin-coated acrylic beads (Sigma) were washed several times in phosphate buffered saline (PBS) and then soaked in purified recombinant human FGF-4 (Sigma) or mouse FGF-8b (R&D systems and Sigma) at 10µg/µl in PBS for 3 hours on ice. Control beads were soaked in PBS alone. Beads were then washed in PBS and implanted in the embryos.

Transfected cells

COS cells were grown in DMEM containing 10% new born calf serum and 1µg DNA transfection was performed using Lipofectamine Plus (Gibco). Control cells were "mock transfected" with 1µl water instead of the DNA. 24 hrs after transfection, pellets of about 1 000 cells each were generated by setting up hanging drop cultures. 24 hrs later the hanging drops were ready for being placed in the embryos.

The following expression constructs were used for transfection: Dkk1 (kind gift from E. Laufer), Crescent (kind gift from E Laufer and M Marvin) and soluble Nfz8 (Deardorff et al., 1998)(kind gift from S. Sokol).

Whole mount *in situ* hybridization

Whole mount in situ hybridization was performed using DIG- or fluoresceine-labeled probes. Below is a table with all the DNAs used for transcription:

DNA	**Restriction/ transcription**	**Kind gift from**
BMP4	BamHI/T3	Karel Liem (Liem et al., 1995)
Bra	Xba/T3	Jim Smith (Kispert et al., 1995)
Cash4	BamHI/T3	Kate Storey (Henrique et al., 1997)
cNR1	NotI/T7	Michael Kuehn (Levin et al., 1995)
CCRT	BamHI/T3	(present work)
CFbln short	ClaI/T7	(present work)
Chd	EcoRI/Sp6	(Streit et al., 1998)
Dlx5	NcoI /T7	Gail Lizarraga (Ferrari et al., 1998)
ERNI	KpnI/T3	(Streit et al., 2000a)
FCrt	XbaI/T7	Marnie Halpern (Rubinstein et al., 2000)
FGF8	Not1/T3	Izpisua-Belmonte (Vogel et al., 1996)
follistatin	ClaI/T3	Laura Paganess (Hemmati-Brivanlou et al., 1994a)
GATA2	NdeI/T7	(Sheng et al., 1997)
GATA3	NdeI/T7	(Sheng et al., 1997)
Geminin	EcoRI/T3	(Papanayotou et al., 2008)
Hoxb9	HindIII/T7	Linda McNaughton (Grapin-Botton et al., 1995)
msx1	BglII/T3	Karel Liem (Liem et al., 1995)
Nhbr90	ClaI/T7	(present work)
noggin	XhoI/T3	Karel Liem (Connolly et al., 1997)
Pax6	EcoRI/T7	M Goulding (Goulding et al., 1993)
Pax7	SalI/T7	(Kawakami et al., 1997)

Sax1	Asp718/T7	Kate Storey (Spann et al., 1994)
Slug	XhoI/T3	David Wilkinson (Nieto et al., 1994)
Smad6	Xba/T7	Ed Laufer (Yamada et al., 1999)
Smad7	Xba/T7	Ed Laufer (Unpublished)
Sox2	PstI/T7	Paul Scotting (Uwanogho et al., 1995)
Sox3	PstI/T7	Paul Scotting (Uwanogho et al., 1995)

The plasmids were linearized with the enzyme indicated above, extracted with 1:1 phenol:chloroform, ethanol precipitated and ressuspended in clean water. Transcriptions were performed using 1µg of linearized plasmid, the appropriate enzyme and either Digoxigenin-nucleotide mix (Boerhinger) or fluorescein isothiocyanate-(FITC) nucleotide mix (Boerhinger) for 2 hours at 37°C. RNase-free DNase (1µl/µg) was then added to destroy the DNA template and the resulting RNA was ethanol precipitated with 4M LiCl. In order to reduce the background in the *in situs*, the precipitations were carried out twice and in the case of *Sox2* and *Sox3*, three times. The resulting RNA was resuspended in RNase-free water and stored in hybridization buffer (50% formamide, 1.3x SSC pH5.3, 5mM EDTA, 50µg/ml yeast tRNA, 100µg/ml Heparin, 0.2% Tween-20 and 0.5% CHAPS).

The embryos were collected at the required stages or time after manipulation in calcium-magnesium-free PBS (CMF) and fixed in fresh 4% formaldehyde in CMF containing 2mM EGTA overnight at 4°C. Embryos were then transferred to absolute methanol and stored at –20°C for up to a week.

Embryos were progressively rehydrated in 75%, 50% and 25% methanol in PBS containing 0.1% Tween (PTW). Following two more washes in PTW, the embryos were treated for 15 minutes with 1µg/µl Proteinase K, rinsed in PTW and post-fixed in 4% formaldeheyde containing 0.1% glutaraldehyde for 20 to 30 minutes at room temperature. Embryos were then washed again in PTW, transferred to hybridization solution and pre-hybridized at 70°C for 4 hrs. Hybridization solution was replaced by the labelled RNA probe and hybridization proceeded overnight at 70°C.

The following day, the embryos were washed at 70°C in hybridization solution (3x 30 minutes) and in 1:1 hybridization solution: TBST (TBS with 1% Tween) for 20 minutes. Embryos were then brought to room temperature, washed in TBST alone (3x 30 minutes) and then blocked with 5% heat inactivated goat serum and 1mg/ml bovine serum

albumin in TBST (blocking buffer) for 3 hours at room temperature. Embryos were incubated in anti-Digoxigenin-AP antibody (Roche) 1:5000 in blocking buffer or in anti-fluorescein-AP (Roche) 1:2000 in blocking buffer.

Embryos were extensively washed in TBST for a minimum of 5 hours with frequent changes of washing solution. *Sox2 and Sox3 in situs* benefited if the post antibody washes were extended until the following day at 4ºC.For the detection of alkaline phosphatase, embryos were rinsed in NTMT (0.1M NaCl, 0.1M Tris-Hcl pH9.5, 0.05M $MgCl_2$, 1% Tween; 2x 10 minutes) and then incubated in one of the following solutions:

- 1.5 ml NTMT containing 4.5 µl NBT (Sigma) and 3.5 µl BCIP (Roche) - develops into a dark blue colour;
- 1 ml NTMT containing 7 µl NBT – develops into a light blue colour;
- 1 ml NTMT containing 7µl INT/BCIP (Roche) – develops into a brick red colour.

When double *in situs* were to be performed, the two probes FITC-labelled and DIG-labelled were combined for the hybridization step. Embryos were washed as described above and the anti-DIG and anti-FITC antibodies, both coupled with alkaline phosphatase were then detected sequentially. The anti-DIG antibody was normally detected first (either with NBT alone or with INT/BCIP) and the remaining alkaline phosphatase activity was inactivated by fixing the embryos overnight and then transferring them to TBST (containing 0.01% Tween) for 2 hours at 70ºC. Detection of the anti-FITC antibody was normally carried out with NBT/BCIP. After the *in situs* were developed embryos were kept in 4% formaldehyde.

Immunostaining

GFP protein in the electroporated embryos was detected with antiGFP antibody. The embryos were washed in PTW (3x 1 hour), placed in blocking buffer for 3 hours at room temperature and left in mouse anti-GFP (Molecular Probes) antibody 1:2000 in blocking buffer overnight at 4ºC. The following day, embryos were washed with PTW (5x1hour) and incubated in the secondary antibody, GαR HRP (Santa Cruz) 1:5000 in blocking buffer, overnight at 4ºC. After three washes for one hour each, HRP was detected using DAB in 1mMTris pH 7.4. Oxidation was aided by adding H_2O_2 and the reaction stopped when a brown precipitated was detected.

Histology

After post-fixing, the embryos were incubated for 5 minutes in absolute methanol and 10 minutes in propan-2-ol (2-isopropanol), followed by clearing in absolute tetrahydronaphthalene for 30 minutes. The embryos were infiltrated in 1:1 tetrahydronaphthalene:paraffin wax for 30 minutes at 60°C, followed with 3 changes (30 minutes) of pure wax at 60°C and placed into a mould. The wax was then left to set and 8-10µm sections were performed in a microtome. The sections were placed on gelatin-albumen subbed glass slides and dried overnight at 37°C. Sections were then de-waxed in Histoclear and mounted in Canada Balsam.

Photography

Whole mounts were normally photographed from the dorsal side using a dissecting microscope and oblique lighting from a fibra optics source. Photographs were taken with a digital camera (Zeiss Axiovision) attached to a computer with Axiovsion software. Sections were photographed on an Olympus Vanox-T compound microscope with Nomarski Differential Interference Contrast or bright field optics.

Library screening and isolation of full length clones

The initial partial length clones nhbr34, nhbr90 and nhbr307 were used to screen a stage 2-4 chick cDNA library (kind gift of Juan Carlos Izpisua-Belmonte), directly cloned in Uni-Zap (Stratagene), under stringent conditions (0.1xSSC, 65°C). The radioactive probes were synthesized with Prime IT II labelling kit (Stratagene) using 20ng of the template DNA fragment and 5µl (50µCi) [α-^{32}P]dCTP. Incorporated nucleotides were removed using a Probe Quant G-50 Micro Column (Pharmacia Biotech). 1 mg salmon sperm DNA (Sigma) was added to the probes and the mixtures were boiled for 5 minutes, allowed to cool on ice for 5 minutes and then added directly to the pre-hybridization solution. About $2x10^5$ clones were screened. Up to 5 positive phage plaques were replated and a secondary screen performed using the same radiolabelled probes, under the same conditions (0.1xSSC, 65°C). The positive plaques were *in vitro* excised and cloned into pBlueScript plasmids using ExAssist™ Interference-Resistence helper Phage (Stratagene). Clones were then PCR amplified with T3 and T7 primers (94°C, 1 min.; 55°C, 2 min.; 72°C, 2 min.; 30 cycles) and the longest clones were sequenced.

Northern Blot

Total RNA was isolated from approximately 30 embryos each at stage 3, 5 and 7-8. Embryos were collected in PBS and the area opaca removed. The embryos were rapidly

transferred to GUA-SCN (4M guanidinium thiocyanate, 26mM Na-citrate, 0.5% Na-Sarcosyl, 0.7% mercaptoethanol), phenol extracted (pH4.0) once and chloroform extracted twice. After ethanol precipitation, the pellets were resuspended in GUA-SCN, re-precipitated and resuspended in 0.1% SDS. 10µg total RNA at each stage (3, 5 and 7-8) was run on a 1.5% agarose gel containing 2.2M formaldehyde, for about 3 hours at 85V. The gel was then soaked in 0.05M NaOH (20 minutes) and neutralized in 10xSSC (45 minutes). The RNA was transferred overnight and the blot was pre-hybridized (0.4M Sodium Phosphate buffer pH7.2, 1mM EDTA pH8.0, 1% BSA, 7% SDS) and hybridized at 65°C with radiolabelled probes [α-^{32}P]dCTP made from both the initial partial clones and the full length clones obtained after the library screnning (mentioned above). The filters were exposed to X-ray film (Fuji) overnight at –80°C and developed using an X-O-Mat.

Chapter 3

Challenging the Default Model of Neural Induction

Introduction

Around the time of gastrulation in vertebrate embryos, the nervous system is induced from part of the ectoderm under the influence of signals emanating from the organizer. This interaction is known as neural induction (Hemmati-Brivanlou and Melton, 1997a; Hemmati-Brivanlou and Melton, 1997b; Munoz-Sanjuan and Brivanlou, 2002; Stern, 2005; Streit and Stern, 1999). The discovery of neural induction in 1924 by Spemann and Mangold (Spemann and Mangold, 1924) generated considerable interest in identifying the signals responsible. Little progress was made until some 15 years ago when it was proposed that Bone Morphogenetic Proteins (BMP), expressed ubiquitously in the early embryo, act as epidermal inducers and that they need to be inhibited in the prospective neural plate for this structure to form (Harland, 2000; Hemmati-Brivanlou and Melton, 1997a; Hemmati-Brivanlou and Melton, 1997b; Munoz-Sanjuan and Brivanlou, 2002). However, there has been considerable controversy concerning whether or not this "default" model provides an adequate explanation for this phenomenon, as there appears to be considerably more complexity to the cell interactions that lead to establishment of a functional neural plate (Linker and Stern, 2004; Streit and Stern, 1999).

BMPs are members of the transforming growth factor β (TGF-β) family of secreted proteins and the main pathway for TGF-β signals is mediated by heterodimeric receptors with serine/threonine receptor kinases and cytoplasmic proteins called Smads (Derynck et al., 1998; Heldin et al., 1997; Massague and Chen, 2000; Nakao et al., 1997a). TGF-β binds to serine/threonine kinase receptors, consisting of both type I (TβRI) and type II (TβRII). The activated type I receptor transmits the intracellular signals through the phosphorylation of receptor-regulated Smad proteins (R-Smads), Smad1, Smad2, Smad3,

Smad5 and Smad8. Smad1, Smad5 and Smad8 serve as substracts for the BMP receptors whereas Smad2 and Smad3 function to transduce for the TGFβ, activin and nodal signals. Activated R-Smads form heteromeric complexes with a common partner, Smad4 (Co-Smad) and translocate into the nucleus (Chen et al., 1998; Hata et al., 1998; Heldin et al., 1997; Kretzschmar et al., 1997b; Lagna et al., 1996; Liu et al., 1997a; Liu et al., 1997b; Macias-Silva et al., 1998; Massague and Chen, 2000). Once localized within the nucleus, the Smad heterocomplex recruits either transcriptional activators or co-repressors to target their action upon a specific subset of target genes (Massague and Chen, 2000; Massague and Gomis, 2006).

The transduction of the TGF-β signals is tightly regulated by the inhibitory Smads (I-Smads), Smad6 and Smad7 (Imamura et al., 1997; Nakao et al., 1997b). Smad6 preferentially inhibits BMPs, whereas Smad7 inhibits signalling by all TGF-β family members including TGF-β, activin and BMP (Ishisaki et al., 1999; Itoh et al., 1998). Both I-Smads compete with R-Smads for binding to activated type I receptors and therefore inhibiting the phosphorylation of the R-Smads (Shi and Massague, 2003). Furthermore, they both recruit Smurf ubiquitin ligases and induce degradation of the receptors (Wicks et al., 2006). Smad6 also inhibits BMP signalling by competing with Smad4 for binding with phosphorylated Smad1, yielding inactive Smad1—Smad6 complexes (Hata et al., 1998). Recent studies further suggest that Smad7 also inhibits TGF-beta signalling in the nucleus, by disrupting the formation of the TGF-beta-induced functional Smad-DNA complex (Zhang et al., 2007).

Whether or not the default model provides a good enough explanation for neural induction, it is clear that BMP inhibition plays some part in the process. In this chapter we aim to re-address the role of BMP and BMP antagonism during neural induction. Misexpression of *BMP* transcripts inhibits the expression of the definitive neural marker *Sox2*, confirming BMP inhibition as a necessary step in neural induction. However, inhibition of BMP signals alone is not sufficient to neuralise competent the ectoderm: by manipulating the BMP pathway intracellularly, using the inhibitory Smads, *Smad6* and *Smad7*, we show that inhibiton of BMP signals does not result in neural induction. Even a combination of *Smad6*, *Smad7* and other BMP antagonists together with FGF, *Cerberus* and *Wnt* antagonists is unable to induce neural markers in competent epiblast. Finally we reveal that the only cells that can be made to express neural markers in response to BMP antagonists are at, or connected with, the border of the neural plate.

Material and Methods

Fertilized hens eggs (Brown Bovan Gold; Henry Stewart and Company) were incubated at 38ºC to reach the desired stages.

All the factors used in the present work were introduced to the area opaca of the chick embryo at stage3+/4 by electroporation, by grafting cells expressing factors or as proteins in heparin-coated beads. Electroporations were performed as previously described (Sheng et al., 2003). The coding region of xSmad7 (Casellas and Brivanlou, 1998), cSmad6 (Yamada et al., 1999), cChordin (Streit et al., 1998), Xenopus truncated BMP receptor (Suzuki et al., 1994) and cCerberus (Zhu et al., 1999) were cloned into pCAβ-IRES-GFP. FGF8 (R&D systems, at a concentration of 50µg/ml) was delivered bound to heparin beads, as previously described (Streit et al., 2000a). Secreted proteins Noggin (Streit and Stern, 1999a) and the Wnt inhibitors Dkk1 (kind gift of E. Laufer), Crescent (Kind gift of M. Marvin and E. Laufer) or soluble NFz8 (Deardorff et al., 1998) were used to transfect COS cells, as previously described (Streit et al., 1998)

The *Sox2* enhancer N2, in *ptKEGFP* (a kind gift fromH. Kondho, (Uchikawa et al., 2003), was subloned into *ptkLacZ* (a kind gift from O. Voisculescu).

Node grafts were performed as previously described (Streit et al., 2000a). *In situ* hybridization and whole mount immunocytochemistry were carried out as described in Chapter 2. Clones for chick *Smad6* and chick *Smad7* were a kind gift from Ed Laufer; *Sox2* and *Sox3* were provided by R. Lovell-Badge and P. Scotting (Uwanogho et al., 1995) and chick *Brachyury* was provided by Jim Smith (Kispert et al., 1995). Following *in situ* hybridization with *Sox2*, grafted cell pellets produce background staining. In those cases, sections were performed in order to access for *Sox2* epiblast expression.

More detailed description of the procedures followed can be found on Chapter 2.

Results

Neural induction: the inhibitors, the inducers and the readouts - fitting almost neatly with the default model

This chapter explores the role of BMP inhibition in neural induction and, albeit extensively studied in various reports (Connolly et al., 1997; Connolly et al., 1995; Graham et al., 1994; Houston et al., 1994; Rex et al., 1997a; Rex et al., 1994; Streit et al., 1998; Uwanogho et al., 1995), it seemed appropriate to re-analyse the expression pattern of some of the BMPs, *BMP2* and *BMP4*, the "neural inducers" *Chordin*, *Noggin* and *Follistatin*, and the "readouts" of neural induction, *Sox3* and *Sox2*, during the developmental stages neural induction is believed to be taking place.

At stage 3/3$^+$ *Chordin* transcripts concentrate in the anterior tip of the primitive streak (**Fig 3.1 D**). At stage 4$^+$ (**Fig 3.1 K**) and thereafter (**Fig 3.1 R**) *Chordin* is restricted to the Hensen's node and the entire length of the notochord (node derivative).

Regarding *noggin*, it has been reported that it is first detected in the anterior part of the primitive streak at stage 3 (Connolly et al., 1997). Our results, however, reveal that *noggin* only starts to be expressed, very weakly (and if at all) at stage 4/4+ (**Fig 3.1 J**) and its signal becomes stronger by stage 5 and 6 (**Fig 3.1 Q**) with transcripts in the notochord and forming neural plate.

In the original paper (Connolly et al., 1995) where chick *follistatin* expression was first described, the authors detected expression at stage 4 in the anterior part of the node. This is in contrast with mouse expression, where the primitive streak and not the node express the gene (Albano et al., 1994). In our results, however, chick *follistatin* only starts to be detected at stage 5 (**Fig 3.1 S**) with strong expression in the head process and the regions lateral to the node. Expression is never seen in the node or in the primitive streak (**Fig 3.1 E**, **L** and **S**).

Sox2 and *Sox3* present a very similar expression pattern, confined to the prospective neural plate and neural plate (**Fig 3.1 F**, **G**, **M**, **N**, **T** and **U**). But whereas *Sox3* starts to be expressed even before primitive streak formation (not shown), *Sox2* transcripts only start to be detected at around stage 4 (**Fig 3.1 N**).

The expression of *BMP genes* after the full primitive streak stage in the chick has been described (Liem et al., 1995; Schultheiss et al., 1997; Watanabe and Le Douarin, 1996)Here we decided to re-analise the expression of *BMP2* and *BMP4* during the developmental stages neural induction is occurring. At stage 3/3+, *BMP2* expression is present in the posterior area *pellucida* epiblast, including the primitive streak (**Fig 3.1 A**), then expands until it surrounds the forming neural plate, where expression persists throughout most of the non-neural ectoderm (**Fig 3.1 H** and **O**). *BMP4* transcripts start to be detected, very weakly, at stage 3, in the most posterior epiblast of the area *pellucida* (**Fig 3.1 B**). By stage 4, expression expands anteriorly, forming a ring of epiblast cells surrounding the future neural plate (**Fig 3.1. I**) and then condenses into a line of cells at the boundary between neural and non-neural ectoderm (**Fig 3.1 P**).

Some of the expression patterns presented above correlate with the default model. However, it is important to note that, there is no overlap of expression between the *BMPs* and the neural inducers *Chordin*, *noggin* and *Follistatin*. Furthermore, *Noggin* just starts to be expressed in the node when the neural inducing ability of the node starts to decrease (Storey et al., 1992; Storey et al., 1995) and its expression persists after the node has lost the ability to induce neural tissue (Connolly et al., 1997). This is also the case for *follistatin* (Connolly et al., 1995).

The Inhibitory Smads (*I-Smads*), *Smad6* and *Smad7* are expressed at the border of the neural plate

In vertebrates, Smad6 and Smad7 function as intracellular inhibitors of BMP, TGF-β and activin signalling pathways (Imamura et al, 1997; Topper et al, 1997; Hata et al, 1998, Kleeff et al, 1999). Whereas Smad6 inhibits specifically the BMP pathway (Hata et al., 1998; Imamura et al., 1997) and the BMP pathway involving TCF3/Lef1/β-catenin (von Bubnoff and Cho, 2001), Smad7 inhibits signals of all TGF-β family members (Hayashi et al., 1997; Nakao et al., 1997a).

Despite being largely studied, the Inhibitory Smads expression pattern is not very well documented in the chick embryo, at least not at gastrula stages of development (Yamada and colleagues (Yamada et al., 1999) have reported the cloning and expression of chick *Smad6*, focusing mainly on heart development stages). In order to determine the spatiotemporal expression of *Smad6* and *Smad7* during neural induction, whole mount *in situ* hybridization was performed in chick embryos form pre-streak stages to the appearance of the first somites. *cSmad6* expression (**Fig 3.2 A-G**) is first detected at stage 4

in the posterior most part of the embryo, including the primitive streak and at the margin of the embryo and excluding the prospective neural plate (**Fig 3.2 B**, **E-G**); As development proceeds, the *Smad6* mRNA remains excluded from the neural plate, but accumulates at the border and expands into the blood mesoderm in the area *opaca* (**Fig 3.2 C**,**D**). *Smad7* expression follows a very similar pattern (**Fig 3.2 H-N**), with the exception that its transcript is detected earlier, very weakly at stage 3 embryos, in a crescent type expression around the future neural plate (**Fig 3.2 H**). By stage 4, the expression becomes strongly localized to the border of the neural plate and very posterior streak (**Fig 3.2 I**, **L-N**).

Like in the case of *BMP* expression, *Smad6* and *Smad7* are expressed predominantly at the border of the neural plate, more consistent with their possible roles in positioning the neural plate border than of acting in the process of neural induction.

Smad7 can activate the N2 Sox2 enhancer

Sox2 expression in the chick embryo was recently found to be controlled by a large number of different enhancers, of which two (N1 and N2) are responsible for the initial domain of expression in the prospective neural plate of stage 4^{+}-5 embryos (Uchikawa et al., 2003). N2 directs *Sox2* expression to the largest and earliest, anterior domain, whereas N1 activates *Sox2* in the paranodal region, destined to give rise to posterior hindbrain and the entire spinal cord (Takemoto et al., 2006; Uchikawa et al., 2003). Uchikawa and colleagues (Uchikawa et al., 2003) also demonstrated that N1 is induced by a graft of Hensen's node in the area opaca. To test weather a node can activate the N2 enhancer, a N2-GFP construct was electroporated, together with a node graft, in the area *opaca* of a chick stage 3^{+} host (**Fig 3.3 A**). After 18-22 hours of culture, the activation of the N2 enhancer could be detected by fluorescence (**Fig 3.3 B**). The embryos were then probed for *Sox2*, with expression in the induced secondary axis in all the cases tested (12/12), of which, 9 revealed activation of the N2 enhancer as shown by the GFP antibody staining (**Fig 3.3 C** and **D**). Further evidence that the N2 construct is functional is provided when N2-TK-GFP is electroporated into a large domain of the neural and prospective neural plate at stage 3+ (**Fig 3.3 E**), revealing the accumulation of GFP as shown by fluorescence (**Fig 3.3 F**) and by antibody staining (**Fig 3.3 H**) in all of the 12 embryos tested.

Smad7, a multifunctional Smad antagonist which inhibits not only Smad1/5/8 (BMP effectors) but also Smad2/3 (Nodal/Activin effectors; (Bhushan et al., 1998; Casellas and Brivanlou, 1998; Pogoda and Meyer, 2002), is reported to be a potent neural inducer in

Xenopus (Bhushan et al., 1998; Chang and Harland, 2007). We decided, therefore, to test if *Smad7* could act as a neural inducer in our chick experiments.

To check if Smad7 could mimic the effect of a node graft in activating N2, the N2-TK-LacZ and pCAβ-Smad7-ires-GFP constructs were co electroporated in a broad domain of the area *opaca* of stage 3+ chick embryos (**Fig 3.3 I**). LacZ staining after O/N culture confirmed the ability of *Smad7* for activating N2 in 7 out of the 12 embryos tested (**Fig 3.3 J** and **K**). In control experiments where the N2 construct was co-electroporated with an empty *pCAβ-GFP*, no LacZ staining was obtained (0/5; not shown).

Inhibition of TGF-β signalling is not sufficient for neural induction in the chick

Smad7 alone can activate the N2 enhancer, but is it sufficient to cause competent epiblast cells to acquire *Sox2* expression? In order to test this, *pCAβ-Smad7-IRES-GFP* was electroporated in a small domain of the area *opaca* of stage 3+ chick embryos (**Fig 3.4 A**). Following incubation for 18-20 hours, no expression of the mesodermal marker *Brachyury* or the neural marker *Sox2* was observed (0/12; **Fig 3.4 P-R**). It is conceivable that the amount of *Smad7* introduced is insufficient to block all BMP signalling in this assay, or that Smad7 is not sufficiently potent. To investigate this, other BMP antagonists were tested in the same assay, alone or in combination, resulting in no *Sox2* or *Brachyury* induction in all the experiments performed for the different factors: Noggin (0/6; **Fig 3.4 B** and **C**), *Chordin* (0/10**; Fig 3.4 D-F**), *dnBMPR* (0/5; **Fig 3.4 G-I**), *Cerberus* (0/4; **Fig 3.4 J-L**), *Smad6* (0/12; **Fig 3.4 M-O**) or all the factors together (0/9; not shown).

These results confirm previous observations (Linker and Stern, 2004; Streit et al., 1998) that inhibition of BMP is not sufficient to induce *Sox2* in competent chick epiblast. We also show that, even though *Smad7* is unable to induce *Sox2*, it does activate the isolated N2 enhancer of *Sox2*, suggesting the existence of silencer elements outside of the N2 enhancer.

Inhibition of TGF-β signalling is not sufficient for neural induction in the chick even when combined with Wnt antagonists and FGF

It has been recently reported that neural induction is initiated by FGF signals (Streit et al., 2000a) and that this, together with the inhibition of Wnt signals, can induce the neural marker *Sox2* (Wilson and Edlund, 2001; Wilson et al., 2001). This later experiments were conduced in cell culture and the results could not be reproduced when performed *in vivo*, in the chick embryo, even when BMPs where inhibited together with FGFs and Wnt antagonists (Linker and Stern, 2004). Further repeating those experiments, we obtained similar results (**Fig 3.5 I**, **J**, **J'**, **Q**, **R** and **R'**). FGF8 alone is able to induce the early neural marker *Sox3* in the extraembrionic area *opaca* in all the embryos tested (11/11; **Fig 3.8 D** and **E**). No *Brachyury* or *Sox2* (0/10; **Fig 3.5 A** and **B**) were induced by FGF8 alone or FGF8 combined with either Smad6 (0/7; not shown), or with Smad7 (0/7; not shown) or with both together (0/9, **Fig 3.5 C-E**). Different combinations of the BMP-Smad and TGF-β/activin pathways inhibitors together with the inhibition of Wnts and with FGF signals always resulted in no *Brachyury* or *Sox2* induction: FGF8+*Smad6*+*Smad7*+αWnt (0/5; **Fig 3.5 F-H** and **H'**); FGF8+*Smad6*+αWnt+*cerberus*+noggin+*dnBMPR*+*Chordin* (0/6, **Fig 3.5 K-M** and **M'**); FGF8+*Smad7*+αWnt+*cerberus*+noggin+*dnBMPR*+*Chordin* (0/10, **Fig 3 N-P** and **P'**) or all the factors together FGF8+*Smad7*+*Smad6*+αWnt+*cerberus*+noggin+*dnBMPR*+*Chordin* (0/15, **Fig 3.5 S-U** and **U'**).

These results confirm the previous conclusion (Linker and Stern, 2004; Streit et al., 1998) that BMP antagonism is insufficient to induce *Sox2* expression, even when combined with Wnt-antagonists and FGF.

BMP inhibition is required for the formation of the neural plate

The experiments performed so far suggest that BMP inhibition is not sufficient for neural induction, but is it necessary? A previous study (Linker and Stern, 2004) demonstrated that overexpression of *BMP4* into the prospective neural plate of stage 3^+ embryos does not have an effect on the early neural marker *Sox3* in the first 15 hours of the experiment, while *Sox2* is strongly downregulated. At 20 hours both *Sox3* and *Sox2* are downregulated and the neural plate morphology is lost in the electroporated region. Is the neural plate border shifted laterally in the electroporated side of the embryos?

To address this, *Xenopus BMP4* (*pCAβ-XBMP4-IRES-GFP*) was electroporated into the prospective neural plate of stage 3^+ embryos. After 18-20 hours, the expected reduction of

the neural plate was observed in all the embryos tested (35/35; **Fig 3.6 A**, **D**, **G** and **J**), together with a lateral shift of the domain of expression of the border markers *Dlx5* (8/8; **Fig 3.6 B** and **C**), *msx1* (9/9; **Fig 3.6 E** and **F**), *Pax7* (9/9; **Fig 3.6 H** and **I**) and *Slug* (9/9; **Fig 3.6 K** and **L**).

This results, together with previous observations (Linker and Stern, 2004), show that BMP inhibition is necessary for expression of the definitive neural plate marker *Sox2* and for neural plate formation. Moreover, BMP modulation plays a role in positioning the border of the neural plate.

The border of the neural plate is uniquely sensitive to BMP antagonists

In the chick embryo, it was previously shown, using grafts of pellets of heterologous cells secreting BMP4 or its antagonists (Chordin or Noggin), that only the border of the neural plate (prospective neural crest and placode region) is sensitive to BMP signalling: in this region, misexpression of BMP4 narrows the neural plate while misexpression of Chordin or Noggin expands it into the prospective epidermis (Streit et al., 1998; Streit and Stern, 1999a; Streit and Stern, 1999b). To test whether intracellular BMP antagonists exert the same effect, expression constructs were electroporated as a line extending from the prospective neural plate to the edge of the area *opaca* in chick embryos at stages 3^{+}-4 (**Fig 3.7 A**). Electroporation of *Smad7* produced a marked extension in the expression domains of *Sox3* (14/15; **Fig 3.7 D** and **E**) and *Sox2* (16/19; **Fig 3.7 F** and **G** and **Fig 3.9 G** and **H**). Under the same conditions, we also reported the expansion of the expression domains of the neural plate border markers *Pax7* (11/11; **Fig 3.7 L** and **M**) and *Slug* (9/9**; Fig 3.7 N** and **O**) and of *msx1* (10/10; **Fig 3.7H** and **l**), *Dlx5* (10/10; **Fig 3.7 J** and **K**) and also *BMP4* (8/8; **Fig 3.7 B** and **C**) into the non-neural ectoderm.

We carried out a similar experiment but using *Smad6* instead, obtaining comparable results (**Fig 3.8**). *Smad6* overexpression dramatically expands the domain of expression of *Sox2* in the electroporated region (60/61; **Fig 3.8 A**, **D**, **G** and **J**; **Fig 3.9 J** and **K**) as well as of *msx1* (15/16; **Fig 3.8 E** and **F**), *Pax7* (18/18; **Fig 3.8 H** and **I**) and *Slug* (11/12; **Fig 3.8 K** and **L**).

We went further and tested several other BMP inhibitors on their ability to extend the border of the neural plate and found that all the factors tested were able to extend the domain of *Sox2* expression (4/5 for *dnBMPR*; **Fig 3.9 M** and **N**; 6/6 for *Cerberus*; **Fig 3.9 P** and **Q**; 7/9 for *Chordin*; **Fig 3.9 S** and **T**).

It is important to note that in all of the experiments performed, in which there was expansion of *Sox2* or *Sox3* domains, no mesoderm was ever induced (0/29; **Fig 3.9**; *Bra* expression in light blue).

Control experiments had no effect on any of the markers tested (0/5 for *BMP4*; 0/8 for *Sox3*; 0/8 for *Sox2*; 0/4 for *msx1*; 0/6 for *Dlx5*; 0/6 for *Pax7* and 0/7 for *Slug*; not shown).

BMP inhibition induces border markers in cell populations not in contact with the neural plate

While the experiments above were being carried out, a colleague in the lab reported that *Pax7* expression was not cell-autonomous to the *Smad*-electroporated cells: it extended many cell diameters away from transfected cells, but always extended as a continuous line from the normal neural plate even if the line of electroporated cells was discontinuous (Linker et al., 2009). This observation raised the possibility that cells from the host neural plate are stimulated to migrate laterally when BMP signalling is inhibited. This idea has been refuted in a recent report (Linker et al., 2009) where cell movements between the electroporated side and the contralateral side (which had been marked with DiI) were compared by time-lapse video microscopy and no differences were observed in the patterns of cell movements between the two sides.

Can BMP inhibition in the non-neural ectoderm, and in an area discontinuous with the neural plate, still result in the expression of neural and border markers? To test this, (*pCAβ-Smad6-IRES-GFP*) was electroporated into the non-neural ectoderm of stage 3^{+} embryos, away from the prospective neural plate. While this experiment resulted in no induction of *Sox2* (0/57; **Fig 3.10 A**, **D**, **G** and **J**), we observed an induction of all the border/neural crest markers tested (12/12 for *Dlx5*; **Fig 3.10 B** and **C**; 6/15 for *msx1*; **Fig 3.10 E** and **F**; 15/18 for *Pax7*; **Fig 3.10 H** and **I**; 10/12 for *Slug*; **Fig 3.10 K** and **L**). No effect was observed in control experiments where *pCAβ-GFP* was electroporated (0/8 for *Sox2*; 0/8 for *Dlx5*; 0/7 for *msx1*; 0/6 for *Pax7*; 0/7 for *Slug*; not shown).

This experiment confirms that the expansion of neural plate and border markers caused by inhibiting BMP signalling is due to an induction of these markers in the lateral epidermis and not to an alteration of cell movements.

Discussion

Neural induction by inhibitory Smads cannot be separated from mesendoderm formation in *Xenopus* or chick

Two previous studies showed that a combination of eFGF (FGF4; (Isaacs et al., 1992) signalling together with BMP inhibition is sufficient to induce neural tissue in the ventral epidermis of Xenopus embryos in the absence of expression of a set of endodermal or mesodermal markers (de Almeida et al., 2008; Delaune et al., 2005; Linker et al., 2009; Linker and Stern, 2004) On the other hand when a similar experiment (FGF4+*Smad6*) is performed in chick, *brachyury* a marker for mesendoderm precursors, is induced along with neural markers, suggesting that the induction of neural markers is an indirect consequence of mesendoderm induction (Linker and Stern, 2004). This difference is puzzling. One possible explanation for the absence of mesendodermal marker expression in the *Xenopus* experiment is that the set of markers chosen in *Xenopus* excludes markers for some very early mesendodermal state, or for a particular cell type, which is responsible for emitting the presumed neural inducing signals. To address this, and based on the finding that Nodal signalling is required for mesendoderm formation (Conlon et al., 1994; De Robertis and Kuroda, 2004; Driever, 1995; Jones et al., 1995; Kuroda et al., 2004; Perea-Gomez et al., 2001; Weng and Stemple, 2003), a recent study (Linker et al., 2009) examined the effect of blocking this with the specific inhibitor CerS (Piccolo et al., 1999) in combination with eFGF+*Smad6* in the A4 blastomere of *Xenopus*. Indeed, this abolishes the expression of *Sox2* and greatly reduces *Sox3*, more consistent with the results from chick (Linker and Stern, 2004; Streit et al., 2000a). Virtually identical results were obtained with a different cell-autonomous BMP inhibitor, ΔSmad7 (a Smad1-specific truncated version of Smad7, which otherwise inhibits all Smads; (Wawersik et al., 2005), was co-injected with eFGF, with and without CerS. In contrast, when the full-length *Smad7* was injected, dorsal mesoderm (*brachyury/chordin*-expressing cells) was induced alongside neural markers (*Sox3* and *Sox2*). As expected (because Smad7 should already block Nodal), CerS did not block the induction of dorsal mesoderm in this assay. In the chick, however, Smad7 did not induce either mesodermal (*brachyury*) or neural (*Sox3, Sox2*) markers. One possible explanation for this is that the chick experiments are conducted at the mid-/late gastrula stage, when competence for mesendoderm induction by activin/nodal signalling is rapidly declining (Dias and Schoenwolf, 1990; Gallera and Ivanov, 1964; Storey et al., 1992; Streit and Stern, 1997a). The type of FGF may also be important – in the chick it was shown that when combined with Smad6, FGF4, but not FGF2, -3 or -8, can induce *brachyury* as well as neural markers

(Linker and Stern, 2004). All of these results make it impossible to separate mesendodermal induction from induction of neural markers: neural markers are only expressed in both species when mesendoderm is also induced. Taken together these results suggest that both in *Xenopus* and in chick, FGF signalling together with BMP inhibition triggers a mesendodermal tissue (or state), which in turn is able to induce the expression of neural markers as a secondary effect.

Mechanism of regulation of *Sox2* expression

In the chick embryo, the three genes of the SoxB1 class are expressed in a precise temporal sequence: *Sox3* is activated before gastrulation in a broad domain that includes the prospective neural plate, followed by *Sox2* in the entire presumptive nervous system at late primitive streak stages (stage $4^{+}/5$) and finally by *Sox1* in a similar domain to the latter (Rex et al., 1997a; Rex et al., 1994; Rex et al., 1997b; Uwanogho et al., 1995). Grafts of Hensen's node induce *Sox3* within 3 hours, *Sox2* after 9 hours and *Sox1* later still (Streit et al., 2000a; Streit et al., 1998; Streit and Stern, 1999a). This timing of *Sox2* activation corresponds approximately to the time when the grafted node can be removed and the responding tissue will still continue to develop into a mature neural plate – for this reason *Sox2* is considered as a marker for induced neural plate in the chick.

Sox2 expression is regulated by a complex array of 25 separate enhancer elements situated both up- and downstream of the coding sequence (Uchikawa et al., 2003; Uchikawa et al., 2004). Of these, two account for the early expression of this gene in its earliest domain in the chick embryo: N2 drives expression in a large region anterior to the tip of the primitive streak (which eventually gives rise to forebrain, midbrain and the most rostral hindbrain) while N1 is activated in a small paranodal domain at the same stage and will eventually give rise to the remaining hindbrain and spinal cord (Takemoto et al., 2006; Uchikawa et al., 2003; Uchikawa et al., 2004). Uchikawa (Uchikawa et al., 2003) demonstrated that N1 can be activated by a graft of Hensen's node. Here we show that N2 can also be activated by a similar graft, consistent with the fact that such grafts can induce a complete CNS (Dias and Schoenwolf, 1990; Storey et al., 1992).

More puzzling is our finding that *Smad7* activates N2, but not expression of the endogenous *Sox2* gene. This result strongly suggests the existence of undescribed silencer elements outside of the N2 enhancer, which contribute to regulate the expression of *Sox2*. This is especially surprising considering that the combined activity of N1+N2 recapitulate the entire initial domain of expression of *Sox2*, and suggests that *Smad7*

induces N2 through a mechanism that does not entirely correspond to the normal process of neural induction in the embryo or by a graft of Hensen's node. Moreover (and unlike N1), the N2 enhancer lacks obvious FAST1 binding sites, which might be expected to respond to the BMP pathway (data not shown). These findings suggest again that the node, as well as the normal embryo environment responsible for generating the early neural plate, must contain signals that are not identical to those activated by *Smad7*, and reinforces the idea that signals in addition to inhibitors of TGFβs must be involved.

BMP-inhibited cells express neural markers only when they form a continuous trail to the neural plate or its border

The default model proposes that BMP inhibition is the only signal necessary for neural induction. Although its simplicity made it very attractive, there has been considerable debate about whether this mechanism is sufficient to explain neural induction (Stern, 2005; Stern, 2006; Streit and Stern, 1999). The current prevailing view is that additional factors are required, and in particular that FGF signaling is important. At least in the chick, BMP inhibitors alone have not been shown to induce any markers (neural or otherwise) *in vivo* to date. What was previously reported was hat the secreted BMP antagonists Chordin and Noggin can expand the neural plate only when applied directly to the neural/epidermal border, and likewise that BMP4 can only narrow the neural plate when applied to the same region (Streit and Stern, 1999a). Here we have observed a similar effect with the cell-autonomous BMP antagonists *Smad6* and Smad7: the neural markers *Sox2* and *Sox3* and the border markers *Slug* and *Pax7,* as well as *msx1* and *Dlx5* and BMP4 can be induced to extend away from their normal domains when *Smad6* or *Smad7* are electroporated as a line between the neural plate and the lateral non-neural ectoderm.

We also show that BMP inhibition induces border markers in the non-neural ectoderm, but neural induction in the same cells only occurs if the BMP-inhibited cells form a continuous trail connecting them to the neural plate and/or its border. These findings suggest that neuralizing factors emanating from the neural plate spread through the ectoderm ("homeogenetic induction", or induction of neural plate by neural plate (Mangold, 1929; Servetnick and Grainger, 1991), but only between BMP-inhibited cells.

We propose a relay mechanism by which homeogenetic signals can spread from the neural plate only through cells in which BMP signaling is inhibited. Over-expression of BMP inhibitors in cells adjacent to the neural plate or its border allows these cells to

respond to homeogenetic neural inducers emanating from the neural plate, resulting in an expansion of the neural territory. In contrast, cells distant from the endogenous neural plate (e.g. the distant epiblast cells in chick, which are competent to make neural tissue in response to an organizer graft) cannot receive homeogenetic inducing signals unless they are connected to it by a continuous trail of BMP-inhibited cells. However, these results also generate a paradox. BMP inhibition in prospective epidermis induces border markers but not neural markers, while inhibition of BMP at the border does induce neural markers. Despite this, increasing the amount of BMP inhibition (even by a combination of *Smad6* + *Smad7* + *dnBMPR* + Noggin + *Chordin* + *Cerberus*, together with FGF and Wnt inhibitors) outside the border is not sufficient to induce neural markers. This suggests that the border markers induced by BMP inhibitors alone (*Slug*, *Pax7*, *Dlx5*, *Msx1*) are not indicative of induction of a full-fledged border, and that other factors must also be important. This is consistent with one model of neural crest induction proposing that signals from the underlying mesoderm are required along with BMP-inhibition for neural crest to be specified (Meulemans and Bronner-Fraser, 2004; Steventon et al., 2005; Streit and Stern, 1999a).

What could be the missing signals, present in the neural plate, which can only travel between BMP-inhibited cells? A possible candidate is the Notch pathway, which has been implicated in establishing the border of the neural plate (Cornell and Eisen, 2002; Endo et al., 2002; Glavic et al., 2004; Kintner, 1992) and as well as generating boundaries between adjacent domains in many other systems (Bray, 1998; Bray, 2006; Sanson, 2001) and this idea requires further investigation.

Conclusion

This study reveals that the only cells that can be made to express neural markers in response to BMP antagonists are at, or connected with, the border of the neural plate.
We further extend previous observations suggesting that BMP inhibition is not sufficient for neural induction. In the chick, inhibition of BMP signalling, even together with Wnt antagonists and FGF, is not sufficient to induce neural markers in competent epiblast. We therefore challenge the Default Model and propose that neural induction does not take place “by default” but involves a sequence of signalling events, where some players are yet to be identified.

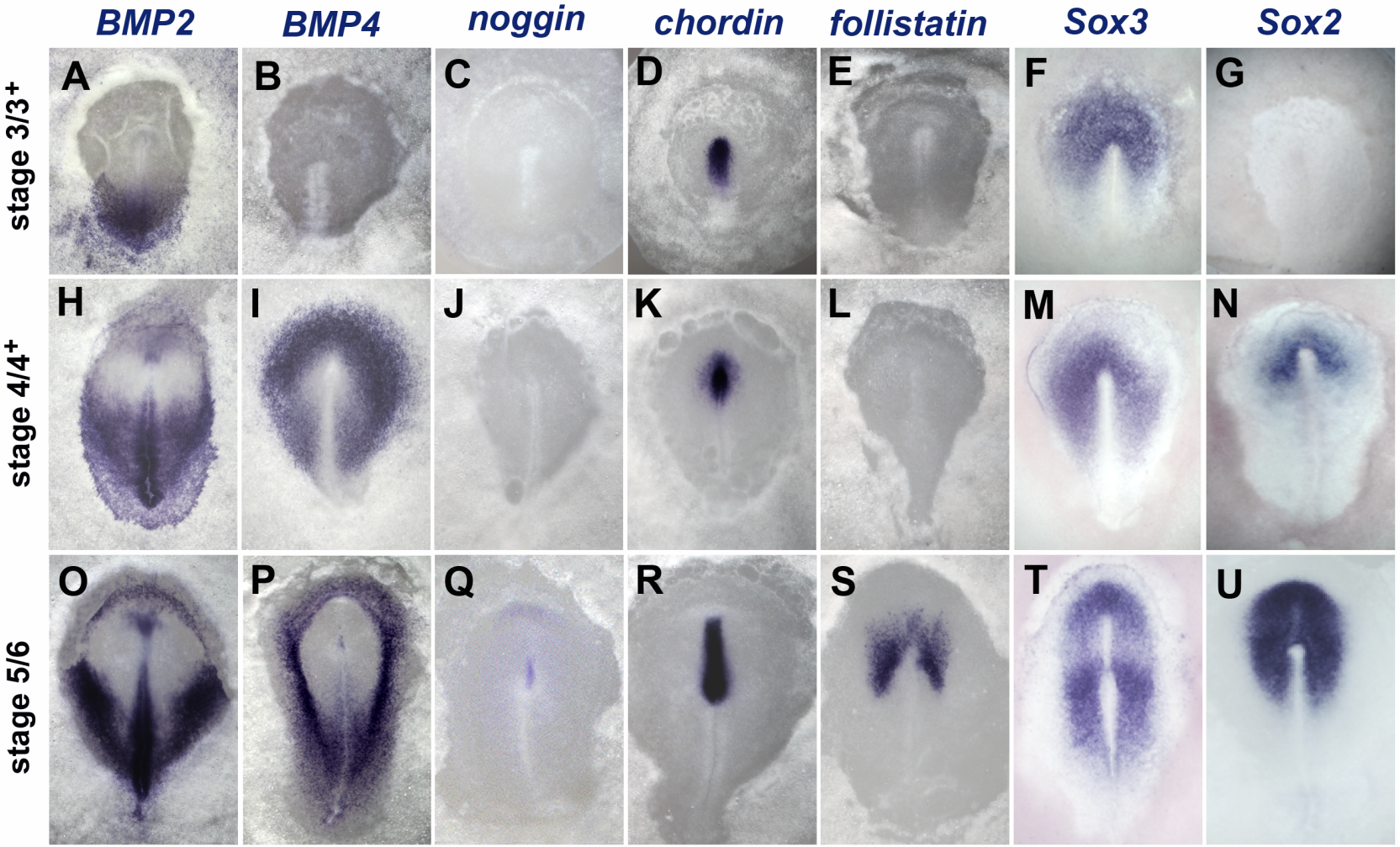

Fig 3.1. Expression patterns of *BMP2*, *BMP4*, *noggin*, *Chordin*, *follistatin*, *Sox3* and *Sox2* in the early chick embryo.

Fig 3.1. Expression patterns of *BMP2*, *BMP4*, *noggin*, *Chordin*, f*ollistatin*, *Sox3* and *Sox2* in the early chick embryo. At stage 3/3^{+}, *BMP2* is expressed in the posterior area *pellucida* epiblast, including the primitive streak (**A**); the domain of expression then expands until it surrounds the forming neural plate where transcripts are present throughout most of the non-neural ectoderm (**H** and **O**). *BMP4* transcripts start to be detected, very weakly, at stage 3, in the most posterior epiblast of the area *pellucida* (**B**); by stage 4, expression expands anteriorly, marking a ring of epiblast cells surrounding the future neural plate (**I**) and then condenses into a line of cells at the boundary between neural and non-neural ectoderm (**P**). *Noggin* transcripts seem to be absent up to stage 4^{+} (**C** and **J**); by stage 5, expression is present in the notochord (**Q**). Chordin is strongly expressed in the node and anterior streak at stage 3 (**D**) and 4^{+} (**K**); from stage 5, *Chordin* expression is present in the node and notochord (**R**). *Follistatin* transcripts are not detected at stage 3^{+} (**E**) or 4^{+} (**L**); by stage 5, expression is present in the head process and the regions lateral to the node (**S**). *Sox3* and *Sox2* follow a similar expression in the prospective neural plate and neural plate (**F**, **M**, **N**, **T** and **U**), with the exception that, while expression of *Sox2* only starts to be detected at stage 4/4^{+} (**N**), *Sox3* transcripts are detected earlier (**F**).

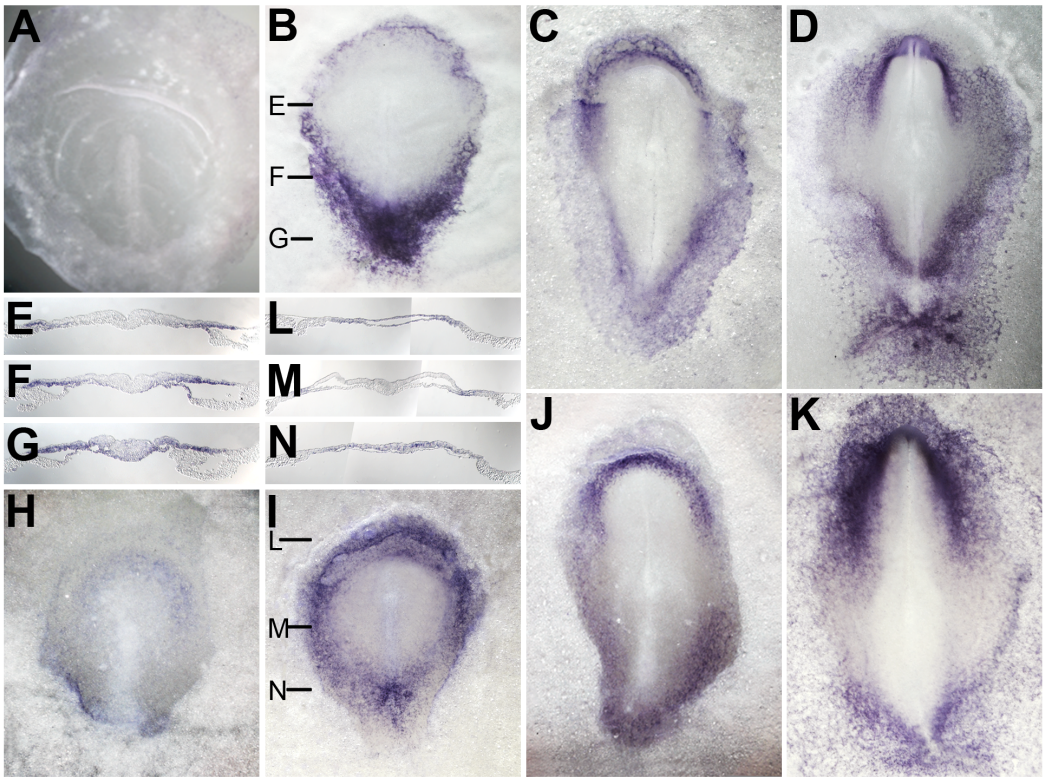

Fig 3.2. Expression pattern of *Smad6* and *Smad7* in the early chick embryo. Whole-mount *in situ* hybridisation was performed with DIG-labelled probes for *Smad6* (**A**-**G**) and *Smad7* (**H**-**N**). *cSmad6* transcripts are not detected up to stage 3^{+} (**A**); At stage 4 expression is detected at the posterior most part of the embryo, including the primitive streak and at the margin of the embryo and excluding the prospective neural plate (**B**, **E**-**G**); As development proceeds, the *Smad6* mRNA remains excluded from the neural plate, but accumulates at the border and expands into the blood mesoderm in the area *opaca* (**C**,**D**). *cSmad7* expression follows a very similar pattern (**H**-**N**), with the exception that its transcript is detected earlier, very weakly at stage 3 embryos, in a crescent type expression around the future neural plate (**H**); By stage 4, the expression becomes strongly localized to the border of the neural plate and very posterior streak (**I**, **L**-**N**).

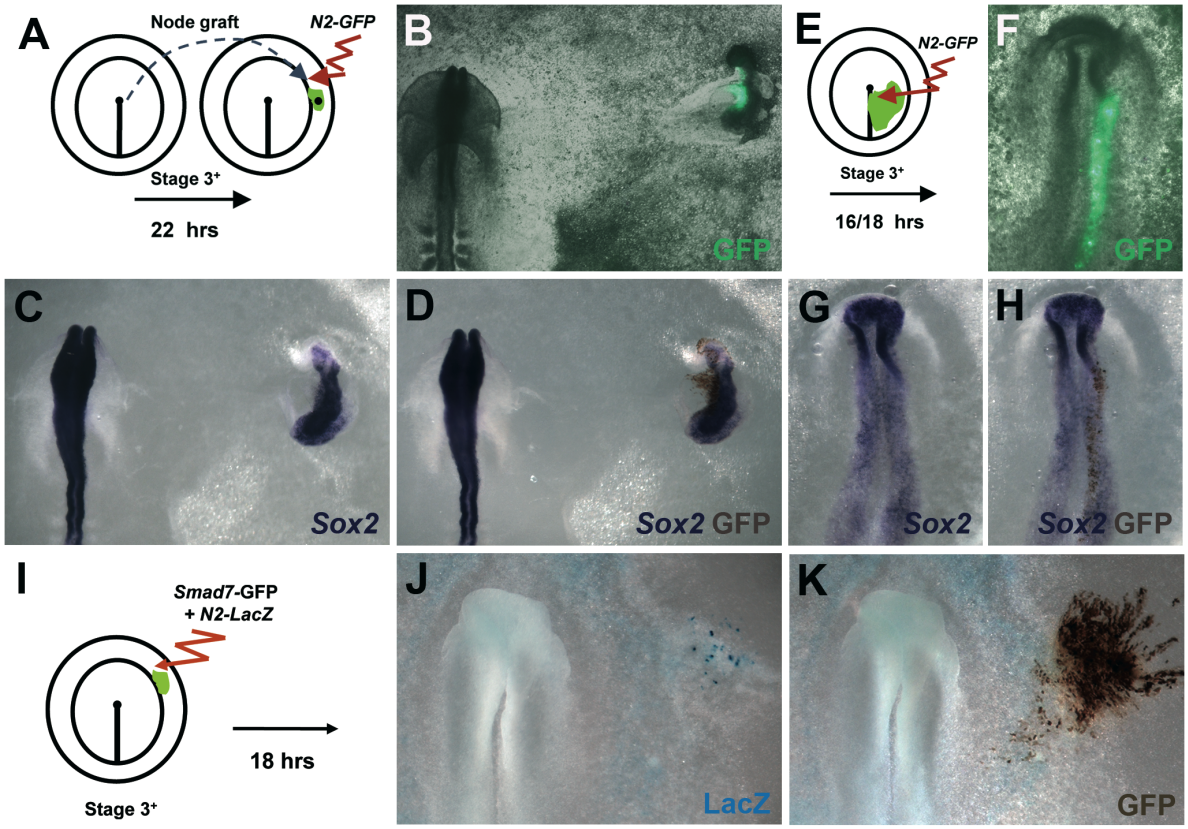

Fig 3.3. *Smad7* activates the N2 enhancer of *Sox2*. Control experiments show that the N2 enhancer is active when a node graft is placed in the area *opaca* (**A**-**D**). Similarly, when *N2-GFP* construct is electroporated in a broad domain in the prospective neural plate, N2 is activated (**E**-**H**). *Smad7* activates the N2 enhancer when electroporated in the competent epiblast of the area *opaca* (**I**-**K**); *LacZ* marks the cells with the enhancer active (**J**).

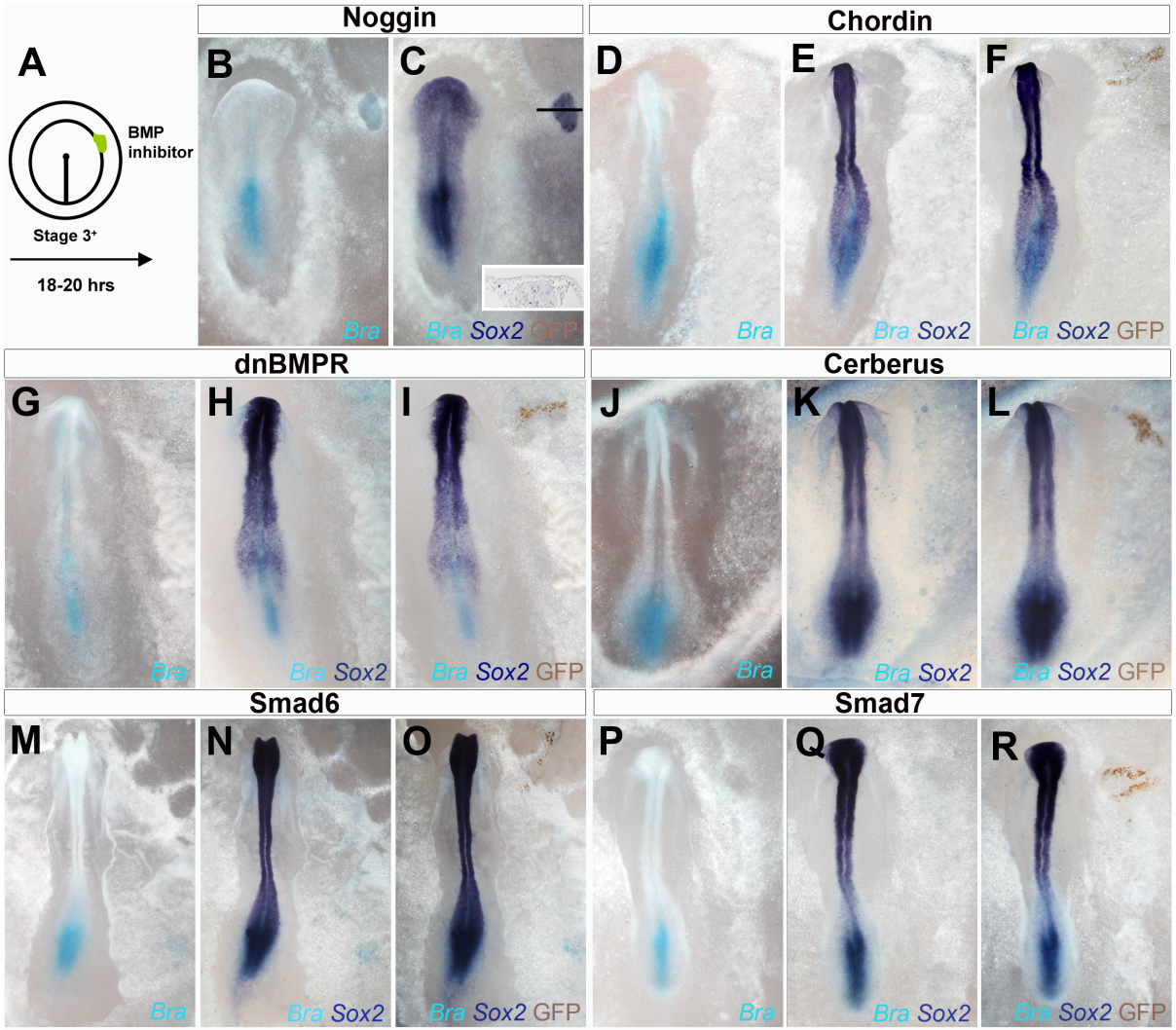

Fig 3.4. BMP inhibition is not sufficient for neural induction.

Fig 3.4. BMP inhibition is not sufficient for neural induction. Experiments were performed in the competent epiblast of the area *opaca* (**A**). Inhibition of BMP by missexpression of Noggin (**B and C**), *Chordin* (**D**-**F**), *dnBMPR* (**G**-**I**), *Cerberus* (**J**-**L**), *Smad6* (**M**-**O**) and *Smad7* (**P**-**R**) is not sufficient to induce *Sox2* (or *Brachyury*, light blue in all the panels). All cell pellets produce background staining after *Sox2 in situ* hybridization and sections through the embryos, at the level indicated, were performed to show absence of expression in the epiblast (**D**).

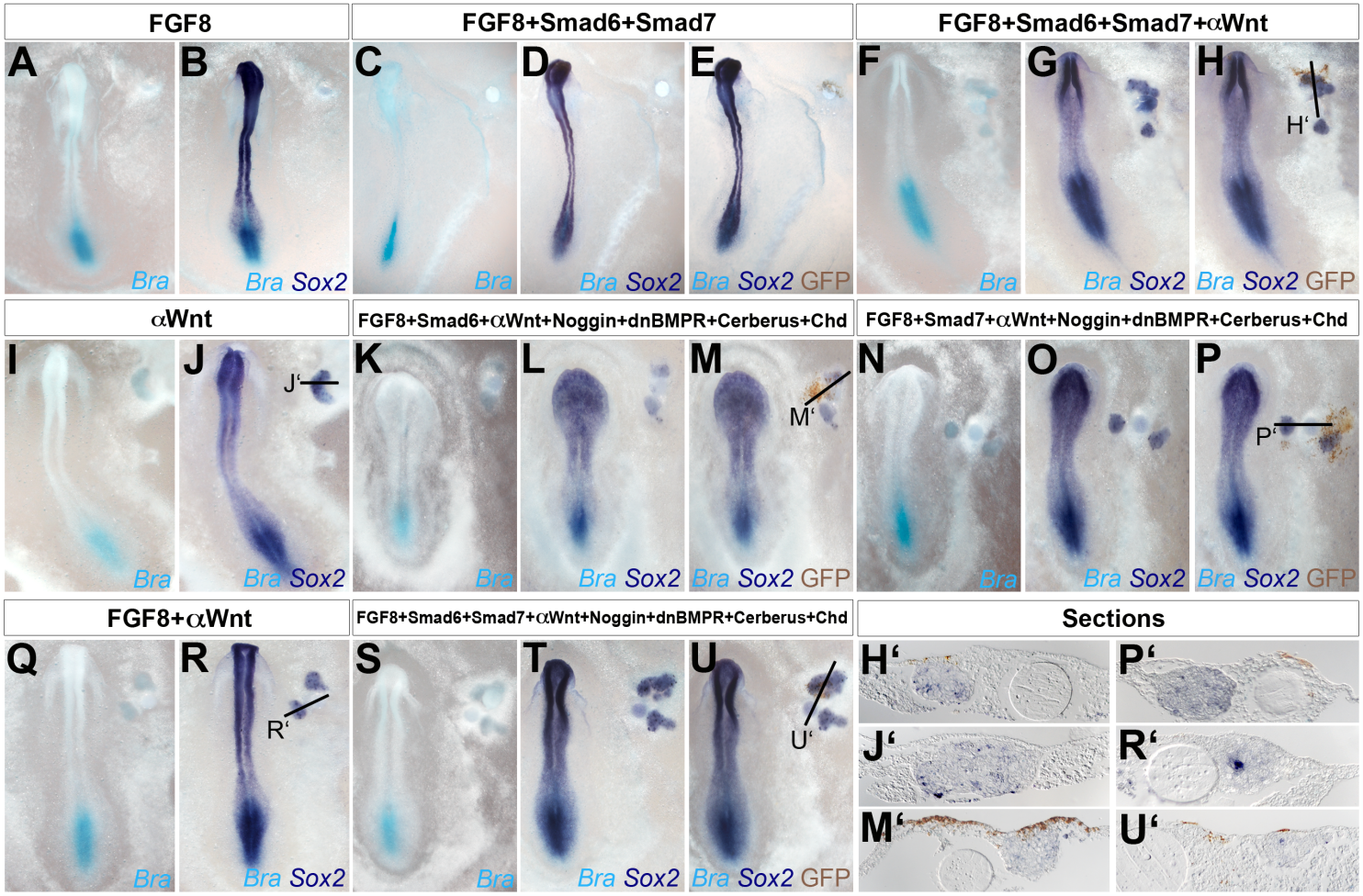

Fig 3.5. Inhibition of BMP and Wnt, together with activation of FGF signaling, does not induce neural or mesodermal tissue in the chick.

Fig 3.5. Inhibition of BMP and Wnt, together with activation of FGF signaling, does not induce neural or mesodermal tissue in the chick. None of the following combinations induces either *Brachyury* (**A**, **C**, **F**, **I**, **K**, **N**, **Q** and **S**) or *Sox2* (**B**, **D**, **G**, **J**, **L**, **O**, **R** and **T**): FGF alone (**A** and **B**); FGF + *Smad6* + *Smad7* (**C**-**E**); FGF + *Smad6* + *Smad7* + Wnt antagonists (*Dkk1+NFz8+Crescent*) (**F**-**H**); Wnt antagonists alone (**I** and **J**); FGF + *Smad6* + Wnt antagonists + Noggin + *dnBMPR* + *Cerberus* + *Chordin* (**K** – **M**); FGF + *Smad7* + Wnt antagonists + Noggi*n* + *dnBMPR* + *Cerberus* + *Chordin* (**N** - **P**); FGF + Wnt antagonists (**Q** and **R**); FGF + *Smad6* + *Smad7* + Wnt antagonists + Noggin + *dnBMPR* + *Cerberus* + *Chordin* (**S** – **U**). Electroporated cells were recognized by GFP expression (**E**, **H**, **M**, **P** and **U**). *In situ* hybridization with *Sox2* always produces background staining in the grafted cell pellets and sections were performed to show the absence of Sox2 expression in the epiblast (the plane of section is indicated by a black line) (**H'**, **J'**, **M'**, **P'**, **R'** and **U'**).

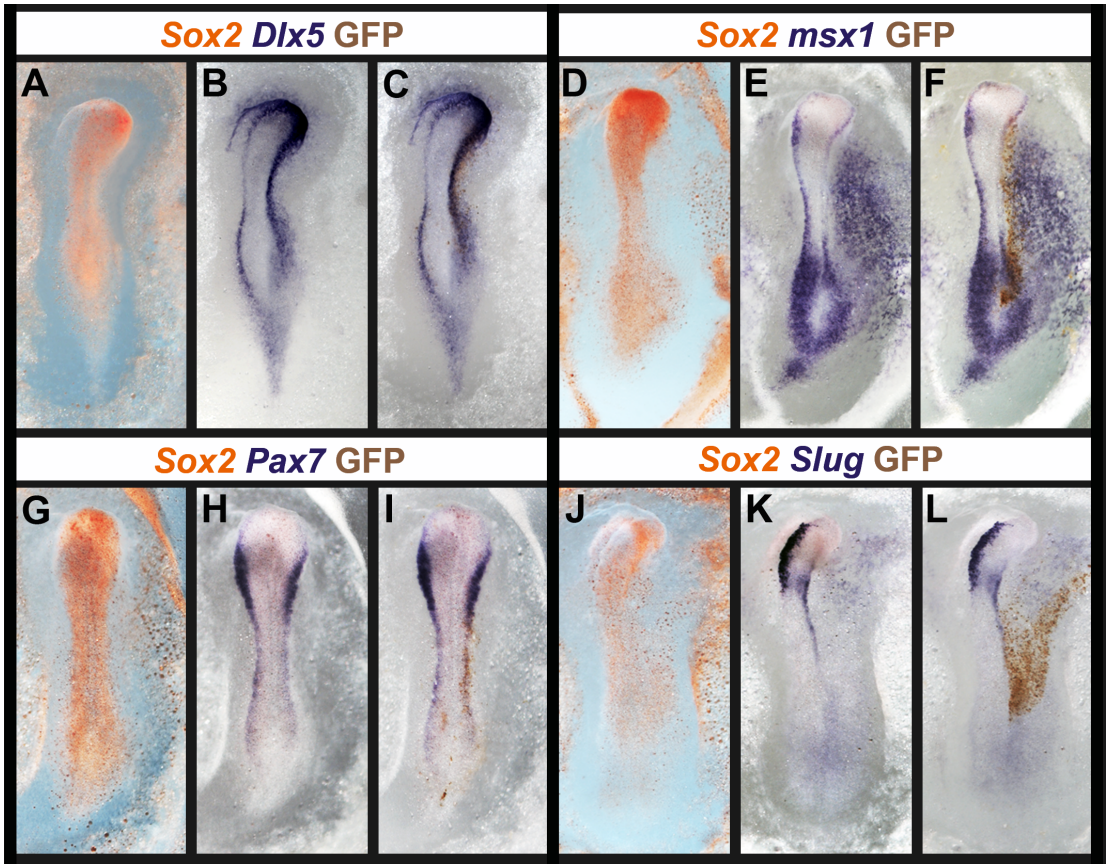

Fig 3.6. *BMP* overexpression inhibits the formation of the neural plate. *BMP4* was electroporated as a patch in the prospective neural plate at stage 3^{+}. 18-20 hours later, a reduction in the domain of the neural plate is observed in the electroporated side, as seen by the narrowing of the domain of expression of *Sox2* (**A**, **D**, **G** and **J**). This is followed by a lateral shift in the expression of the border markers *Dlx5* (**B** and **C**), *msx1* (**E** and **F**), *Pax7* (**H** and **I**) and *Slug* (**K** and **L**); The electroporated region is marked by α-GFP antibody staining, in brown (**C**, **F**, **I** and **L**).

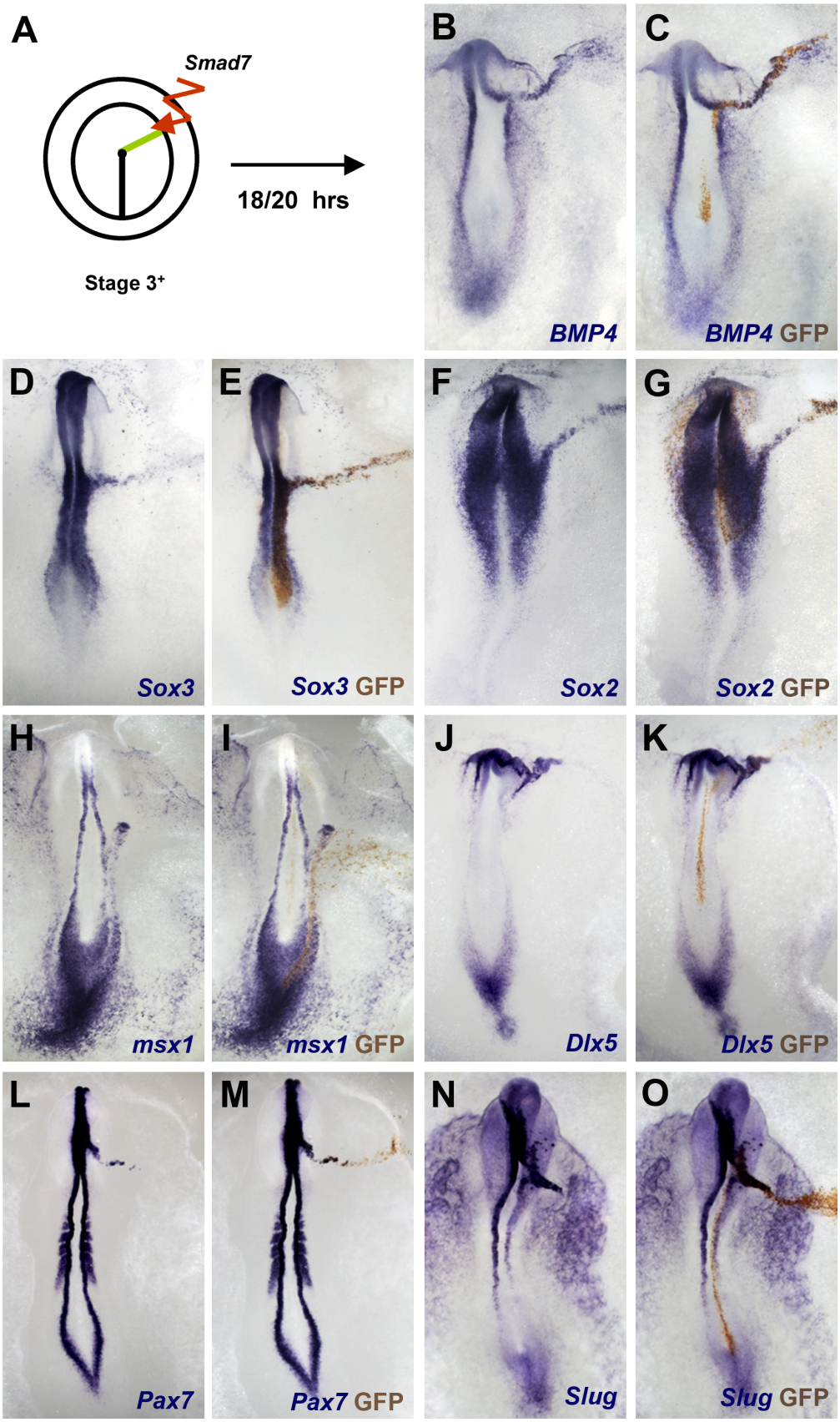

Fig 3.7. ***Smad7*** **overexpression extends the domain of the neural plate.**

Fig 3.7. *Smad7* overexpression extends the domain of the neural plate. Experiments were performed at stage 3^{+}, when *Smad7* was electroporated in a line spanning from the prospective neural plate into the area *opaca* (**A**). This resulted in the expansion of the neural plate, as marked by *Sox3* (**D** and **E**) and *Sox2* (**F** and **G**); Induced expression was also seen for *BMP4* (**B** and **C**), *msx1* (**H** and **I**) *Dlx5* (**J** and **K**), *Pax7* (**L** and **M**) and *Slug* (**N** and **O**); Electroporated cells are shown in brown, after α-GFP antibody staining (**C**, **E**, **G**, **I**, **K**, **M** and **O**).

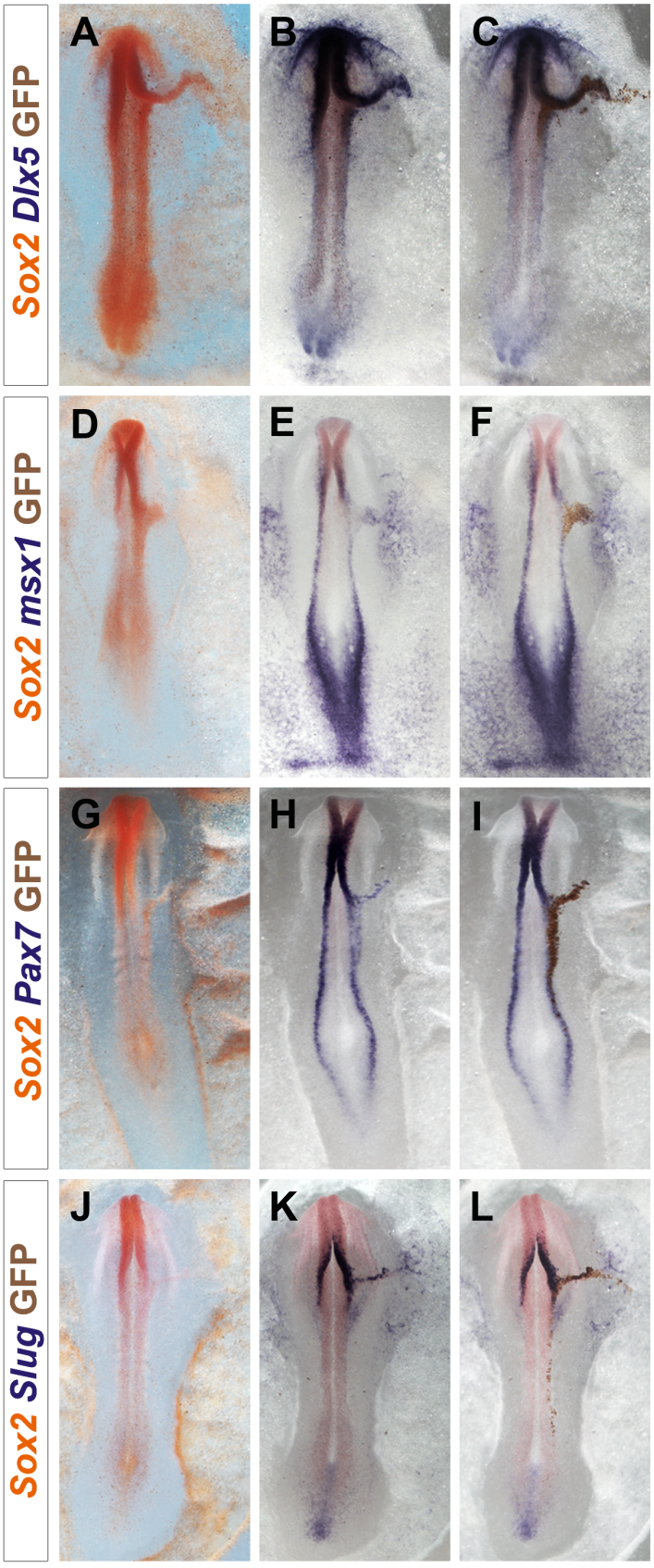

Fig 3.8. Smad6 overexpression extends the domain of the neural plate.

Fig 3.8. *Smad6* overexpression extends the domain of the neural plate. Experiments were performed at stage 3^{+}, when *Smad6* was electroporated in a line spanning from the prospective neural plate into the area *opaca*. This resulted in the expansion of the neural plate, as marked by *Sox2* (**A**, **D**, **G** and **J**); Induced expression was also seen for *Dlx5* (**B** and **C**), *msx1* (**E** and **F**) *Pax7* (**H** and **I**) and *Slug* (**K** and **L**); Electroporated cells are shown in brown, after α-GFP antibody staining (**C**, **F**, **I** and **L**).

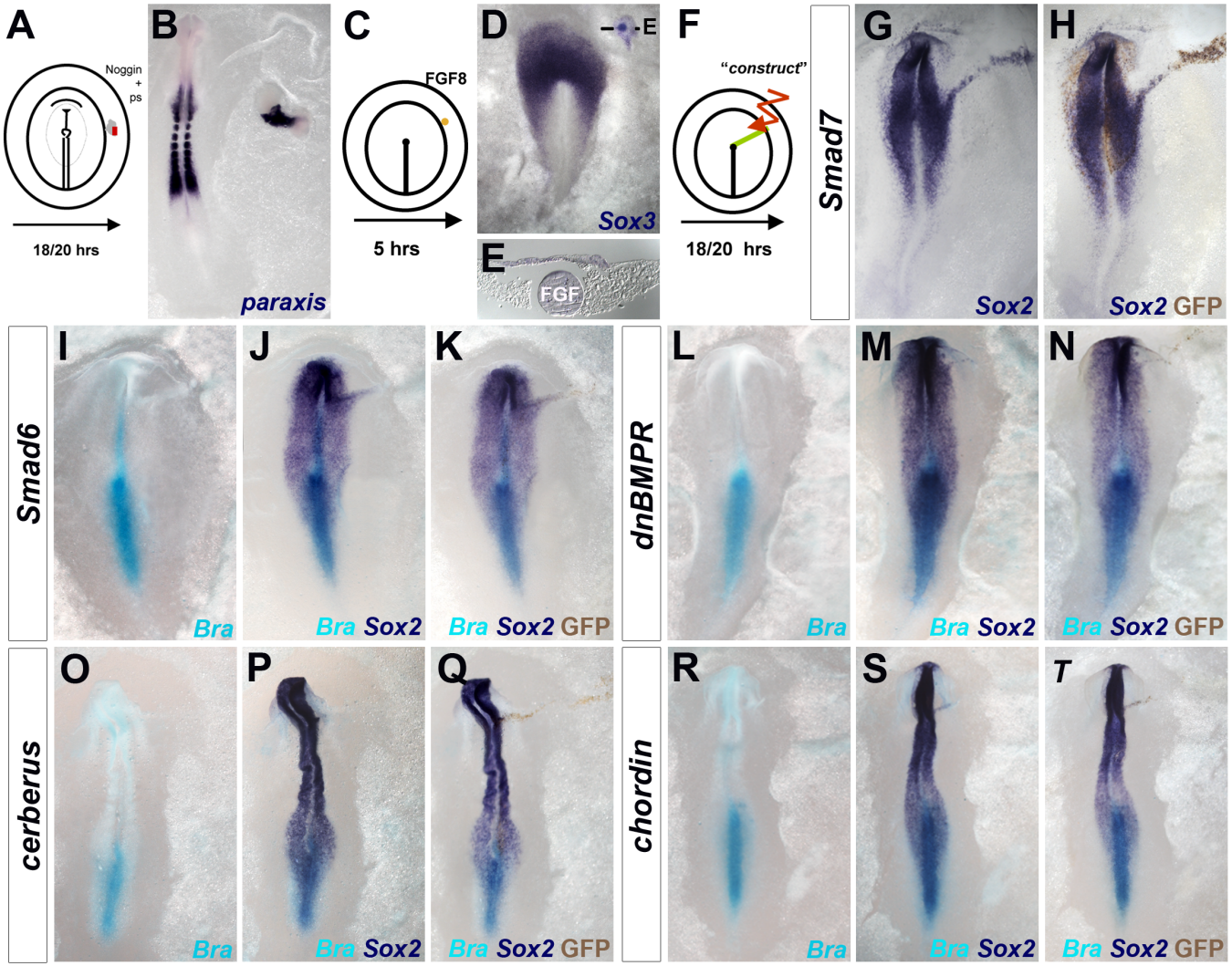

Fig 3.9. The border of the neural plate is uniquely sensitive to BMP antagonists.

Fig 3.9. The border of the neural plate is uniquely sensitive to BMP antagonists. Experiments were performed at stage 3^{+}, when the *BMP* inhibitors were electroporated in a line spanning from the prospective neural plate into the area *opaca* (**F**). This procedure always resulted in the extension of the domain of expression of *Sox2* (shown in dark blue), without induction of *Brachyury* (shown in light blue): *Smad7* (**G** and **H**), *Smad 6* (**I** – **K**), *dnBMPR* (**L** – **N**), *Cerberus* (**O** – **Q**) and *Chordin* (**R** – **S**); Electroporated cells are shown in brown, after α-GFP antibody staining. Some positive controls for this chapter are also presented: Noggin expressing cells are active as, when grafted together with a piece of primitive streak (**A**) induce *paraxis* (**B**); FGF8 used in this study is active as it is able to induce the early neural marker *Sox3* whithin 5 hours (**C** and **D**); this can be clearly seen, through a section, in the epiblast exposed to the FGF bead (**E**).

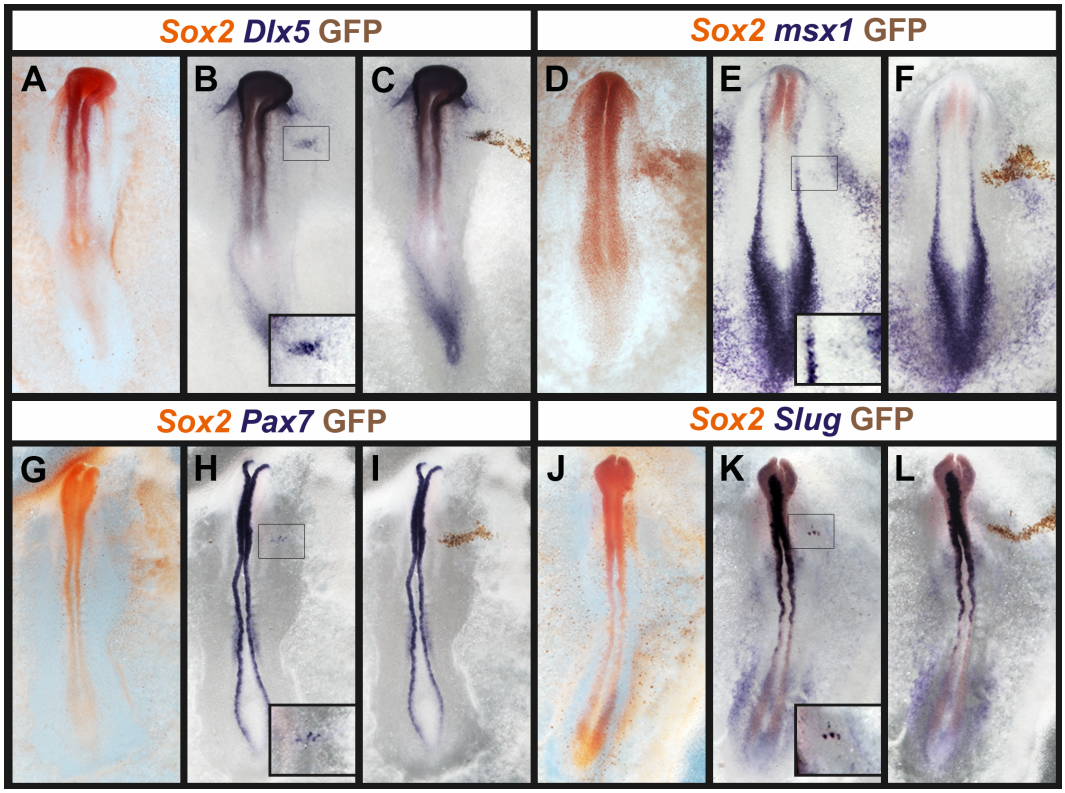

Fig 3.10. BMP inhibition induces border markers in cell populations not in contact with the neural plate. Experiments were performed at stage 3^{+}, when *Smad6* was electroporated, as a small patch, in the non-neural ectoderm, not in contact with the neural plate. This resulted in no induction of the neural marker *Sox2* (**A**, **D**, **G** and J) and in the induction of the border and/or neural crest markers *Dlx5* (**B** and **C**, see **inset in B**), *msx1* (**E** and **F**, low level of induction, **inset in E**), *Pax7* (**H** and **I**, see **inset in H**) and *Slug* (**K** and **L**, see **inset in K**); Electroporated cells are shown in brown, after α-GFP antibody staining (**C**, **F**, **I** and **L**).

Chapter 4

Screen for secreted molecules from the Organizer

Introduction

The organizer and neural induction

The formation of the vertebrate nervous system is generally thought to start at gastrula stages of development when signals from the organizer induce neural development in the ectoderm (Spemann and Mangold, 1924). Some of the molecular players involved have been identified based mainly on work in amphibians, and a model proposed – the Default Model (Sasai et al., 1995; Wilson and Hemmati-Brivanlou, 1995). The model states that neural inducing signals function by inhibiting epidermis and that, in the absence of these signals, cells acquire neural fate as a default. Several lines of evidence support this general idea. The BMP antagonists *Chordin* (Piccolo et al., 1996; Sasai et al., 1994), *noggin* (Lamb et al., 1993; Smith and Harland, 1992; Zimmerman et al., 1996), *follistatin* (Hemmati-Brivanlou et al., 1994a) and *Xnr3* (Hansen et al., 1997; Smith et al., 1995) are expressed by the amphibian organizer at an appropriate stage and share the property of inhibiting BMP signals, allowing the surrounding ectoderm to differentiate into neural (for review see (Harland, 2000; Streit and Stern, 1999; Weinstein and Hemmati-Brivanlou, 1999; Wilson and Hemmati-Brivanlou, 1995; Wilson and Edlund, 2001). However, other work, performed in various species suggest more complexity.

In the mouse, *follistatin* mutants have no neural defects (Matzuk et al., 1995c) and *noggin* mutants do not have an early phenotype, developing a normal neural plate (McMahon et al., 1998). BMP4 mutants, although early embryonic lethal, seem to have both a nervous system and epidermis (Winnier et al., 1995) and BMP7 deficient mice do not exhibit a neural phenotype (Dudley and Robertson, 1997).

In the chick, as presented in the previous Chapter, the time of expression of the neural inducing molecules does not correlate with the default model. *Noggin* just starts to be

expressed in the node when the neural inducing ability of the node starts to decrease (Storey et al., 1992; Storey et al., 1995) and its expression persists after the node has lost the ability to induce neural tissue (Connolly et al., 1997). This is also the case for *follistatin* (Connolly et al., 1995).

Furthermore, ectopic expression of either *Chordin* or *noggin* fails to induce an ectopic neural plate in a region of the area *opaca* that is competent to respond to neural inducing signals from the node (Streit et al., 1998; Streit and Stern, 1999; Streit and Stern, 1999a; Streit and Stern, 1999b). Furthermore, although Chordin cannot induce neural tissue when ectopically expressed, it can stabilize *Sox3* expression in cells that have been exposed fro 5 hours to neural inducing signals from the node (Streit et al., 1998).

Taking together, these observations suggest that, at least in the chick, BMP inhibition is not the only component in neural induction and that other upstream signals from the organizer may also be required.

Secreted molecules have a signal sequence

Proteins destined to cross the cell membrane, including both transmembrane (eg. cell surface, transmembrane receptors) and secreted (eg. hormones, growth factors) components, contain a characteristic hydrophobic sequence (Signal Sequence). The presence of this signal sequence was first detected by Blobel and Dobberstein (Blobel and Dobberstein, 1975a; Blobel and Dobberstein, 1975b) and later confirmed by others that further added that although these signal sequences are unique, they are largely interchangeable among secreted proteins and even between different organisms (Brown et al., 1994; Hitzeman et al., 1990; Miller et al., 1994; Walter and Johnson, 1994). It has also been demonstrated that there is considerable functional interchangeability between some components of the eukaryotic and prokaryotic protein secretion pathways (Hallenberger et al., 1993; Hartman et al., 1994).

A method for isolating secreted molecules

Jacobs and colleagues (Jacobs et al., 1997) have designed a rapid method for isolating large numbers of cDNAs encoding secreted proteins. Their strategy consists of a genetic selection performed in a strain of *Saccharomyces cerevisiae* that is deleted for its endogenous invertase gene. When the yeast is grown in a medium containing either sucrose or raffinose, it has to secrete invertase to break down these sugars and survive. A cDNA cloning vector ("yeast signal sequence trap vector") carries a modified invertase gene lacking the signal sequence and is introduced into this strain. Heterologous

secreted genes that correctly fuse upstream of the defective invertase provide the necessary signals to restore invertase secretion and yeast survival in restrictive media.

This chapter describes a screen performed to isolate secreted molecules expressed in Hensen's node or anterior primitive streak of stage 3^{+}-4 chick embryos. The initial screen was performed in collaboration with the original authors of this method (Edward Lavallie and Lisa Collins-Racie) at the Genetics Institute in Boston (later acquired by Wyeth Pharmaceuticals) and resulted in the isolation of 442 clones. Sequence analyses revealed a 70% contamination with mitochondrial and Ribosomal DNA and the remaining 137 clones were used to perform an *in situ* hybridization screen on chick embryos from stage 3 to stage 7-8. Most genes seem to be expressed ubiquitously, with the exception of 23 that are discussed in more detail.

Material and methods

Molecular screen for Hensen's node secreted factors

Hensen's nodes were dissected from about 1200 chick embryos at stage $3^+/4$ and total RNA extracted using the GUA-SCN method (Chomczynski and Sacchi, 1987) (Chapter II). PolyA$^+$ mRNA was then isolated with the PolyATtract mRNA isolation system (Promega) and converted to double-stranded cDNA using the Superscript Choice System (Gibco) and the oligo/random primer 5'-TCCCGATTGAATTCTAGACCTGCGTCGACNNNNNN-3'. EcoRI adaptors were ligated onto the cDNA which was then digested with SalI; The resulting 300-600 base pair fragments (aproximately) were ligated into pSUC2T7M13ORI pre-digested with EcoRI and XhoI. Electrocompetent DH10B cells (Gibco) were transformed and $5x10^6$ were pooled to prepare the amplified plasmid cDNA library (Sambrook et al., 1989).

A *Saccharomyces cerevisiae* mutant for invertase (SUC2$^-$) was used for the selection. SUC2$^-$ yeast, transformed using lithium acetate, were selected by growth on complete minimal plates lacking triptophan (CMD-W) (Ausubel et al., 1995) for three days before being replicated onto YPR plates (1% yeast extract, 2% peptone, 2% raffinose, 2 µg/ml antimycin A) to select for plasmids encoding signal sequences. Seven days later, yeast colonies were purified by streaking onto new YPR plates. Individual colonies were grown overnight on CMD-W plates and the used to inoculate duplicates into deep-well trays with CMD-W medium. After overnight incubation, glycerol was added (1:1) to one of the sets and frozen (Yeast glycerol stocks). The other set was used to prepare plasmid DNA as previously described (Blanchard and Nowotny, 1994) and the cDNA inserts sequenced.

Bioinformatics

The sequences obtained were compared against the NCBI database for *Homo sapiens* and *Gallus gallus* using BLAST. For prediction of a signal peptide in DNA sequences the Signal P3.0 software was used (http://www.cbs.dtu.dk/services/SignalP/) (Bendtsen et al., 2004; Nielsen et al., 1997a; Nielsen et al., 1997b; Nielsen et al., 1996).

PCR amplification from yeast stocks

Yeast glycerol stocks containning the clones were defrosted and 25µl of each stock was used to inoculate 300µl of CMD-W medium with 15% glycerol. The overnight cultures

were resuspended and 5µl of each lysed with 20µl Lysis buffer (1% Triton X-100, 20nM Tris-HCL pH8.9, 2mM EDTA) at 100°C for 10 minutes, followed by a 7 minute spin at 11500 RPM at 4°C. Clones were amplified by PCR using 2µl of lysis product per reaction and the primers COLPCR3 (5'-GGTGTGAAGTGGACCAAAGGTCTA-3') and INV-UNI (5'-CCTCGTCATTGTTCTCGTTCCCTT-3') (94°C, 1 minute; 55°C, 45 seconds, 68°C, 5 minutes; 30 cycles).

In situ hybridization

In situ hybridization was performed as described in Chapter 2. DIG labelled RNA probes were transcribed using the yeast PCR products and T7 Polymerase (Promega) (The pSUC2T7M13ORI vector contains a T7 polymerase recognition site and the cloning was directional).

Results

The molecular screen resulted in the isolation of 442 sequences

To isolate sequences that code for secreted proteins a Yeast Sequence Trap Screen (Jacobs et al., 1997) was performed using cDNAs isolated from stage 3^{+}-4 Hensen's nodes from chick embryos. Two rounds of screening were performed, resulting in the isolation of 227 clones and 215 clones in the other set, denominated nhbr and nhbw respectively.

Sequence analyses revealed that of the total 442 clones, 4 (0.9%) correspond to 18S RNA genes (accession numbers AF173612 and SCA419876) and 301 clones (69.9%) were mitochondrial DNA sequences (either homologous to *Gallus gallus* mitochondrial genome, X523992, or to *Gallus gallus spadiceus* mitochondrial genome: AP003321). The remaining 137 clones (29.4%) were selected for further analysis.

137 clones are selected for further study

The sequence analyses of the clones is summarized on **Tables 4.I-II**. BLAST searches revealed that of the total 137 clones, 39 (28.5%) have no homology to known genes in humans and of these, 7 (5% of the total) are not annotated in *Gallus gallus*.

The 137 sequences were further analysed for the presence of a signal sequence using the SignalP 3.0 algorithm (hhttp://www.cbs.dtu.dk/services/SignalP/) (Bendtsen et al., 2004; Nielsen et al., 1997a; Nielsen et al., 1997b). This revealed that less than 25% of the sequences (34/137) are known or predicted not to be secreted (**Tables 4.I-II**, last columns headed SP). These might have been survived the screen because of internal peptides that mimic signal sequences. The proportion of sequences without a signal peptide is very close to that obtained by others in similar screens (about 20%; E. Lavallie, personal communication), and apparently to be expected in this type of selection (Kaiser et al., 1987). The presence or absence of a signal peptide (Y or N in column SP, **Tables 4.I-II**) are only predictions based on an algorithm for hydrophobic domains and are not absolute certainties of whether they contain a functional signal sequence (Bendtsen et al., 2004).

An *in situ* screen revealed 23 sequences with spatio-temporally defined expression

To assess whether the clones isolated are likely candidate players in neural induction, DIG-labelled RNA probes for the 137 clones were transcribed and *in situ* hybridization performed in chick embryos ranging from about stage 3 to stage 7/9 (in some cases older embryos). *In situ* analyses revealed that 107 sequences were ubiquitously expressed and 23 sequences have a defined spatio-temporal expression. Their molecular homologies (if any) and expression patterns are summarised below.

Nhbr7 (No similarity)

Nhbr7 mRNA expression cannot be detected at early primitive streak stages (**Fig 4.2 A-B**). At stages 4 and 4^+ expression is confined to the prospective neural plate (**Fig 4.2 C-D**) and stops being detected by the time the first somite forms at stage 7 (**Fig 4.2 E**).

Nhbr10, nhbr116, nhbw63, nhbw153 (Fatty acid elongase; ELOVL family member5, elongation of long chain fatty acids)

Long chain fatty acids are major components of membrane and storage lipids in eukaryotes (Inagaki et al., 2002), mostly located in the Endoplasmic Reticulum or in its vicinity (Beaudoin et al., 2000; David et al., 1998; Karan et al., 2004; Michelsen et al., 2005; Toke and Martin, 1996; Tvrdik et al., 2000; Zhang et al., 2003). In terms of protein topology, all members of the elongase family have, or are predicted to have five or six transmembrane domains, due to the presence of large hydrophobic aminoacid stretches (Monne et al., 1999; Moore et al., 1995). Fatty acid elongases are enzymes involved in the biosynthesis and elongation of fatty acids in a process known as the fatty acid chain elongation system (FACES). FACES has been found in many tissues including liver, brain, kidney, lung, adrenals, retina, testis, small intestine, blood cells (lymphocytes and neutrophils) and fibroblasts, with the exception of the heart, which has no measurable activity (Cinti et al., 1992). All the studies in fatty acid elongation have been carried out mainly with cell lines and no information is available on either fatty acid elongase expression or function during embryonic development.

Detection of these clones by *in situ* hybridization was very difficult to achieve, given the low levels of expression in the embryonic region and strong staining of the inner third of the area *opaca*. Nevertheless for three of the clones (*nhbr10*, *nhbr116* and *nhbw63*) consistent patterns were observed with embryonic expression in the prospective neural plate being detected at stage 4 (**Fig. 4.3 A**). The weak expression is maintained

throughout the neural plate from stage 4+ to stage 8 (**Fig 4.3 B-E**), after which the expression in the area *opaca* is so strong that the embryos become completely stained (not shown).

The remaining clone *nhbw153*, although also similar to fatty acid elongase, resulted in a different *in situ* hybridization pattern from the one described above. At stage 3+ the mRNA localizes to the anterior third of the primitive streak and the node as well as to the prospective neural plate (**Fig. 4.21 A**). At stage 4+ the primitive streak expression is extended posteriorly and there is also strong expression in the emerging head process (**Fig 4.21 B**). At stage 5, expression expands to the "mesodermal wings" and is maintained in the neural plate and head process (**Fig 4.21 C**). Similar expression is observed at stage 6, where the notochord is now well stained (**Fig 4.21 D**). By stage 7, expression is present in the entire neural plate, with the exception of the area surrounding the node and first formed somite; extraembryonic mesoderm also continues to express *nhbw153* (**Fig 4.21 E**). Stage 10 embryos present strong expression in the blood islands and in the neural tube and borders of the posterior neural plate (**Fig 4.21 F**).

Nhbr34 (Fibulin 2)

Fibulin2 was first studied in the mouse. It is a matrix protein containing tandem arrays of calcium binding epidermal growth factor-like motifs (Argraves et al., 1990; Grassel et al., 1999; Pan et al., 1993b). It is present in the stroma and in the basement membrane of many tissues and its expression pattern previously suggested a role in organogenesis, particularly in embryonic heart development (Zhang et al., 1995; Zhang et al., 1996). More recently it has been reported that some fibulins, and in particular fibulin1, is required for the directed migration and survival of cranial NCCs contributing to the development of pharyngeal glands, craniofacial skeleton, cranial nerves, aortic arch arteries, cardiac outflow tract and cephalic blood vessels (Cooley et al., 2008).

Nhbr34 mRNA does not seem to be detected at early primitive streak stages (**Fig. 4.4 A**). There follows an upregulation of expression at stages 4-4+ (**Fig 4.4B**) in the primitive streak, neural plate and underlying mesoderm. Expression seems to decline completely by stage 6 (**Fig 4.4C**).

Nhbr90 (No similarity)

Nhbr90 mRNA is detected at stage 3/3+ at a low level in the prospective neural plate and strongly in the anterior primitive streak (**Fig 4.5 A**). The organizer expression is

maintained through the stages analysed (**Fig 4.5 B-F**); neural plate expression becomes stronger and restricted to regions anterior to the node at around stage 7 (**Fig 4.5 D**), with the formation of the first pair of somites; This pattern of expression is maintained, with its anterior boundary around the first somite and its posterior boundary just below the node (**Fig 4.5 F**).

Nhbr91 (Similar to nuclear autoantigenic sperm protein, NASP)

In the human testis, nuclear autoantigenic sperm protein (NASP) is localized predominantly in the nucleous of primary spermatocytes and round spermatids (Welch and O'Rand, 1990; Welch et al., 1990) and human spermatozoa contains NASP in the acrosomal region. NASP is hypothesised to play a role in regulating the early events of spermatogenesis (O'Rand et al., 1992). NASP has also been reported in somatic cells mouse embryonic cells, skin, neuroepithelium and mammary gland (Batova et al., 2000; Richardson et al., 2000) where it is coupled with the cell cycle, increasing its amounts when histones also increase. Because NASP has histone binding sites, it has been postulated that it may function in the transport and/or storage of histones (Richardson et al., 2000). In a recent study, Richardson and colleagues (Richardson et al., 2006) explored the role of NASP in cell cycle progression in cell lines and in mouse embryonic development. Their results indicate that, without sufficient NASP, both HeLa and U2OS cells fail to replicate their DNA and progress through the cell cycle; mouse NASP$^{-/-}$ null mutation is lethal due to failure in cell proliferation. NASP also seems to play a role in neuronal survival. *In vitro* studies of induced neuronal hypoxia have revealed that NASP is downregulated (Jin et al., 2004a; Jin et al., 2004b).

Nhbr91 is expressed in the primitive streak and prospective neural plate at stage 4 (**Fig 4.6 A-B**). At stage 6, expression continues to be detected in the primitive streak and head process and clears from the centre of the neural plate, forming a horseshoe shape including the border of the neural plate (**Fig 4.6 C**).

Nhbr111 (Similar to hypothetical protein INO80 subunit B)

INO80 belongs to the SWI/SNF family of chromatin-remodelling complex proteins (Peterson et al., 1994) with orthologues and homologues identified in yeast (Kobor et al., 2004; Krogan et al., 2003; Mizuguchi et al., 2004; Shen et al., 2000), *Drosophila* (Klymenko et al., 2006; Kusch et al., 2004), plants (Deal et al., 2007; Fritsch et al., 2004) and mammals (Ikura et al., 2000; Jin et al., 2005; Ruhl et al., 2006), where INO80 has been shown to regulate gene expression directly (Cai et al., 2007; Deal et al., 2007; Fritsch et al., 2004; Klymenko et al., 2006; Mizuguchi et al., 2004; Shen et al., 2000; Shimada et al., 2008; Wong

et al., 2007). Recent studies have also implicated INO80 in many other essential processes, including DNA repair (Fritsch et al., 2004; Kawashima et al., 2007; Morrison et al., 2004; van Attikum et al., 2007; Wu et al., 2007), checkpoint regulation (Morrison et al., 2007; Papamichos-Chronakis et al., 2006) DNA replication (Papamichos-Chronakis et al., 2006; Shimada et al., 2008; Vincent et al., 2008), telomere maintenance (Collins et al., 2007; Yu et al., 2007) and chromosome segregation (Ben-Aroya et al., 2008; Krogan et al., 2004; Measday et al., 2005; Morrison et al., 2004). There are no reported studies directly implicating INO80 in embryonic development.

At stage 3, *nhbr11*1 expression is detected in the entire *area pellucida* (**Fig 4.7 A**), becoming more restricted to the neural plate as the embryos reach stage 4 (**Fig. 4.7 B**). Although expression is quite widespread up to stage 7, later stages reveal a sharp expression in the neural plate and in extraembryonic blood islands (**Fig 4.7 D**).

Nhbr121 (Similar to Integrator Complex subunit 3)

The Integrator Complex participates in the maintenance of genomic stability (Huang et al., 2009; Richard et al., 2008) and participates in the cellular DNA damage response (Skaar et al., 2009; Zhang et al., 2009). Specifically, INTS3 is a subunit of single-stranded DNA (ssDNA)-binding complexes involved in the maintenance of genome stability (Huang et al., 2009). INTS3 is also reported to associate with the C-terminal domain of RNA polymerase II large subunit and mediates 3′ end processing of small nuclear RNAs (Baillat et al., 2005). There are no reports on expression or roles of INTS3 during embryonic development and its existence in the chick is only predicted on the basis of genomic analyses.

Nhbr121 is expressed in the stage 4 node and prospective neural plate (**Fig 4.8 A**). By stage 4^{+}, expression in the node becomes stronger while clearing in the prospective neural plate surrounding the node (**Fig 4.8 B**). As development proceeds, expression is maintained in the node, asymmetrically at stage 6 with strong expression on the right side. Expression is also strong in the head process and in the "mesoderm wings" (**Fig 4.8 C**). At stage 8^{-} (**Fig 4.8 D**) expression appears to be in the neural plate and in the node.

Nhbr225 (Similar to peptidyl-propyl isomerase G; Cyclophilin G)

Peptidyl-propyl isomerases, also known as Cyclophilins, were first identified as the host cell receptors for the potent immunossupressive drug cyclosporin A and described as being ubiquitously distributed (Bukrinsky, 2002). They have also been shown to possess

peptidyl-prolyl *cis–trans* isomerase activity (Bukrinsky, 2002), which is thought to contribute to the proposed role of cyclophilins as mediators of protein folding and as chaperones (Ivery, 2000). Although most studies to date have focused on intracellular activities of cyclophilins, accumulating evidence suggests a role for these proteins as mediators of intercellular communication (Allain et al., 2002; Brazin et al., 2002; Carpentier et al., 2002; Gothel and Marahiel, 1999; Nagata et al., 2000; Sherry et al., 1992; Xu et al., 1992). There is no information on the role of these molecules during embryonic development.

Nhbr225 transcripts are detected at stage 3 in the primitive streak and the prospective neural plate (**Fig 4.9 A**). By stage 4^{+} the expression in the primitive streak seems to have disappeared or is extremely weak. Expression is present in the node and emerging head process (**Fig 4.9 B**). At stage 7 the mRNA marks the entire neural plate, albeit stronger in the anterior part of the embryo (**Fig 4.9 C**). At stage 8^{-} expression remains in the neural plate, although it seems to clear away from the area surrounding the remaining primitive streak, that, together with the node, seem to express the transcript by this stage (**Fig 4.9 D**). In embryos at stage 11, expression is mainly present in the neural tube and anteriorly in the brain region (**Fig 4.9 E**); in the extraembryonic region at the same developmental stage, the blood islands are strongly stained (**Fig 4.9 F**).

Nhbr231 (E3 ubiquitin protein ligase)

Targeting proteins to degradation is an essential mechanism to ensure normal cellular function and the ubiquitination-dependent degradation of proteins involves the sequential activity of at least three types of enzymes: E1 ubiquitin-activating enzyme, E2 ubiquitin-carrier enzyme and E3 ubiquitin-protein ligase (You and Pickart, 2001). E3 ubiquitin ligases are responsible for the specificity of ubiquitin-mediated degradation, determining which target proteins are degraded and how efficiently that process is carried out (Pickart, 2001). The regulation of E3 ligases and, therefore, the efficiency of degradation of their target proteins can take place by several means. E3 ligases can be regulated by abundance, and in some instances autoubiquitination and degradation have been implicated in the regulation of these proteins (Canning et al., 2004; Wu et al., 2004). In addition, post-translational modifications such as phosphorylation, ubiquitination and modification by ubiquitin-like proteins have been demonstrated to play central roles in the regulation of E3 ligases (Hotton and Callis, 2008; Meek and Hupp; Moon et al., 2004; Parry and Estelle, 2004; Snyder, 2009; Xu et al., 2009). Malfunction and/or dysregulation of E3 ligase function has been implicated in various neurodegenerative disorders and in

cancer (Aplin et al., 2006; Boulton, 2006; Carnevale et al., 2007; Chen et al., 2006; Dawson, 2006; Morris et al.; Polanowska et al., 2006). Interestingly, in the context of embryonic neural development, the E3 ubiquitin protein ligase seems to be responsible for Notch ubiquitination and degradation (Lai, 2002).

Stage 4 embryos express *nhbr231* in the prospective neural plate, stronger at the edge (**Fig 4.10 A**). At stage 4^{+}, expression continues to clear away from the central region of the neural plate, resulting in a horseshoe shaped expression domain (**Fig 4.10 B**). At stage 7^{-}, expression is completely abolished in the midline and is strong in the anterior neural plate and mesoderm (**Fig 4.10 C**). By stage 12, *nhbr231* transcripts are strongly localized in the brain and anterior neural tube. Expression is also strong in the blood islands (**Fig 4.10 D**).

Nhbr241 (HT7 antigen; Homo sapiens CD147/basigin)

The HT7 antigen was first isolated in 1986 (Risau et al., 1986a; Risau et al., 1986b) as a highly glysosylated protein. The authors reported its expression in mouse as starting at E10 in endothelial cells of the brain capillaries, which form the blood-brain barrier. Additional expression is seen in erythroblasts and epithelial cells of kidney tubules, choroid plexus and retinal pigment layer (Albrecht et al., 1990; Risau et al., 1986a) and suggests that the HT7 protein may participate in transport processes in these cells. Another possible function of the HT7 protein may be in cell adhesion. Cultured brain endothelial cells have the antigen concentrated in areas of cell-cell contact (Albrecht et al., 1990; Seulberger et al., 1990). Further evidence supporting this stems from the fact that HT7 antigen shares homology with the cell adhesion molecules N-CAM (Cunningham et al., 1987), ICAM-2 (Staunton et al., 1989) and carcinoembryonic antigen CEA (Benchimol et al., 1989), all of which are members of the immunoglobulin superfamily. CD147/basigin is a transmembrane protein belonging to the immunoglobulin superfamily (Biswas, 1982; Biswas et al., 1982). It is strongly related to cancer progression and highly expressed by various cancer cells including malignant melanoma cells, playing important roles in tumor invasiveness, metastasis, cellular proliferation, and in vascular endothelial growth factor production, tumour cell glycolysis, and multi-drug resistance (Kanekura and Chen; Li et al.; Lu et al.). Whilst increased expression of CD147 occurs in many tumors, its expression is not confined to tumor cells (Bordador et al., 2000; Muraoka et al., 1993; Polette et al., 1997; Sameshima et al., 2000) and it plays a critical role in fetal development and retinal function. CD147 has also been shown to play

a role in thymic T cell development and nervous system development (Muramatsu and Miyauchi, 2003) and is involved in spatial learning (Naruhashi et al., 1997) and Alzheimer's amyloid plaque formation (Zhou et al., 2005; Zhou et al., 2007).

At stage 3 expression of *nhbr241* is very weak but starts to be detected in the primitive streak (**Fig 4.11 A**). By stage 4, expression becomes strong in the primitive streak, node and the entire embryonic region (**Fig 4.11 B**). At stage 4+ the node and primitive streak expression are very strong; transcripts are also strongly detected in the prospective neural plate (**Fig 4.11 C**). By stage 6 the expression becomes very weak again and seems to be mainly detected in the neural plate (**Fig 4.11 D**).

Nhbr251 (Similar to nociceptin-like receptor; *Homo sapiens* opiate receptor-like 1, OPRL1)

Nociceptin was first identified in 1995 as orphanin FQ/nociceptin (OFQ/N), a 17aminoacid peptide and the ligand for the "orphan" opioid receptor ORC-1 (Boom et al., 1999; Gouarderes et al., 1999). Nociceptin is present throughout the central nervous system, from the forebrain to the spinal cord (Neal et al., 1999a; Neal et al., 1999b). In terms of its function, it seems to act in a manner similar to that of opioid agonists by inhibiting adenylate cyclase and calcium currents and hyperpolarizing neurons by opening calcium channels (Moran et al., 2000). In the vast literature available, there are no reports on nociceptin distribution during embryonic development and all the functional studies explore its role in neural physiology rather than neural differentiation or induction. OPRL1 encodes a G protein-coupled receptor and all the published data results from studies done in either rats or humans and always in relation to substance abuse and addiction (Briant et al.; Homberg et al., 2009; Kuzmin et al., 2009; Rutten et al.; Rutten et al.; Xuei et al., 2008).

Nhbr251 is expressed at stage 3+ in the entire embryonic region and strongly in the primitive streak and node (**Fig 4.12 A**). By stage 6 transcripts start to become restricted to the neural plate; stronger expression is observed in the head process and the sides of the primitive streak (**Fig 4.12 B**). Expression at stage 7 remains strong in the primitive streak and notochord; transcripts are also detected in the neural plate and posterior mesoderm (**Fig 4.12 C**). Stage 9 embryos reveal the presence of *nhbr251* in the head, particularly in the head folds, the closing neural tube, posterior neural plate and in the remaining streak;

a strong patch of expression is present on the right side of the extraembryonic *area opaca* (**Fig 4.12 D**).

Nhbr260 (No similarity)

At stage 3, *nhbr260* mRNA localizes strongly to the primitive streak and, more weakly, to the epiblast (**Fig 4.13 A**). At stage 4, expression remains similar and includes the node (**Fig 4.13 B**). Expression at stage 4^+ is strong in the lateral sides of the primitive streak and node and in the mesoderm (**Fig 4.13 C**). Stage 8^+ embryos present the transcript in the entire neural plate, stronger at the border, and in the posterior mesoderm. Some expression starts to be detected in what seem to be blood islands (**Fig 4.13 D**).

Nhbr307: Similar to calreticulin

Calreticulin, a highly conserved eukaryotic protein, is localized primarily to the endoplasmic reticulum (ER), but has also been reported to occur in many other locations, including the nucleus, the nuclear envelope, the cytosol and the outer surface of the plasma membrane (Michalak et al., 1991; Rauch et al., 2000). Initially it was identified as a high-affinity calcium-binding protein (Ostwald and MacLennan, 1974) and as an ER calcium storage molecule (Baksh et al., 1992). In the last few years, Calreticulin has become recognised as a multifunctional protein, which can act with a large number of proteins and is involved in a wide variety of different processes (Michalak et al., 1992), including regulation of steroid-dependent gene expression, regulation of integrin activity and interaction with extracelluar matrix proteins (White et al., 1995). During development, it has been shown that Calreticulin is essential for cardiac development (Mesaeli et al., 1999); mice mutant for calreticulin have heart, brain and body wall defects (Rauch et al., 2000).

Nhbr307 transcripts are detected at very low levels throughout the embryonic and non embryonic regions at stage $3/3^+$ (**Fig 4.14 A**). Expression becomes localized at stage 4, weakly in the neural plate and very strong in the primitive streak and node (**Fig 4.14 B**). By stage 4^+ the expression in the primitive streak seems to be downregulated (**Fig 4.14 C**). For the later developmental stages analysed, *nhbr307* seems to maintain its expression restricted to neural structures, the neural plate and neural tube, and somites (**Fig 4.14 D-F**). From stage $9^+/10$ the expression becomes ubiquitous (not shown).

Nhbr313 (*Homo sapiens* AF4/FMR2 family, member1; AFF1)

AF4 is a cofactor of RNA polymerase II elongation and chromatin remodelling (Bitoun et al., 2007) and several studies have linked AF4 to infant leukemia (Bach et al., 2009; Mueller et al., 2009; Vogel and Gruss, 2009). In the mouse mutant, Purkinje cells start to degenerate soon after birth, leading to impaired motor coordination at 5 weeks. Progressive cell death occurs from week 8, affecting most severely the anterior lobes of the cerebellum. The mutant further displays general growth retardation, defects in T-cell maturation and cataract (Isaacs et al., 2003).

Stage 3^{+}-4 embryos express *nhbr313* weakly throughout the embryonic region and strongly in the primitive streak and node (**Fig 4.15 A** and **B**). At stage 5 expression is difficult to detect but can be seen in the primitive streak and in the anterior neural plate (**Fig. 4.15 C**). By stage 7 the expression becomes more defined and clearly localizes to the neural plate and the remaining streak (**Fig 4.15 D**).

Nhbr330 (Polyvirus receptor-related 1, isoform 2; nectin)

Nectins are Ca^{2+}-independent immunoglobulin (Ig)-like cell-cell adhesion molecules. Structurally they are transmembrane proteins with an extracellular region with three Ig-like loops, a single transmembrane region and a cytoplasmic tail region (Takahashi et al., 1999). Nectins contribute to the formation of a variety of cell-cell junctions, acting cooperatively with, or independently of, cadherins. In addition, nectins interact with nectin-like molecules (Necls), playing an important role cell adhesion, migration, and proliferation (Irie et al., 2004; Sakisaka and Takai, 2004). Nectins and Necls can also function as viral receptors and have been associated with human diseases (including cancer) when mutated or upregulated (Sakisaka and Takai, 2004). Nectins also play a role in intracellular signalling. They induce the activation of Cdc42 and Rac small G proteins through c-Src, which in turn regulates the formation of the cadherin-based adherens junctions through reorganization of the actin cytoskeleton (Izumi et al., 2004), gene expression through activation of a mitogen-activated protein cascade and cell polarization through cell polarity proteins (Shimizu and Takai, 2003; Takai et al., 2003).

At stage 4, expression is detected in the posterior two thirds of the primitive streak and some weak expression may be seen in the epiblast (**Fig 4.16 A**). At stage 4^{+}, *nhbr330* transcript is completely absent from the node but is otherwise strongly detected in the rest of the embryo (**Fig 4.16 B**). By stage 5 expression starts to become restricted to the neural plate, with the node and head process clear of transcript (**Fig 4.16 C**). At stage 8,

expression is present in the entire neural plate, being stronger at the anterior border (**Fig 4.16 D**).

Nhbw23 (Similar to receptor protein tyrosine phosphatase LAR)

Receptor tyrosine phosphatases have been implicated in the regulation of axonal growth, promoting neurite outgrowth (Yang et al., 2003) and guiding vertebrate motor axons during development (Carulli et al., 2005). In the *Drosophila* compound eye, LAR is required for the proper connections between different photoreceptor neurons and their specific targets in the optic nerve (Clandinin et al., 2001). Similarly, in *Xenopus*, protein tyrosine phosphatases regulate retinal ganglion cell axon outgrowth in the developing visual system (Johnson et al., 2001). Frydman and colleagues (Frydman and Spradling, 2001) have found that LAR is required for both epithelial planar polarity and for axis determination within the ovarian follicles in *Drosophila*.

Nhbw23 is expressed in the prospective neural plate and is absent from the node (**Fig 4.17 A**). Expression remains mostly restricted to the neural plate from stage 4^+ (**Fig 4.17 B**) to stage 7^+ (**Fig 4.17 C**).

Nhbw 57 (Chemokine, C-X-C motif, ligand 1)

CXC chemokines are heparin-binding proteins that display pleiotropic effects in immunity, regulating angiogenesis, and mediating organ-specific metastases of cancer (Strieter et al., 2005). The family has four highly conserved cysteine amino acid residues, with the first two cysteines separated by a non-conserved amino acid residue. A second structural domain dictates their functional activity. The NH2-terminus of several CXC chemokines contains three amino acid residues (Glu-Leu-Arg; 'ELR' motif), which immediately precedes the first cysteine amino acid residue (Belperio et al., 2000; Luster et al., 1998; Poppas et al., 1998; Strieter et al., 1995a; Strieter et al., 1995b). While the CXC chemokines with the 'ELR' motif (ELR^+) promote angiogenesis, the CXC chemokines that lack the ELR motif (ELR^-) inhibit angiogenesis (Strieter et al., 1995a).

Before gastrulation, at stage XIII, transcripts are present in the entire epiblast (**Fig 4.18 A**). Stage 3^+ embryos present expression in the entire epiblast, the node and primitive streak (**Fig 4.18 B**). By stage 4^+ expression starts to become restricted to the prospective neural plate (**Fig 4.18 C**). In stage 6 embryos expression detected in the neural plate and in the forming notochord (**Fig 4.18 D**). Later, at stage 10, expression is strongly localized to the brain and closing neural tube and in the blood islands (**Fig 4.18 E**).

Nhbw87 (Calnexin)

Calnexin is a conserved, abundant integral membrane phosphoprotein of the endoplasmic reticulum (ER) of eukaryotic cells, where it plays a important role in glycoprotein folding (Chevet et al., 2009) Immediately after sequencing the cDNA of Calnexin, it was recognized as a paralogue of Calreticulin (Wada et al., 1991). Similarly to Calreticulin, Calnexin recognizes the protein-folding status of client glycoproteins via their glycans (Michalak et al., 2009). The ER quality control machinery enables the retention of misfolded proteins within the ER lumen (Hebert and Molinari, 2007). While correctly folded glycoproteins transit the calnexin cycle relatively quickly, misfolded glycoproteins have a prolonged association with constituents of the calnexin cycle and subsequently, are targeted to the ER-associated degradation pathway for degradation by the proteasome (Helenius and Aebi, 2004; Pearse and Hebert; Schrag et al., 2003).

It proved extremely difficult to produce clear *in situ* staining for *nhbw87*. It seems that by stage 3 there is some weak expression in the epiblast (**Fig 4.19 A**). Stage 7 embryos present expression in the neural plate, stronger in the head region (**Fig 4.19 B**). By stage 9, expression remains stronger in the head and in the neural tube and some expression remains in other parts of the neural plate (**Fig 4.19 C**).

Nhbw95 (CD151)

CD151 was first cloned in 1995 (Fitter et al., 1995) as a member of the tetraspanin superfamily (transmembrane 4 super family) of proteins. Tetraspanins form membrane complexes with integrin receptors and are implicated in integrin-mediated cell migration (Berditchevski and Odintsova, 1999; Sugiura and Berditchevski, 1999). In addition to cell motility, it seems that tetraspanins are involved in cell adhesion and metastasis as well as cell activation and signal transduction (Maecker et al., 1997). Immunohistochemical performed in adult human tissue specimens have demonstrated that CD151 is expressed in the epithelium, muscle and Schwann cells (Sincock et al., 1997). Within haematopoietic cells, CD151 is seems to be restricted to platelets and megakaryocytes, where it may be involved in recognition of the subendothelial matrix during thrombus formation and in trombopoiesis, respectively (Sincock et al., 1997). In cultured human umbilical vein endothelial cells CD151 is present on the plasma membrane and predominantly localises to regions of cell-cell contact (Sincock et al., 1999). Anti-CD151 monoclonal antibody inhibits endothelial cell migration and modulates in vitro angiogenesis. CD151 associates with several integrins both on the plasma membrane and within intracellular vesicles,

suggesting a possible role in regulating integrin trafficking and/or function (Fitter et al., 1999; Maecker et al., 1997; Sincock et al., 1999).

Nhbw95 seems to be almost ubiquitous. However, it is absent from the *area pellucida* up to stage 3^+ (**Fig 4.20 A**) and is more strongly expressed in the neural plate at stage 6 (**Fig 4.20 C**). Stage 9 embryos present a distinct expression in the head, edge of the neural tube and the remnants of the streak in the posterior part of the embryo (**Fig 4.20 D**).

Discussion

Advantages and Limitations of the Screen

The YSST and conventional protein secretion

Most eukaryotic secreted proteins (or those membrane bound) contain amino-terminal or internal signal peptides that direct their sorting to the endoplasmic reticulum (ER). From the ER, proteins are transported to the extracellular space or the plasma membrane through the ER-Golgi secretory pathway (Lee et al., 2004a; Osborne et al., 2005).

The Yeast Signal Sequence Trap (YSST) is a genetic method developed to isolate and identify secreted proteins. The YSST uses a strain of *Saccharomyces cerevisiae* with a genomic deletion at the SCU2 locus (Klein et al., 1996); the SUC2-deficient yeast strain does not secrete invertase and, therefore, is unable to grow on sucrose or raffinose as the sole carbon source. The second component of the YSST is a vector with a SUC2 gene lacking the signal sequence and the start codon. Only if a partial cDNA provides these sequence elements is the fusion protein translocated into the secretion pathway. All transformants carrying a secretion signal should be able to grow on sucrose or raffinose as their only source of carbon (Jacobs et al., 1997).

The major advantage of performing a genetic screen in yeast, particularly the YSST, is that it is a rapid and relatively simple method for isolating large numbers of cDNAs putatively encoding for secreted proteins. However, the screen also has two major limitations. First, it can yield false positives and second, it does not always identify known secreted molecules that should be present in the library.

Among the sequences isolated, and after removing ribosomal and mitochondrial sequences, 34 (24.8%) were false positives, i.e., clones coding for proteins known, or predicted, not to be secreted. These false positives could contain sequences that mimic a signal peptide. Kaiser and colleagues (Kaiser et al., 1987) have shown that amongst a large population of sequences, about 20% can work as signal sequences in yeast if an initiating methionine is provided and that many random sequences can functionally replace the secretion signal sequence of yeast invertase.

It was expected from this screen that we would obtain some clones encoding well characterized molecules known to be expressed in the node at the developmental stage the RNA was extracted for the screen. *Chordin*, for example, is abundantly expressed in

the chick node at stage 3^+ (Streit et al., 1998) and is a secreted protein (Piccolo et al., 1996; Sasai et al., 1994). Several hypothesis can be put forward as why *chordin* was not obtained. One possibility is that some cDNAs may not fuse appropriately in frame with the invertase and are therefore not selected. It could also be caused by failure of the yeast translational machinery to initiate for some heterologous mRNA sequences. In fact, it has been shown that some signal sequences, namely in human proteins, are not active in the yeast secretion machinery (Born et al., 1987).

Non-conventional protein secretion

Most eukaryotic secreted proteins are transported to the extracellular space or the plasma membrane through the ER-Golgi secretory pathway (Disatnik et al., 2004; Lee et al., 2004a; Osborne et al., 2005). Even though this ER-Golgi secretory pathway is very efficient and is generally considered the most common mode of protein transport to the cell surface (Trombetta and Parodi, 2003), cytoplasmic, nuclear and even signal peptide containing proteins have been shown to reach the cell surface by non-conventional transport pathways – unconventional protein secretion (Nickel and Seedorf, 2008). Two distinct mechanisms seem to exist. In one, proteins with a signal sequence reach the ER but are exported to the cell surface bypassing the Golgi apparatus. Examples of this are the heat shock protein 150 (HSP150) (Fatal et al., 2004), the cystic fibrosis transmenbrane conductance regulator (CFTR) (Yoo et al., 2002), the protein-tyrosine phosphatase CD45 (Baldwin and Ostergaard, 2002) and the Drosophila melanogaster α integrin subunit (Juschke et al., 2005). The second nonconventional mechanism of protein secretion includes cytoplasmic and nuclear proteins that lack a signal peptide and exit the cell through a mechanism independent from both the ER and the Golgi. In this category, and relevant to developmental processes, are fibroblast growth factor2 (FGF2) (Engling et al., 2002; Florkiewicz et al., 1995; Nickel, 2003; Schafer et al., 2004), β-galactosidase-specific lectins (Nickel, 2003), certain members of the interleukin family (Muesch et al., 1990; Rubartelli et al., 1990) and engrailed homeoprotein (Dupont et al., 2007; Joliot et al., 1998; Maizel et al., 2002), amongst others. The study of unconventional protein secretion is still in its early days and the transport of these proteins is triggered by unconventional means and through mechanisms still very poorly understood.

It is conceivable that the presence of false positives, i.e., proteins lacking a signal sequence and that were selected in the screen belong to the category of proteins secreted through a mechanism of unconventional protein secretion. In fact, it has been suggested (Lee et al., 2006; Monteoliva et al., 2002) that the YSST is able to retrieve proteins secreted

through alternative secretion processes that are not based on the canonical secretion-signal peptide (Nombela et al., 2006).

The next three chapters deal with the cloning, molecular characterization and functional analyses of *nhbr34*, *nhbr90* and *nhbr307*. The main selection criteria were, first, their spatiotemporal expression: all three clones are expressed quite strongly in the organizer at stage $3^{+}/4$ and produce clear expression patterns. Second, their molecular nature: *nhbr34*, homologue to *Fibulin2* was never studied in connection with neural induction; *nhbr307*, homologue to *Calreticulin,* coding for a calcium binding protein, seemed particularly interesting, given the possible implications of calcium in neural induction (Leclerc et al., 1997; Leclerc and Duprat, 1995; Leclerc et al., 1999; Leclerc et al., 2003; Leclerc et al., 2001; Leclerc et al., 2000; Leclerc et al., 2008; Lee et al., 2009; Moreau et al., 1994; Moreau et al., 2008); *nhbr90* for being a completely novel and unusual sequence and, therefore, posing a great challenge.

Table 4.1. *Nhbr* sequences and their homologies in Human (*Homo sapiens*) and in the Chick (*Gallus gallus*).

Original ID	Accession ID	Gene Symbol (*H sapiens*)	Description (*Homo sapiens*)	Gene Symbol (*G gallus*)	Description (*Gallus gallus*)	SP
NHBR10	CR385946	ELOVL5	Homo sapiens ELOVL family member 5, elongation of long chain fatty acids	N/A	Similar to CR385946, "Gallus gallus finished cDNA, clone ChEST154e23", score 232, e-value 5e-58	Y
NHBR111	AJ719645	N/A	Homo sapiens INO80 complex subunit B (INO80B)	INO80B	Similar to AJ719645, "Gallus gallus mRNA for hypothetical protein, clone 4o13", score 199, e-value 5e-48	Y
NHBR116	CR385946	ELOVL5	Homo sapiens ELOVL family member 5, elongation of long chain fatty acids	N/A	Similar to CR385946, "Gallus gallus finished cDNA, clone ChEST154e23", score 189, e-value 7e-45	Y
NHBR117	CR385946	ELOVL5	Homo sapiens ELOVL family member 5, elongation of long chain fatty acids	N/A	Similar to CR385946, "Gallus gallus finished cDNA, clone ChEST154e23", score 308, e-value 2e-80	Y
NHBR121	XM_428600	INTS3	Homo sapiens integrator complex subunit 3 (INTS3)	Ints3	Similar to XM_428600, "PREDICTED: Gallus gallus similar to Ints3 protein (LOC431048), mRNA", score 175, e-value 1e-40	N
NHBR125	CR338931	N/A	N/A	N/A	Similar to CR338931, "Gallus gallus finished cDNA, clone ChEST980a3", score 341, e-value 1e-90	Y
NHBR130	X07352	CHRNA4	Homo sapiens cholinergic receptor, nicotinic, alpha 4 (CHRNA4)	CHRNA4	Similar to X07352, "Chicken nicotinic acetylcholine receptor alpha4 gene exon 5", score 260, e-value 2e-66	Y
NHBR132	CR385946	ELOVL5	Homo sapiens ELOVL family member 5, elongation of long chain fatty acids	N/A	Similar to CR385946, "Gallus gallus finished cDNA, clone ChEST154e23", score 123, e-value 5e-25	Y
NHBR133	AC192754	N/A	N/A	N/A	Similar to AC192754, "Gallus gallus BAC clone CH261-87N12 from chromosome z, complete sequence", score 119, e-value 7e-24	N
NHBR135	CR385946	ELOVL5	Homo sapiens ELOVL family member 5, elongation of long chain fatty acids	N/A	Similar to CR385946, "Gallus gallus finished cDNA, clone ChEST154e23", score 211, e-value 2e-51	Y
NHBR137	NM_001012847	ELL	Homo sapiens elongation factor RNA polymerase II (ELL)	ELL	Similar to NM_001012847, "Gallus gallus elongation factor RNA polymerase II (ELL), mRNA >gi|53128621|emb|AJ719659.1| Gallus gallus mRNA for hypothetical protein, clone 5a13", score 266, e-value 4e-68	N
NHBR140	XR_026835	N/A	N/A	LOC422070	Similar to XR_026835, "PREDICTED: Gallus gallus hypothetical LOC422070 (LOC422070), mRNA", score 66, e-value 1e-07	Y
NHBR148	XM_426204	ELOVL5	Homo sapiens ELOVL family member 5, elongation of long chain fatty acids	ELOVL5	Similar to XM_426204, "PREDICTED: Gallus gallus similar to Elongation of very long chain fatty acids (FEN1/Elo2, SUR4/Elo3, yeast)-like 2 (LOC428646), mRNA", score 115, e-value 1e-22	Y
NHBR149	XM_417693	ARID1A	Homo sapiens AT rich interactive domain 1A (SWI-like) (ARID1A)	ARID1A	Similar to XM_417693, "PREDICTED: Gallus gallus similar to AT rich interactive domain 1A (LOC419542), partial mRNA", score 476, e-value 8e-131	Y
NHBR151	NM_001030757	N/A	N/A	ST13	Similar to NM_001030757, "Gallus gallus suppression of tumorigenicity 13 (colon carcinoma) (Hsp70 interacting protein) (ST13), mRNA >gi|53130128|emb|AJ719784.1| Gallus gallus mRNA for hypothetical protein, clone 6h13", score 345, e-value 7e-92	N
NHBR152	XR_027128	N/A	N/A	NXN	Similar to XR_027128, "PREDICTED: Gallus gallus similar to red-1 (LOC417619), mRNA", score 678, e-value 8e-192	N
NHBR166	XM_001231865	N/A	N/A	FBXO5	Similar to XM_001231865, "PREDICTED: Gallus gallus similar to F-box protein 5, transcript variant 1 (LOC421642), mRNA", score 397, e-value 3e-107	Y
NHBR17	CR385946	ELOVL5	Homo sapiens ELOVL family member 5, elongation of long chain fatty acids	ELOVL5	Similar to CR385946, "Gallus gallus finished cDNA, clone ChEST154e23", score 373, e-value 4e-100	Y
NHBR174	CR406504	N/A	N/A	CR406504	Similar to CR406504, "Gallus gallus finished cDNA, clone ChEST735g14", score 106, e-value 1e-19	Y
NHBR179	AC009104	N/A	N/A	N/A	Weakly similar to AC009104, "Homo sapiens chromosome 16 clone RP11-44L9, complete sequence", score 48, e-value 0.041	N

NHBR193	AC186532	N/A	N/A	AC186532	Similar to AC186532, "Gallus gallus BAC clone CH261-169B23 from chromosome z, complete sequence", score 74, e-value 7e-10	N
NHBR198	NM_205518	ACTB	Homo sapiens actin, beta (ACTB)	ACTB	Similar to NM_205518, "Gallus gallus actin, beta (ACTB), mRNA >gi|211236|gb|L08165.1|CHKBACTN Gallus gallus beta-actin mRNA, complete cds", score 373, e-value 6e-100	N
NHBR20	CR385365	RPL7A	Homo sapiens ribosomal protein L7a (RPL7A)	CR385365	Similar to CR385365, "Gallus gallus finished cDNA, clone ChEST418c10", score 827, e-value 2e-236	Y
NHBR219	NM_001031294	GPR177	Homo sapiens G protein-coupled receptor 177 (GPR177)	GPR177	Similar to NM_001031294, "Gallus gallus G protein-coupled receptor 177 (GPR177), mRNA >gi|53128766|emb|AJ719673.1| Gallus gallus mRNA for hypothetical protein, clone 5c7", score 502, e-value 7e-139	Y
NHBR22	NM_205518	ACTB	Homo sapiens actin, beta (ACTB)	ACTB	Similar to NM_205518, "Gallus gallus actin, beta (ACTB), mRNA >gi|211236|gb|L08165.1|CHKBACTN Gallus gallus beta-actin mRNA, complete cds", score 219, e-value 6e-54	N
NHBR225	XM_422008	PPIG	Homo sapiens peptidylprolyl isomerase G (cyclophilin G) (PPIG)	PPIG	Similar to XM_422008, "PREDICTED: Gallus gallus peptidylprolyl isomerase G (cyclophilin G) (PPIG), mRNA", score 752, e-value 8e-214	Y
NHBR231	BC037687	UBR5	Homo sapiens ubiquitin protein ligase E3 component n-recognin 5 (UBR5)	N/A	Similar to BC037687, "Mus musculus E3 ubiquitin protein ligase, HECT domain containing, 1, mRNA (cDNA clone IMAGE:3666455), containing frame-shift errors", score 334, e-value 2e-88	N
NHBR234	BX934171	C10orf119	Homo sapiens chromosome 10 open reading frame 119 (C10orf119)	BX934171	Similar to BX934171, "Gallus gallus finished cDNA, clone ChEST444n21", score 647, e-value 3e-182	Y
NHBR237	XM_416595	TTF2	Homo sapiens transcription termination factor, RNA polymerase II (TTF2)	TTF2	Similar to XM_416595, "PREDICTED: Gallus gallus similar to MGC81081 protein (LOC418376), mRNA", score 817, e-value 1e-233	Y
NHBR241	X52751	BSG	Homo sapiens basigin (Ok blood group) (BSG)	BSG	Similar to X52751, "Chicken mRNA for HT7 antigen", score 288, e-value 1e-74	Y
NHBR243	XM_418237	UPF1	Homo sapiens UPF1 regulator of nonsense transcripts homolog (yeast) (UPF1)	UPF1	Similar to XM_418237, "PREDICTED: Gallus gallus UPF1 regulator of nonsense transcripts homolog (yeast) (UPF1), mRNA", score 726, e-value 4e-206	N
NHBR249	BX950486	PVRL3	Homo sapiens poliovirus receptor-related 3 (PVRL3)	PVRL3	Similar to BX950486, "Gallus gallus finished cDNA, clone ChEST539i24", score 141, e-value 3e-30	Y
NHBR251	XM_417424	OPRL1	Homo sapiens opiate receptor-like 1 (OPRL1)	OPRL1	Similar to XM_417424, "PREDICTED: Gallus gallus similar to ORL1-like opioid receptor (LOC419251), mRNA", score 496, e-value 4e-137	Y
NHBR259	N/A	N/A	N/A	N/A	-(not annotated)-	Y
NHBR260	N/A	N/A	N/A	N/A	-(not annotated)-	Y
NHBR267	NM_205518	ACTB	Homo sapiens actin, beta (ACTB)	ACTB	Similar to NM_205518, "Gallus gallus actin, beta (ACTB), mRNA >gi|211236|gb|L08165.1|CHKBACTN Gallus gallus beta-actin mRNA, complete cds", score 653, e-value 4e-184	N
NHBR271	CR386508	N/A	N/A	N/A	Similar to CR386508, "Gallus gallus finished cDNA, clone ChEST649o12", score 264, e-value 3e-67	Y
NHBR276	CR390811	UBE2E1	Homo sapiens ubiquitin-conjugating enzyme E2E 1 (UBC4/5 homolog, Yeast) (UBE2E1)	CR390811	Similar to CR390811, "Gallus gallus finished cDNA, clone ChEST460n14", score 207, e-value 3e-50	Y
NHBR279	XM_414529	N/A	N/A	STK10	Similar to XM_414529, "PREDICTED: Gallus gallus similar to protein kinase (LOC416204), mRNA", score 441, e-value 2e-120	Y
NHBR28	AF195629	LOC100288871	Homo sapiens similar to cytochrome b (LOC100288871)	AF195629	Similar to AF195629, "Gallus gallus haplotype C cytochrome b gene, complete cds; mitochondrial gene for mitochondrial product", score 756, e-value 5e-215	Y
NHBR282		N/A	N/A	N/A	-(not annotated)-	Y
NHBR285	NM_001048076	VIM	Homo sapiens vimentin (VIM)	VIM	Similar to NM_001048076, "Gallus gallus vimentin (VIM), mRNA", score 234, e-value 2e-58	Y
NHBR29	CR385946	ELOVL5	Homo sapiens ELOVL family member 5, elongation of long chain fatty acids	ELOVL5	Similar to CR385946, "Gallus gallus finished cDNA, clone ChEST154e23", score 205, e-value 1e-49	Y

NHBR290	NM_001006420	NRBP1	Homo sapiens nuclear receptor binding protein 1 (NRBP1)	NRBP1	Similar to NM_001006420, "Gallus gallus nuclear receptor binding protein 1 (NRBP1), mRNA >gi|53136891|emb|AJ721116.1| Gallus gallus mRNA for hypothetical protein, clone 35j18", score 669, e-value 7e-189	N
NHBR298	CR389017	MEX3D	Homo sapiens mex-3 homolog D (C. elegans) (MEX3D)	CR389017	Similar to CR389017, "Gallus gallus finished cDNA, clone ChEST343d14", score 292, e-value 1e-75	Y
NHBR299	NM_001030620	CANX	Homo sapiens calnexin (CANX)	CANX	Similar to NM_001030620, "Gallus gallus calnexin (CANX), mRNA >gi|53127409|emb|AJ719429.1| Gallus gallus mRNA for hypothetical protein, clone 2d15", score 791, e-value 1e-225	Y
NHBR30	XM_415665	ZNF207	Homo sapiens zinc finger protein 207 (ZNF207)	ZNF207	Similar to XM_415665, "PREDICTED: Gallus gallus zinc finger protein 207 (ZNF207), mRNA", score 385, e-value 8e-104	N
NHBR307	NM_001006495	CALR	Homo sapiens calreticulin (CALR)	CALR	Gallus gallus calreticulin (CALR)	Y
NHBR308	NM_205518	ACTB	Homo sapiens actin, beta (ACTB)	ACTB	Similar to NM_205518, "Gallus gallus actin, beta (ACTB), mRNA >gi|211236|gb|L08165.1|CHKBACTN Gallus gallus beta-actin mRNA, complete cds", score 425, e-value 1e-115	N
NHBR313	XM_420549	AFF1	Homo sapiens AF4/FMR2 family, member 1 (AFF1)	AFF1	Similar to XM_420549, "PREDICTED: Gallus gallus similar to AF-4 (LOC422590), mRNA", score 621, e-value 1e-174	Y
NHBR314	XM_422300	TPR	Homo sapiens translocated promoter region (to activated MET oncogene), TPR	TPR	Similar to XM_422300, "PREDICTED: Gallus gallus similar to translocated promoter region (to activated MET oncogene) (LOC424457), mRNA", score 379, e-value 6e-102	N
NHBR315	M55660	N/A	N/A	DSTN	Similar to M55660, "Chicken (clones pCMA-1 and pCMA-8) depolymerizing factor (ADF) mRNA, complete cds", score 125, e-value 5e-26	N
NHBR330	XM_417892	PVRL1	Homo sapiens poliovirus receptor-related 1 (herpesvirus entry mediator C), (PVRL1)	TRIM29	Similar to XM_417892, "PREDICTED: Gallus gallus similar to Tripartite motif-containing 29 (LOC419754), mRNA", score 276, e-value 9e-71	Y
NHBR331	XM_416161	PCTK2	Homo sapiens PCTAIRE protein kinase 2 (PCTK2)	PCTK2	Similar to XM_416161, "PREDICTED: Gallus gallus similar to PCTAIRE protein kinase 2 (LOC417920), mRNA", score 268, e-value 9e-69	N
NHBR334	BX935775	RPS24	Homo sapiens ribosomal protein S24 (RPS24)	RPS24	Similar to BX935775, "Gallus gallus finished cDNA, clone ChEST1014f24", score 361, e-value 2e-96	Y
NHBR34	AC145911	N/A	Homo sapiens fibulin 2 (FBLN2)	FBLN2	Similar to AC145911, "Gallus gallus BAC clone CH261-47H12 from chromosome unknown, complete sequence", score 805, e-value 5e-230	Y
NHBR37	AJ719645	N/A	N/A	WDR44	Similar to AJ719645, "Gallus gallus mRNA for hypothetical protein, clone 4o13", score 270, e-value 2e-69	N
NHBR4	CR385946	ELOVL5	Homo sapiens ELOVL family member 5, elongation of long chain fatty acids	ELOVL5	Similar to CR385946, "Gallus gallus finished cDNA, clone ChEST154e23", score 238, e-value 9e-60	Y
NHBR42	CR385946	ELOVL5	Homo sapiens ELOVL family member 5, elongation of long chain fatty acids	ELOVL5	Similar to CR385946, "Gallus gallus finished cDNA, clone ChEST154e23", score 90, e-value 5e-15	Y
NHBR47	NM_205477	MYH9	Homo sapiens myosin, heavy chain 9, non-muscle (MYH9)	MYH9	Similar to NM_205477, "Gallus gallus myosin, heavy chain 9, non-muscle (MYH9), mRNA >gi|212382|gb|M26510.1|CHKMYHN Chicken nonmuscle myosin heavy chain (MHC) gene, complete cds", score 492, e-value 7e-136	N
NHBR48		N/A	N/A	N/A	-(not annotated)-	Y
NHBR52	XM_417443	C20orf54	Homo sapiens chromosome 20 open reading frame 54 (C20orf54)	C20orf54	Similar to XM_417443, "PREDICTED: Gallus gallus similar to chromosome 20 open reading frame 54 (LOC419270), partial mRNA", score 349, e-value 4e-93	N
NHBR55	M81779	CDH13	Homo sapiens cadherin 13, H-cadherin (heart) (CDH13)	CDH13	Similar to M81779, "G.gallus T-cadherin mRNA, complete cds", score 916, e-value 2e-263	Y
NHBR58	NM_001030620	CANX	Homo sapiens calnexin (CANX)	CANX	Similar to NM_001030620, "Gallus gallus calnexin (CANX), mRNA >gi|53127409|emb|AJ719429.1| Gallus gallus mRNA for hypothetical protein, clone 2d15", score 902, e-value 4e-259	Y
NHBR59	NM_001030620	CANX	Homo sapiens calnexin (CANX)	CANX	Similar to NM_001030620, "Gallus gallus calnexin (CANX), mRNA >gi|53127409|emb|AJ719429.1| Gallus gallus mRNA for hypothetical protein, clone 2d15", score 930, e-value 2e-267	Y
NHBR65	CR385946	ELOVL5	Homo sapiens ELOVL family member 5, elongation of long chain fatty acids	ELOVL5	Similar to CR385946, "Gallus gallus finished cDNA, clone ChEST154e23", score 419, e-value 8e-114	Y

NHBR69	XM_416106	NAP1L1	Homo sapiens nucleosome assembly protein 1-like 1 (NAP1L1)	NAP1L1	Similar to XM_416106, "PREDICTED: Gallus gallus nucleosome assembly protein 1-like 1 (NAP1L1), mRNA", score 542, e-value 1e-150	N
NHBR7	CR387685	N/A	N/A	CR387685	Similar to CR387685, "Gallus gallus finished cDNA, clone ChEST76p7", score 115, e-value 4e-23	Y
NHBR70	XM_416106	NAP1L1	Homo sapiens nucleosome assembly protein 1-like 1 (NAP1L1)	NAP1L1	Similar to XM_416106, "PREDICTED: Gallus gallus nucleosome assembly protein 1-like 1 (NAP1L1), mRNA", score 653, e-value 6e-184	N
NHBR72	N/A	N/A	N/A	N/A	-(not annotated)-	Y
NHBR73	CR385946	ELOVL5	Homo sapiens ELOVL family member 5, elongation of long chain fatty acids	ELOVL5	Similar to CR385946, "Gallus gallus finished cDNA, clone ChEST154e23", score 203, e-value 5e-49	Y
NHBR76	N/A	N/A	N/A	N/A	-(not annotated)-	Y
NHBR77	XR_026955	MBTD1	Homo sapiens mbt domain containing 1 (MBTD1)	LOC417387	Similar to XR_026955, "PREDICTED: Gallus gallus hypothetical LOC417387 (LOC417387), mRNA", score 300, e-value 3e-78	Y
NHBR78	BX931207	MME	Homo sapiens membrane metallo-endopeptidase (MME)	BX931207	Similar to BX931207, "Gallus gallus finished cDNA, clone ChEST1021m6", score 966, e-value 3e-278	Y
NHBR8	CR386843	RPSA	Homo sapiens ribosomal protein SA (RPSA)	CR386843	Similar to CR386843, "Gallus gallus finished cDNA, clone ChEST38a1", score 585, e-value 9e-164	Y
NHBR83	CR386508	N/A	N/A	CR386508	Similar to CR386508, "Gallus gallus finished cDNA, clone ChEST649o12", score 328, e-value 3e-86	Y
NHBR89	EU826449	N/A	N/A	ATP8	Similar to EU826449, "Gallus gallus ATP synthase F0 subunit 8 (ATP8) gene, partial cds; and ATP synthase F0 subunit 6 (ATP6) gene, complete cds; mitochondrial", score 266, e-value 6e-68	Y
NHBR90	AF002986	N/A	N/A	N/A	Weakly similar to AF002986, "Homo sapiens platelet activating receptor homolog (H963) mRNA, complete cds", score 46, e-value 0.035	Y
NHBR91	XM_001235059	N/A	N/A	NASP	Similar to XM_001235059, "PREDICTED: Gallus gallus nuclear autoantigenic sperm protein (histone-binding) (NASP), mRNA", score 534, e-value 2e-148	N
NHBR95	X52751	BSG	Homo sapiens basigin (Ok blood group) (BSG)	BSG	Similar to X52751, "Chicken mRNA for HT7 antigen", score 234, e-value 1e-58	Y
NHBR97	CR352609	YIPF3	Homo sapiens Yip1 domain family, member 3 (YIPF3)	YIPF3	Similar to CR352609, "Gallus gallus finished cDNA, clone ChEST151l13", score 379, e-value 5e-102	N
NHBR99	N/A	N/A	N/A	N/A	-(not annotated)-	Y

Table 4.2. *Nhbw* sequences and their homologies in Human (*Homo sapiens*) and in the Chick (*Gallus gallus*).

Original ID	Accession ID	Gene Symbol (*H Sapiens*)	Description (*Homo Sapiens*)	Gene Symbol (*G gallus*)	Description (Gallus gallus)	SP
NHBW100	BX934439	N/A	N/A	N/A	Similar to BX934439, "Gallus gallus finished cDNA, clone ChEST966n20", score 262, e-value 6e-67	Y
NHBW105	AC192748	SEMA6A	Homo sapiens sema domain, transmembrane domain (TM), and cytoplasmic domain, (semaphorin) 6A (SEMA6A)	N/A	Similar to AC192748, "Gallus gallus BAC clone CH261-166H21 from chromosome z, complete sequence", score 133, e-value 4e-28	Y
NHBW12	CR385946	ELOVL5	Homo sapiens ELOVL family member 5, elongation of long chain fatty acids (FEN1/Elo2, SUR4/Elo3-like, yeast) (ELOVL5)	N/A	Similar to CR385946, "Gallus gallus finished cDNA, clone ChEST154e23", score 185, e-value 1e-43	Y
NHBW121	CR391670	N/A	N/A	N/A	Similar to CR391670, "Gallus gallus finished cDNA, clone ChEST158n2", score 108, e-value 1e-20	Y
NHBW124	NM_205518	ACTB	Homo sapiens actin, beta (ACTB)	ACTB	Similar to NM_205518, "Gallus gallus actin, beta (ACTB), mRNA >gi|211236|gb|L08165.1|CHKBACTN Gallus gallus beta-actin mRNA, complete cds", score 155, e-value 8e-35	N
NHBW128	L16770	N/A	N/A	N/A	Weakly similar to L16770, "Anas platyrhynchos mitochondrial complete transfer RNA-Glu, transfer RNA-Phe, transfer RNA-Val, transfer RNA-Leu, 12S ribosomal RNA, and 16S ribosomal RNA genes", score 52, e-value 0.001	Y
NHBW13	AY145522	LOC100008588	Homo sapiens 18S ribosomal RNA (LOC100008588), non-coding RNA	N/A	Similar to AY145522, "Rana chensinensis 18S ribosomal RNA gene, partial sequence", score 345, e-value 7e-92	Y
NHBW138	CR524036	N/A	N/A	NOL5A	Similar to CR524036, "Gallus gallus finished cDNA, clone ChEST591p9", score 127, e-value 2e-26	Y
NHBW148	BX934736	TUBA4A	Homo sapiens tubulin, alpha 4a (TUBA4A)	N/A	Similar to BX934736, "Gallus gallus finished cDNA, clone ChEST559b14", score 290, e-value 6e-75	N
NHBW15	D38360	LOC100008588	Homo sapiens 18S ribosomal RNA (LOC100008588), non-coding RNA	D38360	Similar to D38360, "Gallus gallus gene for 18S rRNA, partial sequence", score 153, e-value 6e-34	Y
NHBW153	CR385946	ELOVL5	Homo sapiens ELOVL family member 5, elongation of long chain fatty acids (FEN1/Elo2, SUR4/Elo3-like, yeast) (ELOVL5)	N/A	Similar to CR385946, "Gallus gallus finished cDNA, clone ChEST154e23", score 189, e-value 8e-45	Y
NHBW16	CR352609	YIPF3	Homo sapiens Yip1 domain family, member 3 (YIPF3)	YIPF3	Similar to CR352609, "Gallus gallus finished cDNA, clone ChEST151l13", score 429, e-value 7e-117	N
NHBW161	CR385946	ELOVL5	Homo sapiens ELOVL family member 5, elongation of long chain fatty acids (FEN1/Elo2, SUR4/Elo3-like, yeast) (ELOVL5)	N/A	Similar to CR385946, "Gallus gallus finished cDNA, clone ChEST154e23", score 135, e-value 1e-28	Y
NHBW175	AC175394	N/A	N/A	AC175394	Similar to AC175394, "Gallus gallus BAC clone TAM31-49F22 from chromosome w, complete sequence", score 185, e-value 2e-43	Y
NHBW180	NM_001006472	CD151	Homo sapiens CD151 molecule (Raph blood group) (CD151)	CD151	Similar to NM_001006472, "Gallus gallus CD151 molecule (Raph blood group) (CD151), mRNA >gi|53135765|emb|AJ720796.1| Gallus gallus mRNA for hypothetical protein, clone 25m21", score 714, e-value 1e-202	Y
NHBW184	CR385946	ELOVL5	Homo sapiens ELOVL family member 5, elongation of long chain fatty acids (FEN1/Elo2, SUR4/Elo3-like, yeast) (ELOVL5)	N/A	Similar to CR385946, "Gallus gallus finished cDNA, clone ChEST154e23", score 171, e-value 1e-39	Y
NHBW190	NM_001031023	N/A	N/A	UBXN2B	Similar to NM_001031023, "Gallus gallus UBX domain protein 2B (UBXN2B), mRNA >gi|53129506|emb|AJ719732.1| Gallus gallus mRNA for hypothetical protein, clone 5m7", score 127, e-value 2e-26	N

NHBW201	NM_001006219	YWHAE	Homo sapiens tyrosine 3-monooxygenase/tryptophan 5-monooxygenase activation protein, epsilon polypeptide (YWHAE)	YWHAE	Similar to NM_001006219, "Gallus gallus tyrosine 3-monooxygenase/tryptophan 5-monooxygenase activation protein, epsilon polypeptide (YWHAE), mRNA >gi|53126522|emb|AJ719304.1| Gallus gallus mRNA for hypothetical protein, clone 1e8", score 169, e-value 4e-39	N
NHBW203	CR407495	ATP6V0C	Homo sapiens ATPase, H+ transporting, lysosomal 16kDa, V0 subunit c (ATP6V0C)	ATP6V0C /// TBC1D24	ATPase, H+ transporting, lysosomal 16kDa, V0 subunit c /// TBC1 domain family, member 24	Y
NHBW213	XM_415612	TNRC6C	Homo sapiens trinucleotide repeat containing 6C (TNRC6C)	TNRC6C	Weakly similar to XM_415612, "PREDICTED: Gallus gallus trinucleotide repeat containing 6C (TNRC6C), mRNA", score 50, e-value 0.004	Y
NHBW220	BX934439	EVPL	Homo sapiens envoplakin (EVPL)	N/A	Similar to BX934439, "Gallus gallus finished cDNA, clone ChEST966n20", score 312, e-value 8e-82	Y
NHBW221	BX934439	EVPL	Homo sapiens envoplakin (EVPL)	N/A	Similar to BX934439, "Gallus gallus finished cDNA, clone ChEST966n20", score 312, e-value 8e-82	Y
NHBW223	NM_205518	ACTB	Homo sapiens actin, beta (ACTB)	ACTB	Similar to NM_205518, "Gallus gallus actin, beta (ACTB), mRNA >gi|211236|gb|L08165.1|CHKBACTN Gallus gallus beta-actin mRNA, complete cds", score 520, e-value 4e-144	N
NHBW226	CR352609	YIPF3	Homo sapiens Yip1 domain family, member 3 (YIPF3)	YIPF3	Similar to CR352609, "Gallus gallus finished cDNA, clone ChEST151l13", score 441, e-value 2e-120	Y
NHBW23	XM_001233493	PTPRF	Homo sapiens protein tyrosine phosphatase, receptor type, F (PTPRF)	PTPRF	Similar to XM_001233493, "PREDICTED: Gallus gallus similar to receptor protein tyrosine phosphatase LAR (LOC424568), mRNA", score 482, e-value 7e-133	Y
NHBW237	N/A	N/A	N/A	N/A	-(not annotated)-	N
NHBW246	CR385946	ELOVL5	Homo sapiens ELOVL family member 5, elongation of long chain fatty acids (FEN1/Elo2, SUR4/Elo3-like, yeast) (ELOVL5)	N/A	Similar to CR385946, "Gallus gallus finished cDNA, clone ChEST154e23", score 80, e-value 5e-12	Y
NHBW252	XM_424960	SEMA6A	Homo sapiens sema domain, transmembrane domain (TM), and cytoplasmic domain, (semaphorin) 6A (SEMA6A)	SEMA6A	Similar to XM_424960, "PREDICTED: Gallus gallus sema domain, transmembrane domain (TM), and cytoplasmic domain, (semaphorin) 6A (SEMA6A), mRNA", score 169, e-value 1e-38	Y
NHBW256	AJ721056	DHX33	Homo sapiens DEAH (Asp-Glu-Ala-His) box polypeptide 33 (DHX33)	DHX33	Similar to AJ721056, "Gallus gallus mRNA for hypothetical protein, clone 33j19", score 278, e-value 1e-71	N
NHBW258	AJ721056	DHX33	Homo sapiens DEAH (Asp-Glu-Ala-His) box polypeptide 33 (DHX33)	DHX33	Similar to AJ721056, "Gallus gallus mRNA for hypothetical protein, clone 33j19", score 280, e-value 3e-72	N
NHBW260	CU683875	N/A	N/A	N/A	Similar to CU683875, "Zebrafish DNA sequence from clone CH73-23L24 in linkage group 6, complete sequence", score 125, e-value 1e-25	Y
NHBW263	BC146737	LOC730041	Homo sapiens similar to small GTP binding protein TC10 (LOC730041)	BC146737	Similar to BC146737, "Danio rerio zgc:165551, mRNA (cDNA clone MGC:165551 IMAGE:7219026), complete cds", score 377, e-value 2e-101	Y
NHBW264	CU683875	N/A	N/A	N/A	Similar to CU683875, "Zebrafish DNA sequence from clone CH73-23L24 in linkage group 6, complete sequence", score 125, e-value 6e-26	Y
NHBW266	BC092921	LYZL2	Homo sapiens lysozyme-like 2 (LYZL2)	N/A	Similar to BC092921, "Danio rerio cDNA clone IMAGE:7160567", score 716, e-value 3e-203	Y
NHBW268	CU683875	N/A	N/A	N/A	Similar to CU683875, "Zebrafish DNA sequence from clone CH73-23L24 in linkage group 6, complete sequence", score 125, e-value 6e-26	Y
NHBW40	XM_419518	BPTF	Homo sapiens bromodomain PHD finger transcription factor (BPTF)	HEATR5B	Similar to XM_419518, "PREDICTED: Gallus gallus hypothetical LOC421469 (LOC421469), mRNA", score 96, e-value 1e-16	Y
NHBW45	NM_001030620	CANX	Homo sapiens calnexin (CANX)	CANX	Similar to NM_001030620, "Gallus gallus calnexin (CANX), mRNA >gi|53127409|emb|AJ719429.1| Gallus gallus mRNA for hypothetical protein, clone 2d15", score 345, e-value 1e-91	Y
NHBW49	N/A	N/A	N/A	N/A	-(not annotated)-	Y
NHBW51	NM_001030620	CANX	Homo sapiens calnexin (CANX)	CANX	Similar to NM_001030620, "Gallus gallus calnexin (CANX), mRNA >gi|53127409|emb|AJ719429.1| Gallus gallus mRNA for hypothetical protein, clone 2d15", score 571, e-value 2e-159	Y

NHBW57	BC037997	CXCL2	Homo sapiens chemokine (C-X-C motif) ligand 2 (CXCL2)	CXCL2	Similar to BC037997, "Mus musculus chemokine (C-X-C motif) ligand 1, mRNA (cDNA clone IMAGE:5321155), partial cds", score 351, e-value 1e-93	Y
NHBW62	CR385946	ELOVL5	Homo sapiens ELOVL family member 5, elongation of long chain fatty acids (FEN1/Elo2, SUR4/Elo3-like, yeast) (ELOVL5)	N/A	Similar to CR385946, "Gallus gallus finished cDNA, clone ChEST154e23", score 191, e-value 2e-45	Y
NHBW63	CR385946	ELOVL5	Homo sapiens ELOVL family member 5, elongation of long chain fatty acids (FEN1/Elo2, SUR4/Elo3-like, yeast) (ELOVL5)	N/A	Similar to CR385946, "Gallus gallus finished cDNA, clone ChEST154e23", score 189, e-value 8e-45	Y
NHBW64	BX935106	KCMF1	Homo sapiens potassium channel modulatory factor 1 (KCMF1)	N/A	Similar to BX935106, "Gallus gallus finished cDNA, clone ChEST70g5", score 230, e-value 2e-57	Y
NHBW7	BC037997	CXCL2	Homo sapiens chemokine (C-X-C motif) ligand 2 (CXCL2)	CXCL2	Similar to BC037997, "Mus musculus chemokine (C-X-C motif) ligand 1, mRNA (cDNA clone IMAGE:5321155), partial cds", score 349, e-value 5e-93	Y
NHBW73	J04596	CXCL2	Homo sapiens chemokine (C-X-C motif) ligand 2 (CXCL2)	N/A	Similar to J04596, "Mouse platelet-derived growth factor-inducible KC protein mRNA, complete cds", score 147, e-value 4e-32	Y
NHBW74	CR385946	ELOVL5	Homo sapiens ELOVL family member 5, elongation of long chain fatty acids (FEN1/Elo2, SUR4/Elo3-like, yeast) (ELOVL5)	N/A	Similar to CR385946, "Gallus gallus finished cDNA, clone ChEST154e23", score 189, e-value 8e-45	Y
NHBW8	BC037997	CXCL2	Homo sapiens chemokine (C-X-C motif) ligand 2 (CXCL2)	N/A	Similar to BC037997, "Mus musculus chemokine (C-X-C motif) ligand 1, mRNA (cDNA clone IMAGE:5321155), partial cds", score 351, e-value 1e-93	Y
NHBW82	CR385946	N/A	N/A	N/A	Similar to CR385946, "Gallus gallus finished cDNA, clone ChEST154e23", score 171, e-value 2e-39	Y
NHBW85	NM_001112806	N/A	N/A	CKS1B	Similar to NM_001112806, "Gallus gallus CDC28 protein kinase regulatory subunit 1B (CKS1B), mRNA >gi|41631786|emb|BX931258.1| Gallus gallus finished cDNA, clone ChEST683j9", score 189, e-value 6e-45	Y
NHBW87	NM_001030620	CANX	Homo sapiens calnexin (CANX)	CANX	Similar to NM_001030620, "Gallus gallus calnexin (CANX), mRNA >gi|53127409|emb|AJ719429.1| Gallus gallus mRNA for hypothetical protein, clone 2d15", score 914, e-value 1e-262	Y
NHBW90	XM_417424	OPRL1	Homo sapiens opiate receptor-like 1 (OPRL1)	OPRL1	Similar to XM_417424, "PREDICTED: Gallus gallus similar to ORL1-like opioid receptor (LOC419251), mRNA", score 472, e-value 6e-130	Y
NHBW94	CR385946	ELOVL5	Homo sapiens ELOVL family member 5, elongation of long chain fatty acids (FEN1/Elo2, SUR4/Elo3-like, yeast) (ELOVL5)	N/A	Similar to CR385946, "Gallus gallus finished cDNA, clone ChEST154e23", score 185, e-value 1e-43	Y
NHBW95	NM_001006472	CD151	Homo sapiens CD151 molecule (Raph blood group) (CD151)	CD151	Similar to NM_001006472, "Gallus gallus CD151 molecule (Raph blood group) (CD151), mRNA >gi|53135765|emb|AJ720796.1| Gallus gallus mRNA for hypothetical protein, clone 25m21", score 732, e-value 6e-208	Y
NHBW97	CR385946	ELOVL5	Homo sapiens ELOVL family member 5, elongation of long chain fatty acids (FEN1/Elo2, SUR4/Elo3-like, yeast) (ELOVL5)	N/A	Similar to CR385946, "Gallus gallus finished cDNA, clone ChEST154e23", score 185, e-value 1e-43	Y
NHBW98	N/A	N/A	N/A	N/A	-(not annotated)-	Y

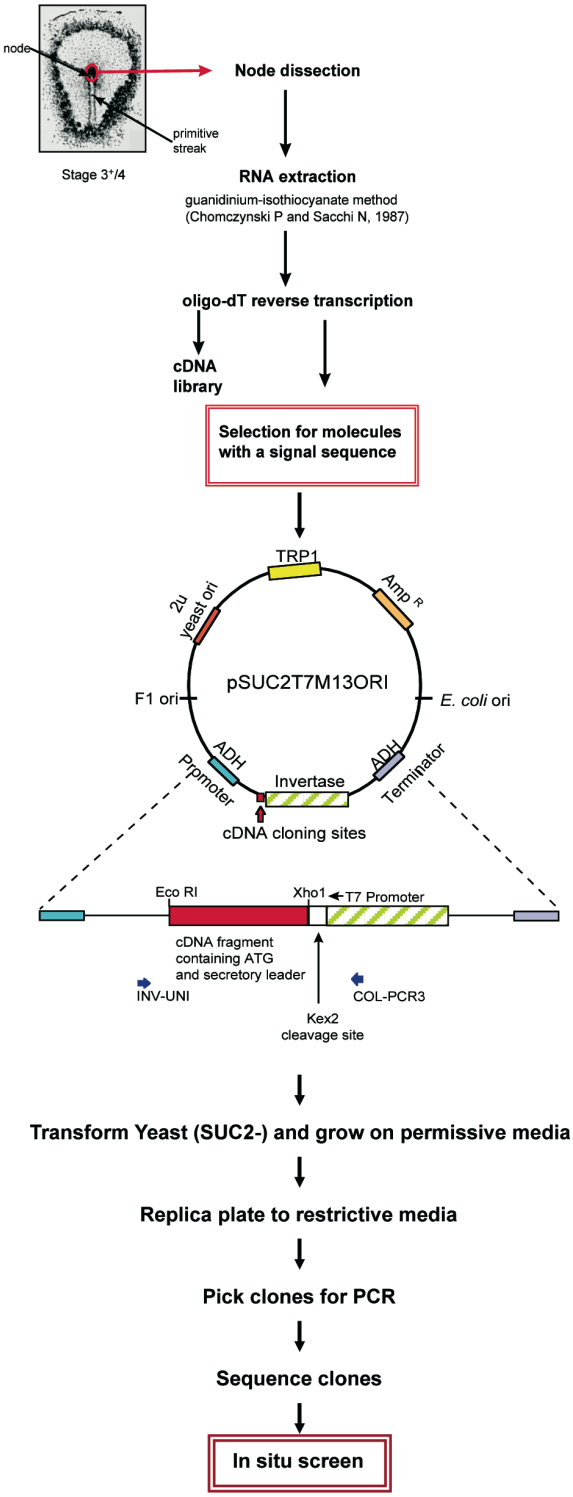

Fig 4.1. Selection for molecules with a Signal Sequence. Nodes were dissected from Stage 3^{+}/4 chick embryos; After RNA extraction and reverse transcription the clones were put through the secretion selection and the resulting sequences further screened by *in situ* hybridization.

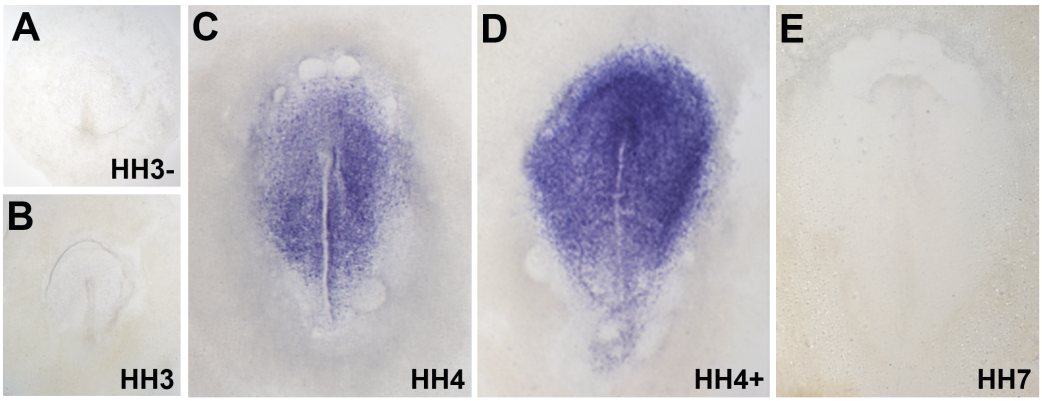

Fig 4.2. *Nhbr7* expression pattern. Strong expression is detected in the early neural plate at stage 4 **(C)** and 4^+ **(D)** followed by a dramatic downregulation **(E)**.

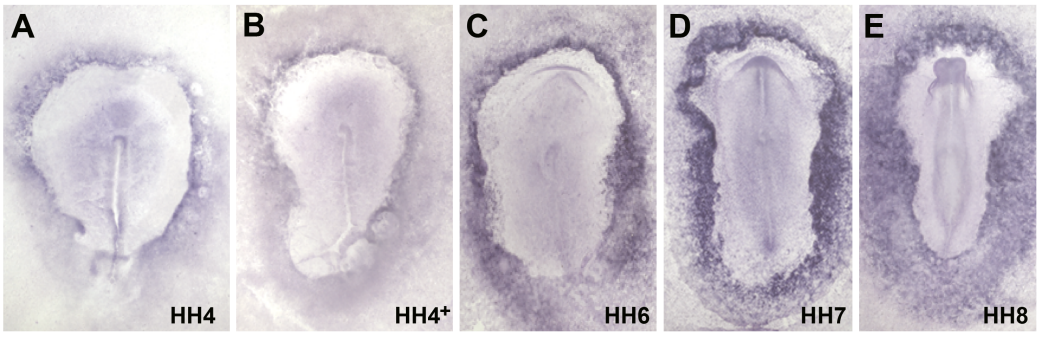

Fig 4.3. *Nhbr10*, *nhbr116* and *nhbw63* expression pattern. Weak but consistent expression is detected in the neural plate form stage 4 (**A**) and this expression is maintained to at least stage 8 (B to E); There seems to be an increased expression in the node region at stages 4^+ (**B**), 6 (**C**) and 7 (**D**) but this might be due to tissue thickening rather than expression amount.

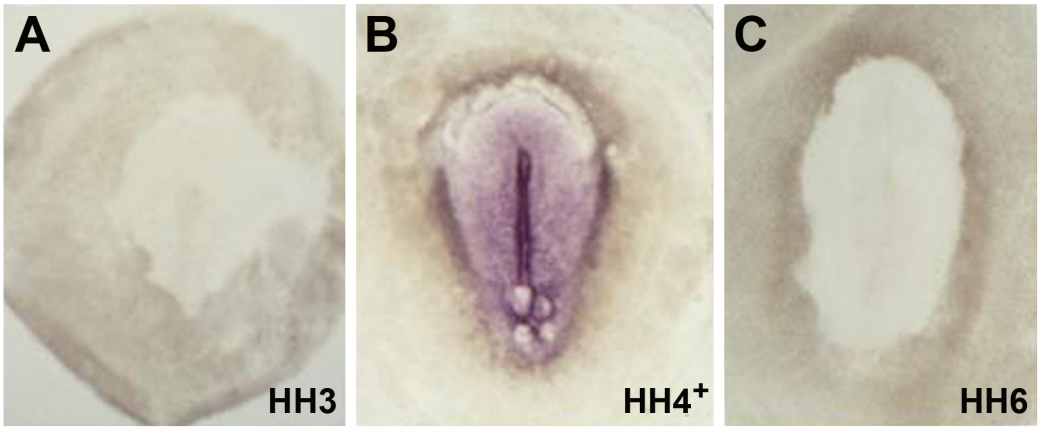

Fig. 4.4. *Nhbr34* expression pattern. Very dynamic expression is observed, with strong detection of transcripts, very transiently, at stage 4^+ (**B**). Prior and after fully elongate primitive streak, no expression is detected (**A**,**C**).

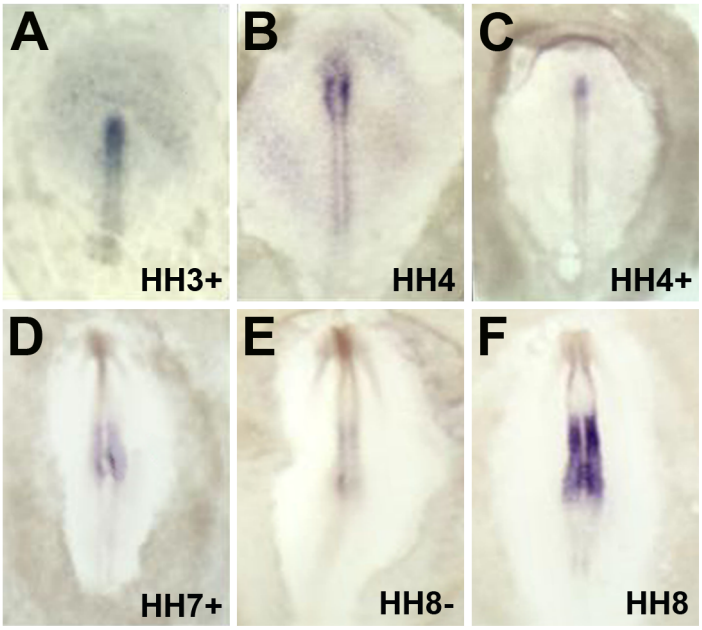

Fig 4.5. *Nhbr90* expression pattern. *Nhbr90* transcripts are first detected in the node at stage 3^+ (**A**) and the node expression is maintained throughout the stages analysed (**A-F**).

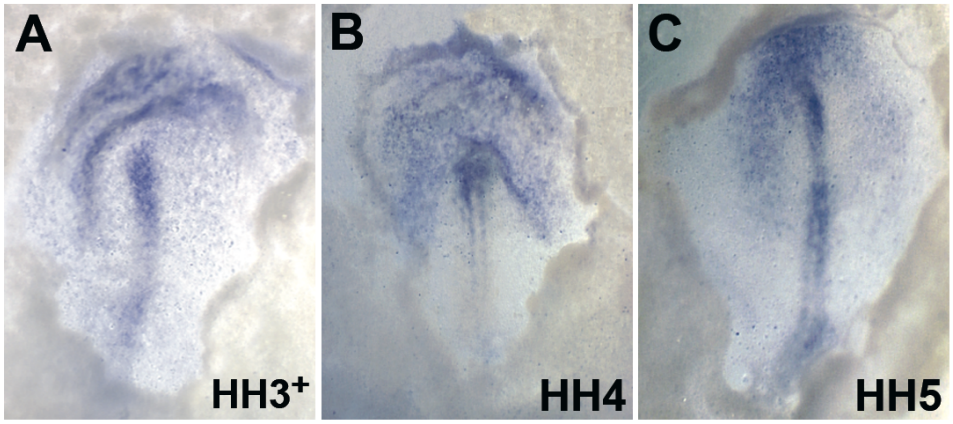

Fig 4.6. *Nhbr91* expression pattern. *Nhbr91* transcripts are detected in the anterior streak and node at stage 3^{+} (**A**) with low level of expression throughout the embryonic region. By stage 4, the expression becomes defined to the prospective neural plate and node (**B**) and reappears in the primitive streak at stage 5 (**C**).

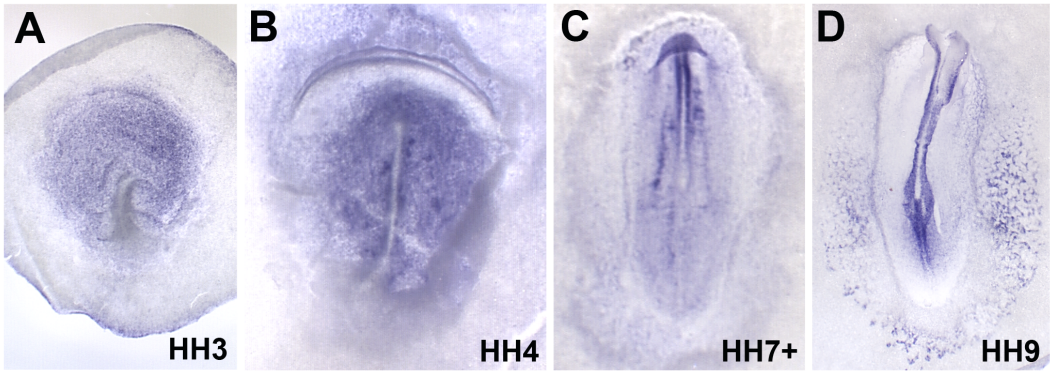

Fig 4.7. *Nhbr111* expression pattern. *Nhbr111* transcripts are present throughout the embryonic region at stage 3 (**B**) and become more defined to the prospective neural plate by stage 4 (**B**). Later stages reveal neural plate and blood islands expression (**C** and **D**).

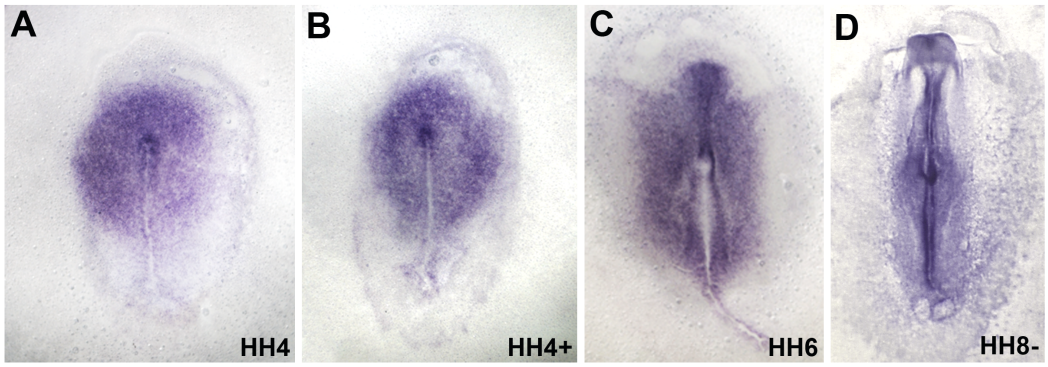

Fig 4.8. *Nhbr121* expression pattern. Nhbr121 is expressed in the node and prospective neural plate at stages 4 (**A**) and 4^{+} (**B**). Transcripts continue to be detected in the neural plate and underlying mesoderm at later stages (**C** and **D**).

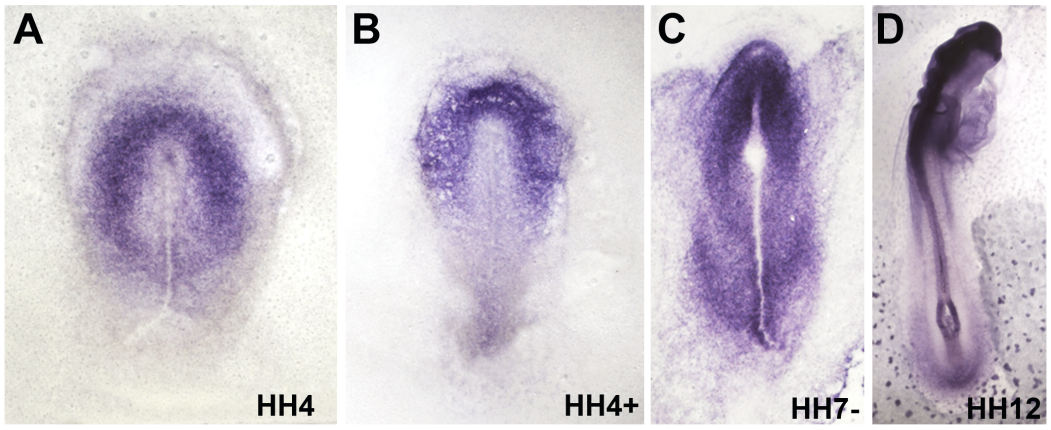

Fig 4.10. *Nhbr231* expression pattern. Stage 4 embryos express *nhbr231* in the prospective neural plate, stronger at the border (**A**); Stage 4^{+} transcripts continue to clear away from the central region of the neural plate, resulting in a horseshoe shaped expression domain (**B**); At stage 7^{-}, expression is completely abolished in the midline and is strong in the anterior neural plate and mesoderm (**C**); By stage 12, *nhbr231* transcripts are strongly localized in the head region and anterior neural tube. Expression is also strong in the blood islands (**D**).

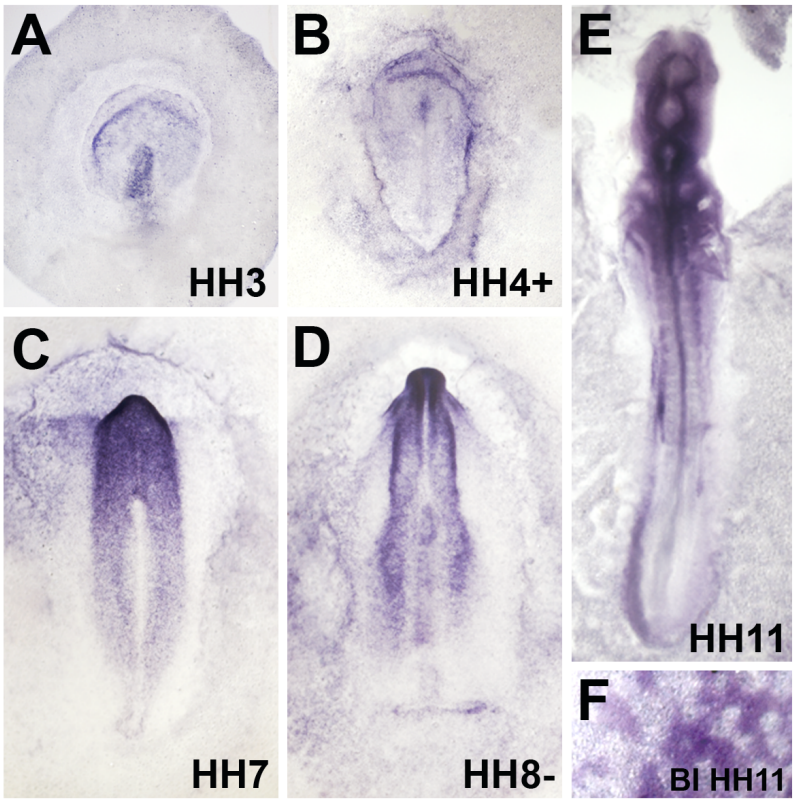

Fig 4.9. *Nhbr225* expression pattern. Transcripts are detected at stage 3 in the primitive streak and the prospective neural plate (**A**); By stage 4^{+} the expression in the primitive streak seems to have disappeared or is extremely weak; Expression is present in the node and emerging head process (**B**); At stage 7 the *nhbr225* mRNA is detected in the entire neural plate, albeit stronger in the anterior part of the embryo (**C**); At stage 8^{-} expression remains in the neural plate, although it seems to clear away from the area surrounding the remaining primitive streak that, together with the node, seem to express the transcript by this stage (**D**); At stage 11, expression is mainly present in the neural tube and in the head region (**E**), as well as in the blood islands (**F**).

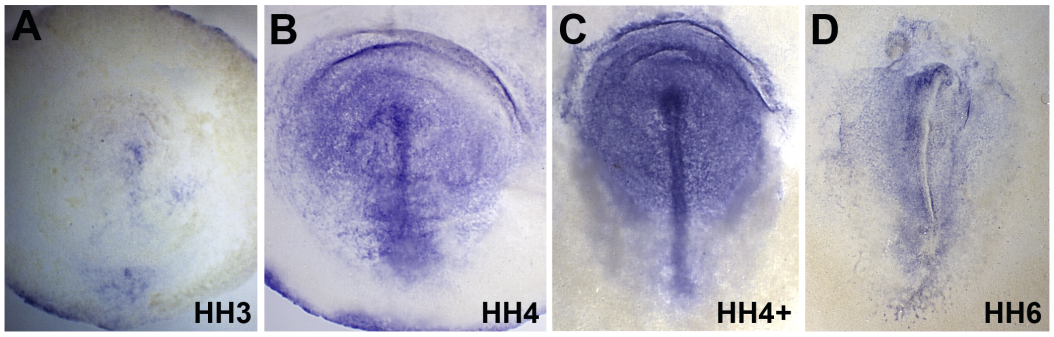

Fig 4.11. *Nhbr241* expression pattern. Nhbr241 expression starts, very weakly, at stage 3 and is detected in the primitive streak (**A**); By stage 4, expression stronger expression is detected in the primitive streak, node and the entire embryonic region (**B**); At stage 4^{+} the node and primitive streak expression is very strong; transcripts are also strongly detected in the prospective neural plate (**C**); By stage 6 the expression becomes very weak again and seems to be mainly detected in the neural plate (**D**).

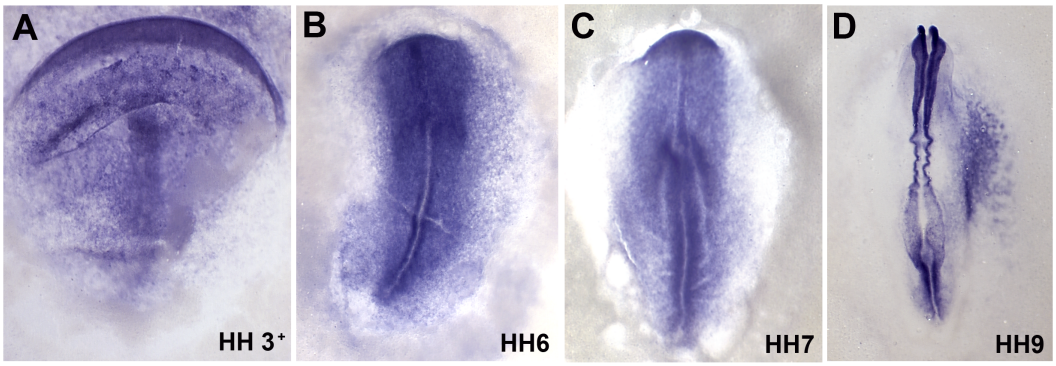

Fig 4.12. *Nhbr151* expression pattern. At stage 3^{+} expression is detected in the entire embryonic region and strongly in the primitive streak and node (**A**); By stage 6 transcripts start to become restricted to the neural plate with stronger expression observed in the head process and the sides of the primitive streak (**B**); Expression at stage 7 remains strong in the primitive streak and notochord; transcripts are also detected in the neural plate and posterior mesoderm (**C**); At stage 9 expression is present in the head region, the closing neural tube, posterior neural plate and in the remaining streak; a strong patch of expression is present on the right side of the extraembryonic *area opaca* (**D**).

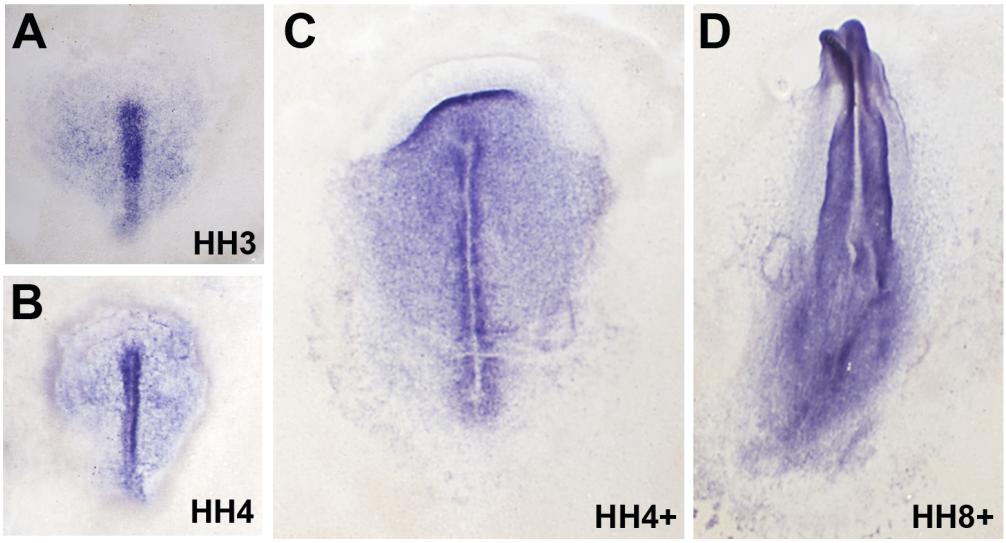

Fig 4.13. *Nhbr260* expression pattern. At stage 3, *nhbr260* is strongly expressed in the primitive streak and, more weakly, in the epiblast (**A**); At stage 4, expression remains similar and includes the node (**B**); Expression at stage 4^{+} is strong in the lateral sides of the primitive streak and node and in the mesoderm (**C**); Stage 8^{+} embryos present the transcript in the entire neural plate, stronger at the border, and in the posterior mesoderm. Some expression starts to be detected in what seem to be blood islands (**D**).

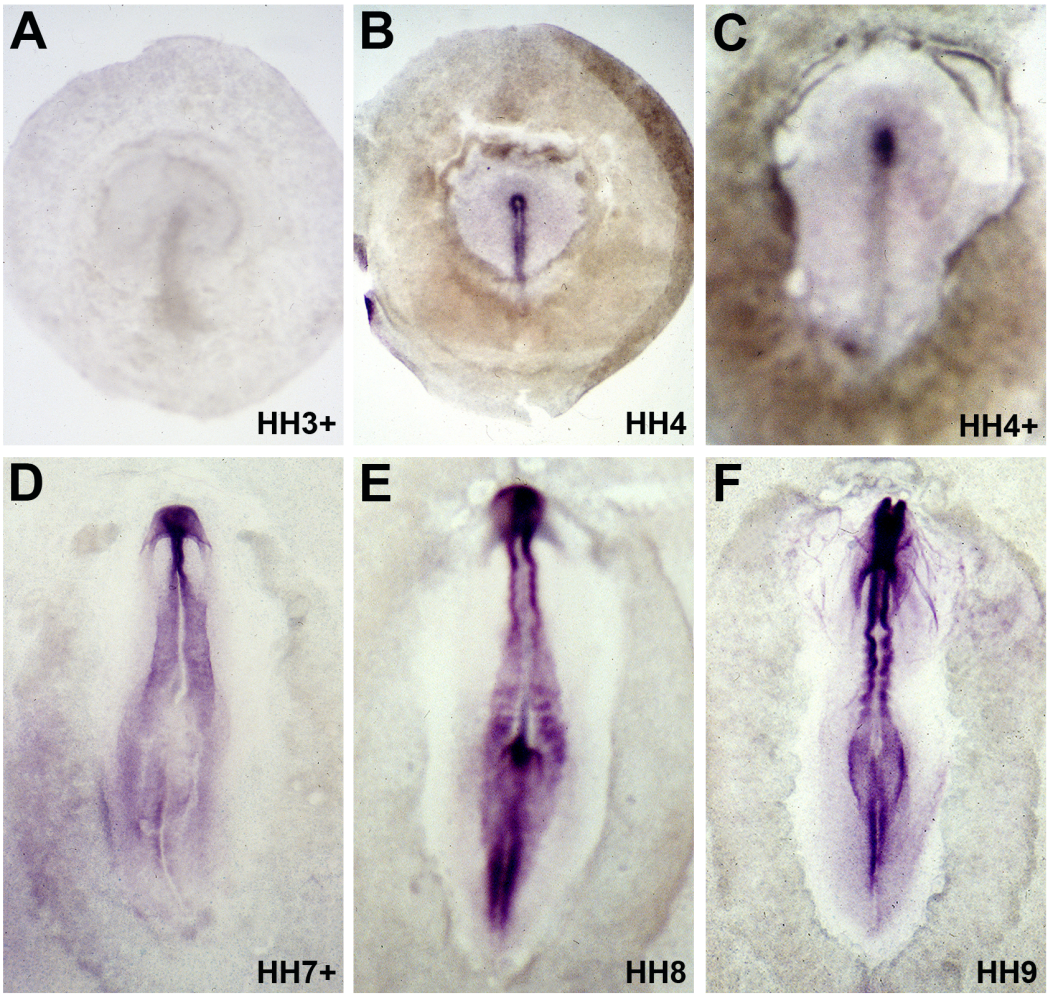

Fig 4.14. *Nhbr307* expression pattern. *Nhbr307* is expressed at very low levels throughout the embryonic and non embryonic regions at stage 3/3^{+} (**A**); Expression becomes localized at stage 4, weakly in the neural plate and very strong in the primitive streak and node (**B**); By stage 4^{+} the expression in the primitive streak seems to be downregulated (**C**). For the later developmental stages analysed, *nhbr307* seems to maintain its expression restricted to neural structures, the neural plate and neural tube, and somites (**D-F**).

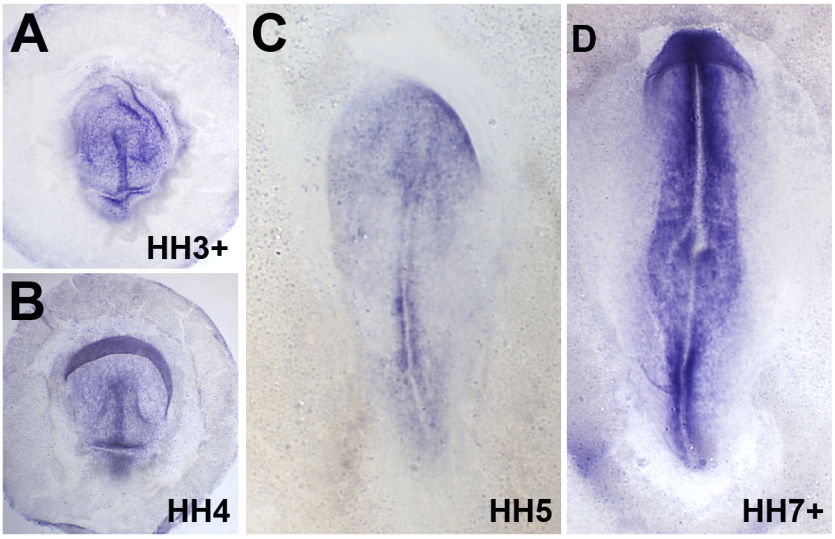

Fig 4.15. *Nhbr313* expression pattern. Stage 3^{+}-4 embryos express *nhbr313* weakly throughout the embryonic region and strongly in the primitive streak and node (**A** and **B**); At stage 5 expression is difficult to detect but can be seen in the primitive streak and in the anterior neural plate (**C**); By stage 7 the expression becomes more defined and clearly localizes to the neural plate and the remaining streak (**D**).

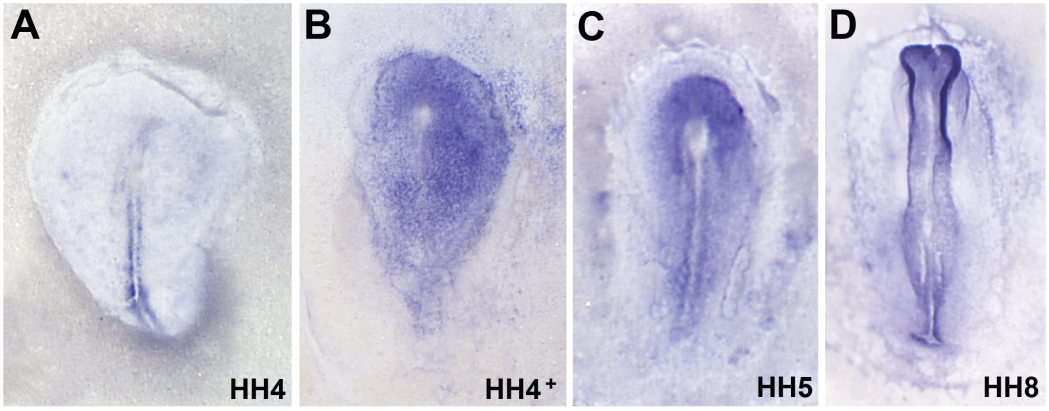

Fig 4.16. *Nhbr330* expression pattern. At stage 4, *nhbr330* expression is detected in the posterior two thirds of the primitive streak and some weak expression may be seen in the epiblast (**A**); At stage 4^{+}, transcripts are completely absent from the node but are otherwise strongly detected in the rest of the embryo (**B**); By stage 5 expression starts to become restricted to the neural plate, with the node and head process not expressing the transcript (**C**);At stage 8, expression is present in the entire neural plate, being stronger at the anterior border (**D**).

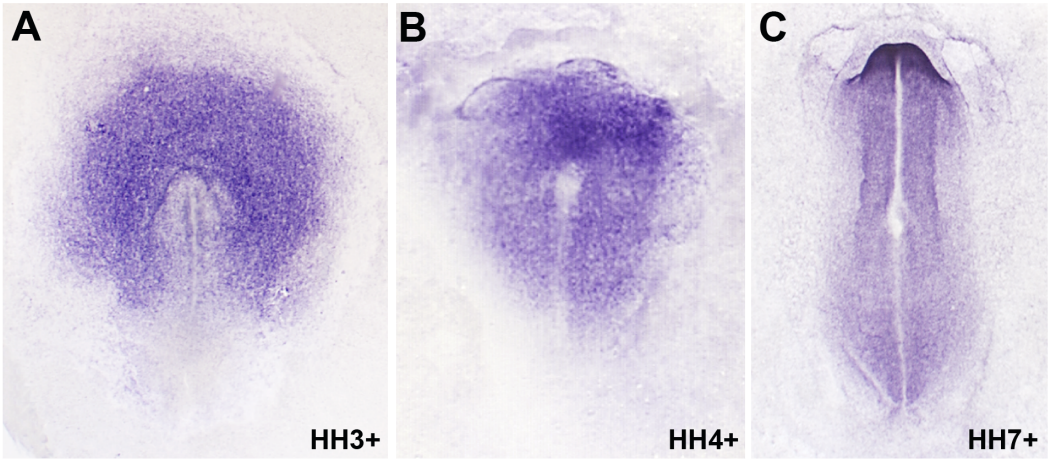

Fig 4.17. *Nhbw23* expression pattern. Transcripts are detected in the prospective neural plate and is absent from the node at stage 3^+ (**A**). Expression remains mostly restricted to the neural plate from stage 4^+ (**B**) to stage 7^+ (**C**).

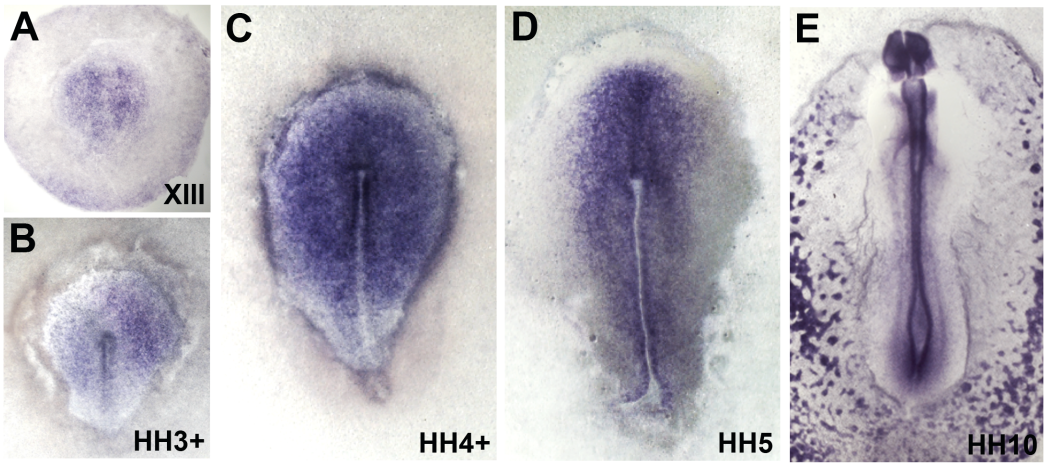

Fig 4.18. *Nhbw57* expression pattern. At stage XIII, transcripts are present in the entire epiblast (**A**); Stage 3^+ embryos present expression in the entire epiblast, the node and primitive streak (**B**). By stage 4^+, expression starts to become restricted to the prospective neural plate (**C**); In stage 6 embryos expression detected in the neural plate and in the forming notochord (**D**); Later, at stage 10, expression is strongly localized to the cephalic region and closing neural tube and in the blood islands (**E**).

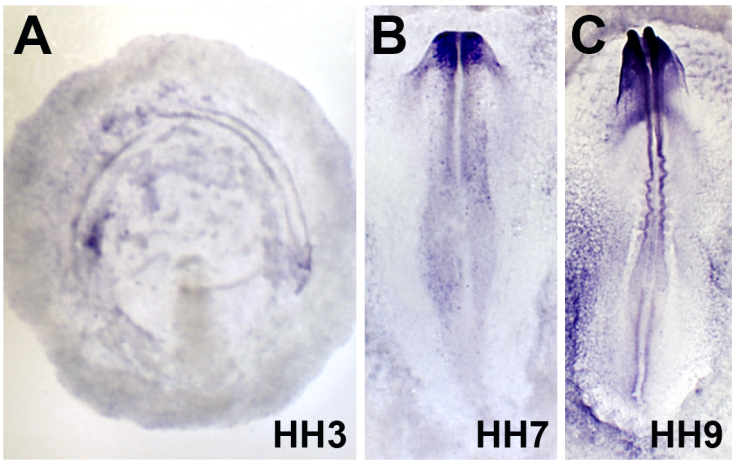

Fig 4.19. *Nhbw87* expression pattern. This *in situ* proved very difficult. By stage 3, there is some weak expression in the epiblast (**A**); Stage 7 embryos present expression in the neural plate, stronger in the head region (**B**); By stage 9, expression remains stronger in the head and in the neural tube and some expression remains in other parts of the neural plate (**C**).

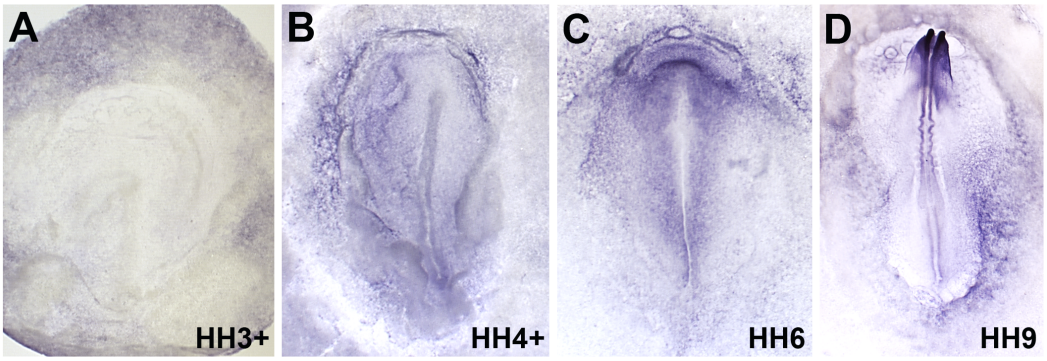

Fig 4.20. *Nhbw95* expression pattern. Expression seems almost ubiquitous, but it is absent from the *area pellucida* up to stage 3^{+} (**A**) and is more strongly expressed in the neural plate at stage 6 (**C**). Stage 9 embryos present a distinct expression in the head, edge of the neural tube and the remnants of the streak in the posterior part of the embryo (**D**).

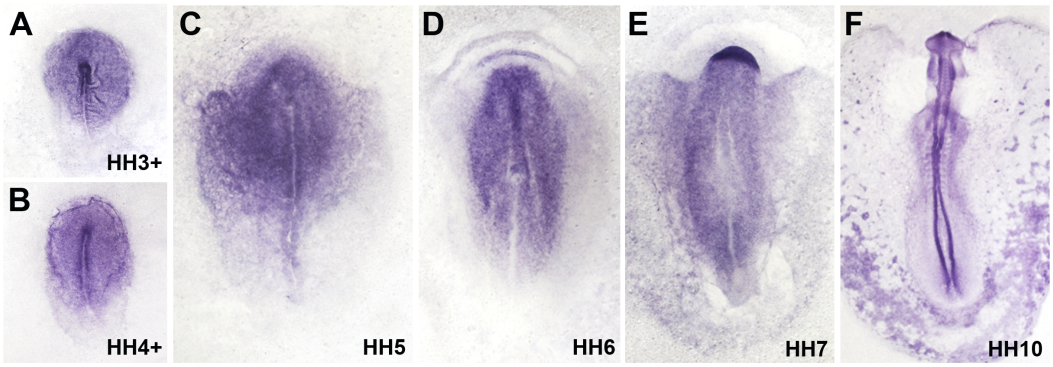

Fig. 4.21. *Nhbw153* expression pattern. Expression is detected in the the anterior third of the primitive streak and the node as well as to the prospective neural plate (**A**); At stage $4^{+, ex}$ expression in the primitive streak extended posteriorly and there is also strong expression in the emerging head process **(B**); At stage 5, expression expands to the "mesodermal wings" and is maintained in the neural plate and head process (**C**); Similar expression is observed at stage 6, where the notochord is now well stained (**D**); By stage 7, expression is present in the entire neural plate, with the exception of the area surrounding the node and first formed somite; the extraembryonic mesoderm also continues to express *nhbw153* (**E**). Stage 10 embryos present strong expression in the blood islands and in the neural tube and borders of the posterior neural plate (**F**).

Chapter 5

nhbr 34: Fibulin 2

Introduction

Fibulins are a family of extracellular matrix (ECM) proteins. Within a decade of the identification of the founding member of the family, Fibulin 1 (Argraves et al., 1989), several others were identified, mostly in mouse and humans, defining a family. These molecules are Fibulin 2 (Pan et al., 1993b), Fibulin 3 (Tran et al., 1997a), Fibulin 4 (Gallagher et al., 2001; Giltay et al., 1999) and Fibulin 5 (Kowal et al., 1999a; Nakamura et al., 2002). A possible sixth member of the family – Fibulin 6 or Hemicentin – has been identified recently in the nematode (Vogel and Hedgecock, 2001). Because its inclusion in the fibulin family remains controversial, it will not be described further.

Fibulin protein structure

Fibulins vary greatly in size from 360 to about 1200 residues and all the family members can be modified further by alternative splicing (Argraves et al., 2003; Argraves et al., 1990; Pan et al., 1993b; Timpl et al., 2003; Tran et al., 1997a). Like most ECM proteins Fibulins have a distinct arrangement in modules, which can be grouped in domains classed as types I, II and III (**Fig 5.1**).

Domain I of Fibulin 1, at the amino-terminus, consists of three anaphylatoxin-like (AT) modules (Huber et al., 1980). Domain II follows, with 9 epidermal growth factor (EGF)-like modules, most of which can have a consensus sequence for calcium binding (also known as calcium-binding EGF-like modules). The carboxy-terminal domain III (FC module) is characteristic of fibulins and fibrillins (Giltay et al., 1999). Fibulin 2 has an extra amino-terminal domain, which can be subdivided into a cysteine-rich segment (Na) and a cysteine-free segment (Nb) (Pan et al., 1993b). Fibulins 3, 4 and 5 are much shorter members of the family, lacking the AT modules, and characterized by only 5 EGF-like repeats (which can present modifications for calcium binding) (Gallagher et al., 1999; Giltay et al., 1999; Nakamura et al., 1999). All the Fibulins are secreted into the extracellular matrix and are synthesized from a precursor containing a signal peptide that is cleaved before secretion (Timpl et al., 2003).

Fibulin function

All Fibulins are associated with basement membranes and elastic extracellular matrix fibres (Argraves et al, 2003) and are known to bind calcium as well as to interact with many other ECM proteins. It has been hypothesised that they function as intramolecular bridges, stabilising the ECM structures, and that they modulate, to a certain extent, cell morphology, adhesion and motility (Gallagher WM et al, 2005). The next few paragraphs explore some possible roles of Fibulins in development and cellular interactions.

Fibulins and heart development

All the Fibulins isolated to date have been implicated in cardiovascular development (Argraves et al., 1990; Giltay et al., 1999; Kowal et al., 1999a; Kowal et al., 1999b; Nakamura et al., 1999; Pan et al., 1993a; Pan et al., 1993b; Timpl et al., 2003; Tran et al., 1997a; Tran et al., 1995; Tran et al., 1997b) and most studies have focused on Fibulin1 and Fibulin2. Immunostaining studies for Fibulin-1 revealed that in stage 15-22 quail embryos the protein is a constituent of most basement membranes, particularly in areas undergoing epithelial-mesenchymal transitions in the endocardial cushions, developing myotomes and neural crest. In the early heart, Fibulin expression is upregulated in the cardiac jelly at sites where endocardial cushion cells begin the migrations that lead to the formation of valvular and septal primordia (Spence et al., 1992). Avian studies have not been performed for fibulin-2. In the mouse, both fibulin-1 and fibulin-2 have been studied extensively. Both are expressed at sites of epithelial-mesenchymal transformation and cell migration during cardiac valvuloseptal and great vessel development (Tsuda et al., 2001; Zhang et al., 1995; Zhang et al., 1994), in zones lined by basement membrane and in adventitial layers (Miosge et al., 1996); both proteins remain as prominent components of adult valves (Miosge et al., 1998; Tsuda et al., 2001; Zhang et al., 1995). Targeted inactivation of the *fibulin1* gene in mice leads to severe haemorrhages in the skin, muscle and perineural tissues. These defects are first evident at about midgestation and result in the death of almost all homozygous embryos at birth (Kostka et al., 2001). Targeted mutations of other Fibulin family members have not been reported.

Fibulin3 is present in some capillaries, but not in large blood vessels whereas Fibulin4 is present in the medial layers of large veins and arteries and some small capillaries (Giltay et al., 1999). Fibulin5 seems to be restricted to the arterial vasculature and is

predominantly expressed in the vascular smooth muscle cells of adult blood vessels (Kowal et al., 1999a) and in the pulmonary artery endothelium (Kuang et al., 2003).

Fibulins in early development, including the nervous system

Apart from reports of *Fibulin1* and *Fibulin2* expression in the neural crest in avian and murine embryos (Spence et al., 1992) there is very limited information pointing to a role of Fibulins in the development of neural structures. Another study assessed the expression patterns of fibulin1 and fibulin2 in human embryos of gestational weeks 4-10. Differences in staining patterns were observed in various neural structures. Fibulin-1 is prominent in the matrix of the leptomeningeal anlagen, in basement membranes of the neuroepithelium and in the perineurium of peripheral nerves. Fibulin-2 is detected primarily within the neuropithelium, spinal ganglia and peripheral nerves (Miosge et al., 1996). Both fibulin1 and -2 are reported as being expressed in areas of epithelial-mesenchymal interactions such as developing tooth and hair follicles (Zhang et al., 1995; Zhang et al., 1996); the early embryonic expression of both fibulins suggests that they function during organ development and, in particular, in the differentiation of heart, skeletal and neural structures (Miosge et al., 1996).

Fibulins in gonadal morphogenesis

Most developing organs are surrounded by an extracellular matrix (ECM), which must be remodelled to accommodate growth and morphogenesis. The role of ECM proteins in organogenesis is not yet clearly understood. However, experiments in *Caenorhabditis elegans* have started to explore the role of fibulin in gonad morphogenesis, where two secreted proteases, MIG-17 and GON-1, are required for gonad formation. Two independent recent studies (Hesselson et al., 2004; Kubota et al., 2004) have shown that Fibulin 1 can rescue gonadogenesis in the absence of these proteases. MIG-17 acts from outside the gonad to control the migration of gonadal distal tip cells (DTCs) that promote gonad morphogenesis. Kubota and coleagues (Kubota et al., 2004) have also shown that fibulin1 can bypass the requirement for MIG-17 activity in directing DTC migration. GON-1 regulates both elongation and shape of the developing gonad. Fibulin1 mutants have a wider than normal gonad as well as body size defects. Hesselson and coleagues (Hesselson et al., 2004) demonstrated that a fine balance between GON-1 and fibulin1 levels is required for proper gonad formation. Studies in other species have not been performed, but it is likely that fibulins may be involved in similar processes during organ formation.

Fibulins in response to injury

Fibulins have also been implicated in the responses to wound healing and inflammation. Fibulin 2 is upregulated in sun-damaged skin elastosis (Hunzelmann et al., 2001), and in some forms of kidney injuries (Wada et al., 2001). In wounds induced in mouse skin, there is a marked upregulation of *fibulin2* mRNA expression, which declines to normal levels after completion of skin repair. Fibulin1 is present in normal skin but is not upregulated in the wounds during the healing process (Fassler et al., 1996; Raghunath et al., 1999). *Fibulin5* expression is increased in the lung alveolar wall of mice with induced emphysema (Kuang et al., 2003), vascular smooth muscle cells in response to blood vessel injury (Kowal et al., 1999a; Kowal et al., 1999b), the lung vasculature in response to hyperoxia (Kuang et al., 2003; Kuang et al., 2006) and in atherosclerotic plaques (Kowal et al., 1999a). A study performed in rabbits has shown that overxexpression of *fibulin5* in the injured skin accelerates the wound healing process (Lee et al., 2004b).

This chapter presents the cloning, molecular characterization and possible implications in neural induction of a chick homologue of *Fibulin 2* (*Fbln2 short*). Its expression in the chick starts in the epiblast prior to gastrulation and, as cells start to ingress, expression is seen in the forming mesoderm. Thereafter expression is concentrated in the notochord, intermediate mesoderm (Wolffian duct primordia) and derivatives of the somites as well as in branchial arches and diencephalic regions. Misexpression of *Fbln2* short within and outside the prospective neural plate does not alter the normal expression of the early neural markers *Sox3* and *Sox2*. It is also unable to induce *Sox2* in the area opaca even in combination with FGF8. These experiments do not support the hypothesis that fibulin plays an important role in neural induction in the chick embryo.

Materials and methods

Isolation of a full-length clone of chick *fibulin2-short*

The original nhbr34 clone was used to transcribe a radiolabelled RNA probe which was used for library screening (details of the procedure can be found in Chapter 2).

Northern Blots

Northern blots were performed as described in Chapter 2 and the full length clone *Fibulin2-short* was used to transcribe a radiolabelled probe ([α-^{32}P]dCTP) prior to hybridization.

Database searches

Homologous sequences from other species were obtained from GenBank. Alignments were performed using ClustalW software and phylogenetic trees built with TreeView. Tools within Prosite http://www.expasy.org/prosite/ allowed analysis of the protein motifs.

In situ hybridisation

The full length *fibulin2 short* was used to transcribe a digoxigenin-labelled RNA probe and hybridisation performed as described in Chapter 2.

Electroporation construct

cFbln2 short was cloned into *pCAβ-IRES-GFP* (a kind gift from A. Lumsden Lab). The *pBS-Fbln2* plasmid was cut with *SpeI* and the ends blunted with Klenow enzyme (Promega), followed by digestion with *ClaI*. The *pCAβ-IRES-GFP* vector was digested with *BamHI*, Klenow filled and cut with *ClaI*. After ligation, the resulting DNA was sequenced and used for electroporation at a concentration of 1.5 µg/µl.

Results

Cloning of the full length nhbr34: chick *fibulin2-short*

Searches of the chicken genome using the nhbr34 sequence revealed a predicted *fibulin 2* gene located on chromosome 12 (LOC427583). The sequence is 4803 bp long and codes for a putative 1600 amino acid protein. This sequence had been deposited in the NCBI database under accession number XM_425156.

The nhbr34 clone was used to screen a chick stage 2-4 cDNA library, resulting in the isolation of a sequence containing a 1746bp long ORF, coding for a 581aa peptide. When compared with the predicted fibulin 2 from the genome, the shorter isolated sequence is 100% identical at the aminoacid level. It was therefore called *fibulin2-short*. Northern Blot analyses of RNA from chick embryos at stages 3, 5 and 7-8 reveal two bands of 4.7 and 1.8-2Kb respectively (**Fig 5.2 A**). The larger band is likely to correspond to the predicted fibulin2 gene, whereas the size of the smaller band agrees with the predicted length of the shorter version of *fibulin 2* which had been isolated. The smaller *fibulin 2* RNA is much more abundant than the larger transcript which may explain why it was not picked up during the library screening. **Fig 5.2C** shows the aminoacid sequence of chick *Fibulin2 short* (*cFbln2-short*) with the underlined region where the *nhbr34* clone aligns.

Fibulin 2 is a conserved molecule

From the time the first Fibulin 2 was isolated from mouse fibroblasts (Pan et al., 1993b), many other Fibulins have been isolated and characterised. The recent sequencing of the genomes of various species also provides a great tool to predict and compare sequences. ClustalW alignments were performed to compare the sequences of Fibulin2 short with the very well described mouse (NM_007992) and human (NM_001004019) sequences. Predicted sequences from chicken (XM_425156), rat (XM_232197) and chimpanzee (XM_516297) and a smaller version of human fibulin2 (hFBLN2 short) were also used. The resulting alignment (**Fig 5.3**) highlights the conserved structure of fibulin2 amongst the sequences analyzed. Conservation is particularly evident in the characteristic domains of Fibulin2, namely the cystein-rich segment (Na; pink), the three anaphylatoxin modules (AT; green), the EGF-like modules (light blue and light blue and yellow when there is a consensus sequence for calcium binding) and in the carboxy-terminal domain (FC module; red). The signal peptide and the Cysteine-free segment (Nb), represented in dark blue and grey respectivelly, although not conserved at the amino acid level, share

the properties that the first has hydrophobic residues and the second lacks cysteines in all the sequences. **Fig 5.3 B** shows the modular structure of Fibulin2.

The Fibulin family has many members

Since the identification of Fibulin-1 (Argraves S, et al 1989), the founding member of the Fibulin family of proteins, four other members have been identified (Fibulin-2, -3, -5 and -5), mostly in work performed with human and murine cell lines. To compare fibulin2-short with other fibulin family members, sequence comparisons were performed with fibulin 2, fibulin 1 and fibulin 5. Some of the sequences used were predicted from the available genome data. Given the large number of sequences available, only a few were selected for analyses. These were zebrafish fibulin1-D (zfFbln1-D; AF013751), chick Fibulin1 (cFbln1; NM_204165), predicted rat Fibulin1 (rFbln1; XM_243637), mouse Fibulin1 (mFbln1; NM_010180) human Fibulin1-C (hFBLN1-C; NM_001996), predicted chick Fibulin5 (cFbln5; XM_421323), rat Fibulin5 (rFbln5; NM_019153), mouse Fibulin5 (mFbln5; NM_011812), human Fibulin5 (hBBLN5; NM_006329) and the fibulin 2 family member mentioned above. Trees resulting from the alignment are shown in **Fig 5.2B** and **Fig 5.4**. Homonymous family members were clustered and within each family, avian fibulins appear closer to their mammalian counterparts, which group together, than the corresponding fish sequences (eg. **Fig 5.4**). Fibulin2 appears to have diverged earlier than the duplication that led to Fibulins 1 and 5.

Expression pattern of *fbln2* in the chick

Whole mount *in situ* hybridisation was performed in chick embryos ranging from pre-gastrula stages to about stage 20. Expression is first detected very weakly in the epiblast at stage 2-3 (not shown) and by stage 3^+ expression covers the entire epiblast (**Fig 5.5 A**). At stage 4, expression is excluded from the primitive groove but is expressed in the primitive ridges and Hensen's node (white arrowhead) (**Fig 5.5 B**). Thereafter, *fbln2* is expressed in the mesodermal wings of the lateral plate (**Fig 5.5 C**) and emerging head process (**Fig 5.5D** and **Fig 5.6A**) and increasingly strongly in the notochord (white arrow, **Fig 5.5 E-H**; **Fig 5.6 J**, **M-Q**). From stage 6 onwards expression starts to clear from the anterior ectoderm, leaving a fringe of expressing cells at the anterior and lateral borders of the neural plate (**Fig 5.5 E-G**). From stage 7^+ the expression completely clears from the neural plate and becomes restricted to the notochord, somites and border of the neural plate (Fig. 5.5 G). At stage 11 strong expression is observed in the anterior ectoderm and prosencephalon, notochord, somites and a dorsal domain of the intermediate mesoderm (**Fig 5.5 H** and **Fig 5.6 J-S**). Later in development *fbln2-short* is strongly expressed in the

diencephalon (perhaps including periocular neural crest), heart (**Fig 5.6 L, M**), branchial arches (red asterisks in **Fig 5.5 I,J**), lateral mesoderm and myotome (red arrows; **Fig 5.5 I-K**).

fbln2-short misexpression is unable to alter the expression of neural plate markers *Sox3 and Sox2*

Because all fibulins are secreted proteins (Argraves et al., 2003) and *fbln2-short* is expressed in Hensen's node at stages 3$^+$-4 and in the axial mesoderm thereafter, it could play a role in neural induction. To investigate this further, *pCAβ-fbln2-short-IRES-GFP* was electroporated into the epiblast of stage 3$^+$ chick embryos in a line extending from close to the node to the area *opaca*. This does not alter the expression of the early neural plate markers *Sox3* (0/11; **Fig 5.7 A-B**) or *Sox2* (0/14; **Fig 5.7 F-G**) in any of the embryos tested. Control electroporations, where the *pCAβ -IRES-GFP* plasmid was used, had similar results

Since misexpression of a line of *Fbln2-short* does not alter the expression of *Sox3* and *Sox2*, it is unlikely to induce their expression in the *area opaca*. Nevertheless, to rule out this possibility, *pCAβ-fbln2-short-IRES-GFP* was electroporated in a discrete domain in the inner third of the *area opaca* of stage 3$^+$ chick embryos. After overnight culture, no expression of *Sox3* (0/6; not shown), *Sox2* (0/8; **Fig 5.7 C-E**), or *Brachyury* (0/14) was observed in the electroporated region. Combining FGF8-soaked beads with *pCAβ-fbln2-short-IRES-GFP* electroporation also resulted in no induction of *Sox2* or of the mesodermal marker *Brachyury* in any of the embryos tested (0/12; **Fig 5.7 H-J**).

These results do not implicate *Fibulin2* in neural induction.

Discussion

Alternative splicing *vs* truncated fibulins

Alternative splicing has been reported for almost all fibulins studied. It was first demonstrated for domain III of human fibulin1 (Argraves et al., 1990; Tran et al., 1997a), which can vary from being completely eliminated (variant A) to being composed of 137 residues in variant D. Fibulin 2 splicing usually occurs within the EGF-like domains (Pan et al., 1993b); splicing in other regions of fibulin is also detected, including partial or complete deletion of the amino terminal domain I (Gallagher et al., 2001). Descriptions of truncated fibulins are rare in the literature, but it has been reported that human fibulin3 can have its amino terminal truncated to the extent of lacking the signal sequence and therefore presumed failure of secretion of the protein (Lecka-Czernik et al., 1995).

Chick Fibulin2-short seems to be a truncated form of the predicted chick Fibulin2. They both locate to the same position on Chicken chromosome 12 and have identical amino-acid composition. Based on the Northern blot results presented, it seems that *fibulin2-short* transcripts are more abundant than the longer form (*fibulin2*) at these stages in the chick embryo and may explain why the latter was not isolated during the library screening. The functional significance of the two forms remains to be understood.

Interestingly, by checking for other truncated fibulins within the human genome, a truncated form of *fibulin2* was found. This human *fibulin2-short* seems to encode a much smaller protein, lacking the signal peptide, the fibulin2 domain N and domain I. The resulting peptide is identical to the carboxy-terminal half of hFibulin2. Whether these truncations are common in other fibulin family members or why they happen is unclear, as is the presence of alternatively spliced variants. It is conceivable that these modifications could affect binding ability to ECM proteins but this remains to be investigated.

Fibulin2-short in neural induction

No previous studies have explored the function of any fibulin in neural induction. There have been only a few studies of its expression in early embryos, which reported expression of fibulins in the neural crest (Spence et al., 1992), neuroepithelium, spinal ganglia and peripheral nerves (Miosge et al., 1996), but the functioal significance of these patterns was not assessed. In situ hybridisation for *Fibulin2 short* in chick embryos (this study) showed that the mRNA is present transiently in Hensen's node and then strongly

in the axial mesoderm, as well as in a portion of the rostral neural tube and in intermediate mesoderm at later stages. Despite the finding that it is expressed in the node and its derivatives the head process and notochord, misexpression experiments gave negative results: neither fibulin2-short alone nor together with FGF8 is unable to induce neural markers in an ecopic, competent region. It is conceivable that a more complex combination of factors is required to reveal a function of fibulin in the modulation of expression of neural markers. It is therefore difficult to envisage its role as a direct signalling molecule that could act as a neural inducer. Furthermore, cell surface receptors for this protein have not been described; it is therefore impossible at this stage to speculate further on the likelihood that it may play a role in this process at these stages of development, and if it does signal, which tissue responds to such signals.

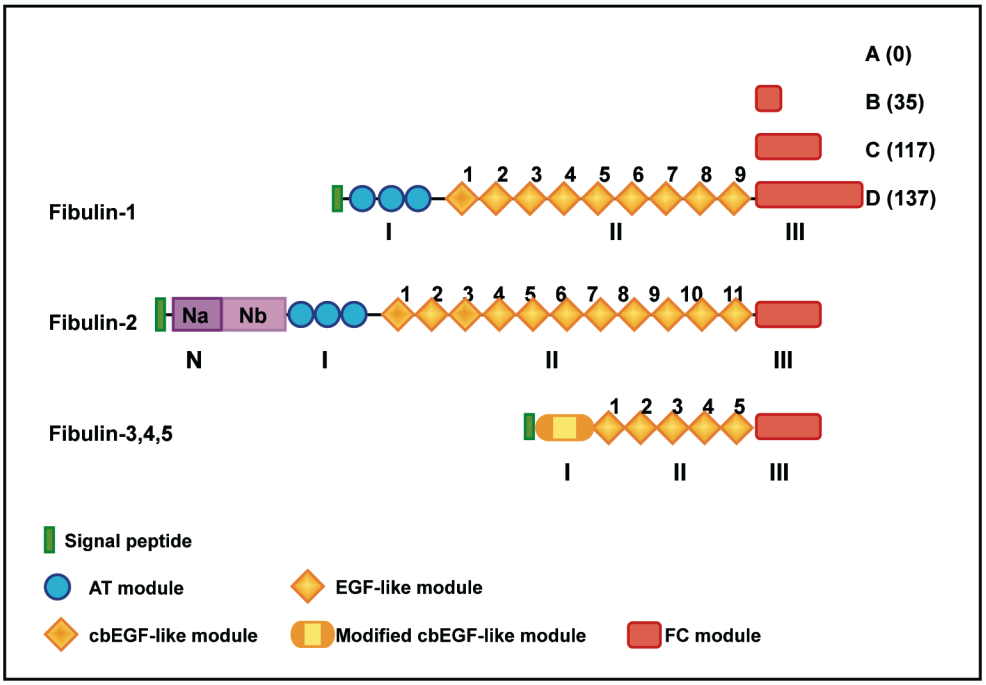

Fig 5.1. Modular structure of Fibulins. Fibulins have a characteristic arrangement of matrix modules, grouped together as domains I, II and III. The four variants of fibulin-1 are shown, being identical in sequence up to the fibulin-type carboxy-terminal (FC) module. Fibulin-2 is unique in that it contains an extra domain, Domain N, which can be subdivided into a cystein-rich segment (Na) and cystein-free segment (Nb). Fibulin-3, fibulin-4 and fibulin-5 have a modified calcium-binding (cb) epidermal growth factor (EGF)-like module at their amino terminus, the Domain I. AT, anaphylatoxin-like.

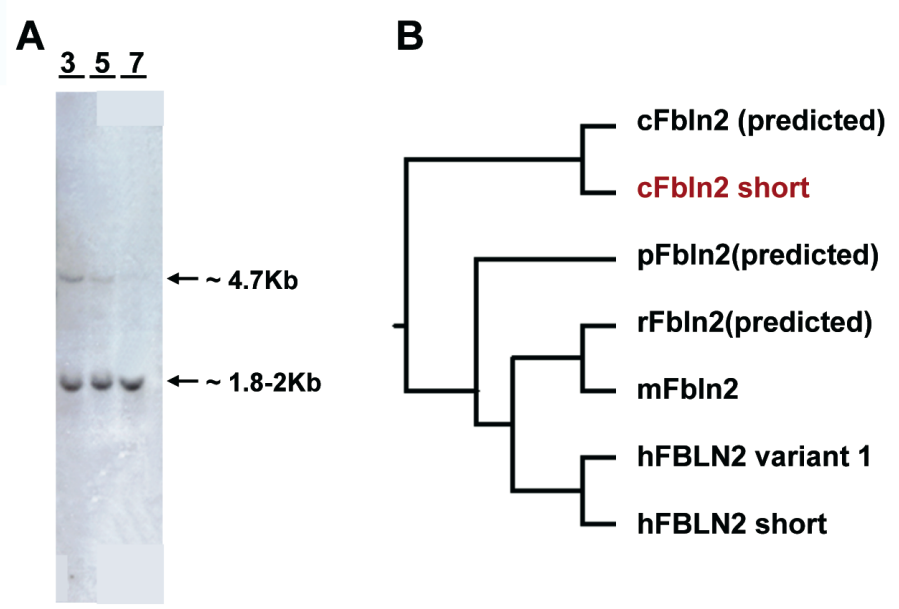

C

cFbln2-short: 581 aa

MDRHQSWQRSCLNAAFFMLLWSGVSHAQRDCTGVECQPLDNCIEDVLEPGECCATCLQH
GCTCEGYQYYDCVNVGFVNGKVPEGQSYFVDFGSTECSCPKGGGKISCQFMLCPELPPN
CIDAVVPADGCPQCGRIGCLHEGQKYVAGHTFHMPPCKVCHCPNAGGELMCYQLPNCNT
FALNTVSPMDAEDNEPERHYDDPYSYDQEAPEGDNAQVESPKKYRSYSSHLEQESISQE
QSEDYDYLPVSIAPSSSAVAGMYAEETTTPLTTPAPKLLSEFRSATERTEWKRVPSTTA
PPPQQTTHKEAPVTTSAPLEHTTATTETPKQLGKLDRRPKGKQGDKEKSEQERTPHSKM
KKHTRKEDPGNSIHLDLKEVNLTEPSSAKSSQETHEGNAFPKVKFSATTSPPVALKEDR
SQSSQKQSQTLYRYHPEEDGDPNSIHANPRLPEDPNCRLESSPATCGPIEDAVANANES
TPKGIVGILLLLEQTLSCFGAIATQAGKDAARKLLQTSFGVALCVQPVRRGDAAVPACR
GMQAELEPRISNWCSFQKLHNMQDEYAYAASAGVWMAHDCWVSDALKRVL*

Fig 5.2. cFibulin2-short. Northern blots reveal that *Fibulin2* is abundantly expressed in the early chick embryo (**A**). Dendogram resulting from the alignment of several Fibulin2 proteins, including another short variant, found in humans (**B**). Fibulin2-short aminoacid sequence, reveals a characteristic modular structure (**C**).

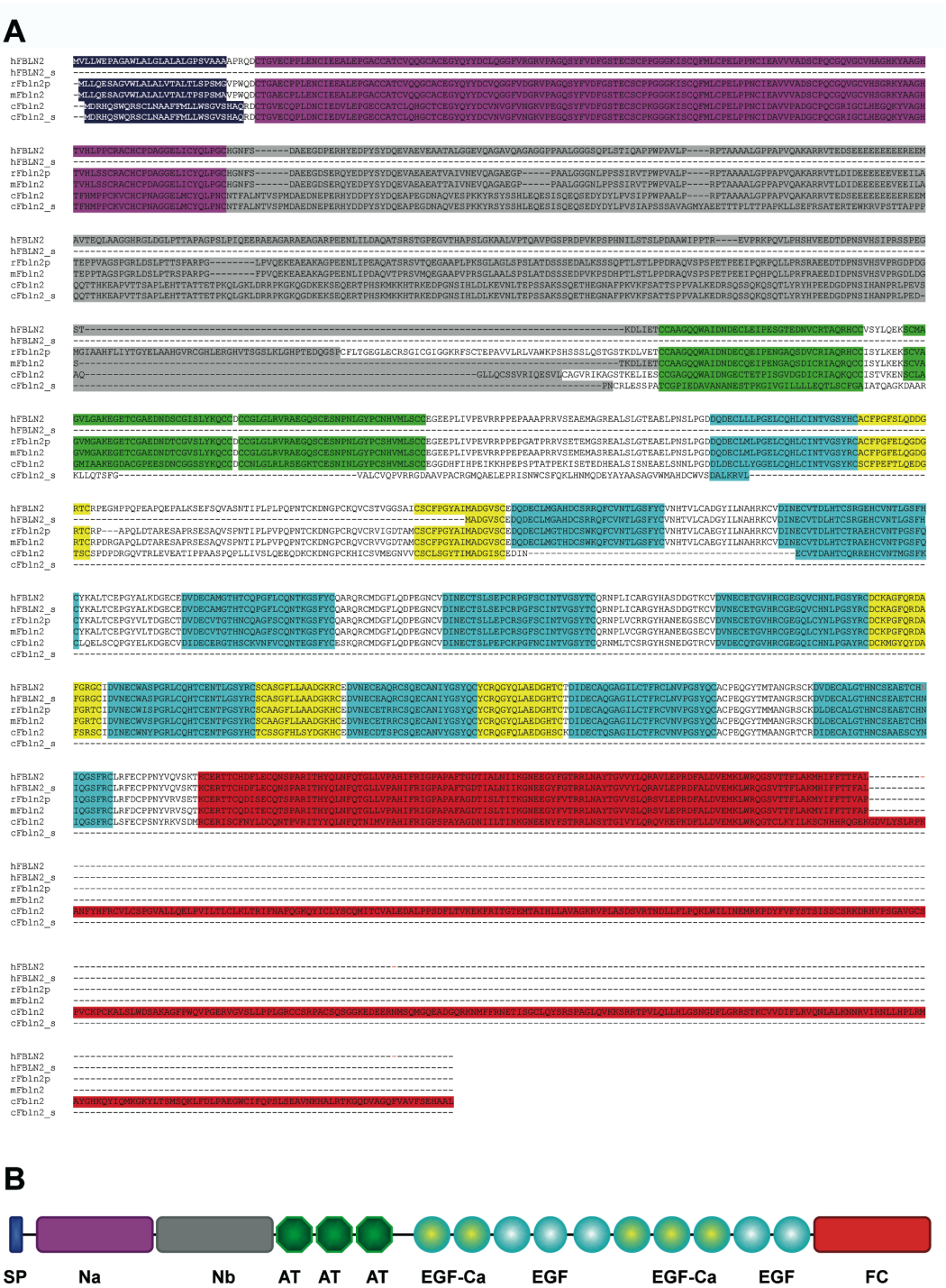

Fig 5.3. Fibulin 2 is a modular protein. Aminoacid alignment of several Fibulin2 proteins , including a human Fibulin2-short (hFBN2_s), very similar with cFibulin2-short; The Fibulin Modules are color coded, both in the alighnment (**A**) and schematic domain structure (**B**).

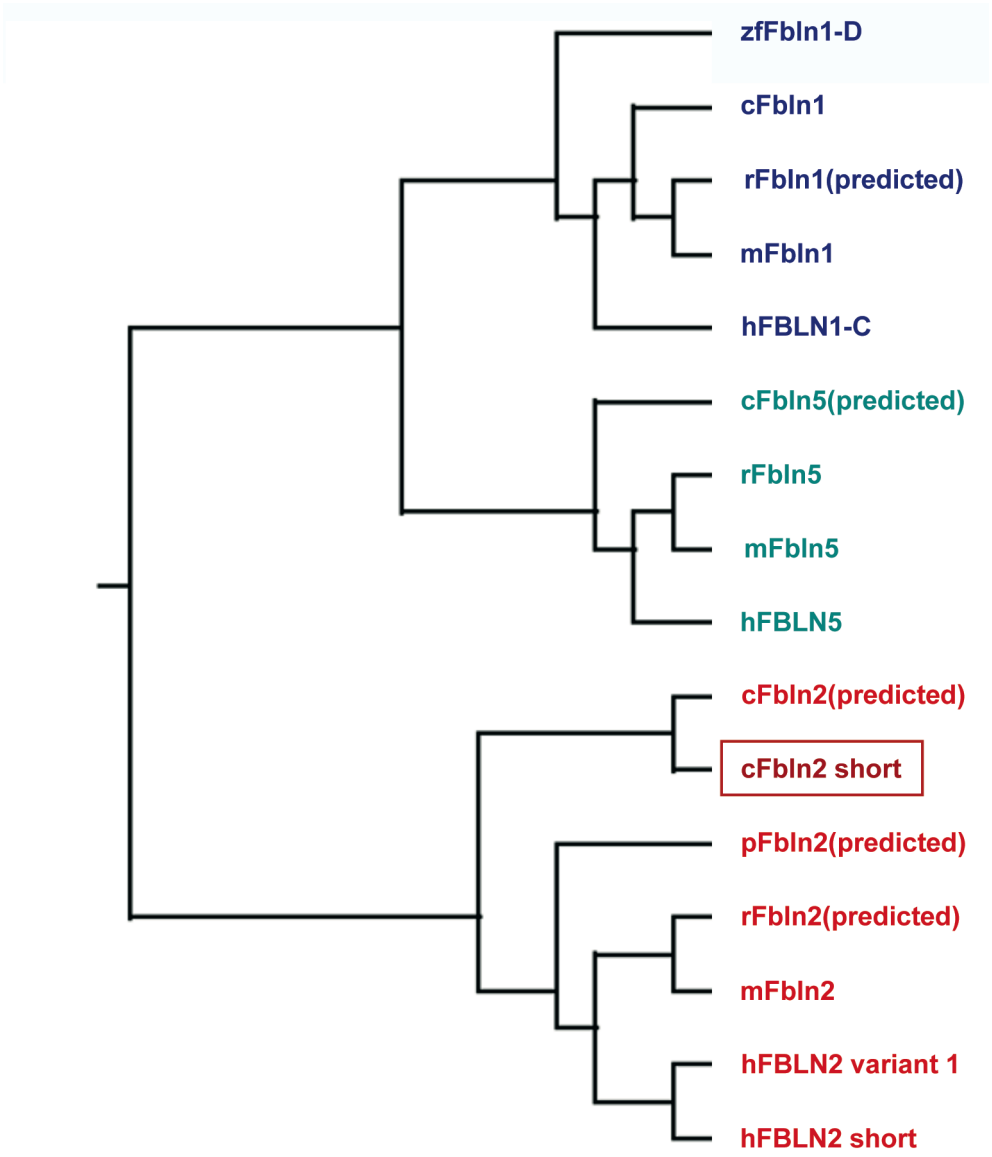

Fig 5.4 Filogenetic tree of fibulin1, fibulin2 and fibulin5 present in various species. Fibulin2-short and other Fibulin 2 protein sequences were compared with other fibulin family members, Fibulin 1 and Fibulin 5. Only a few sequences were selected for the analyses and those were zebrafish fibulin1-D (zfFbln1-D), chick Fibulin1 (cFbln1) predicted rat Fibulin1 (rFbln1), mouse Fibulin1 (mFbln1), human Fibulin1-C (hFBLN1-C), predicted chick Fibulin5 (cFbln5), rat Fibulin5 (rFbln5), mouse Fibulin5 (mFbln5), human Fibulin5 (hBBLN5), mouse Fibulin 2 (mFbln2), human Fibulin 2 (hFBLN2 variant1), a human short version of Fibulin2 (hFBLN2short) and the predicted Fibulin 2 from chicken (cFbln2 predicted), rat (rFbln2predicted) and chimpanzee (pFbln2predicted).

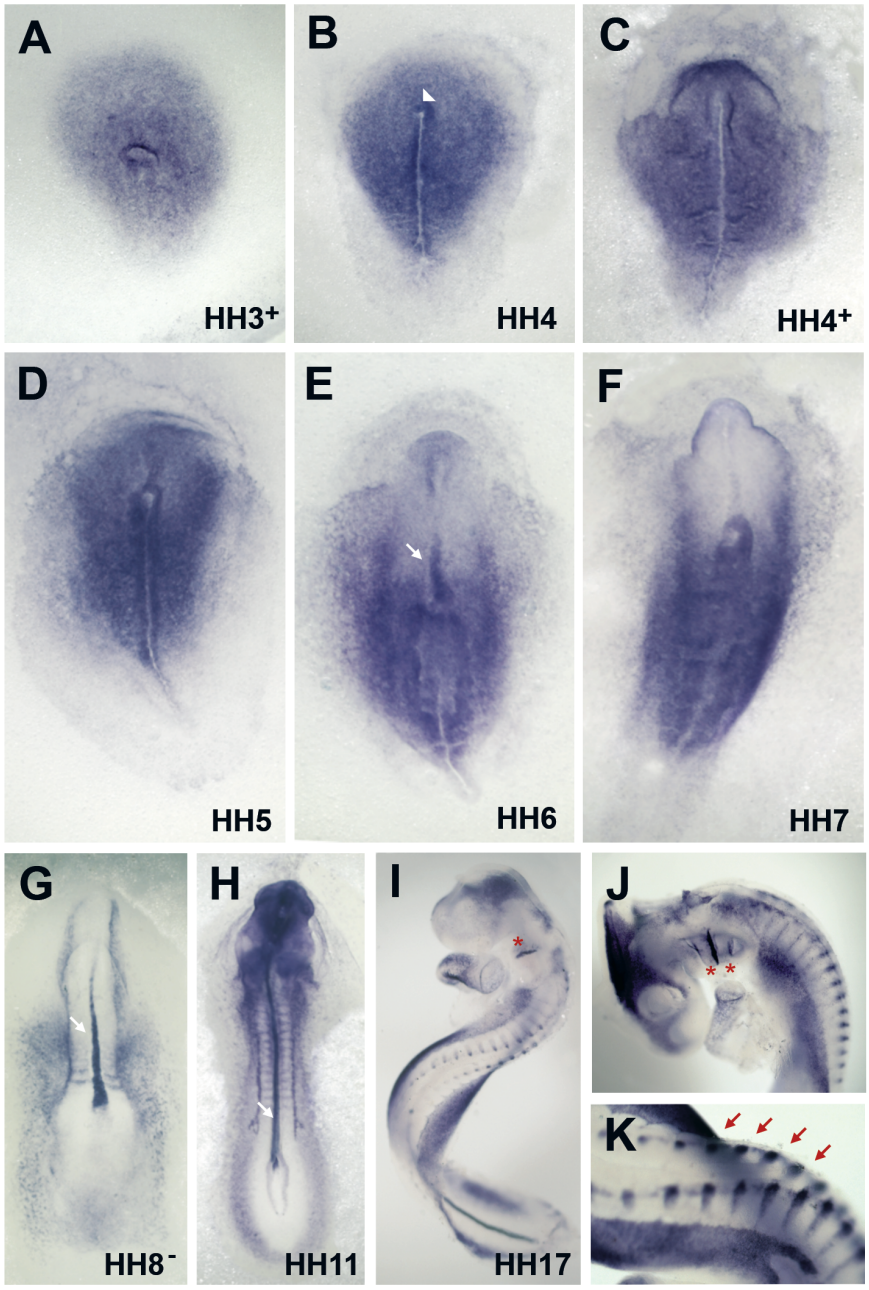

Fig 5.5. *Fibulin2* expression pattern in the developing chick embryo. At stage 3^+ expression is detected in the epiblats epiblast (**A**); By stage 4, expression is excluded from the primitive groove but is present in the primitive ridges and Hensen's node (**B**, white arrowhead); Fibulin 2 is then expressed in the mesodermal wings of the lateral plate (**C**), in the emerging head process (**D**) and in the notochord (**E-H,** white arrow). From stage 6 onwards expression starts to clear from the anterior ectoderm, leaving a fringe of expressing cells at the anterior and lateral borders of the neural plate (**E-G**). From stage 7^+ the expression completely clears from the neural plate and becomes restricted to the notochord, somites and border of the neural plate (**G**). At stage 11 strong expression is observed in the anterior ectoderm and prosencephalon, notochord, somites and a dorsal domain of the intermediate mesoderm (**H**). Later in development *fbln2* is strongly expressed in the branchial arches (red asterisks,**I and J**), lateral mesoderm and myotome (red arrows, **I-K**).

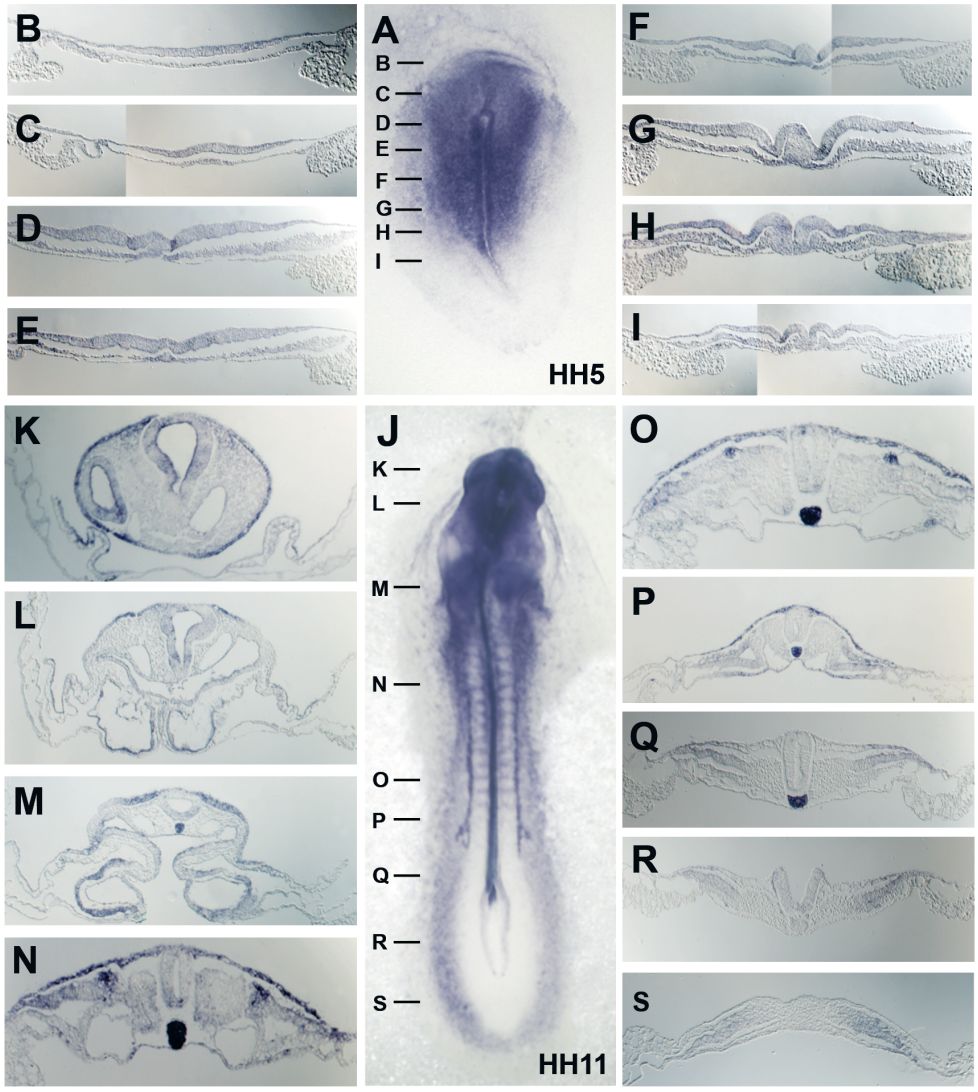

Fig 5.6. Expression of *Fibulin2* in the chick embryo. Expression at stage 5 (**A**) and sections through the embryo (**B-I**); Expression at stage 11 (**J**) and respective sections (**K-S**).

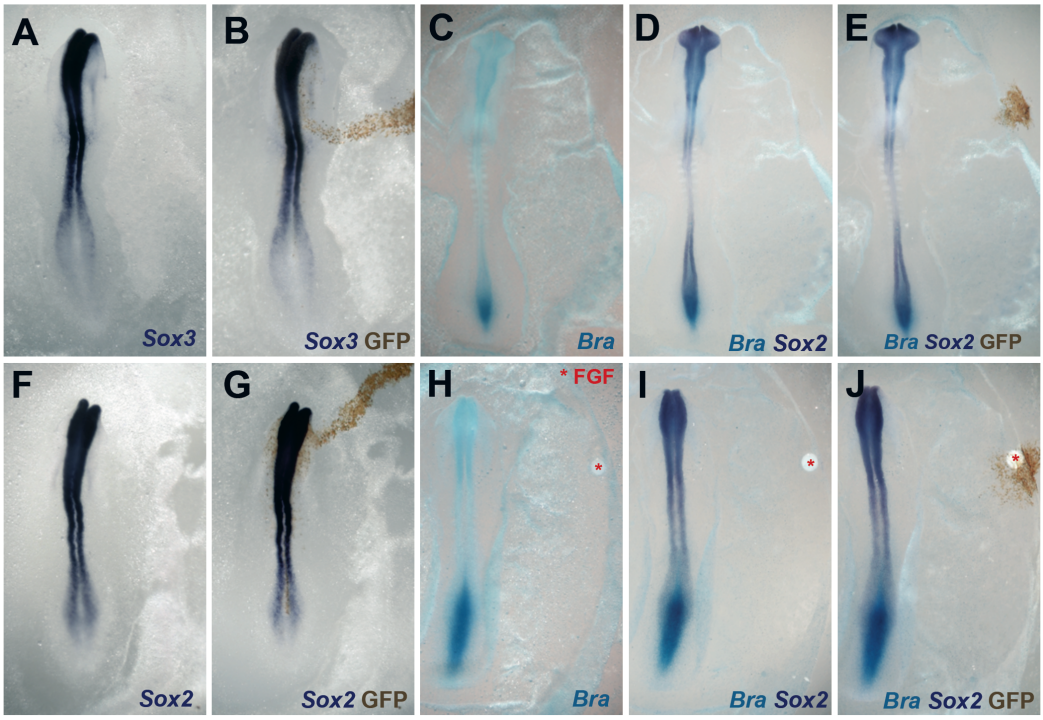

Fig 5.7. *Fibulin2-short* is unable to induce the neural markers Sox3 and Sox2. When electroporated as a line extending from the embryo to the area *opaca*, *fibulin2-short* is unable to induce either *Sox3* (**A** and **B**) or *Sox2* (**F** and **G**). Missexpression in the area *opaca* also results in no *Sox2* induction (**D** and **E**), even when combined with FGF8b (**I** and **J**). No *Brachyury* is induced in the experiments (**C**-**E** and **H**-**J**).

Chapter 6

nhbr307: Calreticulin

Introduction

Calreticulin was first isolated in mammals over thirty years ago (MacLennan et al., 1974; Ostwald and MacLennan, 1974), and this was followed by molecular cloning of the protein from rabbit skeletal muscle (Fliegel et al., 1989a; Fliegel et al., 1989b; Smith et al., 1989). Subsequently, genes encoding Calreticulin were identified in several vertebrates (Liu et al., 1993; Mazzarella et al., 1992), invertebrates (Hawn et al., 1993; Huggins et al., 1995; Jaworski et al., 1996; Khalife et al., 1993a; Khalife et al., 1993b; Labriola et al., 1999) and also in plants (Chen et al., 1994a; Crofts et al., 1998; Dresselhaus et al., 1996; Kwiatkowski et al., 1995) and protozoans (Labriola et al., 1999; Navazio et al., 1998), but no *calreticulin* gene has been found in yeast or prokaryotes.

Molecularly, Calreticulin is a 40-46kDa protein with an N-terminal signal sequence and a C-terminal Endoplasmic Reticulum retrieval sequence (KDEL) (Denning et al., 1997; Fliegel et al., 1989a). Structural predictions suggest that the protein has three domains (Denning et al., 1997; Fliegel et al., 1989a; Michalak et al., 1992) (known as N-, P- and C-domains). The N-domain is highly conserved amongst all known Calreticulin molecules. The P-domain is proline-rich, sharing similarity in aminoacid composition with the Calcium modulator proteins Calnexin and Calmegin (Michalak et al., 1999). This domain contains a high affinity, low capacity Ca^{2+}-binding site (1 mol Ca^{2+}/mol of protein, $K_d \approx$ 1μM). The C-domain is rich in acidic aminoacids (aspartic and glutamic acid) and contains a low-affinity/high capacity Ca^{2+}-binding site (25 mol Ca^{2+}/ mol protein $K_d \approx$ 250μM) (Coppolino and Dedhar, 1998).

The protein appears to fulfil many cellular functions, both within and outside of the ER. In the ER lumen it performs two major functions: chaperoning and regulation of Ca^{2+} homeostasis (Mery et al., 1996; Wada et al., 1994). Calreticuln is a highly versatile lectin-like chaperone (Hebert et al., 1995; Peterson et al., 1995; Spiro et al., 1996) and it

participates in the synthesis of a variety of molecules, including ion channels, surface receptors, integrin and transporters. The protein also affects intracellular Ca^{2+} homeostasis by modulation of ER Ca^{2+} storage and transport. Upregulation of Calreticulin leads to numerous effects in different experimental models, including increased Ca^{2+} storage capacity of the ER (Mery et al., 1996), modulation of cell adhesion (Leung-Hagesteijn et al., 1994), modulation of store-operated Ca^{2+} influx (Mery et al., 2005; Mery et al., 1996), increased propensity to apoptosis (Knee et al., 2003), modulation of steroid sensitive gene expression (Burns et al., 1994) and modulation of the function of another ER calcium pump, SERCA2 (John et al., 1998). In cell culture, downregulation of Calreticulin causes changes in cell adhesion (Coppolino et al., 1997; Rauch et al., 2000), increased resistance to apoptosis (Nakamura et al., 2000), abnormal accumulation of misfolded proteins (Knee et al., 2003), modulation of Ca^{2+}-dependent gene transcription (Mesaeli et al., 1999) and inhibition of agonist-dependent Ca^{2+} release from ER stores (Mesaeli et al., 1999).

However, little is known about the functions of Calreticulin during development. Mouse mutants defective in *calreticulin* die at E14.5 (Mesaeli et al., 1999) with impaired cardiac development and problems in Ca^{2+}-dependent transcriptional pathways (Guo et al., 2002; Mesaeli et al., 2001; Mesaeli et al., 1999). Mutant mice also present brain and body wall defects (Rauch et al., 2000). A zebrafish *calreticulin* homologue was first isolated in a screen for genes whose expression is dependent on Cyclops signalling (a Nodal homologue) but no function was assigned to it (Rubinstein et al., 2000). A subsequent study found that inhibition of the ER Calcium pump during early gastrulation induces cyclopia, phenocopying some of the defects seen in *cyclops*, *squint*, *one-eyed pinhead* and *silberblick* mutant embryos (which have defects in Nodal or Wnt signalling). By contrast, inhibition during mid-gastrulation induces tail defects similar to those observed in *no-tail* (*brachyury*) mutant embryos (Creton, 2004). However since these studies rely on pharmacological inhibition of the ER Ca^{2+} pump, there is no direct evidence that Calreticulin is involved in these processes.

This Chapter reports the cloning, molecular and functional characterization of chick *calreticulin* (*cCrt*) during early development. *cCrt* is expressed in Hensen's node and evidence is provided that its product can be secreted. When misexpressed alone or in combination with FGF8, *Chd*, *Smad6* and/or *Smad7* it is unable to induce the neural marker *Sox2* in competent epiblat of the *area opaca*, although it can expand the neural ectoderm in a similar manner to that observed for BMP antagonists, raising the possibility that Calreticulin acts, directly or indirectly, as a BMP antagonist.

Materials and Methods

Isolation of a full-length clone of chick *calreticulin* (*cCrt*)

The original *nhbr307* clone was used to transcribe the radiolabelled RNA probe used for library screening (for details on the procedure refer to Chapter 2).

Database searches

Homologous sequences from other species were obtained from GenBank. The sequence of fulllength chick *calreticulin* was BLASTed against a Database of Expressed Sequence Tags (dbEST) http://www.chick.umist.ac.uk/ and against the chicken genome using the Ensembl Genome Browser http://www.ensembl.org/Gallus_gallus/index.html. Alignments were performed using ClustalW software and Phylogenetic Trees constructed with TreeView. Tools within Prosite http://www.expasy.org/prosite/ were used to analyse motifs in the protein.

Sub-cellular localisation in COS cells

The open reading frame of *calreticulin* was cloned in pCDNA 3.1/Myc-His (Invitrogen), using the *NotI* and *BamHI* cloning sites. Inserts were generated by PCR using the primers GATCGCGGCCGCATGAGCCGCCTCTGCCTCCCG (adds a *NotI* restriction site prior to the start codon) and GATCGGATCCTCTTCCTCTCAGCCTCC (removes the stop codon from *calreticulin* and adds a BamHI restriction site) and pfuTaq polymerase (Promega) (94°C, 2 minutes; 42°C, 2 minutes; 72°C, 2 minutes; 30 cycles). After digestion of both the PCR fragment and the pCDNA vector with *NotI* and *BamHI*, the DNAs were gel purified using a gel extraction kit (Promega) and ligated with T4 ligase (Promega). The resulting plasmid (*cCrt-Myc*) was checked by sequencing.

$1x10^5$ COS-1 cells were plated in a 35 mm cell culture dish, grown in DMEM containing 10% new born calf serum and transfected with the *cCrt-Myc* construct using Lipofectamine Plus (Gibco). No DNA was used to produce the "Mock transfected" control cells. After 48 hours in culture, the cells were rinsed in PBS and fixed in 4% paraformaldehyde for 30 minutes at room temperature. After washing again in PBS (3x10 minutes), the cells were blocked in PBS containing 0.05% Triton X-100 and 1% goat serum for 30 minutes at room temperature and incubated in anti-myc monoclonal antibody supernatant (1:1 in blocking buffer) overnight at 4°C. The following day, cells were

washed with PBS (5x5 minutes) and incubated in anti-mouse IgG-HRP (Jackson; 1:2500 in blocking buffer) overnight at 4°C. After washing (5x15 minutes in PBS), the cells were rinsed twice with 100 mM Tris pH7.4 and incubated in 0.5 mg/ml DAB for 5 minutes. H_2O_2 was added (0.003%) and the colour developed in the dark. After stopping the reaction with tap water, the cells were fixed with 4% paraformaldeheyde and mounted on a slide. In some experiments anti-calreticulin antibody was used (GαCrt; 1:2500, kind gift of Prof. Michal Michalak); cells were blocked in PBS containing 0.05% Triton X-100 and 1% calf serum and immunoreactivity detected with rabbit anti-goat HRP (Invitrogen; 1:5000).

Western Blotting

$1.5x10^5$ COS-1 cells were transfected with *cCrt-Myc* as described above. A *BMP4* expression construct (Liem et al., 1995) was used as a control. After 24 hours, the culture medium was changed to DMEM with no additives and the cells cultured for another 24 hours. After culture the medium was collected ("secreted fraction") and the cells rinsed twice with PBS and centrifuged at 1100rpm for 5 minutes. The supernatant was discarded and the pellet lysed in PBS with 1mM EDTA, 0.1% Triton X-100, 40 µg/ml PMSF, 5 µg/ml Leupeptin and 1 µg/ml Pepstatin for 30 minutes at 4°C. 1 µl of DNAse was then added for 10 minutes, at room temperature, and the lysis product centrifuged at 10,000 rpm for 10 minutes at 4°C. The supernatant was collected ("lysate").

20 µl of secreted fraction or lysate were boiled at 95°C with 2x SDS-PAGE loading buffer (260 mM Tris pH6.8, 12% w/v SDS, 20% v/v 2-mercaptoethanol, 40% v/v glycerol) for 3 minutes and then centrifuged at 13000 rpm for 3 minutes. The samples were run on 15% SDS-PAGE gels under denaturing and reducing conditions (SDS-running buffer: 0.303% w/v Trizma base, 1.44% w/v glycine, 0.1% w/v SDS). Proteins were transferred onto nitrocellulose membranes (Amersham) and blocked for 2 hours in 4% milk powder in TBST. The membranes were incubated in the primary antibody overnight at 4°C, washed in TBST (3x10 minutes) and incubated in the secondary antibody, goat anti-mouse IgG-HRP (1:2500) overnight at 4°C. The membranes were washed again with TBST (3 x 10 minutes) and detected by chemoluminescence.

Chick *in situ* hybridisation

The full-length clone of *calreticulin* was used to transcribe a digoxigenin-labelled RNA probe. The procedure followed is given in Chapter 2.

Zebrafish embryo collection and *in situ* hybridisation

Breeding fish were maintained at 28.5°C on a 14 hour light/10 hour dark cycle in the UCL Anatomy fish facility (Masa Tada kindly provided the fish). Embryos were collected from the colony by natural spawning, raised in 10% Hank's saline (137 mM NaCl, 5.4 mM KCl, 1.3 mM $CaCl_2$, 1.0 mM $MgSO_4$, 0.25 mM Na_2HPO_4, 4.2 mM $NaHCO_3$) at 28°C and staged. Embryos were fixed in 4% paraformaldehyde in PBS, either overnight at 4°C or for 2 hours at room temperature. After removal of the chorion, the embryos were stored in 100% methanol at –20°C.

In situ hybridisation was performed according to protocols in current use in the Wilson lab. Embryos were rehydrated through 75%, 50% and 25% methanol in PTW (PBS/0.1% Tween-20), washed (4x 5 minutes) in PTW at room temperature, treated for 20 minutes with proteinase K (10 µg/ml) and re-fixed in 4% paraformaldeheyde for 20 minutes. After washing five times with PTW (5 minutes), the embryos were preincubated in hybridization mix (50% formamide, 5x SSC pH 6.0, 50 µg/ml yeast RNA, 50 µg/ml heparin, 0.1%Tween-20) at 65°C for 2 hours and then hybridised overnight in fresh hybridisation mix containing 100 ng of digoxigenin-labelled RNA.

Following hybridisation, the embryos were washed (3x 10 minutes) with 25% hybridisation mix in 2xSSC, once in 2xSSC and twice with 0.2xSSC (30 minutes each wash) at 65°C. The following washes were performed at room temperature and consisted of 5 minutes each in 75%, 50%, 25% 0.2x SSC in PTW and then PTW. After blocking for 2 hours at room temperature in PTW containing 2% sheep serum and 2 mg/ml BSA, the embryos were incubated overnight in anti-DIG-AP antibody (Roche) 1:5000 (in the same blocking solution). The next day, embryos were rinsed in PTW and washed 6-10 times for 15 minutes in PTW with gentle agitation. This was followed by three 5-minute washes in alkaline phosphatase reaction buffer (0.1 M Tris/HCl, pH 9.5, 50 mM MgCl2, 0.1 M NaCl, 0.1% Tween-20). The colour reaction was carried out with NBT/BCIP as described for the chick *in situ* protocol (Chapter 2). The embryos were mounted in 70% glycerol.

Whole mount immunocytochemistry

Embryos were collected in PBS and fixed overnight in 4% paraformaldeheyde containing 2 mM EGTA at 4°C. Embryos were then washed in PTW (3 x 30 minutes) and blocked in TBST containing 5% heat inactivated calf serum and 1mg/ml bovine serum albumin prior to incubation overnight at 4°C in goat anti-Calreticulin (1:2500). Embryos were then washed in PTW (3x 1 hour) and incubated overnight at 4°C in the secondary antibody rabbit anti-goat HRP (Invitrogen; 1:5000). Following 3 washes (one hour each) the

embryos were rinsed with 100mM Tris pH7.4 and incubated in 0.5 mg/ml DAB for 10 minutes, H_2O_2 (0.003%) added and the embryos fixed and stored as described above.

Electroporation constructs

The coding region of chick *calreticulin* (*cCrt*) was cloned in pCAβ-IRES-GFP (a kind gift from A. Lumsden Lab) between the ClaI and BamHI cloning sites. Zebrafish *calreticulin* (*fCrt*) (Rubinstein et al., 2000) was cloned in pCAβ-IRES-GFP between the BsmBI and BamHI cloning sites. The *BMP4* and *Smad6* constructs in pCAβ-IRES-GFP were as described in Chapter 3.

Results

Cloning of the full length nhbr307: chick *calreticulin* (*cCrt*)

The *nhbr307* clone did not contain an entire open reading frame (ORF). Screening a chick stage 2-4 whole embryo cDNA library led to the isolation of a 1162 base pair sequence containing a 1116 bp ORF, a 40 bp long 5' Untranslated Region (UTR). **Fig 6.1A** shows the predicted ORF and corresponding translation into a 381aa protein. This sequence is identical at the aminoacid level (differing by only two nucleotides) to "chick Calreticulin" deposited in current databases (Genbank accession number AY393845, Uniprot Q6EE32) except that the 3' 69 nucleotides (C-terminal 23 aminoacids) of the latter are missing, and both sequences lack the characteristic KDEL sequence found in Calreticulin family members in other species (**Fig 6.1**).

When comparing Calreticulin with other related calcium binding proteins Calnexin (NM_0010309620) and Calmegin (Predicted, XM_420413) it was found that although there is considerable divergence in the amino- and carboxy-termini between the proteins, the central P domain is very conserved. The P domain of Calreticulin is 59% identical to that of Calnexin and 52% identical to the Calmegin central region (not shown).

Northern blot analyses of RNA isolated from chick embryos at stages 3, 5 and 7 reveal the presence of a major transcript of about 1.3 Kb and two larger minor bands (~1.9 and 3.5 Kb) (**Fig 6.1 B**). However there is no published evidence of alternative splicing for *calreticulin* (Michalak et al., 1999) nor are any splice variants apparent from analysis of the intron-exon structure.

The predicted 404 aminoacid (Uniprot Q6EE32) protein sequence was run through several databases all of which pointed to Calreticulin: Prosite BLOCK, Prints and Pfam databases identified the sequence as belonging to the Calreticulin family, with the characteristic amino terminal signal sequence, the Calreticulin family signature 1 (KHEQNIDCGGGYVKLF), the Calreticulin family signature 2 (IHFGODICG) and the characteristic family repeats A (PXXIXDPDAXKPEDWDE) and B (GXWXPPXIXNPXYX). In terms of secondary structure, the protein is divided into three domains, N-domain, P-domain and C-domain (**Fig 6.1 A** and **C**, in blue, red and green, respectively).

Calreticulin is a conserved molecule

Since it was first isolated from rabbit skeletal muscle (Fliegel et al., 1989a; Smith et al., 1988), many other *calreticulin* genes have been isolated and characterised. To compare chick Calreticulin (cCrt) with Calreticulin proteins from other species, ClustalW alignments were performed. Given the large number of sequences in the NCBI database, only a few were chosen for this comparison: human Calreticulin (hCALR, NM_004343), mouse Calreticulin (mCalr, NM_007591), rat Calreticulin (rCalr, NM_022399), *Xenopus* Calreticulin (xCalr, BC046699), zebrafish Calreticulin (zCalr, NM_131047) and *Drosophila* Calreticulin (dCrt, NM_079569). The alignments reveal a high homology between the sequences analysed, particularly within the Calreticulin family signature 1, signature 2 and the characteristic family repeats A and B (**Fig 6.2 A**). A dendogram obtained from these sequences is shown in **Fig. 6.2 B**.

Chicken related sequences

Although Uniprot, Genbank and EBI databases contain entries for chick *calreticulin*, no corresponding sequence can be found, at the present date (February 2011), in the chick genome database (www.ensembl.org). A portion of the sequence (91 nucleotides long) can be found in an "unassigned" (Un) chromosome but this region has not been assembled completely and the sequence lies at the end of a contig which is followed by a gap. However, other related sequences can be found in chomosome 4 (*Calmegin*; ENSGALT00000015978), chromosome 13 (*Calnexin*; ENSGALT00000009563) and chromosome 28 (3625650-3664309) which share some similarity with *cCrt* (not shown).

Calreticulin protein localises to the endoplasmic reticulum, but can also be secreted

The cellular localisation of the protein was predicted using Psort software (Horton and Nakai, 1997) http://www.psort.org/. This reveals a probability of 0.667 of secretion to the extracellular space, whereas the probabilities of being located in the cytoplasm, vacuoles or endoplasmic reticulum were of 0.111 in each case. The SOSOI prediction of transmembrane regions in a protein, http://sosui.proteome.bio.tuat.ac.jp/sosuiframe0.html, predicts cCrt to be a soluble protein, with an average of hydrophobicity of -0.974394. However, Calreticulin has been reported in other species as an endoplasmic reticulum resident protein (Gelebart et al., 2005). In fact Calreticulin characteristically ends with a KDEL ER retrieval sequence (reported in all but *Oncocera volvulus* Calreticulin).

Because prediction analyses suggest it to be a secreted protein, whereas published data point to ER localisation, myc tagged *cCrt* was transfected into COS-1 cells and the accumulation of the produced protein detected using either *anti*-myc or *anti*-Calreticulin antibodies. In both cases, signal is detected in perinuclear granules (**Fig 6.3 A** and **C**). Western blots were also performed from the transfected COS cells; the culture medium and cell lysate were collected separately. Calreticulin was found in both fractions (**Fig 6.9 A**), confirming that it can indeed be secreted from cells.

Expression pattern of *Calreticulin* (*cCrt*) in the chick

To assess the expression of *calreticulin* at early stages of development in normal chick embryos, both whole mount *in situ* hybridisation, using the full length *cCrt* clone, and whole mount antibody staining were performed. At the mRNA level (**Fig 6.4 A-F**), transcripts are first detected at stage 3-3$^+$ (**Fig 6.4 A**) and the signal is strongest in the anterior half to one-third of the primitive streak. At stages 4$^+$-5 expression becomes concentrated in Hensen's node, with a lower level of expression seen in the anterior epiblast (**Fig 6.4 B, C**). Expression is maintained in the node and from stage 7 onwards it is markedly asymmetric, with expression on the right side (**Fig 6.4 D-E**; inset **D'**). At this stage expression begins in the neural plate, always more pronounced anteriorly (**Fig 6.4 E-F**); this increases at stage 9. From stage 10 onwards, expression becomes ubiquitous (not shown).

Antibody staining only produces a weak signal, but also reveals accumulation of Calreticulin protein in the primitive streak from stage 3$^+$ (**Fig 6.4 G-J**) as well as the asymmetry in the node at stages 7 and 8 (**Fig 6.4 I** and **J**; inset **J'**).

Expression pattern of *Calreticulin* (*fCrt*) in Zebrafish

For comparison, *in situ* hybridisation was also performed in zebrafish using the full-length zebrafish clone. At shield stage expression is present in the shield (**Fig 6.5 A1**). Expression persists at the midline and most anterior part of the embryo through epiboly and tail bud stages (**Fig 6.5 B-D**). By the 3 somite stage, expression starts to become ubiquitous, although remaining stronger anteriorly (**Fig 6.5 E1** and **E2**). Therefore expression of this gene in zebrafish embryos is comparable to the results obtained for the chick.

Misexpression of *Calreticulin* expands the neural plate

Since *calreticulin* is expressed in Hensen's node during gastrulation and appears to be secreted, can it induce ectopic expression of neural markers? To answer this, *pCAβ-cCrt-IRES-GFP* was electroporated into the epiblast of stage 3+ chick embryos in a line extending from the node to the area *opaca* (**Fig 6.6 A**). *cCrt* overexpression causes an expansion of expression of neural plate markers into the non-neural ectoderm in 7/15 (46.7%) of embryos stained for *Sox3* (**Fig 6.6 D-E**) and 9/20 (45%) of embryos tested for *Sox2* (**Fig 6.6 F-G**). In addition to neural plate markers, the expression of neural plate border markers was also analysed. *msx1* was expanded in 5/12 (41.7%) cases (**Fig 6.6 H-J**) as was *Dlx5* in 6/12 (50%; **Fig 6.6 J-K**), *Pax7* in 6/10 (60%; **Fig 6.6 L-M**) and *BMP4* in 5/11 (45%; **Fig 6.6 B-C**). However, *Slug* is mainly downregulated, especially posteriorly (3/7 - 43%; **Fig 6.6 N-O**). Notably, in all of the embryos showing an expansion of neural plate or border markers, this effect never extended to the area *opaca*.

Since the *cCrt* clone lacks the C-terminal sequence including the KDEL domain, the zebrafish orthologue *fCrt*, which includes a terminal KDEL domain, was used in the same experiment. Similar results were obtained. *fCrt* overexpression caused an expansion in the expression of *Sox3* in 5/9 (55%) and *Sox2* in 4/10 (40%) embryos tested (not shown).

Therefore, ectopic *cCrt* can expand the neural plate including its border. This is reminiscent of the action of the BMP inhibitors *Chordin*, *Noggin*, *Smad6* and *Smad7* when misexpressed in a similar way (see Chapter 3 and (de Almeida et al., 2008; Linker et al., 2009; Linker and Stern, 2004; Streit and Stern, 1999a{de Almeida, 2008 #2383).

Misexpression of *Calreticulin* cannot induce neural markers in the area *opaca*

To test whether *Calreticulin* missexpression can induce the competent epiblast of the area opaca to acquire expression of neural markers, *pCAβ-cCrt-IRES-GFP* was electroporated into a discrete domain within the inner third of the area *opaca* of stage 3+ chick embryos, at approximately the level of Hensen's node (**Fig 6.7A**). After incubation for 15-20hrs, no expression of *Sox3* (0/5, not shown) or *Sox2* (0/8; **Fig 6.7 C-D**) was observed in the electroporated region. As a control, similar electroporations were performed using the *pCAβ-IRES-GFP* without an insert, resulting in no effect on *Sox3* (0/5) or on *Sox2* (0/4) expression (not shown).

FGF signalling is required for initial induction of *Sox3* as well as for cells to respond to BMP antagonists, which maintain *Sox3* expression (Streit et al., 2000a; Streit et al., 1998; Wilson et al., 2000). However, although FGF in combination with BMP antagonists can maintain *Sox3* expression, it does not induce *Sox2* (Linker and Stern, 2004; Streit et al., 1998). Misexpression of FGF8 with c*Crt* also fails to induce *Sox2* in the area *opaca* in all the embryos tested (0/10; **Fig 6.7 E-F'**). However, *Calreticulin* did not maintain FGF-induced *Sox3* expression (0/14; not shown). *Calreticulin* was also unable to induce *Sox2* in the presence of both *Chordin* and FGF8 (0/10; **Fig 6.7 G-H'**). Even a combination of FGF8 and *Calreticulin*, together with BMP antagonists *Chordin* (Streit et al., 1998), *Smad6* (Imamura et al., 1997) and *Smad7* (which inhibits both BMP and activin/nodal-related signals; (Casellas and Brivanlou, 1998) is unable to induce *Sox2* (0/14; **Fig 6.7 I-J'**) in competent epiblast. These results show that *Calreticulin*, either alone or in combination with FGF and BMP inhibitors, is unable to induce *Sox2* in a domain isolated from the host's neural plate.

Calreticulin may inhibit BMP signalling

The results presented above raise the possibility that *cCrt* may be acting by inhibiting *BMP* signals. When *BMP4* is misexpressed by electroporation in the prospective neural ectoderm of the chick embryo at stage 3$^+$, both *Sox3* and *Sox2* are downregulated after overnight culture (Linker and Stern, 2004). To test whether *cCrt* could rescue the effects of *BMP4* overexpression, the two constructs were co-electroporated into prospective neural ectoderm adjacent to the node at stage 3$^+$ (**Fig 6.8 A**). A DNA pool with a minimum concentration of 0.7µg/µl of *pCAβ-BMP4-IRES-GFP* was needed to inhibit *Sox3* in all the embryos tested (11/11; **Fig 6.8 B-C**). 2.5µg/µl of *cCrt* plasmid was required to rescue this phenotype in 55% of the embryos (11/20, **Fig 6.8 H-I**). *Smad6* was used as a control BMP inhibitor; 2 µg/µl of this are able to rescue the *BMP4* effect in 58% of the embryos analysed (7/12; **Fig 6.8 D-E**). These results are consistent with the hypothesis that cCrt might act as a BMP inhibitor.

Calreticulin secreted by COS cells expands the neural plate

It has been reported that Calreticulin localizes mainly to the ER, but a fraction of the protein is secreted (**Fig 6.9 A**). This conclusion is supported by the results of Western blots presented above. However, these experiments do not address whether the secreted Calreticulin is biologically active in the assays described above, which suggested some BMP inhibiting activity. To test whether extracellular Calreticulin could account for the

above results, *myc*-tagged *cCrt* was used to transfect COS cells and pellets of these grafted adjacent to the non-neural epiblast next to the prospective neural plate of stage 3+ chick embryos, a region where misexpression of BMP inhibitors can expand the neural plate (see Chapter 3). In 3/11 (27%) embryos tested, an expansion of *Sox2* expression was detected in the epiblast above the grafted cells (**Fig 6.9 C-C'**); no expansion of the neural plate was seen when mock-transfected cells were implanted (0/6; **Fig 6.9 B-B'**). This result suggests that extracellularly presented Calreticulin can expand the neural plate into the non-neural ectoderm but the effect is weaker than with Chordin (Streit et al., 1998), consistent with the conclusion that Calreticulin may act, directly or indirectly, as a weak BMP antagonist.

Discussion

Calreticulin fullfils the criteria of the screen

Calreticulin was cloned from a screen for secreted factors from the chick organiser at stage 3^{+}-4 (Chapter 4). *In situ* hybridisation performed with the full-length clone shows that it is expressed in the chick node. *In situs* performed in zebrafish with the fish homologue confirm the expression of *calreticulin* in the node. Moreover, because the protein has a sequence likely to function as a signal peptide at its amino terminal, prediction analyses pointed to it being secreted and both Western blots and the results of implantation of transfected COS cells strongly suggest that the protein is secreted. Therefore, *Calreticulin* fullfils the criteria of the screen.

Calreticulin and the border of the neural plate

Calreticulin is expressed at the right time and in the right place to be a neural inducer. Furthermore, a fraction of the protein is secreted. But is it a neural inducer? The misexpression experiments performed led to expansion of the neural plate into the adjacent non-neural epiblast of the area *pellucida*, together with expansion of the neural plate border markers *msx1*, *Dlx5*, *Pax7* and *Slug*. The normal domains of expression of these border markers overlaps to a large extent with the domain of expression of *BMP4* at stages 5-7, and it has previously been suggested that both *msx1* and *Dlx1*, as well as *Slug* and *Pax7* are induced by a threshold of BMP signalling (Streit and Stern, 1999a; Tribulo et al., 2003). These results suggest that Calreticulin may be modulating BMP signals, perhaps contributing with other endogenous BMP antagonists in establishing the interface between the neural and the non-neural ectoderm and thus, positioning the neural plate border.

Calreticulin is not an early neural inducer

When grafted into the inner third of the area *opaca* the organiser can induce a full cascade of events that culminate in formation of an ectopic neural plate. Many studies have been performed in order to dissect the molecular components of this cascade, with FGF having been put forward as the initial step (Alvarez et al., 1998; Kim and Nishida, 2001; Minokawa et al., 2001; Storey et al., 1998; Streit et al., 2000a). BMP inhibition has also been widely reported as being the mechanism by which neural is achieved (the Default model is discussed in Chapter 1). Like other BMP antagonists when misexpressed in this region

(see Chapter 3), *Calreticulin* is unable to mimic the effects of a node graft in the area *opaca* either alone or in combination with FGFs and even with the BMP antagonists *Chd* and *Smad 6* and *Smad7* (the latter also inhibits activin/nodal-related signals). Therefore although *Calreticulin* is not a sufficient neural inducer, the present results suggest that it may be able to act as a relatively weak BMP antagonist, which might contribute, along with other BMP antagonists produced by the node, to the maintenance and/or stabilisation of early-induced markers and perhaps to positioning the border between neural and non-neural territories.

Calcium homeostasis may play a role neural induction

In addition to the more widely studied roles of BMP antagonists, FGF and more recently Wnt inhibition, a few studies point to an involvement of Calcium signalling, perhaps through L-type channels, in neural induction (Leclerc et al., 2000; Lee et al., 2009; Moreau et al., 1994)(references). However neither the mechanism of action nor the relationships between this type of signalling and the others mentioned above have been explored in detail, and it is probably fair to say that this mechanism has very largely been ignored. In particular, if Calcium signalling is indeed involved in neural induction, some important questions that have never been addressed include: how would Calcium be conveyed from the organizer to the responding tissue? What mechanisms might regulate the L-type channels in a non-cell autonomous manner? As a main intracellular function of Calreticulin is as a regulator of Ca^{2+} homeostasis regulator (Groenendyk et al., 2004), it is not improbable that it may function in a similar way upon secretion, perhaps as a "presenter" of Calcium to L-channels in the responding cells.

The evidence implicating Ca^{2+} signalling during neural induction in *Xenopus* is plentiful but rather indirect. At least two genes reported to be involved in early neural development can be activated by high intracellular levels of Ca^{2+}: (high $[Ca^{2+}_i]$): *Zic3* (Batut et al., 2003; Leclerc et al., 2003; Leclerc et al., 2000; Nakata et al., 1998) and *xMPL* (Batut et al., 2003). *Zic3* is a member of the Odd-paired domain family shown to be involved in neural determination in *Xenopus* (Marchal et al., 2009; Moreau et al., 1994; Moreau et al., 2008; Nakata et al.; Nakata et al.). When either intact *Xenopus* embryos or explants are treated with L-type channel inhibitors, the expression of *Zic3* is blocked (Batut et al., 2005; Moreau et al., 1994; Moreau et al., 2008). *xMPL* is expressed in the presumptive neural plate in *Xenopus* and encodes a substrate for protein kinase C (PKC). Its expression is activated by high $[Ca^{2+}_i]$ and can be induced by *noggin* overexpression (Batut et al., 2003). Noggin has been proposed to activate L-type channels (Leclerc et al., 1999). It has been proposed that an increase in $[Ca^{2+}_i]$ can neuralise animal cap ectoderm

(Leclerc et al., 2003); a mechanism for this has been proposed (Batut et al., 2005). According to the authors, neural inducing molecules including noggin could induce increase [Ca^{2+}_i] via activation of L-type channels in the dorsal ectoderm. This in turn would initiate a cascade of events where BMP signals may be inhibited, the early neural precursor *Zic3* is induced and culminates with the stable expression of neural genes (*En2*, *neurogenin* and *NCAM*). However, the proposed mechanism by which [Ca^{2+}_i] might regulate BMP signalling have not been elucidated, and since Noggin is known to bind BMPs directly in the extracellular space (Furthauer et al., 1999; Holley et al., 1996a; McMahon et al., 1998) it is difficult to understand why Calcium signalling might be needed to account for BMP inhibition.

The present results do provide a novel link between Calcium signalling and BMP inhibition, as well as revealing a source of the signals: the organiser itself, since the data obained here strongly suggest that *calreticulin* is expressed in the node and that a fraction of the protein is secreted. It could be that, when missexpressed, the secreted calreticulin binds to calcium and presents it to the L-type Ca^{2+} channel, leading to the increase in intercellular Ca^{2+} concentration. According to the model of Batut and colleagues (Batut et al., 2005), this would lead to expansion of the neural plate (which was indeed observed in the present experiments).

Could calreticulin play an additional role in the activation of L-type channels? An opportunity to answer this question arose serendipitously in the laboratory when a different screen, designed to identify early responses to signals from Hensen's node in the chick (the same screen that led to the identification of ERNI; see Chapter 1) identified one such gene, named *Calfacilitin*, which encodes a protein with features suggestive of it being an L-type Calcium channel itself. This gene is expressed in the very early neural plate, raising the exciting possibility that a Calcium-presenting protein (Calreticulin) is secreted by the organiser while a L-type Calcium channel is induced in the responding tissue. To assess whether Calfacilitin might be such a Calcium channel, we started a collaboration with the laboratory of Prof. Tuck Wah Song in Singapore. Preliminary results indicate that: (a) while Calfacilitin does not by itself function as a Calcium-channel, it does appear to prolong the "open" time of endogenous L-type Calcium channels in the presence of Calcium, and (b) co-expression of Calreticulin with Calfacilitin seems to slightly prolong the "open" time even further. Although these experiments are still in progress, they provide a plausible mechanism to explain the elusive source of L-type activating signals during neural induction.

Calreticulin variants

It is important to note here that almost all of the experiments presented in this Chapter were performed using the chick calreticulin gene. Because Calreticulin is characterised, amongst other domains, by a carboxy-terminal KDEL sequence, and the chick cDNA that was isolated in his study lacks this domain, it is likely that the gene used here may represent a truncated version. Although the full-length zebrafish sequence can also expand the domains of *Sox3* and *Sox2* when overexpressed, it is crucial to repeat the BMP4 rescue experiment using the full length zebrafish *calreticulin* gene.

A role for *Calreticulin* in embryonic left-right asymmetry?

Asymmetry in the node starts early in development with the asymmetric expression of genes encoding *Activin Receptor type IIA*, the transcription factor *HNF3β*, and the signalling proteins *Shh* and *Nodal* (Levin et al., 1995; Lohr et al., 1997). Left-right asymmetry during development is crucial to correctly position the internal organs of the embryo. Here, Calreticulin was found to be expressed asymmetrically in the node from around stage 6-7 onwards, both at the RNA and protein levels. This is about the same stage at which Nodal is first expressed in the lateral plate mesoderm. It was mentioned above that calcium transients in *Xenopous* induce expression of the early neural marker *Zic3* (Leclerc et al., 2003), and it is tantalising to relate this to the finding that Zic3 is involved in left-right specification (Kitaguchi et al., 2002; Kitaguchi et al., 2000). Although the present results do not reveal a specific role for Calreticulin in left-right specification, this is an interesting possibility worthy of further exploration.

Conclusion

Chick *calreticulin* is highly conserved across species. In the chick it is expressed in the node and is secreted. Although it is unable by itself to induce neural markers in competent epiblast of the chick area *opaca*, either alone or in combination with FGF and/or BMP antagonists, it is able to modulate the expression of neural plate border in a manner similar to that observed when BMP signals are attenuated. Furthermore, Calreticulin can partly rescue the effects of BMP overexpression. We propose that Calreticulin may act as a relatively weak BMP antagonist by a mechanism that remains to be elucidated, but which could provide the missing link between Calcium signalling and BMP inhibition.

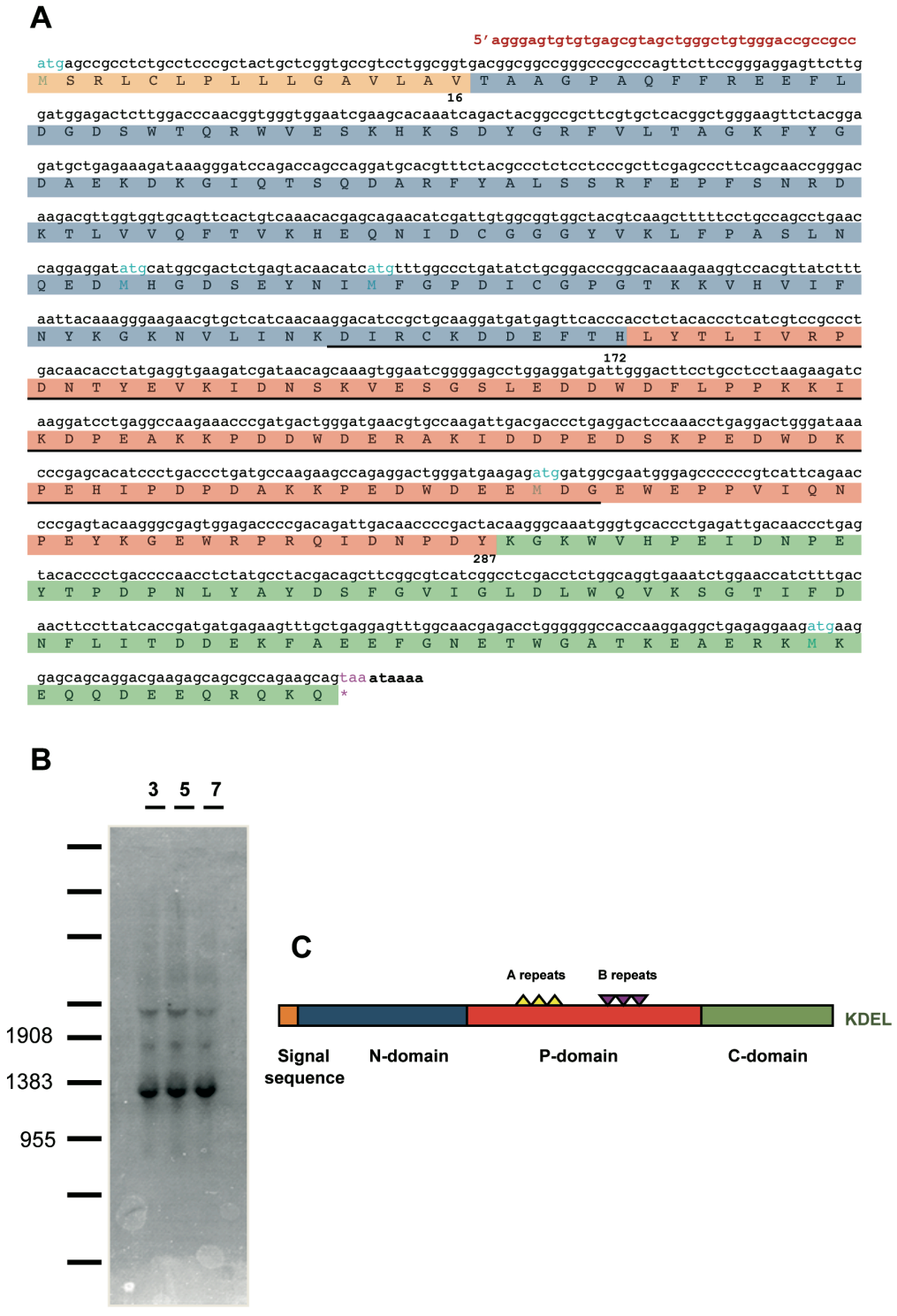

Fig 6.1. *Gallus gallus* Calreticulin (cCrt).

Fig 6.1. *Gallus gallus* Calreticulin (cCrt). Amino acid sequence for *cCrt* revealing the 16aa signal sequence (orange) and the functional domains N-domain (blue), P-domain (red) and C-domain(green); underlined (blak) is the original nhbr307 sequence (**A**). Northern blot for stages HH3, HH5 and HH7 reveals a band of about 1.2kb. Although two other bands (1.9 Kb and 3.5 Kb) are present, there is no evidence for alternative splicing of the *calreticulin* mRNA (**B**). Domain structure of the protein based on the human calreticulin showing the same functional domains and the characteristic A repeats (yellow triangles) and B repeats (purple triangles) as well as the C-terminal KDEL endoplasmic reticulum (ER) retrieval sequence (**C**). Chicken calreticulin lacks the KDEL sequence.

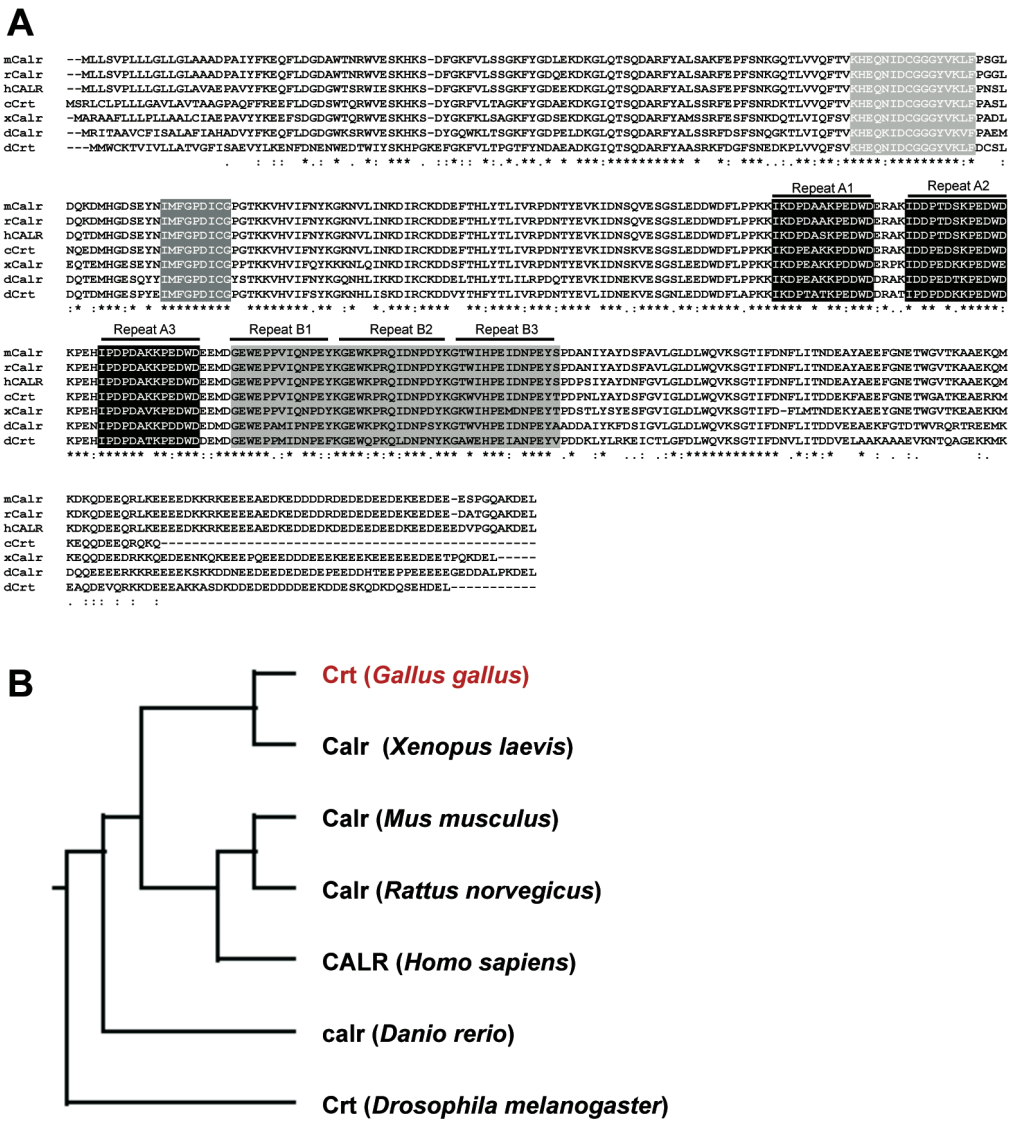

Fig 6.2. Calreticulin is a conserved protein. ClustalW alignment of the calreticulin protein in mouse (mCalr; accession number NM_007591), rat (rCalr; accession number NM_022399), human (hCALR; accession number NM_004343), ,chicken (cCrt), *Xenopus* (xCalr; accession number BC046699)' zebrafish (dCalr; accession number NM_131047) and *Drosophila* (dCrt; accession number NM_079569). The Calreticulin family signature 1 (KHEQNIDCGGGYVKLF) is shown in light grey; Calreticulin family signatire2 (IHFGPDICG) is shown in a darhker shade of grey followed by three blocks of repeats A (PXXIXDPDAXKPEDWDE), in black and three blocks of repeats B (GXWXPPXIXNPXYX) in dark grey. (**A**). Dendogram using the same sequences as in the alignment (**B**).

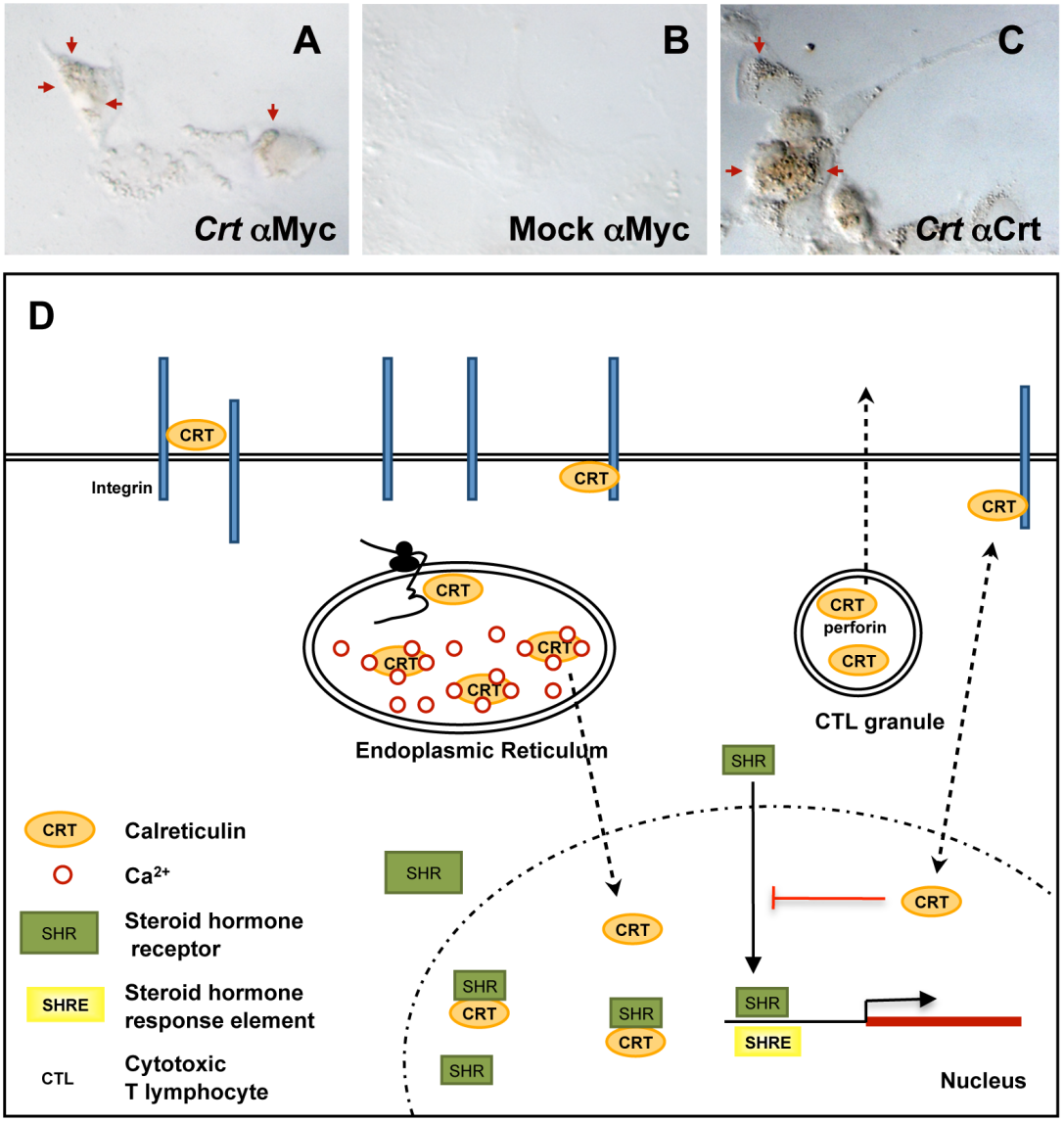

Fig 6.3. Calreticulin sub-cellular localization. Antibody staining of Cos cells transfected with *calreticulin* reveals its abundance in granules around the nucleus (red arrows), corresponding to the endoplasmic reticulum (**A** and **C**). In the control Mock transfected cells no protein is detected (**B**). The scheme (**D**) shows calreticulin proteins present at the cell surface, in the endoplasmic reticulum, CTL granules and in the nucleus and its interactions with integrins, calcium stores, nascent polypeptide chains, perforin and steroid hormone receptors. Dotted arrows indicate possible routes of calreticulin trafficking (Adapted from Coppolino M, 1998).

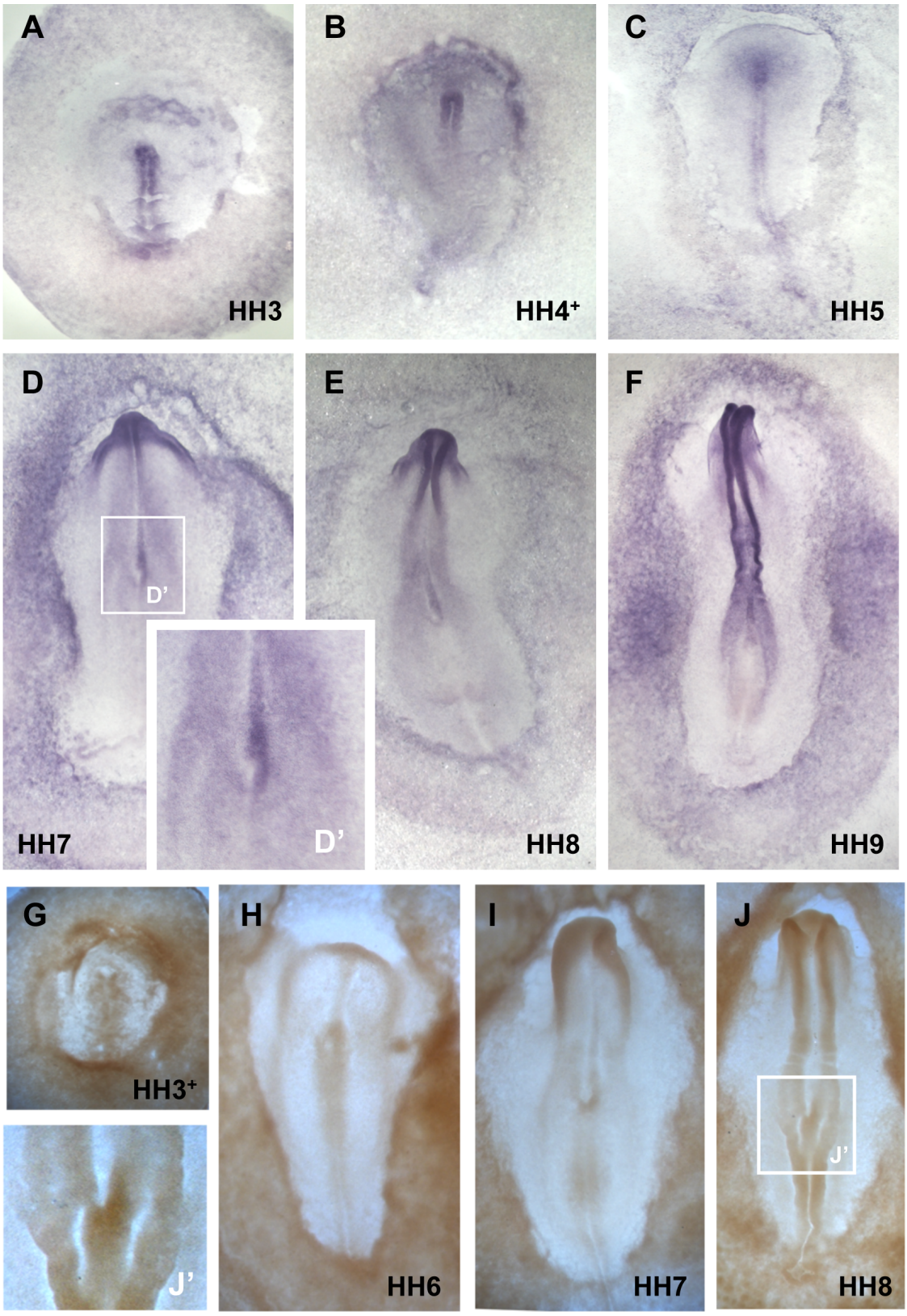

Fig 6.4. Calreticulin (cCrt) expression in the chick embryo.

Fig 6.4. Calreticulin (cCrt) expression in the chick embryo. At the mRNA level, transcripts are detected at stage 3-3^{+} (**A**) and the signal is strongest in the anterior part of the primitive streak. At stages 4^{+}-5 expression becomes concentrated in Hensen's node, with a lower level of expression seen in the anterior epiblast (**B** and **C**). Expression is maintained in the node and, from stage 7 onwards, it is asymmetric and on the right side (**D**, **E** and **D'**). From this stage, expression can be detected in the neural plate (**D**, **E** and **F**). At the protein level, antibody staining reveals the accumulation of Calreticulin protein in the primitive streak from stage 3^{+} (**G**-**J**) as well as the asymmetry in the node at stages 7 and 8 (**I**, **J** and **J'**).

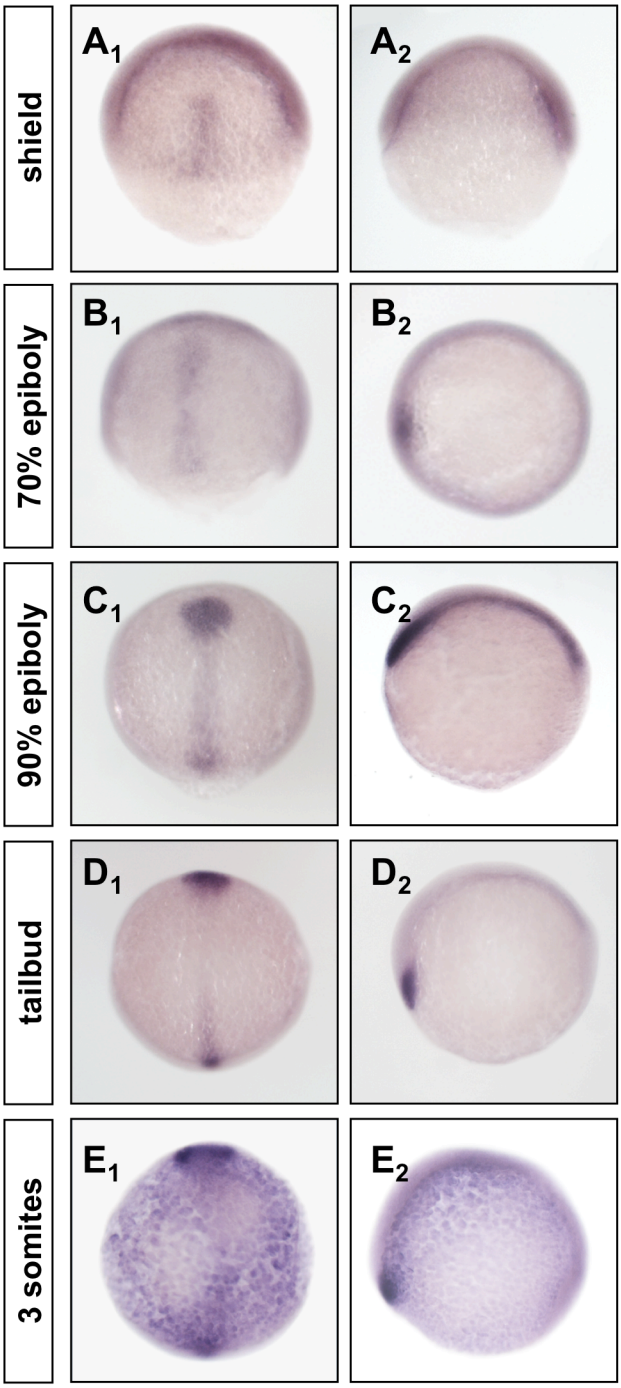

Fig 6.5. *Calreticulin (fCrt)* expression in zebrafish (*Danio rerio*). At shield stage expression is present in the shield (**A1**). Expression persists at the midline and most anterior part of the embryo though epiboly (**B1**, **B2**, **C1** and **C2**) and tail bud stages (**D1** and **D2**). At the 3 somite stage, expression starts to become ubiquitous, although remaining stronger anteriorly (**E1** and **E2**).

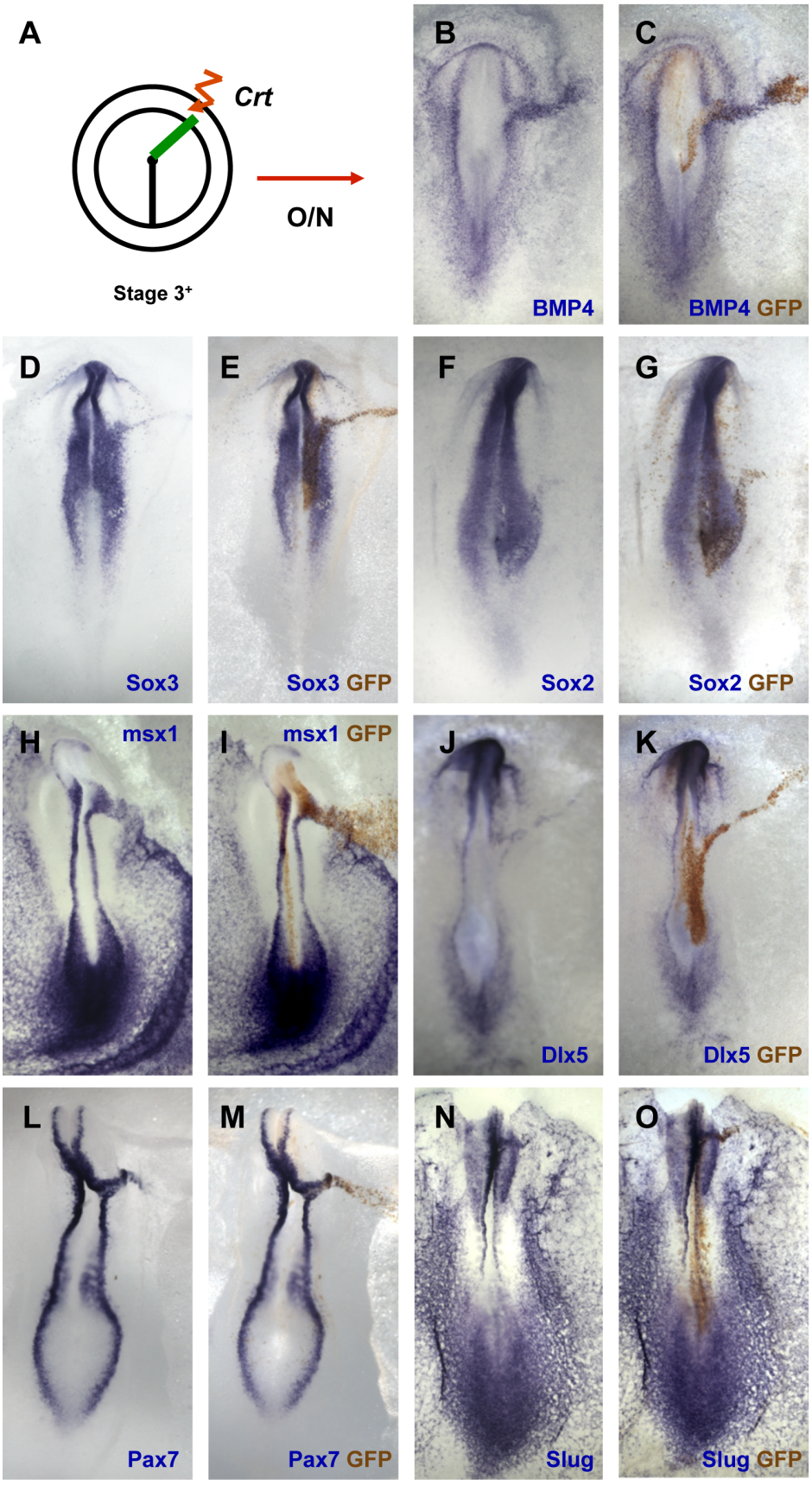

Fig 6.6. Calreticulin overexpression extends the border of the neural plate.

6.6. Calreticulin overexpression extends the border of the neural plate. *pCAβ-cCrt-IRES-GFP* was electroporated into the epiblast of stage 3^{+} chick embryos in a line extending from the node to the area *opaca* (**A**). *cCrt* overexpression causes an expansion of expression of neural plate markers *Sox3* (**D-E**) and *Sox2* (**F**-**G**). The neural plate domain was expanded together with the lateral shift of expression of the border markers *msx1* (**H** and **I**), *Dlx5* (**J** and **K**), *Pax7* (**L** and **M**), *Slug* (**N** and **O**) and *BMP4* (**B** and **C**). The expansion of neural plate or border markers was never extended to the area *opaca*.

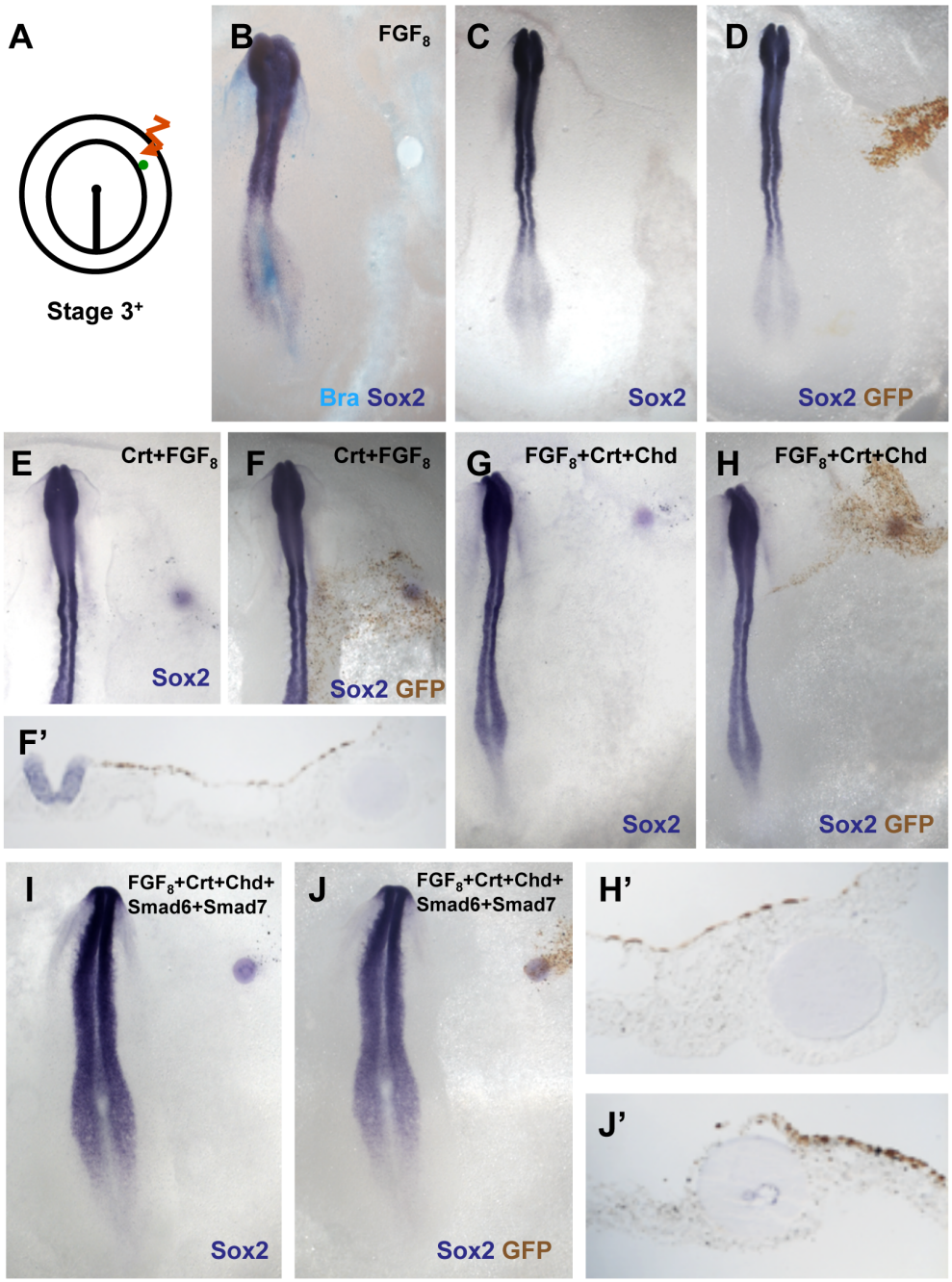

Fig 6.7 Clareticulin, either alone or in combination with FGF and BMP inhibitors, is not able to induce neural markers in the area *opaca*. Experiments were performed in the competent extraembryonic epiblast of the area *opaca* at stage 3+ (**A**). FGF8 alone does not induce the neural marker *Sox2* or the mesodermal marker *Brachyury* (*Bra*) in the area *opaca* (**B**). *Calreticulin* overexpression by electroporation does not induce *Sox2* in the area *opaca* (**C** and **D**), even when combined with FGF8 (**E** and **F**) and the BMP inhibitors, *Chd* (**G** and **H**) and *Smad6* and *Smad7* (**I** and **J**). Staining was observed in some of the FGF beads after *Sox2 in situ* hybridization (**E-J**) and histological sections were performed to show the absence of expression in the epiblast (**F'**, **H'** and **J'**).

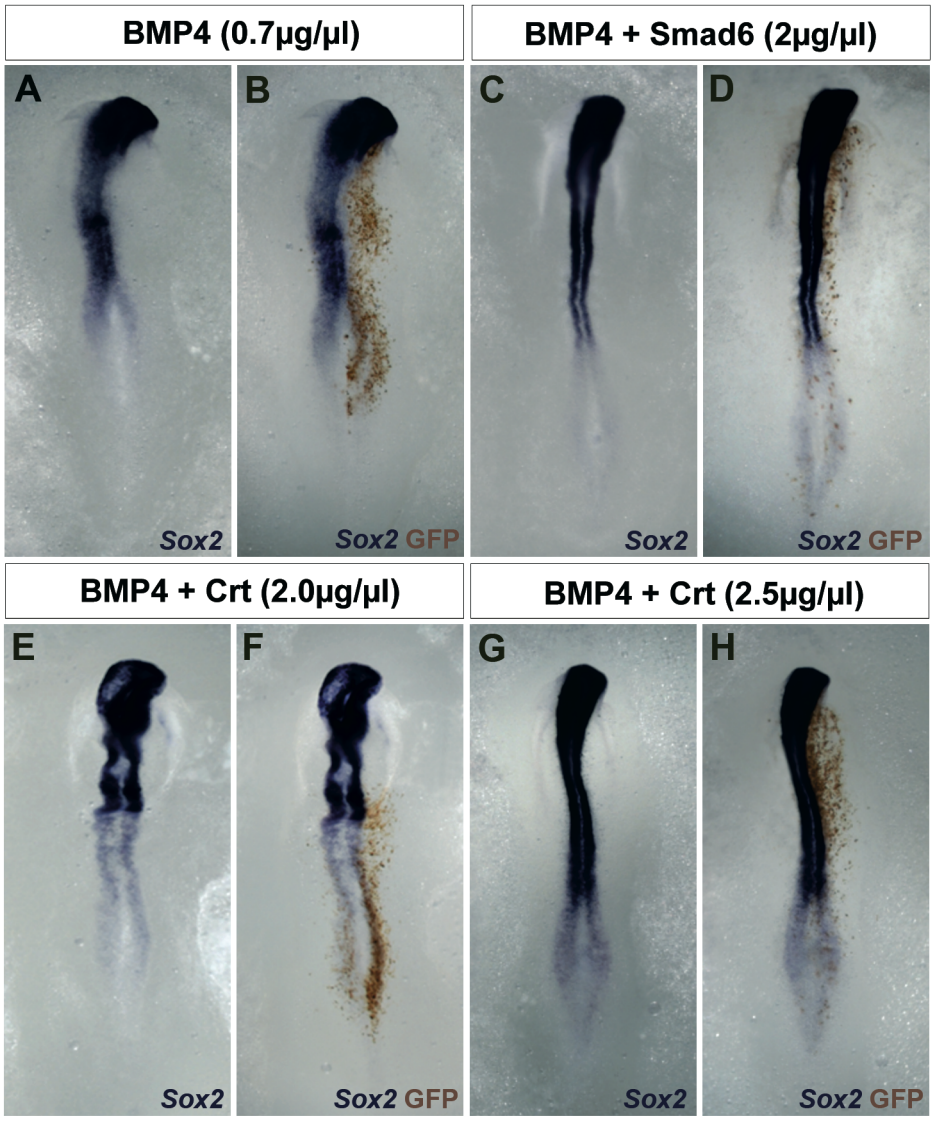

Fig 6.8. *Calreticulin* can rescue the effects of BMP4 *overexpression* in the neural plate. *BMP4* (0.7µg/µl) missexpred by electroporation in the prospective neural plate at stage 3^{+} results in the downregulation of *Sox3* after O/N culture (**A** and **B**). *Smad6*, a *BMP* antagonist, can rescue the effect of *BMP4* overexpression on *Sox3* at a concentration of 2µg/µl (**C** and **D**). *Calreticulin* can also rescue the effect of *BMP* overexpression, but at a higher concentration of 2.5µg/µl (**G** and **H**).

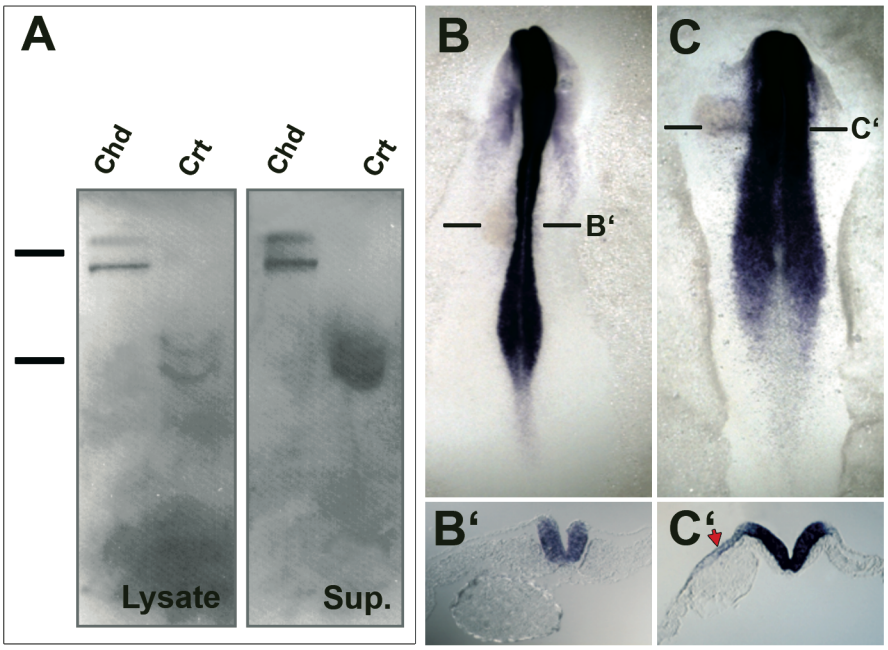

Fig 6.9. Calreticulin, secreted by transfected COS, cells can expand the neural plate domain. Western blots using both the lysate and the supernatant of Cos transfected cells reveal that Calreticulin protein can be secreted (supernatant fraction); Chordin was used as a control (**A**). Pellets of *Calreticulin* transfected cells were placed in the border of the prospective neural plate at stage 3^{+}, resulting in the expansion of the *Sox2* domain of expression (**C**). Mock transfected cells have no effect on *Sox2* expression (**B**).

Chapter7

Nhbr90: A long non-coding RNA

Introduction

Nhbr90 was isolated as a putative secreted factor from the organizer. Given that its transcript is always present in the node and the fact that *nhbr90* has no known homologies, it was decided it would be an interesting molecule to study further.

This chapter deals with the cloning, expression and study of *nhbr90* in the context of neural induction. We report that it is indeed always expressed in the organizer; in fact, nhbr90 starts before primitive streak formation, in the hypoblast. Later expression coincides with embryonic regions of neurogenesis activity, namely the branchial arches and Dorsal Root Ganglia (DRGs).

Nhbr90 does not seem to be translated, but rather be a long non-coding RNA (ncRNA). Overexpression of *nhbr90* reveals that it induces both *Sox3* and *Sox2* in the competent epiblast of the area *opaca* through a mechanism yet to be understood.

Materials and methods

Isolation of a full-length clone of chick *nhbr90*

The original *nhbr90* clone was used to transcribe a radiolabelled RNA probe, which was used for library screening (details of the procedure can be found in Chapter 2).

Northern Blots

Northern blots were performed as described in Chapter 2 and the full length clone *nhbr90* was used to transcribe a radiolabelled probe ([α-^{32}P]dCTP) prior to hybridization.

RNA analyses and structure prediction

RNA prediction analyses and secondary structure was carried out using free software UNAfolf and mfold3.5 (Kuker et al., 1999; Rouillard et al., 2003) from the RNA Institute at the University of Albany, USA. RNA analyser (Burge and Karlin, 1997; Lowe and Eddy, 1997) from the Department of Bioinformatics at the University of Würzburg was also used. The RNA analyses work was done in collaboration with Mario dos Reis (a fromer member of the Stern Lab) and Fabrice Jossinet at the Institut de Biologie Moléculaire et Cellulaire du CNRS, Université Louis Pasteur.

In situ hybridisation

The full length *nhbr90* was used to transcribe a digoxigenin-labelled RNA probe and hybridisation was performed as described in Chapter 2. Further probes were transcribed with smaller fragments of the nhbr90 clone, including a 506 bp probe obtained by cutting the nhbr90 with *ClaI* and *AseI* (*ClaI/AseI* riboprobe), and a 1573bp probe obtained from the *Ase/BamHI* digestion (*AseI/BamHI* riboprobe) (**Fig 7.1B**).

Electroporation constructs

Nhbr90 was cloned into *pCAβ-IRES-GFP* (a kind gift from A. Lumsden Lab). The *pBS-nhbr90* plasmid was cut with *ClaI* and *BamHI* and inserted into *pCAβ-IRES-GFP*. The resulting DNA was sequenced and used for electroporation at a concentration of 1.5 µg/µl. Further electroporation constructs were made using fragments from the full length *nhbr90* clone (2079bp), namely a 1573 bp insert, obtained by digesting the *pBS-*

nhbr90 with *AseI* and *BamHI* and a 1312bp insert, obtained by digesting the the *pBS-nhbr90* with *ClaI* and *XhoI* (**Fig 7.1C**).

Expressing *nhbr90* in COS cells

The full length *nhbr90* sequence (2079bp) was cloned into in pCDNA 3.1/Myc-His (Invitrogen). *pBS-nhbr90* was cut with *ClaI, Klenow* filled in (resulting in a blunted end) and then cut with *BamHI*. Similarly, the pCDNA 3.1/Myc-His vector was cut with *NotI*, *Klenow* filled in and subsequently cut with *BamHI*. The vector and *nhbr90* were ligated and the resulting DNA sequenced and used to transfect COS cells to form pellets of *nhbr90* expressing cells (explained in Chapter 2).

Results

Cloning of the full length *nhbr90*: *nhbr90* doesn't get translated and seems to function as a non-coding RNA

The original 276bp *nhbr90* clone (**Fig 7.2 A**, underlined in red) was used to transcribe a radiolabelled RNA probe, which was used to screen a chick stage 2-4 whole embryo cDNA library, resulting in the isolation of 13 clones. Sequencing the clones revealed they were all identical in nucleotide sequence and 2079bp in length (**Fig 7.2 A**).

No long Open Reading Frame (ORF) was detected in the 2Kb clone, raising the possibility that, perhaps the, full length clone wasn't isolated. To test this, Northern Blots were performed, in triplicate, using RNA isolated from chick embryos at stages 3, 5 and 7. The results were consistently the same and reveal the presence of a unique 2Kb transcript (**Fig 7.2 B**). This indicates that the sequence obtained from library screening is the full length of the *nhbr90* clone.

Further searches were performed using Ensemble. The *nhbr90* sequence spans 2 contigs present in *Gallus gallus* Chromosome 5. In one location the there's a 97.51 percentage identity spanning 1367bp; another hit reveals a 96.84 percentage identity spanning 1392bp. Although not ideal, the fact that the 2KB sequence is not found in its entirety in the chick Genome is not altogether surprising. Given that the sequence spans two contigs, it might be the case that they haven't been properly assembled or that, indeed, some sequencing is missing.

The puzzling fact that a 2KB sequence with no long ORF raised the possibility that, perhaps, we could be dealing with a sequence that never gets to be transcribed. Using RNA prediction software, both my analyses and that of a collaborator, Mario dos Reis, predict that *nhbr90* can fold as a long non-coding RNA (ncRNA) (**Fig 7.2 C**). Another collaborator, Fabrice Jossinet, predicts that a small sub-sequence in the putative 3'-UTR of the *nhbr90* clone is complementary to the 5' stem of a putative miRNA precursor from *Gallus gallus* (not shown). This prediction wasn't further explored.

Despite not having a long ORF, the sequence has, however, 13 small putative ORFs when analysed in all the six frames. And these are, in descending order of size:

Frame	From (bp)	To (bp)	Length (bp)	Length (aa)
-3	701	1045	345	114
+2	35	334	300	99
-2	1473	1655	183	60
-1	1357	1527	171	56
+3	750	896	147	48
+1	745	888	144	47
-1	343	483	141	46
+1	1654	1785	132	43
+3	1740	1868	129	42
-3	1616	1741	126	41
-1	1642	1764	123	40
+2	1544	1663	120	39
+3	405	518	114	37

Further tests are necessary to access if of the small putative ORFs is transcribed and/or functional.

Nhbr90 is expressed in the node and in areas of neurogenic activity

To assess the expression of *nhbr90* at early stages of development in normal chick embryos, whole mount *in situ* hybridization was performed. Because of the presence of the several putative ORFs in the clone, three different probes were transcribed, spanning different regions in the sequence. We used a full length 2079bp riboprobe (Riboprobe 1) and two smaller ones of 506bp and 10573 bp (Riboprobe 2 and Riboprobe 3, respectively) (**Fig 7.1 B**). The three riboprobes resulted in identical expression pattern (not shown) clearly indicating that the *nhbr90* sequence is part of one single transcript.

Expression starts at pre-streak stages, in the hypoblast (**Fig 7.3 A**) and, by the time the streak is formed and fully elongated at stage $3^{+}/4$, expression is strongly localized in the

node (**Fig 4.3 B** and **C**). By stage 4+ the expression persists in the node and starts to appear in the prospective neural plate, just anteriorly to the node (**Fig 7.3 D**). The expression of *nhbr90* is maintained in the node as it regresses and transcripts start to be detected in the notochord, as it's laid down (not shown). At stage 7, expression localizes to the presomitic mesoderm and the anterior boundary of expression overlaps with the first pair of somites formed (not shown). This somite region and presomitic mesoderm expression persists during somite formation. Also maintained is the expression in the node and notochord (**Fig 7.3 E**). Later on, at stages 10 (not shown) and 11, with the neural tube being closed, expression is detected in the neural tube, with its anterior boundary of expression coinciding with the first pair of somites formed. Expression is also detected in the caudal neural plate (**Fig 7.3 F**).

Given the dynamic expression of *nhbr90* and the fact that transcripts are always present in the node, a signalling centre, we decided to examine what happens to the expression at later stages in development. In embryos developed to stage 18, the *nhbr90* transcripts accumulate in the cranial ganglia at the level of the hindbrain and pharyngeal arches (white arrow heads, **Fig 7.4 A**, **B** and **C**), the dorsal neural tube (**Fig 7.4 D**) and the dorsal root ganglia (red arrows, **Fig 7.4 A**, **D** and **D'**). These are areas of active nerve formation and maturation of neurons. This later expression further emphasises the role *nhbr90* may be playing not only in neural induction, but also in neurogenesis.

In sum, *nhbr90* is expressed before node formation, in the hypoblast cells that will contribute to the node. It then strongly localises to the node, and mostly the node up to stage 4. The hypoblast and node expression during the time neural induction is taking place, makes *nhbr90* a very strong candidate to be a neural inducing molecule.

Nhbr90 overexpression results in *Sox3* and *Sox2* induction

Nhbr 90 is expressed in the node, being a very good candidate to act as a neural inducer. It does not contain a long ORF and predictions suggest that can function as a ncRNA. To test if it is indeed functional in our neural induction essay, full length *nhbr90* was overexpressed, by electroporation, in stage 3+/4 chick embryos in a line spanning from the node to the area *opaca* (**Fig 7.5 A**). Results revealed that, indeed, *nbbr90* is able to induce both *Sox3* in almost all the embryos tested (20/20; Fig **7.5 B, C**) and *Sox2* (23/25; **Fig 7.5 D, E**) and that this induction extends to the area *opaca*. To note that the 3 embryos that failed to express *Sox2* ectopically had a very small amount of cells electroporated and

the results might have been due to insufficient missexpression of the construct. The induction of neural markers is not an artefact of electroporation as no induction was observed (0/9 *Sox3*; 0/10 *Sox2*) when control electroporations were performed (**Fig 7.5 F-J**).

Could this induction into the area *opaca* be a result of continuous cell communication from the neural plate? To test this, a discrete patch of cells was electroporated directly into the anterior inner third of the area *opaca* (**Fig 7.5 K**), resulting in remarkable induction of the neural markers *Sox3* (12/13; **Fig 7.5 L, M**) and *Sox2* (16/20 **Fig 7.5 N, O**). No induction was observed in control electroporations (0/6 Sox3 and 0/8 Sox2; **Fig 7.5 P-T**).

These results could be due to some of the small ORFs present in the clone being translated and functional. To test this, two smaller fragments of *nhbr90* (**Fig 7.1 C**) were inserted into the *pCAB-IRES-GFP* and electroporated into the area opaca. Neither of the constructs resulted in Sox2 induction (0/12 for *AseI/BamHI nhbr90*; 0/7 for *ClaI/XhoI nhbr90*). Crucially, when both were electroporated together, no neural markers were induced (0/15) (not shown).

This last experiment is a further indication that a full *nhbr90* sequence is necessary for it to function as a neural inducer as it provides overexpression of all the putative small ORFs at once, without inducing *Sox2*. Only when the full length *nhbr90* sequence is missexpressed, *Sox2* is induced and, as it does not contain a long ORF, it may be acting as a ncRNA.

The embryo looses its competence to respond to neural inducing signals

In normal embryonic development, the competence of the epiblast to respond to neural inducing signals is restricted in early development, rapidly disappearing around or after stage 6 (Dias and Schoenwolf, 1990; Gallera, 1965; Storey et al., 1992; Streit et al., 1995; Streit et al., 1996; Streit and Stern, 1997a; Woodside, 1937).

In order to ascertain the ability of *nhbr90* to signal as a neural inducer in normal chick development and to which extent the embryo maintains its competence to respond to the signals, the following experiment was carried out: Embryos ranging from stage 3^{+} to stage $7/8^{-}$ were electroporated with pCAB-nhbr90-IRES-GFP in a patch area of the inner third of the area *opaca* and left to grow O/N. When missexpression is carried out at stage

3+, *Sox2* induction is seen in 77% of the embryos (17/22; **Fig 7.6 A**, **B** and **C**). Experiments performed at stage 4+ resulted in 70% induction of the neural marker (7/10; Fig 7.6 A); at stage 5/6 only 27% the embryos showed *Sox2* induction and, by stage 7/8-, the embryos had completely lost their ability to respond to the neural induction ability of the *nhbr90* construct (0/12; **Fig 7.6 A**). Control experiments, where electroporations were performed with the *pCAB-GFP* vector, no induction of *Sox2* was observed (0/14 at stage 3+; 0/5 at stage 4+; 0/5 at satge 5/6; 0/6 at stage 7/8-; **Fig 7.6 A**, **D** and **E**).

The timing necessary for induction of neural markers *by nhbr90* mimics that of the node

When a node graft is performed in a chick embryo at stage 3+, it takes approximately 5-6 hours for *Sox3* to be induced in the host embryo, and about 9 hours for *Sox2* induction. Does *nhbr90* mimics this timing for induction of neural markers? To test this, *nhbr90* was electroporated in a small region either in the epiblast adjacent to the future neural plate at stage 3/3+ (**Fig 7.7 A**) or in the inner third of the area *opaca* at the same developmental stage (**Fig 7.7 B**). After 6 hours, *Sox3* is induced in all the embryos tested in the proximity to the neural plate (8/8, **Fig 7.7 B** and **C**) and in 93% (13/14, **Fig 7.7 G** and **H**) of those tested in the area *opaca*. No induction of *Sox2* was observed after 6 hours (0/8 in the area *pellucida*; 0/8 area *opaca*, not shown). In control embryos, where *GFP* alone was electroporated, no *Sox3* (0/6 in the area opacca; 0/5 area *pellucida*, not shown) or *Sox2* (0/5 in the area opacca; 0/4 area pellucida, not shown) were induced.

A minimum of 8 to 9 hours are required for nhbr90 to induce *Sox2* expression both in the area adjacent to the neural plate (13/14, **Fig 7.7 D** and **E**; 0/6 for the control, not shown) and in the area *opaca* (15/15, **Fig 7.7 I** and **J**; 0/5 for the control, not shown).

These results confirm that nhbr90 mimics the node in terms of the timing required for induction of neural markers.

Nhbr90 acts in a non cell autonomous manner

The *nhbr90* clone seems to act as a neural inducer but, as a non coding RNA, if its effect is direct, then it will be cell autonomous, as RNAs are not known to leave the cell. To test if the effect of *nhbr90* is direct we took two different approaches: First, by missexpressing *nhbr90* into the inner third of the area *opaca* of stage 3+ embryos. This set up results in induction of *Sox2* expression in over 90% of the embryos tested (previous sections and **Fig 7.8 A**, **B** and **B'**). When embryos were processed for GFP staining, it was clearly revealed that *Sox2* expressing cells are not exclusively the ones electroporated and that,

not all the electroporated cells express *Sox2*. It seems, therefore, that the effect of *nhbr90* is non-cell autonomous. To further test this idea we took a second approach: *nhbr90* was expressed in COS cells and these grafted in stage 3+ chick embryos, also in the inner third of the area *opaca*. In this case there was also induction of *Sox2* in all the embryos tested (8/8; **Fig 7.8 C** and **C'**).

These results indicate that, by whatever mechanism *nhbr90* working to induce *Sox2*, the effect is not direct and the neural inducing factor is secreted. As there is no evidence of a long non-coding RNA being secreted we speculate that *nhbr90* might be inducing some secreted factor by the expressing cells and this factor will then induce the neural marker *Sox2*.

Nhbr90 is involved in *ERNI* and *Geminin* regulation

In a recent paper (Papanayotou et al., 2008) it was beautifully demonstrated the mechanism by which *Sox2* is activated. *ERNI* is expressed early in the hypoblast and prospective neural plate (Streit et al., 2000b) and needs to be downregulated for neural induction to take place. ERNI interacts with Geminin, inhibiting *Sox2* in the early neural plate. At around stage 4, *Bert* is expressed and disrupts the interaction between Geminin and ERNI, allowing the activation of *Sox2*.

Geminin is a coiled-coiled protein expressed in the early prospective neural plate. When misexpressed in a line extending laterally from the neural plate, *Geminin* strongly induces ectopic *Sox2*. *Geminin* can also induce *Sox2* expression when introduced into the extraembryonic epiblast (Papanayotou et al., 2008). These results resemble the effect of *nhbr90* misexpression. Could there be a relation between *nhbr90* and the three genes, *ERNI*, *Bert and Geminin*, central to *Sox2* regulation? To test this, *nhbr90* was electroporated in line extending from the prospective neural plate and into the extraembryonic ectoderm (**Fig 7.9 F**). This results in the extension of the normal domain of expression of *Geminin* (5/5; **Fig 7.9 I** and **J**; 7 more embryos were processed, all with induction of *Geminin*, but were not taken into account given their abnormal growth). Furthermore, *nhbr90* overexpression downregulates the endogenous *ERNI* expression while extending the prospective neural plate domain. (6/8; **Fig 7.9 G** and **H**). The effect of *nhbr90* in *Bert* expression could not be accessed due to intense background staining and therefore the impossibility to differentiate between induction (if any) and endogenous expression (10 embryos electroporated, not shown).

In control electroporations, no effect was seen in either *ERNI* (0/4; not shown) or *Geminin* (0/6; not shown). Control electroporations in the 6 embryos probed with *Bert* resulted in high levels of background (not shown).

This result extend previous observations that, in order to become neural, cells must first express *ERNI*, forming a pre-neural state, and that *ERNI* needs to be downregulated for the proper neural plate to form and express *Sox2* (Papanayotou et al., 2008). It is conceivable that *nhbr90* is able to induce *Sox2* by both downregulating *ERNI* and upregulating *Geminin* by a mechanism yet to be elucidated.

Nhbr90 induced *Sox2* cells are prevented to gastrulate though the streak

Activation of the transcription factor *Sox2* is strongly correlated with the establishment of the

embryonic neural plate and studies have revealed that, amongst a number or enhancers regulating *Sox2*, enhancer *N1* is responsible for *Sox2* activation in the caudally extending neural plate (Takemoto et al., 2006; Uchikawa et al., 2003). It is further revealed that enhancer *N1* becomes inactive in the mesodermal precursors that have ingressed through the primitive streak, indicative of the release from this cell population from a neural fate (Takemoto et al., 2006). Our studies have revealed that *nhbr90* robustly induced Sox2. What happens to gastrulation, and therefore cell ingression and mesodermal formation if cells are induced to prematurely express *Sox2*? To answer this question, *nhbr90* was electroporated close to the primitive streak at stage 3 (**Fig 7.9 A**; some embryos were even slightly younger than stage 3) and the embryos allowed to grow. These resulted in all the embryos expressing *Sox2* in the electroporated area (5/6; **Fig 7.9 B** and **D**) and also in impaired cell ingression through the streak, as revealed by downregulation of *Brachyury* expression (8/8; **Fig 7.9 D** and **E**). Control electroporation revealed no induction of *Sox2* (0/5; not shown) and normal expression of *Brachyury* (6/6; not shown).

To further examine what happens to the cells that ectopically express *Sox2* during gastrulation, the effect of *nhbr90* electroporation was examined. Embryos were electroporated with *nhbr90* at stage 3^{+} in a patch close to the most anterior primitive streak (**Fig 7.10 A**). All embryos electroporated revealed ectopic expression of *Sox2* after 8-9 hrs hours (6/6; **Fig 7.10 B** and **C**). And sections reveal that, although not all the electroporated cells induce *Sox2*, no *Sox2* expressing cells have ingressed through the streak (**Fig 7.10 A** and **E**). When embryos were allowed to grow for 17 hours, it is still observed that not all the electroporated cells ectopically express *Sox2* (**Fig 7.10 H** and **I**).

However, cells that are induced to express *Sox2*, fail to ingress and accumulate at the "gastrulation edge" (4/5; **Fig 7.10 F**, **H** and **G**, white arrowheads).

No studies on the N1 enhancer were carried out. However, the results presented here are in agreement with recently published data supporting that cells that do ingress through the streak are "released" from their neural fate (Takemoto et al., 2006) or, in other means, the cells adopt either mesodermal or neural character.

Neural induction in the Caudal Neural Plate: FGF induces proneural genes and also *nhbr90*.

The caudal neural plate (CNP), from which the chick posterior hindbrain and spinal cord are derived, is a unique embryonic region, regressing alongside the primitive streak to the tail end of the embryo (Brown and Storey, 2000; Schoenwolf et al., 1992). CNP cells are distinguished by the expression of a number of genes including the proneural gene homologue, *cash4* (Henrique et al., 1997) and the homeobox-containing gene *Sax1* (Spann et al., 1994). It has been shown that these caudal neural genes are induced continuously by the regressing node and that this node activity can be mimicked by FGF signaling (Henrique et al., 1997; Storey et al., 1998), a well established inducer of caudal neural character (reviewed by (Doniach, 1995; Ribisi et al., 2000). FGF signals also limit the posterior boundary of the transcription factor *Pax6* expression (Pituello et al., 1999). Given that *nhbr90* continues to be expressed in the node, at the level of the caudal neural plate we decided to investigate its possible role in regulating caudal neural genes.

We started by examining the expression pattern, at the level of the caudal neural plate of stage 10 chick embryos of *Fgf8*, *Pax6*, *Sax1*, *Cash4* and *nhbr90*. We focused on the posterior expression of these genes, at the level of the caudal neural plate up to the two newly formed somites.

Fgf8 transcription is restricted to the caudal region of the embryo being very strong at the level of the primitive streak and Hensen's node and displaying a decreasing caudo-rostral gradient in the presomitic mesoderm (**Fig 7.12 A'**).

Pax6 expression in the neural tube coincides with the onset of somitogenesis (Pituello et al., 1999). At the level of the caudal neural plate, *Pax6* transcripts are only present at the

level of the somites and completely absent in the pre-somitic mesoderm and remaining CNP (**Fig 7.12 B'**).

Sax1 (Spann et al., 1994) is expressed only in the spinal part of the neural plate. The anterior border of *Sax1* expression is the transverse plane separating the youngest somite from the yet unsegmented mesodermal plate. The posterior border of *Sax1* expression coincides with the posterior end of the neural plate (**Fig 7.12 C'**).

Cash4 is expressed in the caudal neural plate and excluded from the somitic region (Henrique et al., 1997) (**Fig 7.12 D'**).

Nhbr90 is expressed in the anterior half of the CNP and in the neural tube (**Fig 7.12 E'**).

FGF8 has been shown to mimic the node in inducing both *Cash4* (Henrique et al., 1997) and *Sax1* (Storey et al., 1998) and to downregulate *Pax6* (Bertrand et al., 2000). We decided to revisit these results and examine if FGF could also regulate *nhbr90*. FGF8 (or PBS soaked beads, in the controls) soaked beads were placed adjacent and just posterior to the node in stage 5/6 chick embryos and the embryos allowed to grow for about 18/20 hours (**Fig 7.13 A**). FGF8 does indeed downregulate the expression of *Pax6* (7/7; **Fig 7.13 B**) and upregulates *Cash4* (4/6; **Fig 7.13 C**) and *Sax1* (8/8; **Fig 7.13 D**). FGF8 also induces expression of *nhbr90* in almost half of the embryos tested (3/7; **Fig 7.13 E**). Control experiments had no effect on the genes tested (0/5 for *Pax6*, Fig **7.13 F**; 0/6 for *Cash4*, **Fig 7.13 G**; 0/6 for *Sax1*, **Fig 7.13 H**; 0/4 for *nhbr90*, **Fig 7.13 I**).

These results extend the previously published observations that FGF, expressed in the caudal neural plate, regulates the expression of *Cash4* and *Sax1*. Surprisingly, Fgf8 can also, to a certain extent, induce *nhbr90*. Given the low percentage of upregulation of *nhbr90* by FGF (43%), it is likely that FGF might not be the main mechanism of *nhbr90* regulation.

Nhbr90 induce neural tissue but doesn't seem involved in anteriorposterior patterning

There is very little evidence for the existence of a general neuralized cell state that lacks regional character in the embryo (Streit et al., 1995); rather, it seems that early chick neural plate has anterior identity and needs further signals to acquire posterior identity (Muhr et al., 1999. This 'anterior' neural tissue expresses forebrain, markers (for example,

Otx2, {Bally-Cuif, 1995 #137), but does not express 'posterior' markers, such as *En2* (midbrain and hindbrain rhombomere 1, (Hidalgo-Sanchez et al., 1999), *Krox20* (hindbrain rhombomeres 3 and 5, (Marin and Charnay, 2000a; Marin and Charnay, 2000b; Saldivar et al., 1997)) and *Hoxb9* (spinal cord).

Nhbr90 induces neural tissue. Does it also have a function on anterior posterior patterning? To address this question, *nhbr90* was overexpressed, by electroporation, in the extraembryonic area *opaca* of stage 5 embryos (**Fig 7.13 A**). After O/N culture, the embryos were accessed for the expression of various markers. *Sox2* was induced in 33% of the embryos (4/12; **Fig 7.13 A** and **C**). No induction was seen for the anterior marker *Otx2* (0/7; not shown) or the posterior marker *Hoxb9* (0/10; **Fig 7.13 D** and **E**). Similarly, no induction was detected for the caudal neural plate genes *Sax1* (0/9; **Fig 7.13 F** and **G**) or *Cash4* (0/10; **Fig 7.13 H** and **I**). Control electroporations, for all the genes tested had no effect (not shown; 0/5 for *Sox2*; 0/6 for *Hoxb9*; 0/3 for *Otx2*; 0/6 for *Sax1*; 0/4 for *Cash4*).

These results suggest that, in the area *opaca*, *nhbr90* is able to induce the neural marker *Sox2*, but unable to pattern the neural tissue. What happens if a similar experiment takes place in anterior exptraembryonic epiblast of the area *pellucida*? *nhbr90* was electroporated in this region, at stage 5, and the embryos grown O/N (**Fig 7.14 A**). Surprisingly, of all the embryos tested, 50% still revealed induction of *Sox2* (albeit very weak, when compared to previous experiments; 4/8; **Fig 7.14 B** and **C**). The caudal neural marker *Cash4* was induced in 37.5% of the embryos, again very weakly, but noticeably (3/8; **Fig 7.14 J** and **K**). No effect was observed for *Fgf8* (0/7; **Fig 7.14 D** and **E**), *Hoxb9* (0/10; **Fig 7.14 F** and **G**) or *Sax1* (0/8; **Fig 7.14 H** and **I**). Control electroporations had no effect on all the markers tested (not shown; 0/8 for *Sox2*; 0/5 for *Fgf8*; 0/9 for *Hoxb9*; 0/8 for *Sax1*; 0/8 for *Cash4*). The results obtained strongly suggest that *nhbr90* is not involved in the anterior-posterior patterning of the neural tissue.

Discussion

Nhbr90 appears to be a long non-codding RNA (lnc RNA)

The accepted role of the RNA in the cell has been considered mostly in the context of protein gene expression, limiting its functions as mRNA, tRNA, and rRNA. The discovery, in the last few years, of a vast array of transcripts that are not translated to proteins but rather function as RNAs has changed this view profoundly. And it is becoming clear that non-coding RNAs are involved in a variety of processes, including modulation of transcription and gene regulation (He and Hannon, 2004; Mattick, 2005; Mimouni et al., 2009; Umlauf et al., 2008; Yano et al., 2004), maturation of mRNAs, rRNAs, and tRNAs, or X-chromossome inactivation (Gontan et al., 2011; Lee, 2009; Malecova and Morris, 2010; Tian et al., 2010) and even serving as precursors of smaller RNAs (Borden et al.; Grinchuk et al.; Mattick and Makunin, 2006)

Recent studies have identified a variety of regulator paradigms for how long ncRNA function. Transcription by an upstream non coding promoter can affect the expression of a downstream gene by inhibiting RNA polymerase II recruitment (Bernard et al., 2010; Dye et al., 2006; Espinoza et al., 2007) or inducing chromatin remodelling (De Lucia and Dean, 2010; Turner and Morris, 2010). An antisense transcript is able to hybridize to the overlapping sense transcript (Gelfand et al., 2011; Lardenois et al., 2011) and with this, block recognition of the splice sites by the spliceossome, resulting in an alternatively spliced transcript. Alternatively, hybridization of the sense and antisense transcripts can allow Dicer to generate endogenous siRNAs (Murphy et al., 2008). By binding to specific protein partners, a non-coding transcript can modulate the activity of the protein, serve as structural component that allows a larger RNA-protein complex to form, or alter where the protein localizes in the cell. Long RNAs can be processed to yield small RNAs, such as miRNAs and piRNAs (Pauli et al., 2011).

Isolation of a new RNA species with no significant ORF is not sufficient evidence of a new ncRNA gene. There should be evidence of specific and temporal expression, of function, either by computational means (e.g., sequence or structure conservation) or experimental means (e.g., genetic phenotype). There should also be evidence that the RNA does not code for a small protein (Eddy, 2002).

In the context of *nhbr90,* it is important to add that many transcripts are classified as

noncoding on the basis of not having ORFs longer than 50–100 amino acids (Pauli et al.). However, the *Drosophila tarsal-less* (*tal*) gene provides a good example of the importance of validating these bioinformatic predictions. The *tal* gene expresses a 1.5-kb transcript that contains only ORFs smaller than 50 amino acids and was, therefore, originally classified as a long ncRNA. However, it was found that several 33-nt ORFs within the *tal* gene are translated into 11-amino-acid-long peptides that control tissue morphogenesis and pattern formation events during *Drosophila* development (Galindo et al., 2007; Kondo et al., 2007; Pueyo and Couso, 2008). Due to practical and statistical reasons, ORFs as short as these in *tal* are generally eliminated from gene annotations but, as the *tal* gene exemplifies, clearly need to be considered when addressing the function of an unannotated transcript. Additionally, some ncRNA genes, such as *SRA* (*Steroid receptor RNA activator*), seem to produce multiple RNA isoforms, some of which can be translated, allowing the gene to have functions carried out by both RNA and protein (Leygue, 2007).

To make sure that the *nhbr90* effect wasn't due to some of its translated putative ORFs, several constructs were produced. Interestingly, only the full length clone resulted in the induction of *Sox2*. Even if several clones were co-electroporated (spanning the entirety of the full length clone), the resulting embryos had no *Sox3* or *Sox2* induction. This result suggests that, in fact, the effect seem with *nhbr90* overexpression is not due to any of its putative ORFs being translated but rather that the it codes for a functional, non coding RNA.

Nhbr90 is expressed in the right place, and at the right time to function as a neural inducer

The Hensen's node is able to induce a complete secondary axis when grafted to an ectopic position and the extent to which the axes are induced depends, amongst other factors, on the age of both the host epiblast and the age of the grafted node (Galler 1971; Niewkoop, 1985) (see Chapter I). Storey and colleagues (Storey et al., 1992) identified the time frame during which neural inducing signals are present in the Hensen's node and the node age related ability to pattern the neural tissue: nodes at stage $3^{+}/4$ have the most neural inducing ability; young nodes, from stage 2 to 4, induce both anterior and posterior central nervous system; older nodes, from about stage 5/6, have a reduced inducing ability and progressively generate more posterior structures (Dias and

Schoenwolf, 1990; Gallera, 1970b; Storey et al., 1992; Streit et al., 1997b; Tsung et al., 1965; Vakaet, 1965).

The *nhbr90* transcript is strongly localized in the node at stage $3^{+}/4$, the age the node exhibits its maximum inducing ability (Storey et al., 1992), making it a candidate to play a role in neural induction.

Furthermore, the late expression of *nhbr90* in areas of neurogenic activity, suggests that the role of *nhbr90* goes beyond neural induction and might, perhaps, include neurogenesis. *Nhbr90* is expressed, at stage 19, in the branchial arches and the dorsal root ganglia (DRGs), both regions of active neural crest cell migration and neurogenesis (Lefcort and George, 2007; Noden, 1993; Noden and Trainor, 2005).

The neural crest of vertebrate embryos gives rise to a wide variety of adult cell types, including neurons and glial cells of the peripheral nervous system, pigment cells and various endocrine cells and skeletal elements (Le Douarin, 1980).

When it comes to the pharyngeal arches, the cranial neural crest migrates in three streams. The first stream of migration, trigeminal stream, emanates from the midbrain, rhombomeres 1 and 2. It migrates into the upper jaw primordia, underneath the eye, and into the first pharyngeal arch, which forms the lower jaw; The second stream, hyoid stream, from rhombomere 4, migrates into the second pharyngeal arch, forming the jaw support; The third stream, post-otic stream, emerges from rhombomeres 6 and 7 and populates the caudal pharyngeal arches, of which there are three in the chick embryo (Graham et al., 2004).

In the chick dorsal root ganglia (DRGs) there are two waves of neurogenesis (Lefcort and George, 2007). The first wave takes place between stages 15 and 18 and is generated from neural crest cells (NCCs) that migrate ipsilaterally and differentiate in the inner core of what will be the DRG. The second wave, from stages 19 to 26, is derived from NCCs that migrate both ipsilaterally and contrallaterally (between stages 19 and 22). The cells that migrate ipsilaterally, delaminate from the more lateral regions of the dorsal neural tube and tend to migrate directly into the inner core of the DRG. A second population, that tends to delaminate from the very medial region of the dorsal neural tube, includes cells that migrate both ipsilaterally and contralaterally. This medially-derived population of NCCs localize to the DRG perimeter where they remain in the cell cycle and become the

major source of mitotically-active progenitor cells for the second wave of neurogenesis and for glial cells in the DRG (Lefcort and George, 2007).

Nhbr90 might still play a role as a neural inducer in the Caudal Neural Plate (CNP)

Caudal Neural Plate (CNP) cells express of a number of genes, including the proneural gene homologue, *cash4* (Henrique et al., 1997) and the homeobox-containing gene *Sax1* (Spann et al., 1994). Previous studies have shown that these caudal neural genes are induced continuously by the regressing node and that this node activity can be mimicked by FGF signals (Henrique et al., 1997; Storey et al., 1998). Furthermore, *Cash4* misexpression, both in *Xenopus* and *Drosophila*, promote neural cell fates (Henrique et al., 1997).

By misexpressing *cash4* in fly and frog embryos it has also been shown that this gene promotes neural cell fates (Henrique et al., 1997) and the cellular context in which it is expressed in the chick suggests that *cash4* mediates neural specification steps within the CNP (Brown and Storey, 2000). Furthermore, cells derived from the CNP region, but now located above the node, all contribute to the neural tube (Brown and Storey, 2000; Mathis et al., 2001; Selleck and Bronner-Fraser, 1995; Storey et al., 1995). This seems to mean that cells in the CNP may be specified, but not yet committed to a neural fate and, consistent with this, express early neural genes, such as *Sox3* and *Sox2* (Streit et al., 1997b).

cash4 and *Sax1* persist in the CNP, but are both down regulated as cells form the neural plate/neural tube above the level of the primitive streak (Henrique et al., 1997; Spann et al., 1994) and it is here that the first neurons in the caudal nervous system are born (Sechrist and Bronner-Fraser, 1991). The results presented in this study show that *nhbr90* is expressed in the anterior half of the caudal neural plate and is able to induce *Cash4*. It is also able to induce *Sox2* at the level of the CNP, suggesting that its neural inducing role continues beyond the early neural induction at stage $3^{+}/4$.

Protein interactions and *Sox2* activation

A recent paper (Papanayotou et al., 2008) has elucidated the role of three coiled-coiled domain proteins Geminin, ERNI and Bert in the regulation of the neural marker *Sox2*. Geminin is shown to bind to the chromatin remodelling factor Brahma, displacing the HP1α transcriptional repressor from its binding site and allowing the SWI/SNF

chromatin remodelling complex to act as an activator and drive transcription of Sox2. However, ERNI interacts with Geminin and recruits onto the complex HP1γ, another transcriptional repressor, thus inhibiting *Sox2* transcription in the earlier neural plate. At the end of gastrulation, *BERT* starts to be expressed in the neural plate, disrupting the interaction between Geminin and ERNI, displacing HP1 from the SWI/SNF chromatin remodelling complex and allowing it to activate the transcription of *Sox2*.

Papanayotou's studies (Papanayotou et al., 2008) and that of others (Streit et al., 2000a) reveal that FGF signaling activates *ERNI* as well as *Sox3* and *Geminin* expression in the epiblast. However, FGF does not induce *BERT*, whose expression is also not regulated by BMP antagonists or any combination of known factors implicated in neural induction to date (Papanayotou, unpublished data). Future work will detertmine if *nhbr90* plays a role in regulating *BERT*.

The work presented here show that *nhbr90* overexpression induces *Sox2* expression in the extraembryonic epiblast of the area *opaca*. Our analyses further indicate that *nhbr90* does not get transcribed and seems to function as a long non-coding RNA, and plays a role in the regulation of *Geminin* and *ERNI*. In fact, non-coding RNAs seem to be involved in the modulation of transcription and gene regulation (He and Hannon, 2004; Mattick, 2005; Mimouni et al., 2009; Umlauf et al., 2008; Yano et al., 2004) by inhibiting RNA polymerase II recruitment (Bernard et al, 2010; Dye et al., 2006; Espinoza et al., 2007; Goodrich and Kugel) or inducing chromatin remodelling (De Lucia and Dean, 2010; Turner and Morris, 2010). In this context, it is interesting to add that it is possible that *nhbr90* RNA might interact with the chromatin complexes that lead to the activation of *Sox2*.

The non-cell autonomous effect of *nhbr90*

It was shown in the results section that *nhbr90* induces *Sox2* in a non-cell autonomous manner when overexpressed by electroporation or when introduced as pellets of expressing cells (**Fig 7.8** and **Fig 7.10**). This non-cell autonomous effect is very puzzling as the vast majority of the literature refers to the cell autonomous nature of long non-coding RNAs.

The non-cell autonomous effect observed when *nhbr90* is overexpressed could be explained by either of the following hypotheses:

1. *nhbr90* is regulating an intermediary secreted or membrane bound molecule which, in turn, exerts its effect on neighbouring cells;

2. *nhbr90* can be secreted.

For the first hypothesis it is interesting to note that very recent work being carried out by others in the lab has revealed the presence of *Tetraspanin18* (*Tspn18*) upstream of *nhbr90* and that this genomic organization is conserved across different vertebrate classes (unpublished data, not shown). *Tspn18* encodes for a transmembrane protein previously shown to be expressed in the chick embryonic nervous system but not yet studied in relation to embryonic development.

To test the hypothesis that *nhbr90* is exerting its effect via *Tspn18*, it will be necessary to both access if *nbbr90* overexpression can regulate *Tspn18* expression and if *Tspn18* itself is involved in the regulation of *Sox2*.

The second hypothesis, with the idea of RNA being exported to the extracellular space, is starting to gain some interest. The possibility of RNA being exported was first reported almost 40 years ago (Kolodny et al., 1972) and received very little attention until relatively recently, where it was found a mechanism, involving microparticles, for RNA transport to the extracellular space and possible intake by other cells (Chen et al., 2009; Hunter et al., 2008; Rosell et al., 2009; Taylor and Gercel-Taylor, 2008; Valadi et al., 2007). Many long non-coding RNAs are processed to yield small RNAs, such as miRNAs or siRNAs (Eddy, 2002; Pauli et al., 2011) and it is the small RNA particles that can be exported via microparticles (Hunter et al., 2008; Valadi et al., 2007).

Microparticles are lipid vesicles that are <1mm in diameter and are secreted by many cell types (Aharon et al., 2009; Castellana et al., 2009; Chironi et al., 2009; Huttner et al., 2008; Shet, 2008) and provide a way of RNA export. Unlike cellular RNAs, these secreted RNAs are mainly small RNAs or RNAs greater than 500 nt. This suggests that secretion of RNAs is not a random cellular process but a selective process that targets small RNAs such as miRNAs and, most possibly, other small non-coding RNAs, but not the more abundant intact mRNAs or ribosomal RNAs present in cells (Mattick and Makunin, 2005).

In this context of RNA secretion, it is important to access if *nhbr90* serves as precursor of smaller ncRNAs and if the smaller particles can be secreted. And if that is the case, how do the smaller ncRNAs regulate *Sox2*.

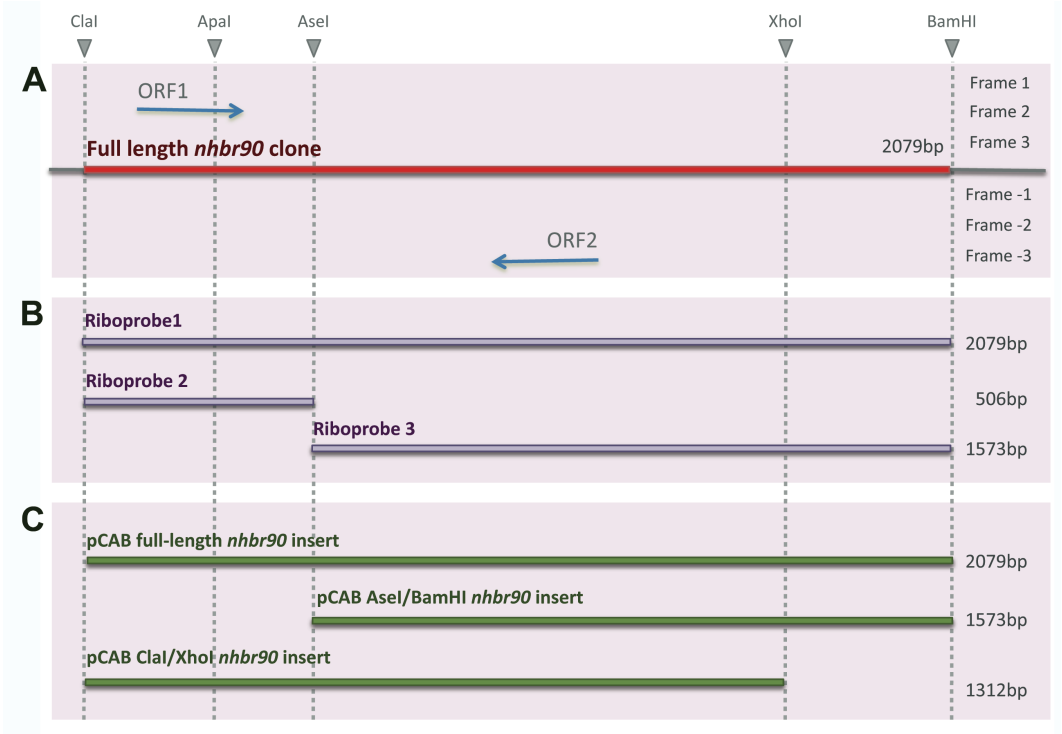

Fig 7.1. Schematic representation of the *nhbr90* clone and constructs used in the present study. *The nhbr90* clone is 2079bp long and contains two putative ORFs : ORF1 (99aa) and ORF2 (114aa) (**A**). *In situ* hybridizations were performed using the full-length clone (Riboprobe1) and also smaller fragments (Riboprobes 2 and 3) (**B**). Constructs for overexpression of *nhbr90* were made using either the full-length clone (*pCAB* full-length *nhbr90* insert) or smaller fragments (*pCAB Ase*I/*Bam*HI *nhbr90* insert and *pCAB Cla*I/*Xho*I *nhbr90* insert) (**C**).

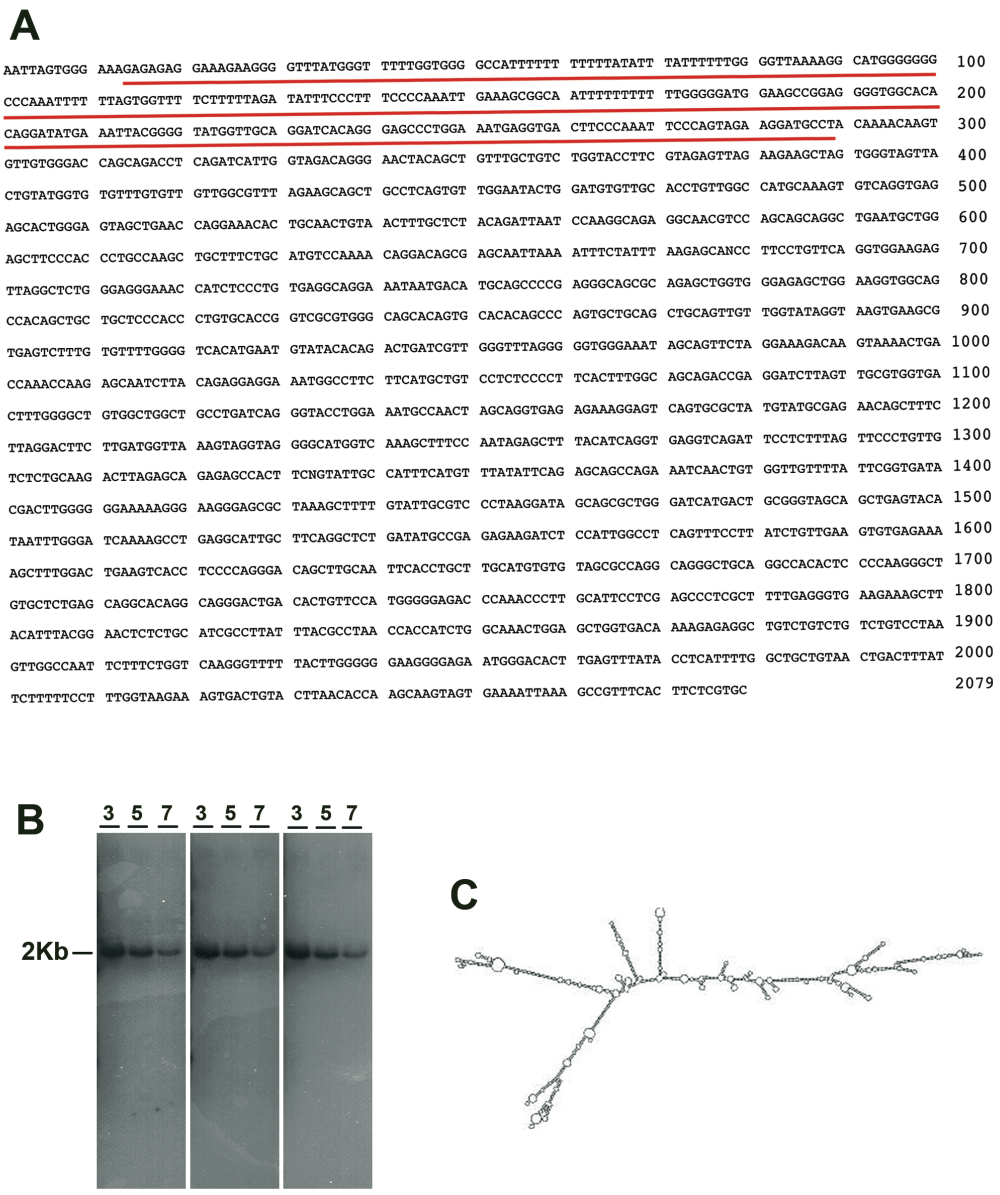

Fig7.2. *Nhbr90* is a 2079bp sequence and can fold as a RNA. Nucleotide sequence of nhbr90; Underlined in red is the original fragment obtained from the screen (**A**). Northern blots reveal the presence of a single *nhbr90* transcript of 2Kb (**B**). *nhbr90* can assume s secondary structure characteristic of long non-coding RNAs (**C**).

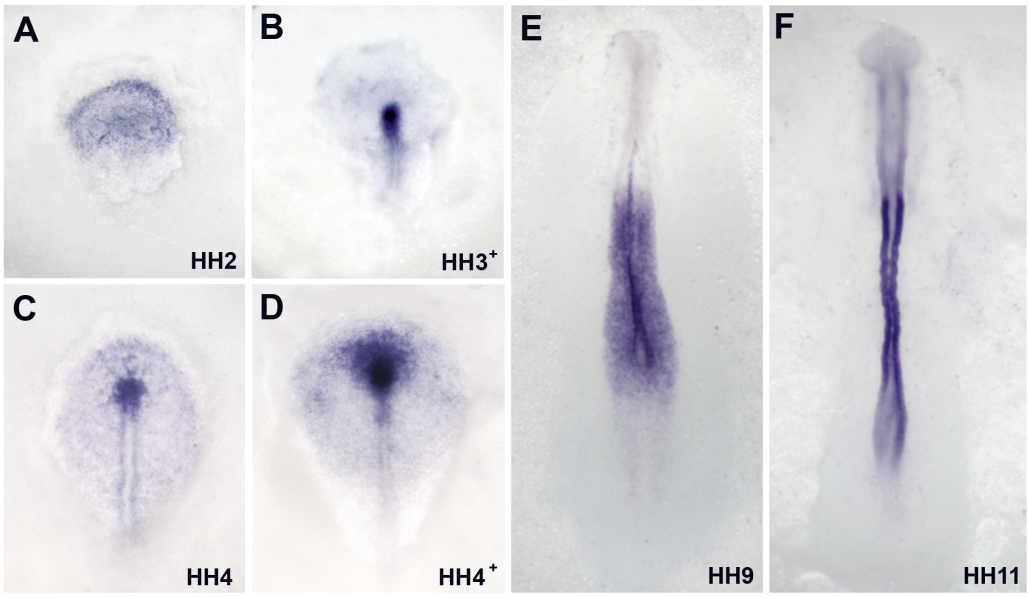

Fig 7.3. *Nhbr90* expression pattern. *Nhbr90* is detected first in the hypoblast (**A**) and then strongly localises to the Hensen's node (**B**, **C** and **D**). Later expression reveals the presence of the transcript in the neural plate (**E**) and neural tube (**F**).

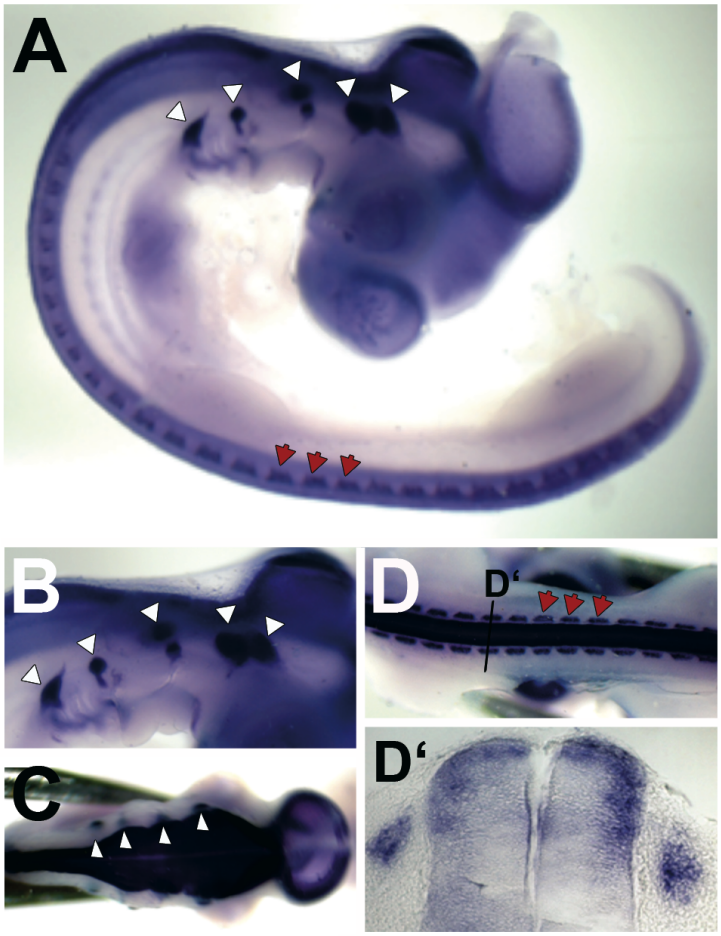

Fig 7.4. *Nhbr90* is expressed in areas of neurogenic activity. Stage 18 embryos express *nhbr90* in the cranial ganglia at the level of the hindbrain and pharyngeal arches (white arrow heads, **A**, **B** and **C**), the dorsal neural tube (**D**) and the dorsal root ganglia (red arrows, **A**, **D** and **D'**).

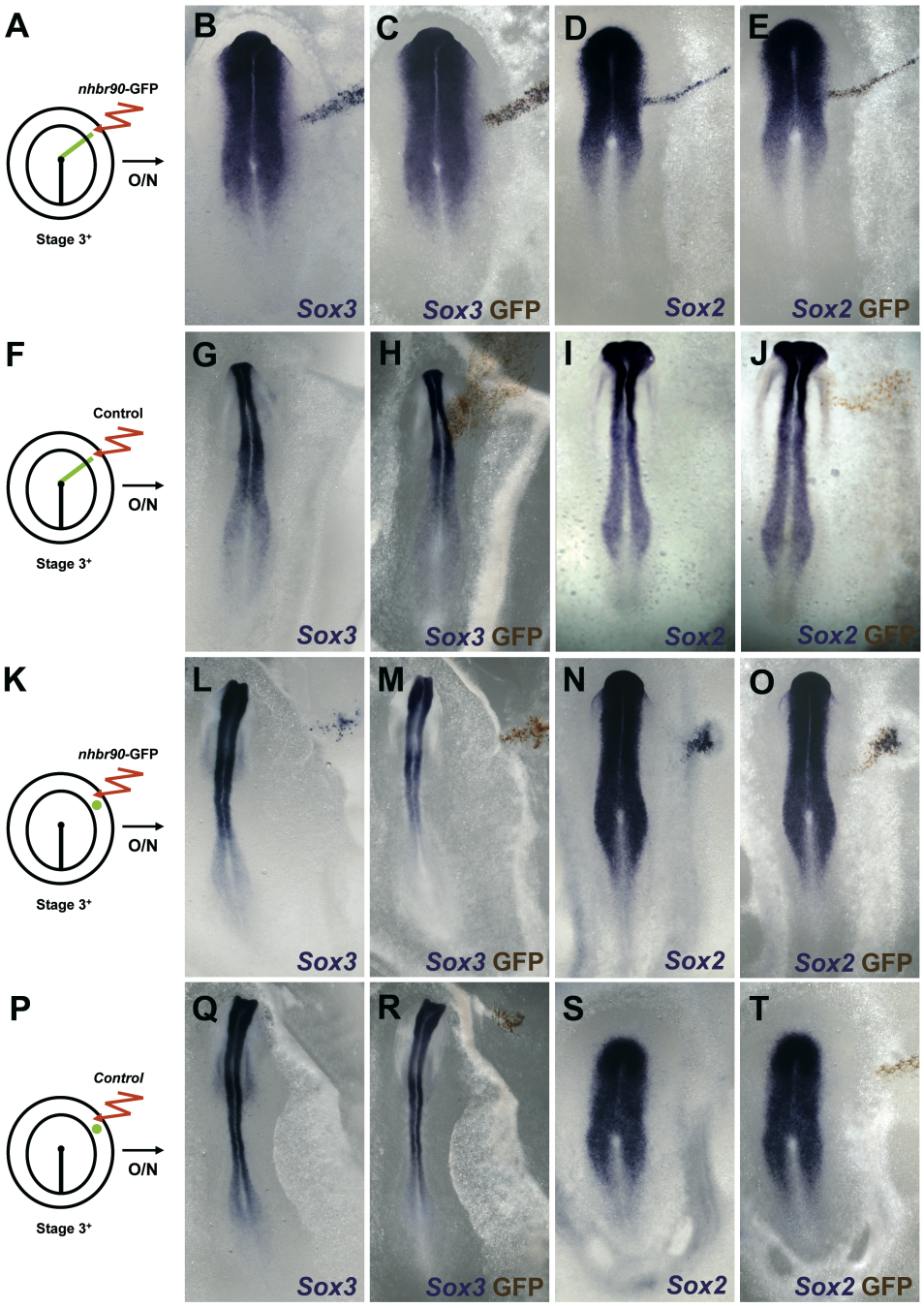

Fig 7.5. *Nhbr90* is able to induce both Sox3 and Sox2. *Nhbr90* overexpression in a line spanning from the node to the area *opaca* (**A**) results in the expansion of the domain of expression of *Sox3* (**B** and **C**) and *Sox2* (**D** and **E**); *nhbr90* electroporated to the inner third of the area *opaca* (**K**) induces the expression of the neural markers *Sox3* (**L** and **M**) and *Sox2* (**N** and **O**). Control electroporations have no effect on the neural markers tested (**F**- **J** and **P**- **T**).

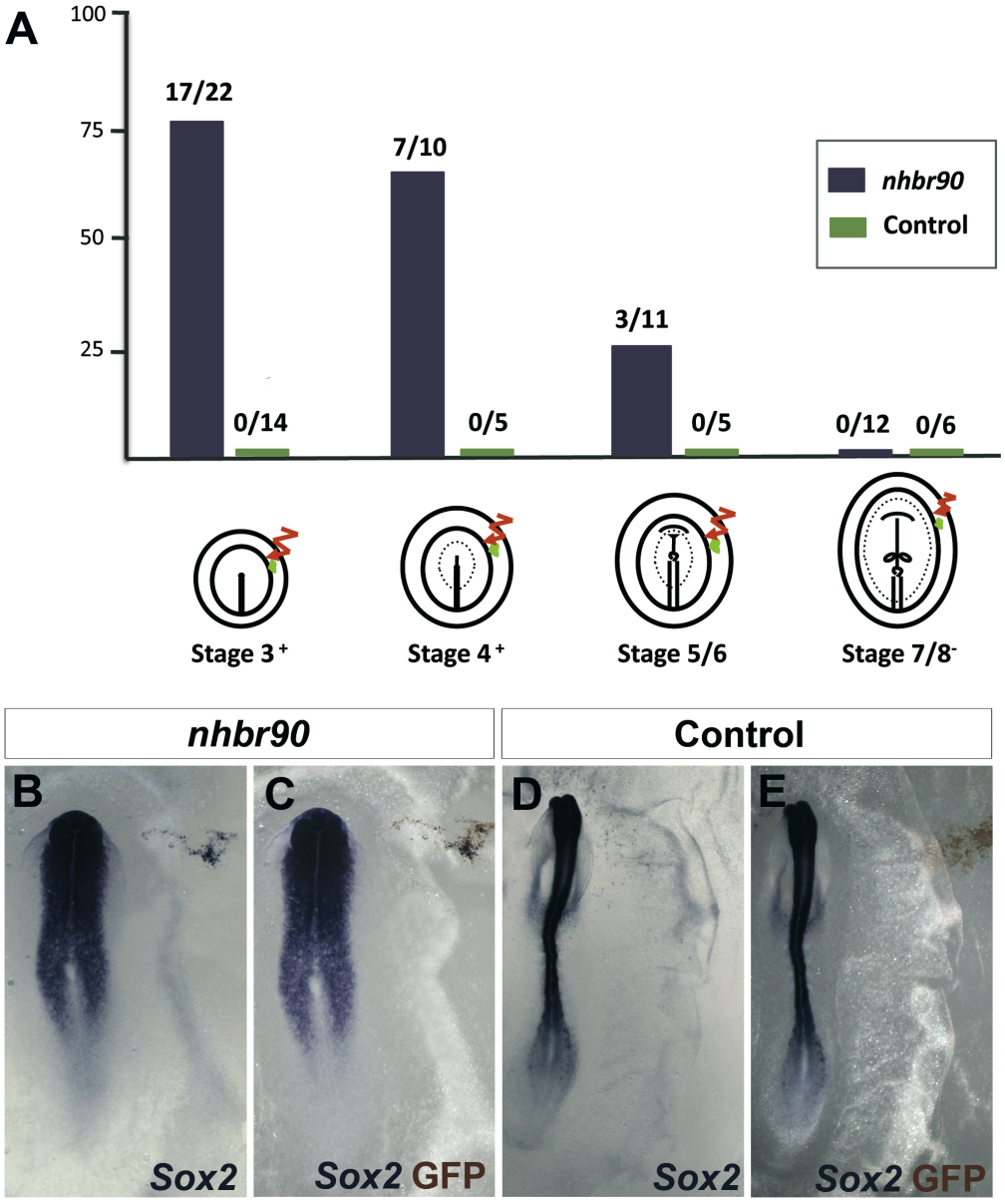

Fig 7.6. The embryo loses the competence to respond to *nhbr90* neural inducing ability after stage 4^{+}. Graphic representation of the decrease in embryonic competence to respond to *nhbr90* (**A**); Example of an embryo electroporated with *nhbr90* in the area opaca at stage 3^{+} with *Sox2* induction (**B** and **C**); Control electroporations have no effect on *Sox2* expression (**D** and **E**).

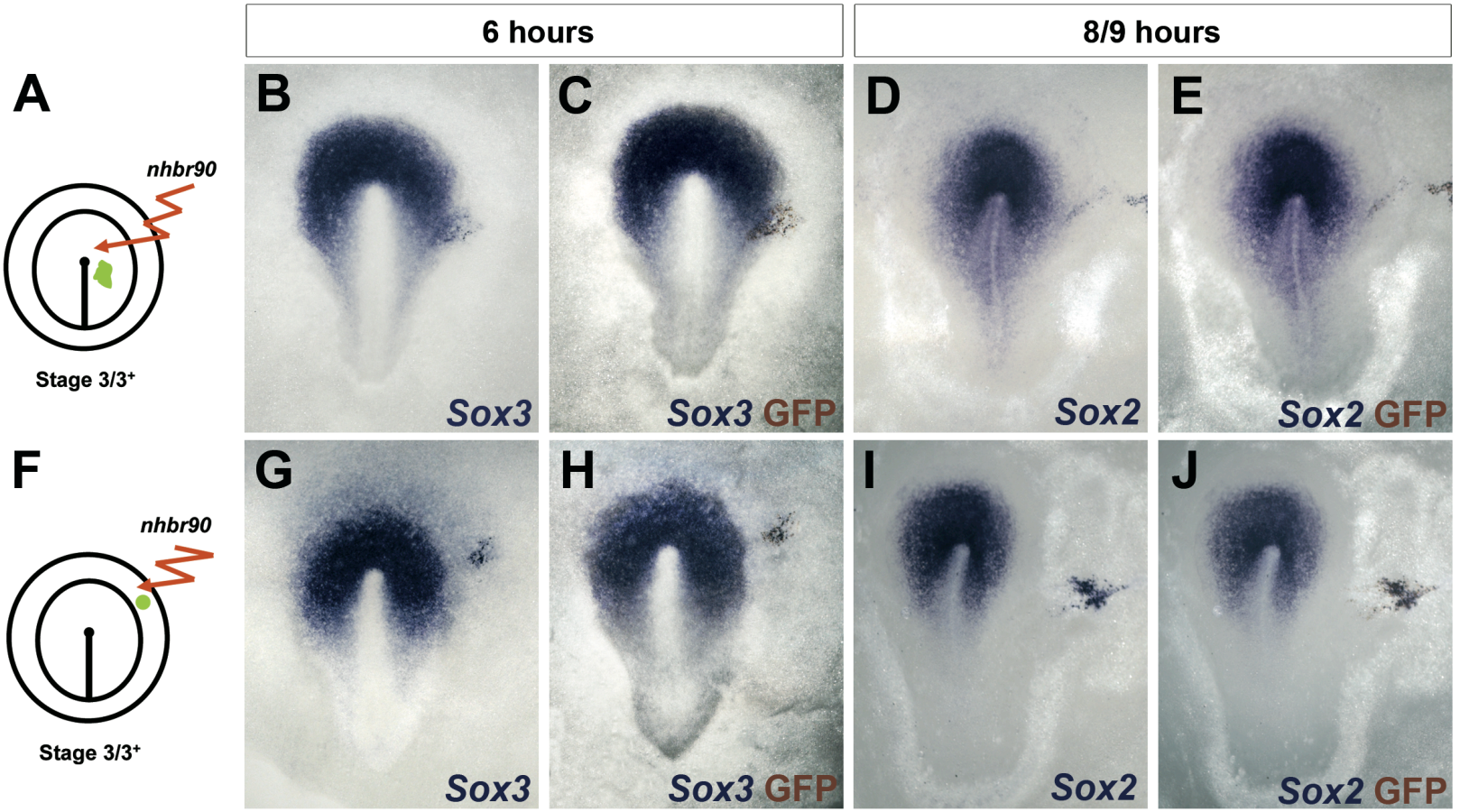

Fig 7.7. *nhbr90* induces *Sox3* before inducing *Sox2*. Electroporations of *nhbr90* in either the epiblast adjacent to the neural plate (**A**) or in the area *opaca* (**F**) result in the induction of *Sox3* within 6 hours (**B**-**C** and **G**-**H**). Similar experiments require at least 8/9 hours for *Sox2* to be upregulated (**D**-**E** and **I**-**J**).

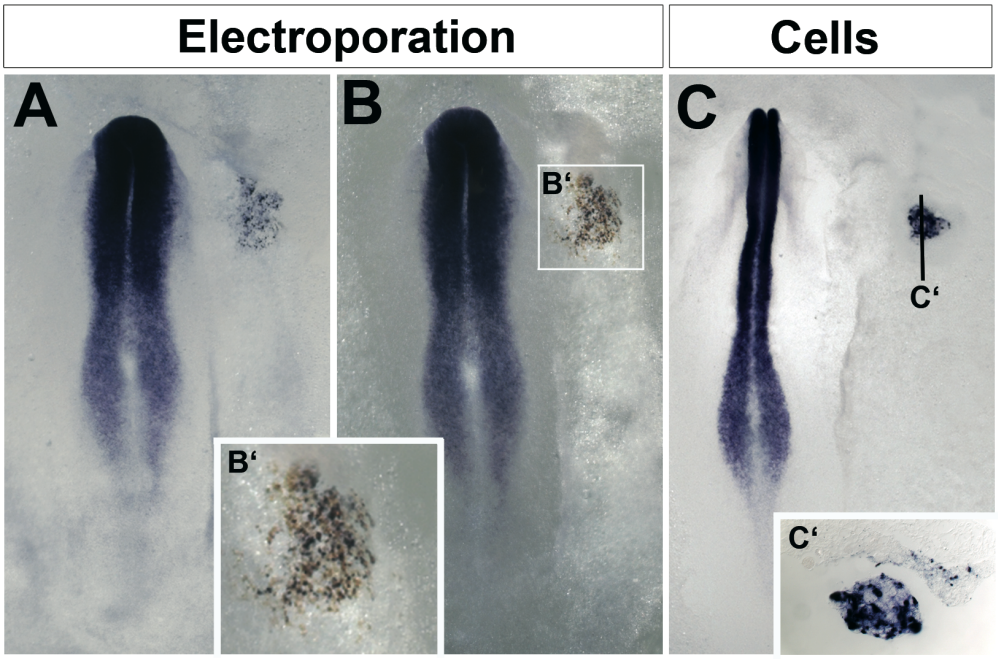

Fig 7.8. The effect of *nhbr90* is non cell autonomous. *nhbr90* overexpression by either electroporation (**A**, **B** and **B’**) or by grafts of expressing cells (**C** and **C’**) results in *Sox2* induction in the neighbouring cells (**B’**) or in the epiblast underlying the graft (as revealed through an histological section in **C’**).

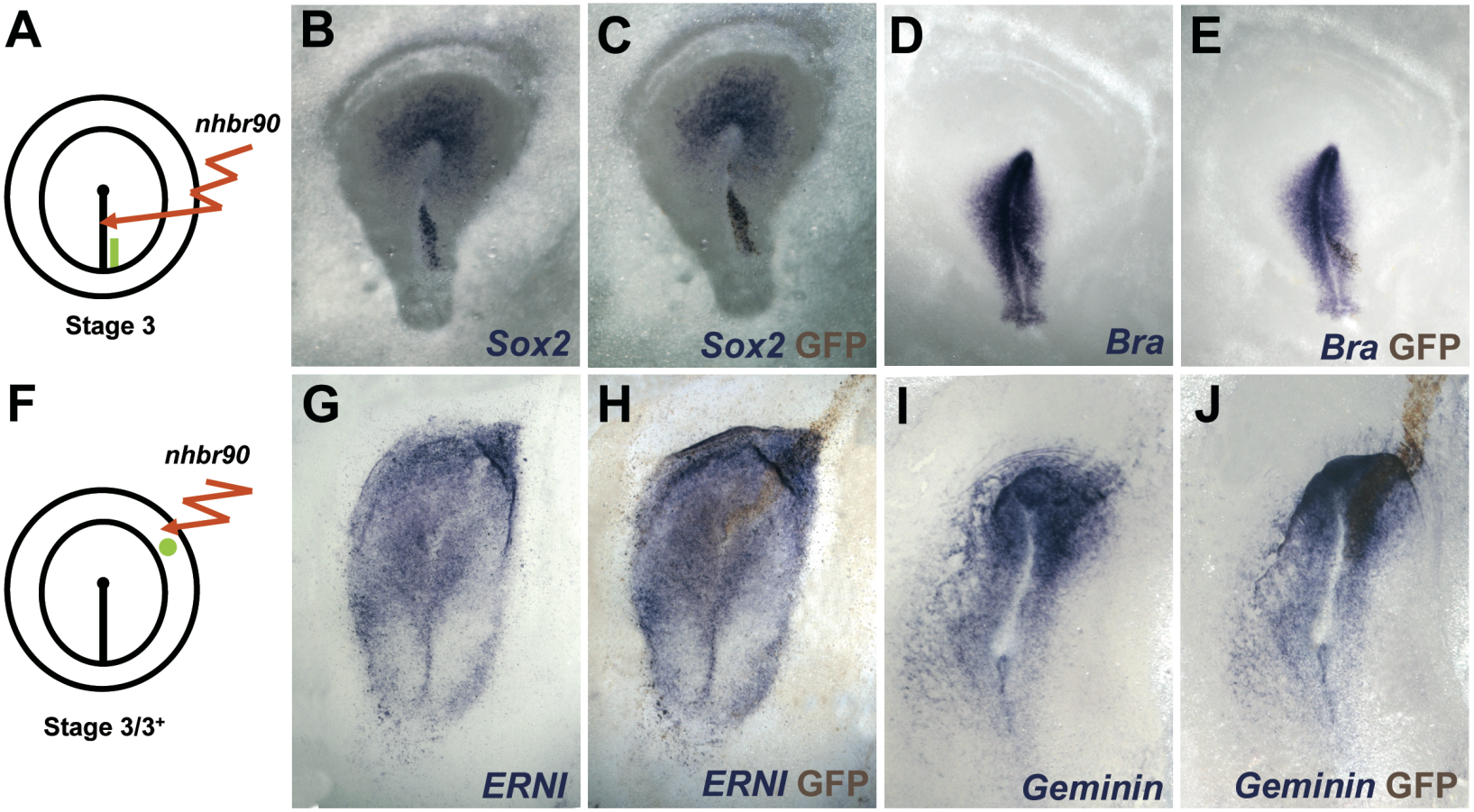

Fig 7.9. *nhbr90* induces *Sox2* at the expense of *Brachiury* and induces *Geminin* whilst dowregulating *ERNI*. Overexpression of *nhbr90* in a line parallel to the primitive streak (**A**) results in the induction of *Sox2* (**B** and **C**) at the expense of *Brachiury* expressing cells (**D** and **E**). *nhbr90* electroporated in a line spanning from the node to the area *opaca* (**F**) results in the downregulation of *ERNI* (**G** and **H**) and in the extension of the *Geminin* domain of expression (**I** and **J**).

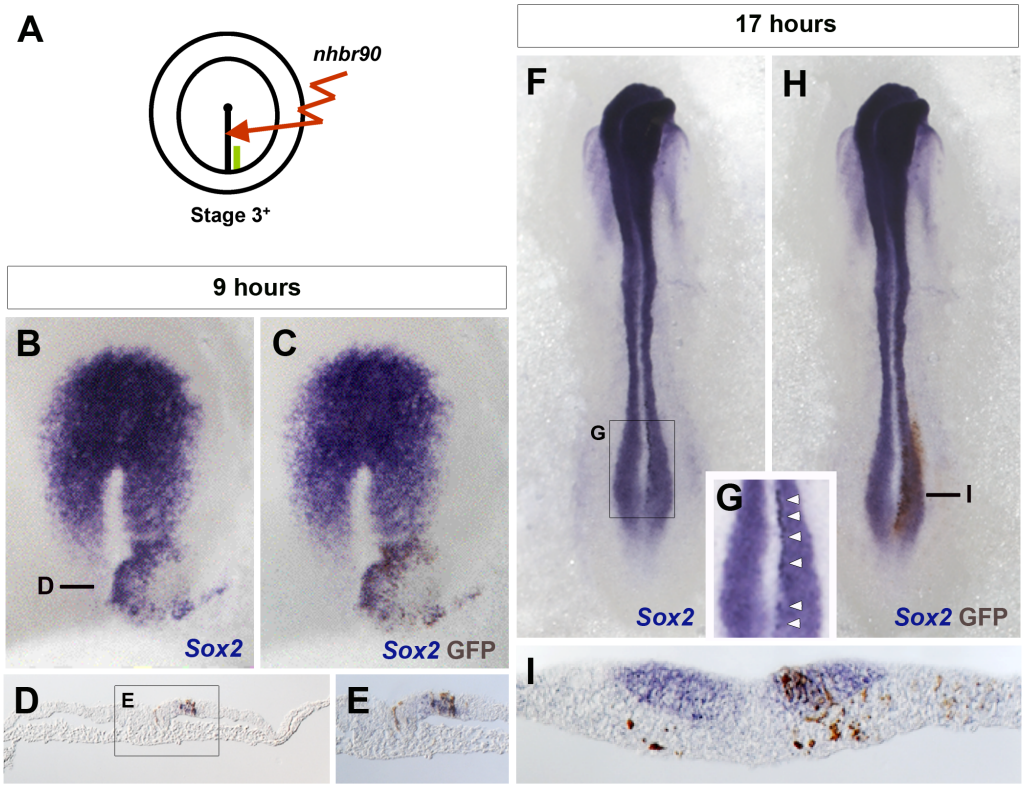

Fig 7.10. Cells induced to express *Sox2* are prevented to ingress through the primitive streak. *Nhbr90* overexpression in a line parallel to the posterior streak at stage 3^+ (**A**) results in the induction of *Sox2* within 9 hours (**B** and **C**) and the induced cells remain in the epiblast (**D** and **E**). After 17 hours (**F** and **H**), and as gastrulation proceeds, the induced *Sox2* cells accumulate at the "gastrulating edge" of the streak but do not ingress (**G**, white arrowheads); Not all the electroporated cells express *Sox2* and those are able to ingress (**I**).

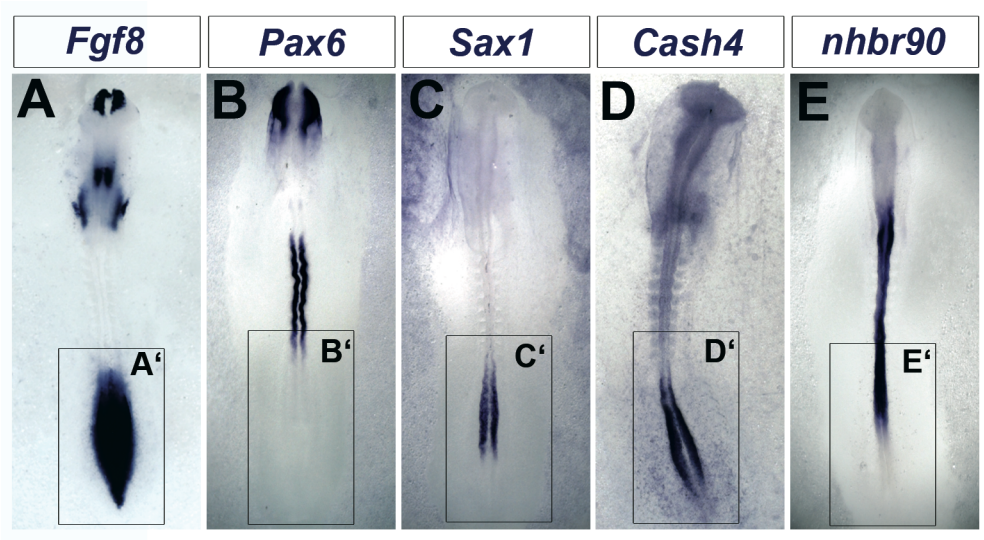

Fig 7.11. Expression profiles of *Fgf8*, *Pax6*, *Sax1, Cash4* and *nhbr90* in the Caudal Neural Plate (CNP). *Pax6* is excluded from the CNP (**B** and **B'**) and its expression is complementary to that of *Fgf8* (**A** and **A'**); *nhbr90* seems to occupy a more anterior domain of the CNP (**E** and **E'**), followed by *Sax1* (**C** and **C'**); *Cash4* expression expands to the most posterior part of the CNP (**D** and **D'**).

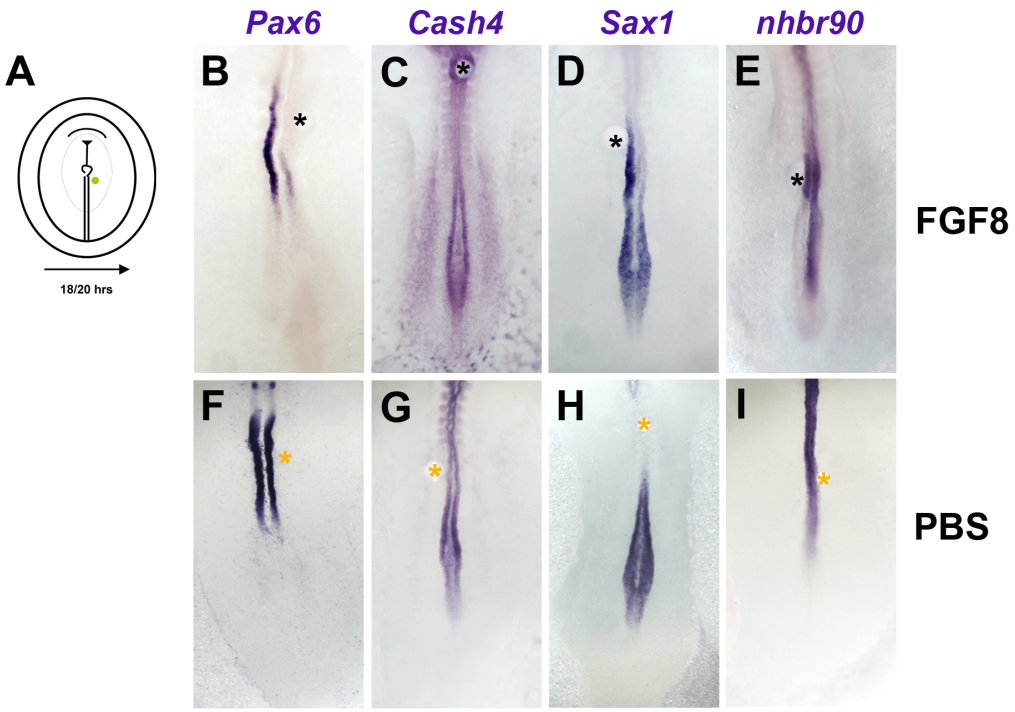

Fig 7.12. FGF8 induces proneural genes and also *nhbr90*. A bead of Fgf8 placed posterior to the node at stage 6 (**A**) downregulates *Pax6* (**B**) and upregulates the proneural genes *Cash4* (**C**) and *Sax1* (**D**) and also *nhbr90* (**E**); Control beads have no effect (**F**-**I**).

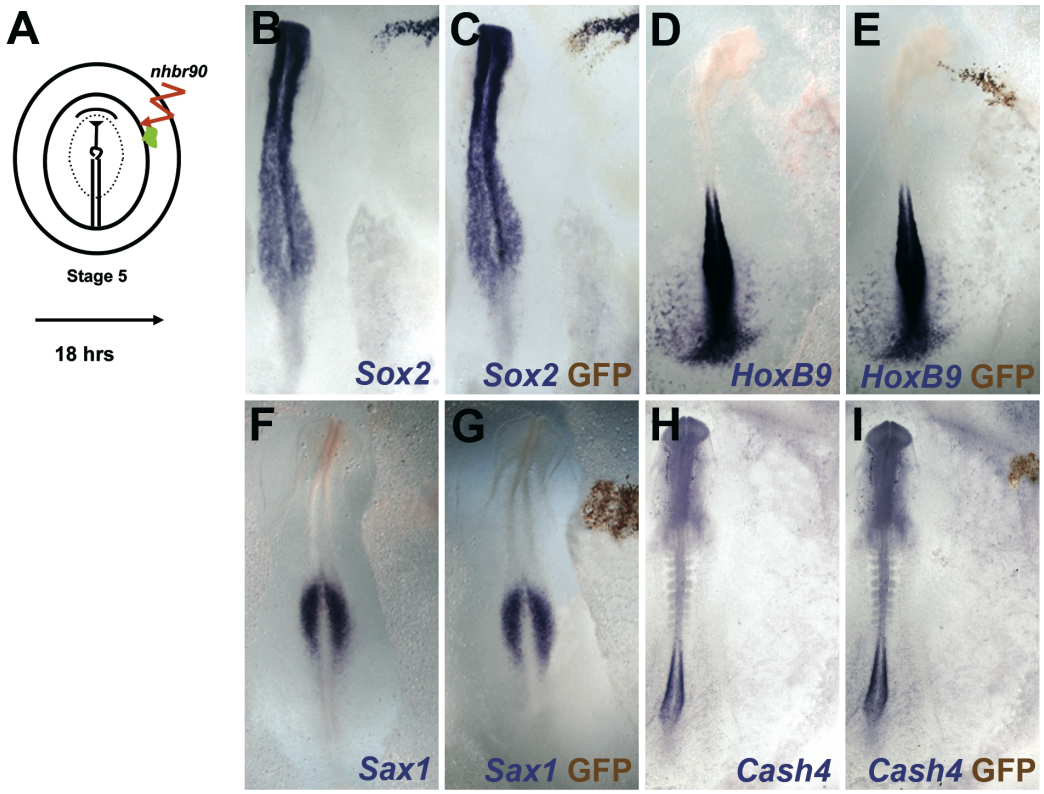

Fig 7.13.Overexpression of *nhbr90* in the area *opaca* has no effect on the proneural markers *Sax1* and *Cash4*. Electroporation of *nhbr90* in the area *opaca* at stage 5 (**A**) results in the induction of *Sox2* in some of the embryos tested (**B** and **C**) but has no effect in the posterior marker *HoxB9* (**D** and **E**) or the proneural markers *Sax1* (**F** and **G**) and *Cash4* (**H** and **I**).

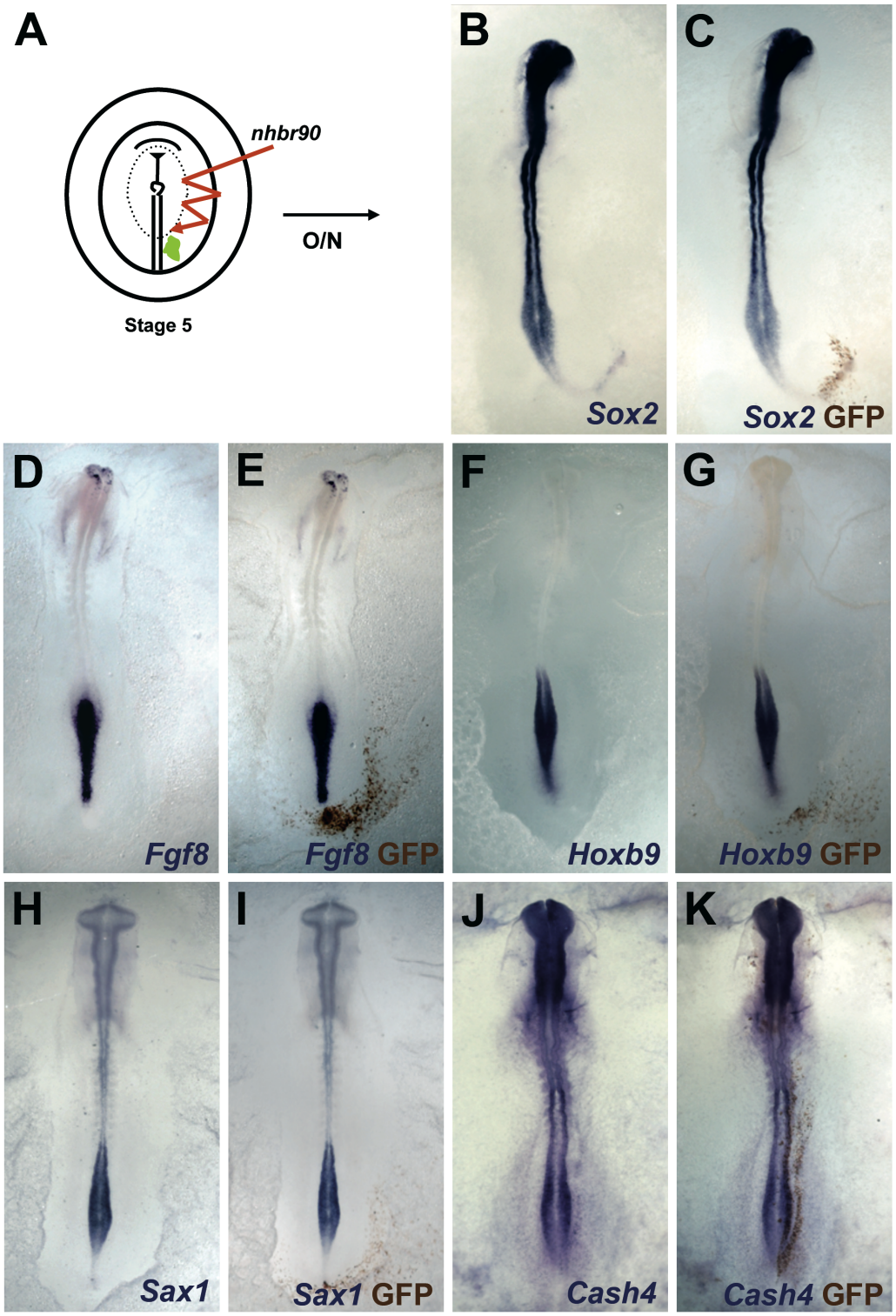

Fig 7.14.Overexpression of *nhbr90* in the area *pellucida* induces neural markers but has no effect in patterning. Electroporation of *nhbr90* in a patch adjacent to posterior end of the streak at stage 5 (**A**) results in the induction of *Sox2* (**B** and **C**) and Cash4 (**J** and **K**) in some of the embryos tested but has no effect on *Fgf8* (**D** and **E**), the posterior marker *HoxB9* (**F** and **G**), or the proneural gene *Sax1* (**H** and **I**).

Chapter 8

General Conclusion

The work presented in this study starts by re-evaluating the role of BMP antagonism in neural induction in the chick embryo. We find that, even though BMP inhibition is a required step during neural induction, it is not sufficient to elicit the expression of the neural plate markers *Sox3* or *Sox2*. Even combinations of BMP inhibitors, together with FGF and Wnt inhibition, is not sufficient to induce neural markers. We do find, however, that non-neural ectoderm can be neuralised by BMP inhibition, but only when the BMP-inhibited cells form a continuous trail from the neural plate or its border.

To uncover novel neural inducing molecules produced by the organizer, a screen to isolate cDNAs encoding for secreted proteins was carried out. 441 clones were obtained and, after sequence analyses, 133 were selected and put through an *in situ* hybridization screen, narrowing down the number of candidate molecules to 21. Based on their expression in the node and/or anterior primitive streak, 3 genes were studied further.

Fibulin2, a secreted extracellular matrix protein, revealed not to be directly involved in inducing neural markers;

Calreticulin is shown to be secreted and acts like a BMP inhibitor, extending the border of the neural plate. However, it is unable to induce neural character in the competent extraembryonic ectoderm of the area opaca. By a mechanism yet to be elucidated, Calreticulin, known as an intracelular Calcium regulator, might provide a link between Calcium concentration and neural induction.

Nhbr90, a novel molecule, seems not to be translated but act as a long non-coding RNA. Crutialy, *nhbr90* has the ability to induce *Sox2* by a mechanism that is yet to be elucidated.

The work presented in this Thesis emphasises the complexity of the neural induction process. Some new players have been identified and many more molecules from the screen are yet to be analysed.

References

Abe, T., Furue, M., Kondow, A., Matsuzaki, K. and Asashima, M. (2005). Notch signaling modulates the nuclear localization of carboxy-terminal-phosphorylated smad2 and controls the competence of ectodermal cells for activin A. *Mech Dev* **122**, 671-80.

Aharon, A., Katzenell, S., Tamari, T. and Brenner, B. (2009). Microparticles bearing tissue factor and tissue factor pathway inhibitor in gestational vascular complications. *J Thromb Haemost* **7**, 1047-50.

Albano, R. M., Arkell, R., Beddington, R. S. and Smith, J. C. (1994). Expression of inhibin subunits and follistatin during postimplantation mouse development: decidual expression of activin and expression of follistatin in primitive streak, somites and hindbrain. *Development* **120**, 803-13.

Albazerchi, A. and Stern, C. D. (2007). A role for the hypoblast (AVE) in the initiation of neural induction, independent of its ability to position the primitive streak. *Dev Biol* **301**, 489-503.

Albrecht, U., Seulberger, H., Schwarz, H. and Risau, W. (1990). Correlation of blood-brain barrier function and HT7 protein distribution in chick brain circumventricular organs. *Brain Res* **535**, 49-61.

Allain, F., Vanpouille, C., Carpentier, M., Slomianny, M. C., Durieux, S. and Spik, G. (2002). Interaction with glycosaminoglycans is required for cyclophilin B to trigger integrin-mediated adhesion of peripheral blood T lymphocytes to extracellular matrix. *Proc Natl Acad Sci U S A* **99**, 2714-9.

Alvarez, I. S., Araujo, M. and Nieto, M. A. (1998). Neural induction in whole chick embryo cultures by FGF. *Dev Biol* **199**, 42-54.

Ang, S. L. and Rossant, J. (1994). HNF-3 beta is essential for node and notochord formation in mouse development. *Cell* **78**, 561-74.

Aplin, A. C., Gelati, M., Fogel, E., Carnevale, E. and Nicosia, R. F. (2006). Angiopoietin-1 and vascular endothelial growth factor induce expression of inflammatory cytokines before angiogenesis. *Physiol Genomics* **27**, 20-8.

Argraves, W. S., Dickerson, K., Burgess, W. H. and Ruoslahti, E. (1989). Fibulin, a novel protein that interacts with the fibronectin receptor beta subunit cytoplasmic domain. *Cell* **58**, 623-9.

Argraves, W. S., Greene, L. M., Cooley, M. A. and Gallagher, W. M. (2003). Fibulins: physiological and disease perspectives. *EMBO Rep* **4**, 1127-31.

Argraves, W. S., Tran, H., Burgess, W. H. and Dickerson, K. (1990). Fibulin is an extracellular matrix and plasma glycoprotein with repeated domain structure. *J Cell Biol* **111**, 3155-64.

Artavanis-Tsakonas, S. (1988). The molecular biology of the Notch locus and the fine tuning of differentiation in Drosophila. *Trends Genet* **4**, 95-100.

Ausubel, F. M., Brent, R., Kingston, R. E., Moore, D. D., Seidman, J. G., Smith, J. A. and Struhl, K. J. (1995). Current Protocols in Molecular Biology. New York, NY: John Wiley.

Bach, C., Mueller, D., Buhl, S., Garcia-Cuellar, M. P. and Slany, R. K. (2009). Alterations of the CxxC domain preclude oncogenic activation of mixed-lineage leukemia 2. *Oncogene* **28**, 815-23.

Bachiller, D., Klingensmith, J., Kemp, C., Belo, J. A., Anderson, R. M., May, S. R., McMahon, J. A., McMahon, A. P., Harland, R. M., Rossant, J. et al. (2000). The organizer factors Chordin and Noggin are required for mouse forebrain development. *Nature* **403**, 658-61.

Baillat, D., Hakimi, M. A., Naar, A. M., Shilatifard, A., Cooch, N. and Shiekhattar, R. (2005). Integrator, a multiprotein mediator of small nuclear RNA processing, associates with the C-terminal repeat of RNA polymerase II. *Cell* **123**, 265-76.

Baksh, S., Burns, K., Busaan, J. and Michalak, M. (1992). Expression and purification of recombinant and native calreticulin. *Protein Expr Purif* **3**, 322-31.

Baldwin, T. A. and Ostergaard, H. L. (2002). The protein-tyrosine phosphatase CD45 reaches the cell surface via golgi-dependent and -independent pathways. *J Biol Chem* **277**, 50333-40.

Barth, L. G. and Barth, L. J. (1974a). Ionic regulation of embryonic induction and cell differentiation in Rana pipiens. *Dev Biol* **39**, 1-22.

Barth, L. J. and Barth, L. G. (1974b). Effect of the potassium ion on induction of notochord from gastrula ectoderm of Rana pipiens. *Biol Bull* **146**, 313-25.

Batova, I. N., Richardson, R. T., Widgren, E. E. and O'Rand, M. G. (2000). Analysis of the autoimmune epitopes on human testicular NASP using recombinant and synthetic peptides. *Clin Exp Immunol* **121**, 201-9.

Batut, J., Neant, I., Leclerc, C. and Moreau, M. (2003). [xMLP is an early response calcium target gene in neural determination in Xenopus laevis]. *J Soc Biol* **197**, 283-9.

Batut, J., Vandel, L., Leclerc, C., Daguzan, C., Moreau, M. and Neant, I. (2005). The Ca2+-induced methyltransferase xPRMT1b controls neural fate in amphibian embryo. *Proc Natl Acad Sci U S A* **102**, 15128-33.

Beaudoin, F., Michaelson, L. V., Hey, S. J., Lewis, M. J., Shewry, P. R., Sayanova, O. and Napier, J. A. (2000). Heterologous reconstitution in yeast of the polyunsaturated fatty acid biosynthetic pathway. *Proc Natl Acad Sci U S A* **97**, 6421-6.

Beddington, R. S. (1994). Induction of a second neural axis by the mouse node. *Development* **120**, 613-20.

Belperio, J. A., Keane, M. P., Arenberg, D. A., Addison, C. L., Ehlert, J. E., Burdick, M. D. and Strieter, R. M. (2000). CXC chemokines in angiogenesis. *J Leukoc Biol* **68**, 1-8.

Ben-Aroya, S., Coombes, C., Kwok, T., O'Donnell, K. A., Boeke, J. D. and Hieter, P. (2008). Toward a comprehensive temperature-sensitive mutant repository of the essential genes of Saccharomyces cerevisiae. *Mol Cell* **30**, 248-58.

Benchimol, S., Fuks, A., Jothy, S., Beauchemin, N., Shirota, K. and Stanners, C. P. (1989). Carcinoembryonic antigen, a human tumor marker, functions as an intercellular adhesion molecule. *Cell* **57**, 327-34.

Bendtsen, J. D., Nielsen, H., von Heijne, G. and Brunak, S. (2004). Improved prediction of signal peptides: SignalP 3.0. *J Mol Biol* **340**, 783-95.

Berditchevski, F. and Odintsova, E. (1999). Characterization of integrin-tetraspanin adhesion complexes: role of tetraspanins in integrin signaling. *J Cell Biol* **146**, 477-92.

Bernard, D., Prasanth, K. V., Tripathi, V., Colasse, S., Nakamura, T., Xuan, Z., Zhang, M. Q., Sedel, F., Jourdren, L., Coulpier, F. et al. A long nuclear-retained non-coding RNA regulates synaptogenesis by modulating gene expression. *Embo J* **29**, 3082-93.

Bertrand, N., Medevielle, F. and Pituello, F. (2000). FGF signalling controls the timing of Pax6 activation in the neural tube. *Development* **127**, 4837-43.

Bertrand, V., Hudson, C., Caillol, D., Popovici, C. and Lemaire, P. (2003). Neural tissue in ascidian embryos is induced by FGF9/16/20, acting via a combination of maternal GATA and Ets transcription factors. *Cell* **115**, 615-27.

Bhushan, A., Chen, Y. and Vale, W. (1998). Smad7 inhibits mesoderm formation and promotes neural cell fate in Xenopus embryos. *Dev Biol* **200**, 260-8.

Biehs, B., Francois, V. and Bier, E. (1996). The Drosophila short gastrulation gene prevents Dpp from autoactivating and suppressing neurogenesis in the neuroectoderm. *Genes Dev* **10**, 2922-34.

Biswas, C. (1982). Tumor cell stimulation of collagenase production by fibroblasts. *Biochem Biophys Res Commun* **109**, 1026-34.

Biswas, C., Bloch, K. J. and Gross, J. (1982). Collagenolytic activity of rabbit V2 carcinoma implanted in the nude mouse. *J Natl Cancer Inst* **69**, 1329-36.

Bitoun, E., Oliver, P. L. and Davies, K. E. (2007). The mixed-lineage leukemia fusion partner AF4 stimulates RNA polymerase II transcriptional elongation and mediates coordinated chromatin remodeling. *Hum Mol Genet* **16**, 92-106.

Blanchard, M. M. and Nowotny, V. (1994). High-throughput rapid yeast DNA extraction. Application to yeast artificial chromosomes as polymerase chain reaction templates. *Genet Anal Tech Appl* **11**, 7-11.

Blobel, G. and Dobberstein, B. (1975a). Transfer of proteins across membranes. I. Presence of proteolytically processed and unprocessed nascent immunoglobulin light chains on membrane-bound ribosomes of murine myeloma. *J Cell Biol* **67**, 835-51.

Blobel, G. and Dobberstein, B. (1975b). Transfer of proteins across membranes. II. Reconstitution of functional rough microsomes from heterologous components. *J Cell Biol* **67**, 852-62.

Blum, M., Gaunt, S. J., Cho, K. W., Steinbeisser, H., Blumberg, B., Bittner, D. and De Robertis, E. M. (1992). Gastrulation in the mouse: the role of the homeobox gene goosecoid. *Cell* **69**, 1097-106.

Boom, A., Mollereau, C., Meunier, J. C., Vassart, G., Parmentier, M., Vanderhaeghen, J. J. and Schiffmann, S. N. (1999). Distribution of the nociceptin and nocistatin precursor transcript in the mouse central nervous system. *Neuroscience* **91**, 991-1007.

Bordador, L. C., Li, X., Toole, B., Chen, B., Regezi, J., Zardi, L., Hu, Y. and Ramos, D. M. (2000). Expression of emmprin by oral squamous cell carcinoma. *Int J Cancer* **85**, 347-52.

Borden, J. R., Jones, S. W., Indurthi, D., Chen, Y. and Papoutsakis, E. T. A genomic-library based discovery of a novel, possibly synthetic, acid-tolerance mechanism in Clostridium acetobutylicum involving non-coding RNAs and ribosomal RNA processing. *Metab Eng* **12**, 268-81.

Born, J., Janeczek, J., Schwarz, W. and Tiedemann, H. (1989). Activation of masked neural determinants in amphibian eggs and embryos and their release from the inducing tissue. *Cell Differ Dev* **27**, 1-7.

Born, W., Freeman, M., Bornstein, W., Rapoport, A., Klein, R. D., Hendy, G. N., Khorana, H. G., Rich, A., Potts, J. T., Jr. and Kronenberg, H. M. (1987). Signal sequence of human preproparathyroid hormone is inactive in yeast. *J Bone Miner Res* **2**, 353-60.

Boulton, S. J. (2006). BRCA1-mediated ubiquitylation. *Cell Cycle* **5**, 1481-6.

Bouwmeester, T., Kim, S.-H., Sasai , Y., Lu, B. and De Robertis, E. M. (1996). Cerberus is a head-inducing secreted factor expressed in the anterior endoderm of Spemann's Organizer. *Nature* **382**, 595-601.

Bray, S. (1998). Notch signalling in Drosophila: three ways to use a pathway. *Semin Cell Dev Biol* **9**, 591-7.

Bray, S. J. (2006). Notch signalling: a simple pathway becomes complex. *Nat Rev Mol Cell Biol* **7**, 678-89.

Brazin, K. N., Mallis, R. J., Fulton, D. B. and Andreotti, A. H. (2002). Regulation of the tyrosine kinase Itk by the peptidyl-prolyl isomerase cyclophilin A. *Proc Natl Acad Sci U S A* **99**, 1899-904.

Briant, J. A., Nielsen, D. A., Proudnikov, D., Londono, D., Ho, A., Ott, J. and Kreek, M. J. Evidence for association of two variants of the nociceptin/orphanin FQ receptor gene OPRL1 with vulnerability to develop opiate addiction in Caucasians. *Psychiatr Genet* **20**, 65-72.

Brown, J. D., Hann, B. C., Medzihradszky, K. F., Niwa, M., Burlingame, A. L. and Walter, P. (1994). Subunits of the Saccharomyces cerevisiae signal recognition particle required for its functional expression. *Embo J* **13**, 4390-400.

Brown, J. M. and Storey, K. G. (2000). A region of the vertebrate neural plate in which neighbouring cells can adopt neural or epidermal fates. *Curr Biol* **10**, 869-72.

Bukrinsky, M. I. (2002). Cyclophilins: unexpected messengers in intercellular communications. *Trends Immunol* **23**, 323-5.

Burge, C. and Karlin, S. (1997). Prediction of complete gene structures in human genomic DNA. *J Mol Biol* **268**, 78-94.

Burns, K., Duggan, B., Atkinson, E. A., Famulski, K. S., Nemer, M., Bleackley, R. C. and Michalak, M. (1994). Modulation of gene expression by calreticulin binding to the glucocorticoid receptor. *Nature* **367**, 476-80.

Cai, Y., Jin, J., Yao, T., Gottschalk, A. J., Swanson, S. K., Wu, S., Shi, Y., Washburn, M. P., Florens, L., Conaway, R. C. et al. (2007). YY1 functions with INO80 to activate transcription. *Nat Struct Mol Biol* **14**, 872-4.

Campos-Ortega, J. A. (1988). Cellular interactions during early neurogenesis of Drosophila melanogaster. *Trends Neurosci* **11**, 400-5.

Camus, A., Perea-Gomez, A., Moreau, A. and Collignon, J. (2006). Absence of Nodal signaling promotes precocious neural differentiation in the mouse embryo. *Dev Biol* **295**, 743-55.

Canning, M., Boutell, C., Parkinson, J. and Everett, R. D. (2004). A RING finger ubiquitin ligase is protected from autocatalyzed ubiquitination and degradation by binding to ubiquitin-specific protease USP7. *J Biol Chem* **279**, 38160-8.

Carnevale, E., Fogel, E., Aplin, A. C., Gelati, M., Howson, K. M., Zhu, W. H. and Nicosia, R. F. (2007). Regulation of postangiogenic neovessel survival by beta1 and beta3 integrins in collagen and fibrin matrices. *J Vasc Res* **44**, 40-50.

Carpentier, M., Allain, F., Slomianny, M. C., Durieux, S., Vanpouille, C., Haendler, B. and Spik, G. (2002). Receptor type I and type II binding regions and the peptidyl-prolyl isomerase site of cyclophilin B are required for enhancement of T-lymphocyte adhesion to fibronectin. *Biochemistry* **41**, 5222-9.

Carulli, D., Laabs, T., Geller, H. M. and Fawcett, J. W. (2005). Chondroitin sulfate proteoglycans in neural development and regeneration. *Curr Opin Neurobiol* **15**, 116-20.

Casellas, R. and Brivanlou, A. H. (1998). Xenopus Smad7 inhibits both the activin and BMP pathways and acts as a neural inducer. *Dev Biol* **198**, 1-12.

Castellana, D., Kunzelmann, C. and Freyssinet, J. M. (2009). Pathophysiologic significance of procoagulant microvesicles in cancer disease and progression. *Hamostaseologie* **29**, 51-7.

Chang, C. and Harland, R. M. (2007). Neural induction requires continued suppression of both Smad1 and Smad2 signals during gastrulation. *Development* **134**, 3861-72.

Chen, C., Seth, A. K. and Aplin, A. E. (2006). Genetic and expression aberrations of E3 ubiquitin ligases in human breast cancer. *Mol Cancer Res* **4**, 695-707.

Chen, F., Hayes, P. M., Mulrooney, D. M. and Pan, A. (1994a). Identification and characterization of cDNA clones encoding plant calreticulin in barley. *Plant Cell* **6**, 835-43.

Chen, T. S., Lai, R. C., Lee, M. M., Choo, A. B., Lee, C. N. and Lim, S. K. (2009). Mesenchymal stem cell secretes microparticles enriched in pre-microRNAs. *Nucleic Acids Res* **38**, 215-24.

Chen, W. S., Manova, K., Weinstein, D. C., Duncan, S. A., Plump, A. S., Prezioso, V. R., Bachvarova, R. F. and Darnell, J. E., Jr. (1994b). Disruption of the HNF-4 gene, expressed in visceral endoderm, leads to cell death in embryonic ectoderm and impaired gastrulation of mouse embryos. *Genes Dev* **8**, 2466-77.

Chen, Y., Huang, L., Russo, A. F. and Solursh, M. (1992). Retinoic acid is enriched in Hensen's node and is developmentally regulated in the early chicken embryo. *Proc Natl Acad Sci U S A* **89**, 10056-9.

Chen, Y. and Solursh, M. (1992). Comparison of Hensen's node and retinoic acid in secondary axis induction in the early chick embryo. *Dev Dyn* **195**, 142-51.

Chen, Y. G., Hata, A., Lo, R. S., Wotton, D., Shi, Y., Pavletich, N. and Massague, J. (1998). Determinants of specificity in TGF-beta signal transduction. *Genes Dev* **12**, 2144-52.

Chevet, E., Smirle, J., Cameron, P. H., Thomas, D. Y. and Bergeron, J. J. (2009). Calnexin phosphorylation: linking cytoplasmic signalling to endoplasmic reticulum lumenal functions. *Semin Cell Dev Biol* **21**, 486-90.

Chironi, G. N., Boulanger, C. M., Simon, A., Dignat-George, F., Freyssinet, J. M. and Tedgui, A. (2009). Endothelial microparticles in diseases. *Cell Tissue Res* **335**, 143-51.

Chomczynski, P. and Sacchi, N. (1987). Single-step method of RNA isolation by acid guanidinium thiocyanate-phenol-chloroform extraction. *Anal Biochem* **162**, 156-9.

Cinti, D. L., Cook, L., Nagi, M. N. and Suneja, S. K. (1992). The fatty acid chain elongation system of mammalian endoplasmic reticulum. *Prog Lipid Res* **31**, 1-51.

Clandinin, T. R., Lee, C. H., Herman, T., Lee, R. C., Yang, A. Y., Ovasapyan, S. and Zipursky, S. L. (2001). Drosophila LAR regulates R1-R6 and R7 target specificity in the visual system. *Neuron* **32**, 237-48.

Coffman, C., Harris, W. and Kintner, C. (1990). Xotch, the Xenopus homolog of Drosophila notch. *Science* **249**, 1438-41.

Coffman, C. R., Skoglund, P., Harris, W. A. and Kintner, C. R. (1993). Expression of an extracellular deletion of Xotch diverts cell fate in Xenopus embryos. *Cell* **73**, 659-71.

Collins, S. R., Miller, K. M., Maas, N. L., Roguev, A., Fillingham, J., Chu, C. S., Schuldiner, M., Gebbia, M., Recht, J., Shales, M. et al. (2007). Functional dissection of protein complexes involved in yeast chromosome biology using a genetic interaction map. *Nature* **446**, 806-10.

Conlon, F. L., Lyons, K. M., Takaesu, N., Barth, K. S., Kispert, A., Herrmann, B. and Robertson, E. J. (1994). A primary requirement for nodal in the formation and maintenance of the primitive streak in the mouse. *Development* **120**, 1919-28.

Connolly, D. J., Patel, K. and Cooke, J. (1997). Chick noggin is expressed in the organizer and neural plate during axial development, but offers no evidence of involvement in primary axis formation. *Int J Dev Biol* **41**, 389-96.

Connolly, D. J., Patel, K., Seleiro, E. A., Wilkinson, D. G. and Cooke, J. (1995). Cloning, sequencing, and expressional analysis of the chick homologue of follistatin. *Dev Genet* **17**, 65-77.

Cooley, M. A., Kern, C. B., Fresco, V. M., Wessels, A., Thompson, R. P., McQuinn, T. C., Twal, W. O., Mjaatvedt, C. H., Drake, C. J. and Argraves, W. S. (2008). Fibulin-1 is required for morphogenesis of neural crest-derived structures. *Dev Biol* **319**, 336-45.

Coppolino, M. G. and Dedhar, S. (1998). Calreticulin. *Int J Biochem Cell Biol* **30**, 553-8.

Coppolino, M. G., Woodside, M. J., Demaurex, N., Grinstein, S., St-Arnaud, R. and Dedhar, S. (1997). Calreticulin is essential for integrin-mediated calcium signalling and cell adhesion. *Nature* **386**, 843-7.

Cornell, R. A. and Eisen, J. S. (2002). Delta/Notch signaling promotes formation of zebrafish neural crest by repressing Neurogenin 1 function. *Development* **129**, 2639-48.

Cornell, R. A., Musci, T. J. and Kimelman, D. (1995). FGF is a prospective competence factor for early activin-type signals in Xenopus mesoderm induction. *Development* **121**, 2429-37.

Creton, R. (2004). The calcium pump of the endoplasmic reticulum plays a role in midline signaling during early zebrafish development. *Brain Res Dev Brain Res* **151**, 33-41.

Crofts, A. J., Leborgne-Castel, N., Pesca, M., Vitale, A. and Denecke, J. (1998). BiP and calreticulin form an abundant complex that is independent of endoplasmic reticulum stress. *Plant Cell* **10**, 813-24.

Cuevas, P. and Llorca, F. O. (1974). [Primary induction of young chick (Gallus gallus) blastoderm by grafting Hensen's node from quail. Preliminary note]. *Acta Anat* **89**, 423-30.

Cunningham, B. A., Hemperly, J. J., Murray, B. A., Prediger, E. A., Brackenbury, R. and Edelman, G. M. (1987). Neural cell adhesion molecule: structure, immunoglobulin-like domains, cell surface modulation, and alternative RNA splicing. *Science* **236**, 799-806.

Dale, L., Howes, G., Price, B. M. and Smith, J. C. (1992). Bone morphogenetic protein 4: a ventralizing factor in early Xenopus development. *Development* **115**, 573-85.

Dale, L. and Slack, J. M. W. (1987b). Regional Specification within the mesoderm of early embryos of Xenopus laevis. *Development* **100**, 279-295.

Darnell, D. K., Stark, M. R. and Schoenwolf, G. C. (1999). Timing and cell interactions underlying neural induction in the chick embryo. *Development* **126**, 2505-2514.

David, D., Sundararabu, S. and Gerst, J. E. (1998). Involvement of long chain fatty acid elongation in the trafficking of secretory vesicles in yeast. *J Cell Biol* **143**, 1167-82.

Dawson, T. M. (2006). Parkin and defective ubiquitination in Parkinson's disease. *J Neural Transm Suppl*, 209-13.

de Almeida, I., Rolo, A., Batut, J., Hill, C., Stern, C. D. and Linker, C. (2008). Unexpected activities of Smad7 in Xenopus mesodermal and neural induction. *Mech Dev* **125**, 421-31.

De Lucia, F. and Dean, C. Long non-coding RNAs and chromatin regulation. *Curr Opin Plant Biol* **14**, 168-73.

De Robertis, E. M. and Kuroda, H. (2004). Dorsal-ventral patterning and neural induction in Xenopus embryos. *Annu Rev Cell Dev Biol* **20**, 285-308.

Deal, R. B., Topp, C. N., McKinney, E. C. and Meagher, R. B. (2007). Repression of flowering in Arabidopsis requires activation of FLOWERING LOCUS C expression by the histone variant H2A.Z. *Plant Cell* **19**, 74-83.

Deardorff, M. A., Tan, C., Conrad, L. J. and Klein, P. S. (1998). Frizzled-8 is expressed in the Spemann organizer and plays a role in early morphogenesis. *Development* **125**, 2687-700.

Delaune, E., Lemaire, P. and Kodjabachian, L. (2005). Neural induction in Xenopus requires early FGF signalling in addition to BMP inhibition. *Development* **132**, 299-310.

Denning, G. M., Leidal, K. G., Holst, V. A., Iyer, S. S., Pearson, D. W., Clark, J. R., Nauseef, W. M. and Clark, R. A. (1997). Calreticulin biosynthesis and processing in human myeloid cells: demonstration of signal peptide cleavage and N-glycosylation. *Blood* **90**, 372-81.

Derynck, R., Zhang, Y. and Feng, X. H. (1998). Smads: transcriptional activators of TGF-beta responses. *Cell* **95**, 737-40.

Di-Gregorio, A., Sancho, M., Stuckey, D. W., Crompton, L. A., Godwin, J., Mishina, Y. and Rodriguez, T. A. (2007). BMP signalling inhibits premature neural differentiation in the mouse embryo. *Development* **134**, 3359-69.

Dias, M. S. and Schoenwolf, G. C. (1990). Formation of ectopic neurepithelium in chick blastoderms: age-related capacities for induction and self-differentiation following transplantation of quail Hensen's nodes. *Anat Rec* **228**, 437-48.

Disatnik, M. H., Boutet, S. C., Pacio, W., Chan, A. Y., Ross, L. B., Lee, C. H. and Rando, T. A. (2004). The bi-directional translocation of MARCKS between membrane and cytosol regulates integrin-mediated muscle cell spreading. *J Cell Sci* **117**, 4469-79.

Doniach, T. (1995). Basic FGF as an inducer of anteroposterior neural pattern. *Cell* **83**, 1067-70.

Dresselhaus, T., Hagel, C., Lorz, H. and Kranz, E. (1996). Isolation of a full-length cDNA encoding calreticulin from a PCR library of in vitro zygotes of maize. *Plant Mol Biol* **31**, 23-34.

Driever, W. (1995). Axis formation in zebrafish. *Curr Opin Genet Dev* **5**, 610-8.

Dudley, A. T. and Robertson, E. J. (1997). Overlapping expression domains of bone morphogenetic protein family members potentially account for limited tissue defects in BMP7 deficient embryos. *Dev Dyn* **208**, 349-62.

Dupont, E., Prochiantz, A. and Joliot, A. (2007). Identification of a signal peptide for unconventional secretion. *J Biol Chem* **282**, 8994-9000.

Dye, M. J., Gromak, N., Haussecker, D., West, S. and Proudfoot, N. J. (2006). Turnover and function of noncoding RNA polymerase II transcripts. *Cold Spring Harb Symp Quant Biol* **71**, 275-84.
Eddy, S. R. (2002). Computational genomics of noncoding RNA genes. *Cell* **109**, 137-40.

Endo, Y., Osumi, N. and Wakamatsu, Y. (2002). Bimodal functions of Notch-mediated signaling are involved in neural crest formation during avian ectoderm development. *Development* **129**, 863-73.

Engling, A., Backhaus, R., Stegmayer, C., Zehe, C., Seelenmeyer, C., Kehlenbach, A., Schwappach, B., Wegehingel, S. and Nickel, W. (2002). Biosynthetic FGF-2 is targeted to non-lipid raft microdomains following translocation to the extracellular surface of CHO cells. *J Cell Sci* **115**, 3619-31.

Espinoza, C. A., Goodrich, J. A. and Kugel, J. F. (2007). Characterization of the structure, function, and mechanism of B2 RNA, an ncRNA repressor of RNA polymerase II transcription. *RNA* **13**, 583-96.

Fainsod, A., Dibler, K., Yelin, R., Marom, K., Epstein, M., Pillemer, G., Steinbeisser, H. and Blum, M. (1997). The dorsalizing and neural inducing gene follistatin is an antagonist of BMP-4. *Mechanisms of Development* **63**, 39-50.

Fainsod, A., Steinbeisser, H. and De Robertis, E. M. (1994). On the function of BMP-4 in patterning the marginal zone of the Xenopus embryo. *Embo J* **13**, 5015-25.

Fassler, R., Sasaki, T., Timpl, R., Chu, M. L. and Werner, S. (1996). Differential regulation of fibulin, tenascin-C, and nidogen expression during wound healing of normal and glucocorticoid-treated mice. *Exp Cell Res* **222**, 111-6.

Fatal, N., Karhinen, L., Jokitalo, E. and Makarow, M. (2004). Active and specific recruitment of a soluble cargo protein for endoplasmic reticulum exit in the absence of functional COPII component Sec24p. *J Cell Sci* **117**, 1665-73.

Faure, S., de Santa Barbara, P., Roberts, D. J. and Whitman, M. (2002). Endogenous patterns of BMP signaling during early chick development. *Dev Biol* **244**, 44-65.

Faure, S., Lee, M. A., Keller, T., ten Dijke, P. and Whitman, M. (2000). Endogenous patterns of TGFbeta superfamily signaling during early Xenopus development. *Development* **127**, 2917-31.

Ferrari, D., Lichtler, A. C., Pan, Z. Z., Dealy, C. N., Upholt, W. B. and Kosher, R. A. (1998). Ectopic expression of Msx-2 in posterior limb bud mesoderm impairs limb morphogenesis while inducing BMP-4 expression, inhibiting cell proliferation, and promoting apoptosis. *Dev Biol* **197**, 12-24.

Fitter, S., Sincock, P. M., Jolliffe, C. N. and Ashman, L. K. (1999). Transmembrane 4 superfamily protein CD151 (PETA-3) associates with beta 1 and alpha IIb beta 3 integrins in haemopoietic cell lines and modulates cell-cell adhesion. *Biochem J* **338 (Pt 1)**, 61-70.

Fitter, S., Tetaz, T. J., Berndt, M. C. and Ashman, L. K. (1995). Molecular cloning of cDNA encoding a novel platelet-endothelial cell tetra-span antigen, PETA-3. *Blood* **86**, 1348-55.

Fliegel, L., Burns, K., MacLennan, D. H., Reithmeier, R. A. and Michalak, M. (1989a). Molecular cloning of the high affinity calcium-binding protein (calreticulin) of skeletal muscle sarcoplasmic reticulum. *J Biol Chem* **264**, 21522-8.

Fliegel, L., Burns, K., Opas, M. and Michalak, M. (1989b). The high-affinity calcium binding protein of sarcoplasmic reticulum. Tissue distribution, and homology with calregulin. *Biochim Biophys Acta* **982**, 1-8.

Florkiewicz, R. Z., Majack, R. A., Buechler, R. D. and Florkiewicz, E. (1995). Quantitative export of FGF-2 occurs through an alternative, energy-dependent, non-ER/Golgi pathway. *J Cell Physiol* **162**, 388-99.

Fritsch, O., Benvenuto, G., Bowler, C., Molinier, J. and Hohn, B. (2004). The INO80 protein controls homologous recombination in Arabidopsis thaliana. *Mol Cell* **16**, 479-85.

Frydman, H. M. and Spradling, A. C. (2001). The receptor-like tyrosine phosphatase lar is required for epithelial planar polarity and for axis determination within drosophila ovarian follicles. *Development* **128**, 3209-20.

Furthauer, M., Thisse, B. and Thisse, C. (1999). Three different noggin genes antagonize the activity of bone morphogenetic proteins in the zebrafish embryo. *Dev Biol* **214**, 181-96.

Galindo, M. I., Pueyo, J. I., Fouix, S., Bishop, S. A. and Couso, J. P. (2007). Peptides encoded by short ORFs control development and define a new eukaryotic gene family. *PLoS Biol* **5**, e106.

Gallagher, W. M., Argentini, M., Sierra, V., Bracco, L., Debussche, L. and Conseiller, E. (1999). MBP1: a novel mutant p53-specific protein partner with oncogenic properties. *Oncogene* **18**, 3608-16.

Gallagher, W. M., Greene, L. M., Ryan, M. P., Sierra, V., Berger, A., Laurent-Puig, P. and Conseiller, E. (2001). Human fibulin-4: analysis of its biosynthetic processing and mRNA expression in normal and tumour tissues. *FEBS Lett* **489**, 59-66.

Gallera, J. (1965). [What is the necessary period of time for obtaining neural inductions in the chicken?]. *Experientia* **21**, 218-9.

Gallera, J. (1970a). Inductions cérébrales et médullaires chez les Oiseaux. *Experientia* **26**, 886-7.

Gallera, J. (1970b). [Difference in reactivity to the neurogenic inductor between the ectoblast of the area opaca and that of the area pellucida in chickens]. *Experientia* **26**, 1353-4.

Gallera, J. (1971). Primary induction in birds. *Adv. Morph* **9**, 149-180.

Gallera, J. (1972). Alteration of the prospective fate and the inductive power of the definitive streak node in the chick. *Experientia* **28**, 1217-8.

Gallera, J. and Ivanov, I. (1964). La compétence neurogéne du feuillet externe du blastoderme de Poulet en fonction du facteur 'temps'. *J Embryol Exp Morphol* **12**, 693.

Gelebart, P., Opas, M. and Michalak, M. (2005). Calreticulin, a Ca2+-binding chaperone of the endoplasmic reticulum. *Int J Biochem Cell Biol* **37**, 260-6.

Gelfand, B., Mead, J., Bruning, A., Apostolopoulos, N., Tadigotla, V., Nagaraj, V., Sengupta, A. M. and Vershon, A. K. (2011). Regulated antisense transcription controls expression of cell-type-specific genes in yeast. *Mol Cell Biol* **31**, 1701-9.

Gerhart, J. (2001). Evolution of the organizer and the chordate body plan. *Int J Dev Biol* **45**, 133-53.

Gibson, A., Robinson, N., Streit, A., Sheng, G. and Stern, C. D. (2010). Regulation of programmed cell death during neural induction in the chick embryo. *Int J Dev Biol* **55**, 33-43.

Giltay, R., Timpl, R. and Kostka, G. (1999). Sequence, recombinant expression and tissue localization of two novel extracellular matrix proteins, fibulin-3 and fibulin-4. *Matrix Biol* **18**, 469-80.

Glavic, A., Silva, F., Aybar, M. J., Bastidas, F. and Mayor, R. (2004). Interplay between Notch signaling and the homeoprotein Xiro1 is required for neural crest induction in Xenopus embryos. *Development* **131**, 347-59.

Godsave, S. F. and Slack, J. M. (1989). Clonal analysis of mesoderm induction in Xenopus laevis. *Dev Biol* **134**, 486-90.

Gontan, C., Jonkers, I. and Gribnau, J. (2011). Long Noncoding RNAs and X Chromosome Inactivation. *Prog Mol Subcell Biol*, 43-64.

Goodrich, J. A. and Kugel, J. F. Dampening DNA binding: a common mechanism of transcriptional repression for both ncRNAs and protein domains. *RNA Biol* **7**, 305-9.

Gothel, S. F. and Marahiel, M. A. (1999). Peptidyl-prolyl cis-trans isomerases, a superfamily of ubiquitous folding catalysts. *Cell Mol Life Sci* **55**, 423-36.

Gouarderes, C., Tafani, J. A., Meunier, J. C., Jhamandas, K. and Zajac, J. M. (1999). Nociceptin receptors in the rat spinal cord during morphine tolerance. *Brain Res* **838**, 85-94.

Goulding, M. D., Lumsden, A. and Gruss, P. (1993). Signals from the notochord and floor plate regulate the region-specific expression of two Pax genes in the developing spinal cord. *Development* **117**, 1001-16.

Grabowski, C. T. (1956). The effects of the axcision of Hensen's node on the development of the chick embryo. *J. Exp. Zool.* **133**, 301-344.

Graham, A., Begbie, J. and McGonnell, I. (2004). Significance of the cranial neural crest. *Dev Dyn* **229**, 5-13.

Graham, A., Francis-West, P., Brickell, P. and Lumsden, A. (1994). The signalling molecule BMP4 mediates apoptosis in the rhombencephalic neural crest. *Nature* **372**, 684-6.

Grapin-Botton, A., Bonnin, M. A., McNaughton, L. A., Krumlauf, R. and Le Douarin, N. M. (1995). Plasticity of transposed rhombomeres: Hox gene induction is correlated with phenotypic modifications. *Development* **121**, 2707-21.

Grassel, S., Sicot, F. X., Gotta, S. and Chu, M. L. (1999). Mouse fibulin-2 gene. Complete exon-intron organization and promoter characterization. *Eur J Biochem* **263**, 471-7.

Grinchuk, O. V., Jenjaroenpun, P., Orlov, Y. L., Zhou, J. and Kuznetsov, V. A. Integrative analysis of the human cis-antisense gene pairs, miRNAs and their transcription regulation patterns. *Nucleic Acids Res* **38**, 534-47.

Gritsman, K., Talbot, W. S. and Schier, A. F. (2000). Nodal signaling patterns the organizer. *Development* **127**, 921-32.

Gritsman, K., Zhang, J., Cheng, S., Heckscher, E., Talbot, W. S. and Schier, A. F. (1999). The EGF-CFC protein one-eyed pinhead is essential for nodal signaling. *Cell* **97**, 121-32.

Groenendyk, J., Lynch, J. and Michalak, M. (2004). Calreticulin, Ca2+, and calcineurin - signaling from the endoplasmic reticulum. *Mol Cells* **17**, 383-9.

Grunz, H. (1997). Neural induction in amphibians. *Curr Top Dev Biol* **35**, 191-228.

Grunz, H. and Tacke, L. (1989). Neural differentiation of Xenopus laevis ectoderm takes place after disaggregation and delayed reaggregation without inducer. *Cell Differ Dev* **28**, 211-7.

Guo, L., Nakamura, K., Lynch, J., Opas, M., Olson, E. N., Agellon, L. B. and Michalak, M. (2002). Cardiac-specific expression of calcineurin reverses embryonic lethality in calreticulin-deficient mouse. *J Biol Chem* **277**, 50776-9.

Gurdon, J. B. (1987). Embryonic induction--molecular prospects. *Development* **99**, 285-306.

Hallenberger, S., Tucker, S. P., Owens, R. J., Bernstein, H. B. and Compans, R. W. (1993). Secretion of a truncated form of the human immunodeficiency virus type 1 envelope glycoprotein. *Virology* **193**, 510-4.

Hansen, C. S., Marion, C. D., Steele, K., George, S. and Smith, W. C. (1997). Direct neural induction and selective inhibition of mesoderm and epidermis inducers by Xnr3. *Development* **124**, 483-92.

Harland, R. (2000). Neural induction. *Curr Opin Genet Dev* **10**, 357-62.

Hartley, D. A., Xu, T. A. and Artavanis-Tsakonas, S. (1987). The embryonic expression of the Notch locus of Drosophila melanogaster and the implications of point mutations in the extracellular EGF-like domain of the predicted protein. *Embo J* **6**, 3407-17.

Hartman, M. L., Pincus, S. M., Johnson, M. L., Matthews, D. H., Faunt, L. M., Vance, M. L., Thorner, M. O. and Veldhuis, J. D. (1994). Enhanced basal and disorderly growth hormone secretion distinguish acromegalic from normal pulsatile growth hormone release. *J Clin Invest* **94**, 1277-88.

Hata, A., Lagna, G., Massague, J. and Hemmati-Brivanlou, A. (1998). Smad6 inhibits BMP/Smad1 signaling by specifically competing with the Smad4 tumor suppressor. *Genes Dev* **12**, 186-97.

Hatta, K. and Takahashi, Y. (1996). Secondary axis induction by heterospecific organizers in zebrafish. *Dev Dyn* **205**, 183-95.

Hawley, S. H., Wunnenberg-Stapleton, K., Hashimoto, C., Laurent, M. N., Watabe, T., Blumberg, B. W. and Cho, K. W. (1995). Disruption of BMP signals in embryonic Xenopus ectoderm leads to direct neural induction. *Genes Dev* **9**, 2923-35.

Hawn, T. R., Tom, T. D. and Strand, M. (1993). Molecular cloning and expression of SmIrV1, a Schistosoma mansoni antigen with similarity to calnexin, calreticulin, and OvRal1. *J Biol Chem* **268**, 7692-8.

Hayashi, H., Abdollah, S., Qiu, Y., Cai, J., Xu, Y. Y., Grinnell, B. W., Richardson, M. A., Topper, J. N., Gimbrone, M. A., Jr., Wrana, J. L. et al. (1997). The MAD-related protein Smad7 associates with the TGFbeta receptor and functions as an antagonist of TGFbeta signaling. *Cell* **89**, 1165-73.

He, L. and Hannon, G. J. (2004). MicroRNAs: small RNAs with a big role in gene regulation. *Nat Rev Genet* **5**, 522-31.

Hebert, D. N. and Molinari, M. (2007). In and out of the ER: protein folding, quality control, degradation, and related human diseases. *Physiol Rev* **87**, 1377-408.

Hebert, D. N., Simons, J. F., Peterson, J. R. and Helenius, A. (1995). Calnexin, calreticulin, and Bip/Kar2p in protein folding. *Cold Spring Harb Symp Quant Biol* **60**, 405-15.

Heldin, C. H., Miyazono, K. and ten Dijke, P. (1997). TGF-beta signalling from cell membrane to nucleus through SMAD proteins. *Nature* **390**, 465-71.

Helenius, A. and Aebi, M. (2004). Roles of N-linked glycans in the endoplasmic reticulum. *Annu Rev Biochem* **73**, 1019-49.

Hemmati-Brivanlou, A., Kelly, O. G. and Melton, D. A. (1994a). Follistatin, an antagonist of activin, is expressed in the Spemann organizer and displays direct neuralizing activity. *Cell* **77**, 283-95.

Hemmati-Brivanlou, A. and Melton, D. (1997a). Vertebrate embryonic cells will become nerve cells unless told otherwise. *Cell* **88**, 13-7.

Hemmati-Brivanlou, A. and Melton, D. (1997b). Vertebrate neural induction. *Annu Rev Neurosci* **20**, 43-60.

Hemmati-Brivanlou, A. and Melton, D. A. (1992). A truncated activin receptor inhibits mesoderm induction and formation of axial structures in Xenopus embryos. *Nature* **359**, 609-614.

Hemmati-Brivanlou, A. and Melton, D. A. (1994b). Inhibition of activin receptor signaling promotes neuralization in Xenopus. *Cell* **77**, 273-81.

Hemmati-Brivanlou, A. and Thomsen, G. H. (1995). Ventral mesodermal patterning in Xenopus embryos: expression patterns and activities of BMP-2 and BMP-4. *Dev Genet* **17**, 78-89.

Henrique, D., Tyler, D., Kintner, C., Heath, J. K., Lewis, J. H., Ish-Horowicz, D. and Storey, K. G. (1997). cash4, a novel achaete-scute homolog induced by Hensen's node during generation of the posterior nervous system. *Genes Dev* **11**, 603-15.

Hesselson, D., Newman, C., Kim, K. W. and Kimble, J. (2004). GON-1 and fibulin have antagonistic roles in control of organ shape. *Curr Biol* **14**, 2005-10.

Hidalgo-Sanchez, M., Simeone, A. and Alvarado-Mallart, R. M. (1999). Fgf8 and Gbx2 induction concomitant with Otx2 repression is correlated with midbrain-hindbrain fate of caudal prosencephalon. *Development* **126**, 3191-203.

Hitzeman, R. A., Chen, C. Y., Dowbenko, D. J., Renz, M. E., Liu, C., Pai, R., Simpson, N. J., Kohr, W. J., Singh, A., Chisholm, V. et al. (1990). Use of heterologous and homologous signal sequences for secretion of heterologous proteins from yeast. *Methods Enzymol* **185**, 421-40.

Holley, S. A., Jackson, P. D., Sasai, Y., Lu, B., De Robertis, E. M., Hoffmann, F. M. and Ferguson, E. L. (1995). A conserved system for dorsal-ventral patterning in insects and vertebrates involving sog and chordin. *Nature* **376**, 249-53.

Holley, S. A., Neul, J. L., Attisano, L., Wrana, J. L., Sasai, Y., O'Connor, M. B., De Robertis, E. M. and Ferguson, E. L. (1996a). The Xenopus dorsalizing factor noggin ventralizes Drosophila embryos by preventing DPP from activating its receptor. *Cell* **86**, 607-17.

Holley, S. A., Neul, J. L., Attisano, L., Wrana, J. L., Sasai, Y., O'Connor, M. B., De Robertis, E. M. and Ferguson, E. L. (1996b). The Xenopus dorsalizing factor noggin ventralizes Drosophila embryos by preventing DPP from activating its receptor. *Cell* **86**, 607-17.

Holtfreter, J., Hamburger, V. (1955). Embryogenesis: Progressive differentiation - amphibians. New York: Haffner.

Homberg, J. R., Mul, J. D., de Wit, E. and Cuppen, E. (2009). Complete knockout of the nociceptin/orphanin FQ receptor in the rat does not induce compensatory changes in mu, delta and kappa opioid receptors. *Neuroscience* **163**, 308-15.

Hornbruch, A., Summerbell, D. and Wolpert, L. (1979). Somite formation in the early chick embryo following grafts of Hensen's node. *J Embryol Exp Morphol* **51**, 51-62.

Horton, P. and Nakai, K. (1997). Better prediction of protein cellular localization sites with the k nearest neighbors classifier. *Proc Int Conf Intell Syst Mol Biol* **5**, 147-52.

Hotton, S. K. and Callis, J. (2008). Regulation of cullin RING ligases. *Annu Rev Plant Biol* **59**, 467-89.

Houston, B., Thorp, B. H. and Burt, D. W. (1994). Molecular cloning and expression of bone morphogenetic protein-7 in the chick epiphyseal growth plate. *J Mol Endocrinol* **13**, 289-301.

Hsu, D.R. (1998). The *Xenopus* dorsalizing factor gremlin identifies a novel family of secreted proteins that antagonize BMP activities. *Molecular Cell* **1**, 673-683.

Huang, J., Gong, Z., Ghosal, G. and Chen, J. (2009). SOSS complexes participate in the maintenance of genomic stability. *Mol Cell* **35**, 384-93.

Huber, R., Scholze, H., Paques, E. P. and Deisenhofer, J. (1980). Crystal structure analysis and molecular model of human C3a anaphylatoxin. *Hoppe Seylers Z Physiol Chem* **361**, 1389-99.

Hudson, C., Darras, S., Caillol, D., Yasuo, H. and Lemaire, P. (2003). A conserved role for the MEK signalling pathway in neural tissue specification and posteriorisation in the invertebrate chordate, the ascidian Ciona intestinalis. *Development* **130**, 147-59.

Hudson, C. and Lemaire, P. (2001). Induction of anterior neural fates in the ascidian Ciona intestinalis. *Mech Dev* **100**, 189-203.

Huggins, M. C., Gibbs, J. and Moloney, N. A. (1995). Cloning of a Schistosoma japonicum gene encoding an antigen with homology to calreticulin. *Mol Biochem Parasitol* **71**, 81-7.

Hunt, T. E. (1929). Hensen's node as an organizer in the fomration of the chick embryo. *Anat Rec* **42**, 22.

Hunter, M. P., Ismail, N., Zhang, X., Aguda, B. D., Lee, E. J., Yu, L., Xiao, T., Schafer, J., Lee, M. L., Schmittgen, T. D. et al. (2008). Detection of microRNA expression in human peripheral blood microvesicles. *PLoS One* **3**, e3694.

Hunzelmann, N., Nischt, R., Brenneisen, P., Eickert, A. and Krieg, T. (2001). Increased deposition of fibulin-2 in solar elastosis and its colocalization with elastic fibres. *Br J Dermatol* **145**, 217-22.

Huttner, H. B., Janich, P., Kohrmann, M., Jaszai, J., Siebzehnrubl, F., Blumcke, I., Suttorp, M., Gahr, M., Kuhnt, D., Nimsky, C. et al. (2008). The stem cell marker prominin-1/CD133 on

membrane particles in human cerebrospinal fluid offers novel approaches for studying central nervous system disease. *Stem Cells* **26**, 698-705.

Iemura, S., Yamamoto, T. S., Takagi, C., Uchiyama, H., Natsume, T., Shimasaki, S., Sugino, H. and Ueno, N. (1998). Direct binding of follistatin to a complex of bone-morphogenetic protein and its receptor inhibits ventral and epidermal cell fates in early Xenopus embryo. *Proc Natl Acad Sci U S A* **95**, 9337-42.

Ikura, T., Ogryzko, V. V., Grigoriev, M., Groisman, R., Wang, J., Horikoshi, M., Scully, R., Qin, J. and Nakatani, Y. (2000). Involvement of the TIP60 histone acetylase complex in DNA repair and apoptosis. *Cell* **102**, 463-73.

Imamura, T., Takase, M., Nishihara, A., Oeda, E., Hanai, J., Kawabata, M. and Miyazono, K. (1997). Smad6 inhibits signalling by the TGF-beta superfamily. *Nature* **389**, 622-6.

Inagaki, K., Aki, T., Fukuda, Y., Kawamoto, S., Shigeta, S., Ono, K. and Suzuki, O. (2002). Identification and expression of a rat fatty acid elongase involved in the biosynthesis of C18 fatty acids. *Biosci Biotechnol Biochem* **66**, 613-21.

Irie, K., Shimizu, K., Sakisaka, T., Ikeda, W. and Takai, Y. (2004). Roles of nectins in cell adhesion, signaling and polarization. *Handb Exp Pharmacol*, 343-72.

Isaacs, A. M., Oliver, P. L., Jones, E. L., Jeans, A., Potter, A., Hovik, B. H., Nolan, P. M., Vizor, L., Glenister, P., Simon, A. K. et al. (2003). A mutation in Af4 is predicted to cause cerebellar ataxia and cataracts in the robotic mouse. *J Neurosci* **23**, 1631-7.

Isaacs, H. V., Pownall, M. E. and Slack, J. M. (1992). Expression of a novel FGF in Xenpus embryo: Anew candidate inducing factor for mesoderm formation and anteroposterior specification. *Development* **114**, 711-720.

Isaacs, H. V., Pownall, M. E. and Slack, J. M. (1994). eFGF regulates Xbra expression during Xenopus gastrulation. *Embo J* **13**, 4469-81.

Ishisaki, A., Yamato, K., Hashimoto, S., Nakao, A., Tamaki, K., Nonaka, K., ten Dijke, P., Sugino, H. and Nishihara, T. (1999). Differential inhibition of Smad6 and Smad7 on bone morphogenetic protein- and activin-mediated growth arrest and apoptosis in B cells. *J Biol Chem* **274**, 13637-42.

Itoh, S., Landstrom, M., Hermansson, A., Itoh, F., Heldin, C. H., Heldin, N. E. and ten Dijke, P. (1998). Transforming growth factor beta1 induces nuclear export of inhibitory Smad7. *J Biol Chem* **273**, 29195-201.

Ivery, M. T. (2000). Immunophilins: switched on protein binding domains? *Med Res Rev* **20**, 452-84.

Izumi, G., Sakisaka, T., Baba, T., Tanaka, S., Morimoto, K. and Takai, Y. (2004). Endocytosis of E-cadherin regulated by Rac and Cdc42 small G proteins through IQGAP1 and actin filaments. *J Cell Biol* **166**, 237-48.

Jacobs, K. A., Collins-Racie, L. A., Colbert, M., Duckett, M., Golden-Fleet, M., Kelleher, K., Kriz, R., LaVallie, E. R., Merberg, D., Spaulding, V. et al. (1997). A genetic selection for isolating cDNAs encoding secreted proteins. *Gene* **198**, 289-96.

Jaworski, D. C., Higgins, J. A., Radulovic, S., Vaughan, J. A. and Azad, A. F. (1996). Presence of calreticulin in vector fleas (Siphonaptera). *J Med Entomol* **33**, 482-9.

Jin, J., Cai, Y., Yao, T., Gottschalk, A. J., Florens, L., Swanson, S. K., Gutierrez, J. L., Coleman, M. K., Workman, J. L., Mushegian, A. et al. (2005). A mammalian chromatin remodeling complex with similarities to the yeast INO80 complex. *J Biol Chem* **280**, 41207-12.

Jin, K., Mao, X. O. and Greenberg, D. A. (2004a). Proteomic analysis of neuronal hypoxia in vitro. *Neurochem Res* **29**, 1123-8.

Jin, K., Minami, M., Xie, L., Sun, Y., Mao, X. O., Wang, Y., Simon, R. P. and Greenberg, D. A. (2004b). Ischemia-induced neurogenesis is preserved but reduced in the aged rodent brain. *Aging Cell* **3**, 373-7.

John, L. M., Lechleiter, J. D. and Camacho, P. (1998). Differential modulation of SERCA2 isoforms by calreticulin. *J Cell Biol* **142**, 963-73.

Johnson, K. G., McKinnell, I. W., Stoker, A. W. and Holt, C. E. (2001). Receptor protein tyrosine phosphatases regulate retinal ganglion cell axon outgrowth in the developing Xenopus visual system. *J Neurobiol* **49**, 99-117.

Joliot, A., Maizel, A., Rosenberg, D., Trembleau, A., Dupas, S., Volovitch, M. and Prochiantz, A. (1998). Identification of a signal sequence necessary for the unconventional secretion of Engrailed homeoprotein. *Curr Biol* **8**, 856-63.

Jones, C. M., Kuehn, M. R., Hogan, B. L., Smith, J. C. and Wright, C. V. (1995). Nodal-related signals induce axial mesoderm and dorsalize mesoderm during gastrulation. *Development* **121**, 3651-62.

Jones, C. M., Lyons, K. M., Lapan, P. M., Wright, C. V. E. and Hogan, B. M. (1992). DVR-4 (Bone Morphogentic Protein-4) as a posterior-ventralizing factor in Xenopus mesoderm induction. *Development* **115**, 639-647.

Joubin, K. and Stern, C. D. (1999). Molecular interactions continuously define the organizer during the cell movements of gastrulation. *Cell* **98**, 559-71.

Juschke, C., Wachter, A., Schwappach, B. and Seedorf, M. (2005). SEC18/NSF-independent, protein-sorting pathway from the yeast cortical ER to the plasma membrane. *J Cell Biol* **169**, 613-22.

Kaiser, C. A., Preuss, D., Grisafi, P. and Botstein, D. (1987). Many random sequences functionally replace the secretion signal sequence of yeast invertase. *Science* **235**, 312-7.

Kanekura, T. and Chen, X. CD147/basigin promotes progression of malignant melanoma and other cancers. *J Dermatol Sci* **57**, 149-54.

Karan, G., Yang, Z. and Zhang, K. (2004). Expression of wild type and mutant ELOVL4 in cell culture: subcellular localization and cell viability. *Mol Vis* **10**, 248-53.

Kawakami, A., Kimura-Kawakami, M., Nomura, T. and Fujisawa, H. (1997). Distributions of PAX6 and PAX7 proteins suggest their involvement in both early and late phases of chick brain development. *Mech Dev* **66**, 119-30.

Kawashima, S., Ogiwara, H., Tada, S., Harata, M., Wintersberger, U., Enomoto, T. and Seki, M. (2007). The INO80 complex is required for damage-induced recombination. *Biochem Biophys Res Commun* **355**, 835-41.

Kengaku, M. and Okamoto, H. (1993). Basic fibroblast growth factor induces differentiation of nerual tube and neural crest lineages of cultured ectoderm cells from Xenopus gastula. *Development* **119**, 1067-1078.

Khalife, J., Pierce, R. J., Godin, C. and Capron, A. (1993a). Cloning and sequencing of the gene encoding Schistosoma mansoni calreticulin. *Mol Biochem Parasitol* **62**, 313-5.

Khalife, J., Trottein, F., Schacht, A. M., Godin, C., Pierce, R. J. and Capron, A. (1993b). Cloning of the gene encoding a Schistosoma mansoni antigen homologous to human Ro/SS-A autoantigen. *Mol Biochem Parasitol* **57**, 193-202.

Kidd, S., Baylies, M. K., Gasic, G. P. and Young, M. W. (1989). Structure and distribution of the Notch protein in developing Drosophila. *Genes Dev* **3**, 1113-29.

Kim, G. J. and Nishida, H. (2001). Role of the FGF and MEK signaling pathway in the ascidian embryo. *Dev Growth Differ* **43**, 521-33.

Kintner, C. (1992). Molecular bases of early neural development in Xenopus embryos. *Annu Rev Neurosci* **15**, 251-84.

Kintner, C. R. and Dodd, J. (1991). Hensen's node induces neural tissue in Xenopus ectoderm. Implications for the action of the organizer in neural induction. *Development* **113**, 1495-505.

Kispert, A., Ortner, H., Cooke, J. and Herrmann, B. G. (1995). The chick Brachyury gene: developmental expression pattern and response to axial induction by localized activin. *Dev Biol* **168**, 406-15.

Kitaguchi, T., Mizugishi, K., Hatayama, M., Aruga, J. and Mikoshiba, K. (2002). Xenopus Brachyury regulates mesodermal expression of Zic3, a gene controlling left-right asymmetry. *Dev Growth Differ* **44**, 55-61.

Kitaguchi, T., Nagai, T., Nakata, K., Aruga, J. and Mikoshiba, K. (2000). Zic3 is involved in the left-right specification of the Xenopus embryo. *Development* **127**, 4787-95.

Klein, C. J., Olsson, L., Ronnow, B., Mikkelsen, J. D. and Nielsen, J. (1996). Alleviation of glucose repression of maltose metabolism by MIG1 disruption in Saccharomyces cerevisiae. *Appl Environ Microbiol* **62**, 4441-9.

Klingensmith, J., Ang, S.-L., Bachiller, D. and Rossant, J. (1999). Neural Induction and Patterning in the Mouse in the Absence of the Node and Its Derivatives. *Developmental Biology* **216**, 535-549.

Klymenko, T., Papp, B., Fischle, W., Kocher, T., Schelder, M., Fritsch, C., Wild, B., Wilm, M. and Muller, J. (2006). A Polycomb group protein complex with sequence-specific DNA-binding and selective methyl-lysine-binding activities. *Genes Dev* **20**, 1110-22.

Knecht, A., Good, P. J., Dawid, I. B. and Harland, R. M. (1995). Dorsal-ventral patterning and differentiation of noggin-induced neural tissue in the absence of mesoderm. *Development* **121**, 1927-1936.

Knee, R., Ahsan, I., Mesaeli, N., Kaufman, R. J. and Michalak, M. (2003). Compromised calnexin function in calreticulin-deficient cells. *Biochem Biophys Res Commun* **304**, 661-6.

Knoetgen, H., Teichmann, U., Wittler, L., Viebahn, C. and Kessel, M. (2000). Anterior neural induction by nodes from rabbits and mice. *Dev Biol* **225**, 370-80.

Kobor, M. S., Venkatasubrahmanyam, S., Meneghini, M. D., Gin, J. W., Jennings, J. L., Link, A. J., Madhani, H. D. and Rine, J. (2004). A protein complex containing the conserved Swi2/Snf2-related ATPase Swr1p deposits histone variant H2A.Z into euchromatin. *PLoS Biol* **2**, E131.

Kolodny, G. M., Culp, L. A. and Rosenthal, L. J. (1972). Secretion of RNA by normal and transformed cells. *Exp Cell Res* **73**, 65-72.

Kondo, T., Hashimoto, Y., Kato, K., Inagaki, S., Hayashi, S. and Kageyama, Y. (2007). Small peptide regulators of actin-based cell morphogenesis encoded by a polycistronic mRNA. *Nat Cell Biol* **9**, 660-5.

Kostka, G., Giltay, R., Bloch, W., Addicks, K., Timpl, R., Fassler, R. and Chu, M. L. (2001). Perinatal lethality and endothelial cell abnormalities in several vessel compartments of fibulin-1-deficient mice. *Mol Cell Biol* **21**, 7025-34.

Kowal, R. C., Jolsin, J. M., Olson, E. N. and Schultz, R. A. (1999a). Assignment of fibulin-5 (FBLN5) to human chromosome 14q31 by in situ hybridization and radiation hybrid mapping. *Cytogenet Cell Genet* **87**, 2-3.

Kowal, R. C., Richardson, J. A., Miano, J. M. and Olson, E. N. (1999b). EVEC, a novel epidermal growth factor-like repeat-containing protein upregulated in embryonic and diseased adult vasculature. *Circ Res* **84**, 1166-76.

Kretzschmar, M., Doody, J. and Massague, J. (1997a). Opposing BMP and EGF signalling pathways converge on the TGF-beta family mediator Smad1. *Nature* **389**, 618-22.

Kretzschmar, M., Doody, J., Timokhina, I. and Massague, J. (1999). A mechanism of repression of TGFbeta/ Smad signaling by oncogenic Ras. *Genes Dev* **13**, 804-16.

Kretzschmar, M., Liu, F., Hata, A., Doody, J. and Massague, J. (1997b). The TGF-beta family mediator Smad1 is phosphorylated directly and activated functionally by the BMP receptor kinase. *Genes Dev* **11**, 984-95.

Krogan, N. J., Baetz, K., Keogh, M. C., Datta, N., Sawa, C., Kwok, T. C., Thompson, N. J., Davey, M. G., Pootoolal, J., Hughes, T. R. et al. (2004). Regulation of chromosome stability by the histone H2A variant Htz1, the Swr1 chromatin remodeling complex, and the histone acetyltransferase NuA4. *Proc Natl Acad Sci U S A* **101**, 13513-8.

Krogan, N. J., Keogh, M. C., Datta, N., Sawa, C., Ryan, O. W., Ding, H., Haw, R. A., Pootoolal, J., Tong, A., Canadien, V. et al. (2003). A Snf2 family ATPase complex required for recruitment of the histone H2A variant Htz1. *Mol Cell* **12**, 1565-76.

Kuang, P. P., Goldstein, R. H., Liu, Y., Rishikof, D. C., Jean, J. C. and Joyce-Brady, M. (2003). Coordinate expression of fibulin-5/DANCE and elastin during lung injury repair. *Am J Physiol Lung Cell Mol Physiol* **285**, L1147-52.

Kuang, P. P., Joyce-Brady, M., Zhang, X. H., Jean, J. C. and Goldstein, R. H. (2006). Fibulin-5 gene expression in human lung fibroblasts is regulated by TGF-beta and phosphatidylinositol 3-kinase activity. *Am J Physiol Cell Physiol* **291**, C1412-21.

Kubota, Y., Kuroki, R. and Nishiwaki, K. (2004). A fibulin-1 homolog interacts with an ADAM protease that controls cell migration in C. elegans. *Curr Biol* **14**, 2011-8.

Kudoh, T., Concha, M. L., Houart, C., Dawid, I. B. and Wilson, S. W. (2004). Combinatorial Fgf and Bmp signalling patterns the gastrula ectoderm into prospective neural and epidermal domains. *Development* **131**, 3581-92.

Kuker, M., D.H., M. and Turner, D. H. (1999). Algorithms and Thermodynamics for RNA Secondary Structure Prediction. In *A Practical Guide in RNA Biochemistry and Biotechnology*, (ed. J. Barciszewski and B. F. C. Clarks), pp. 11-43. Dordrecht: Kluwer Academic Publishers.

Kuroda, H., Fuentealba, L., Ikeda, A., Reversade, B. and De Robertis, E. M. (2005). Default neural induction: neuralization of dissociated Xenopus cells is mediated by Ras/MAPK activation. *Genes Dev* **19**, 1022-7.

Kuroda, H., Wessely, O. and De Robertis, E. M. (2004). Neural induction in Xenopus: requirement for ectodermal and endomesodermal signals via Chordin, Noggin, beta-Catenin, and Cerberus. *PLoS Biol* **2**, E92.

Kusch, T., Florens, L., Macdonald, W. H., Swanson, S. K., Glaser, R. L., Yates, J. R., 3rd, Abmayr, S. M., Washburn, M. P. and Workman, J. L. (2004). Acetylation by Tip60 is required for selective histone variant exchange at DNA lesions. *Science* **306**, 2084-7.

Kuzmin, A., Bazov, I., Sheedy, D., Garrick, T., Harper, C. and Bakalkin, G. (2009). Expression of pronociceptin and its receptor is downregulated in the brain of human alcoholics. *Brain Res* **1305 Suppl**, S80-5.

Kwiatkowski, B. A., Zielinska-Kwiatkowska, A. G., Migdalski, A., Kleczkowski, L. A. and Wasilewska, L. D. (1995). Cloning of two cDNAs encoding calnexin-like and calreticulin-like

proteins from maize (Zea mays) leaves: identification of potential calcium-binding domains. *Gene* **165**, 219-22.

Labriola, C., Cazzulo, J. J. and Parodi, A. J. (1999). Trypanosoma cruzi calreticulin is a lectin that binds monoglucosylated oligosaccharides but not protein moieties of glycoproteins. *Mol Biol Cell* **10**, 1381-94.

Lagna, G., Hata, A., Hemmati-Brivanlou, A. and Massague, J. (1996). Partnership between DPC4 and SMAD proteins in TGF-beta signalling pathways. *Nature* **383**, 832-6.

Lai, E. C. (2002). Protein degradation: four E3s for the notch pathway. *Curr Biol* **12**, R74-8.

Lamb, T. M. and Harland, R. M. (1995). Fibroblast growth factor is a direct neural inducer, which combined with noggin generates anterior-posterior neural pattern. *Development* **121**, 3627-36.

Lamb, T. M., Knecht, A. K., Smith, W. C., Stachel, S. E., Economides, A. N., Stahl, N., Yancopolous, G. D. and Harland, R. M. (1993). Neural induction by the secreted polypeptide noggin. *Science* **262**, 713-8.

Lardenois, A., Liu, Y., Walther, T., Chalmel, F., Evrard, B., Granovskaia, M., Chu, A., Davis, R. W., Steinmetz, L. M. and Primig, M. Execution of the meiotic noncoding RNA expression program and the onset of gametogenesis in yeast require the conserved exosome subunit Rrp6. *Proc Natl Acad Sci U S A* **108**, 1058-63.

Launay, C., Fromentoux, V., Shi, D. L. and Boucaut, J. C. (1996). A truncated FGF receptor blocks neural induction by endogenous Xenopus inducers. *Development* **122**, 869-80.

Le Douarin, N. (1980). Migration and differentiation of neural crest cells. *Curr Top Dev Biol* **16**, 31-85.

Lecka-Czernik, B., Lumpkin, C. K., Jr. and Goldstein, S. (1995). An overexpressed gene transcript in senescent and quiescent human fibroblasts encoding a novel protein in the epidermal growth factor-like repeat family stimulates DNA synthesis. *Mol Cell Biol* **15**, 120-8.

Leclerc, C., Daguzan, C., Nicolas, M. T., Chabret, C., Duprat, A. M. and Moreau, M. (1997). L-type calcium channel activation controls the in vivo transduction of the neuralizing signal in the amphibian embryos. *Mech Dev* **64**, 105-10.

Leclerc, C. and Duprat, A.-M. a. M., M. (1995). In vivo labelling of L-type Ca2+ channels by fluorescent dihydropyridine: correlation between ontogenesis of the channels and the acquisition of neural competence in ectoderm cells from *Pleurodeles waltl* embryos. *Cell Calcium* **17**, 216-224.

Leclerc, C., Duprat, A. M. and Moreau, M. (1999). Noggin upregulates Fos expression by a calcium-mediated pathway in amphibian embryos. *Dev Growth Differ* **41**, 227-38.

Leclerc, C., Lee, M., Webb, S. E., Moreau, M. and Miller, A. L. (2003). Calcium transients triggered by planar signals induce the expression of ZIC3 gene during neural induction in Xenopus. *Dev Biol* **261**, 381-90.

Leclerc, C., Rizzo, C., Daguzan, C., Neant, I., Batut, J., Auge, B. and Moreau, M. (2001). [Neural determination in Xenopus laevis embryos: control of early neural gene expression by calcium]. *J Soc Biol* **195**, 327-37.

Leclerc, C., Webb, S. E., Daguzan, C., Moreau, M. and Miller, A. L. (2000). Imaging patterns of calcium transients during neural induction in Xenopus laevis embryos. *J Cell Sci* **113 Pt 19**, 3519-29.

Leclerc, C., Webb, S. E., Miller, A. L. and Moreau, M. (2008). An increase in intracellular Ca2+ is involved in pronephric tubule differentiation in the amphibian Xenopus laevis. *Dev Biol* **321**, 357-67.

Lee, J. T. (2009). Lessons from X-chromosome inactivation: long ncRNA as guides and tethers to the epigenome. *Genes Dev* **23**, 1831-42.

Lee, K. W., Moreau, M., Neant, I., Bibonne, A. and Leclerc, C. (2009). FGF-activated calcium channels control neural gene expression in Xenopus. *Biochim Biophys Acta* **1793**, 1033-40.

Lee, M. C., Miller, E. A., Goldberg, J., Orci, L. and Schekman, R. (2004a). Bi-directional protein transport between the ER and Golgi. *Annu Rev Cell Dev Biol* **20**, 87-123.

Lee, M. H., Lee, S. H., Kim, H., Jin, J. B., Kim, D. H. and Hwang, I. (2006). A WD40 repeat protein, Arabidopsis Sec13 homolog 1, may play a role in vacuolar trafficking by controlling the membrane association of AtDRP2A. *Mol Cells* **22**, 210-9.

Lee, M. J., Roy, N. K., Mogford, J. E., Schiemann, W. P. and Mustoe, T. A. (2004b). Fibulin-5 promotes wound healing in vivo. *J Am Coll Surg* **199**, 403-10.

Lefcort, F. and George, L. (2007). Neural crest cell fate: to be or not to be prespecified. *Cell Adh Migr* **1**, 199-201.

LeSueur, J. A., Fortuno, E. S., 3rd, McKay, R. M. and Graff, J. M. (2002). Smad10 is required for formation of the frog nervous system. *Dev Cell* **2**, 771-83.

Leung-Hagesteijn, C. Y., Milankov, K., Michalak, M., Wilkins, J. and Dedhar, S. (1994). Cell attachment to extracellular matrix substrates is inhibited upon downregulation of expression of calreticulin, an intracellular integrin alpha-subunit-binding protein. *J Cell Sci* **107 (Pt 3)**, 589-600.

Levin, M., Johnson, R. L., Stern, C. D., Kuehn, M. and Tabin, C. (1995). A molecular pathway determining left-right asymmetry in chick embryogenesis. *Cell* **82**, 803-14.

Leygue, E. (2007). Steroid receptor RNA activator (SRA1): unusual bifaceted gene products with suspected relevance to breast cancer. *Nucl Recept Signal* **5**, e006.

Li, J., Peng, L., Wu, L., Kuang, Y., Su, J., Yi, M., Hu, X., Li, D., Xie, H., Kanekura, T. et al. Depletion of CD147 sensitizes human malignant melanoma cells to hydrogen peroxide-induced oxidative stress. *J Dermatol Sci* **58**, 204-10.

Liem, K. F., Jr., Tremml, G., Roelink, H. and Jessell, T. M. (1995). Dorsal differentiation of neural plate cells induced by BMP-mediated signals from epidermal ectoderm. *Cell* **82**, 969-79.

Linker, C., De Almeida, I., Papanayotou, C., Stower, M., Sabado, V., Ghorani, E., Streit, A., Mayor, R. and Stern, C. D. (2009). Cell communication with the neural plate is required for induction of neural markers by BMP inhibition: evidence for homeogenetic induction and implications for Xenopus animal cap and chick explant assays. *Dev Biol* **327**, 478-86.

Linker, C. and Stern, C. D. (2004). Neural induction requires BMP inhibition only as a late step, and involves signals other than FGF and Wnt antagonists. *Development* **131**, 5671-81.

Liu, F., Massague, J. and Ruiz i Altaba, A. (1998). Carboxy-terminally truncated Gli3 proteins associate with Smads. *Nat Genet* **20**, 325-6.

Liu, F., Pouponnot, C. and Massague, J. (1997a). Dual role of the Smad4/DPC4 tumor suppressor in TGFbeta-inducible transcriptional complexes. *Genes Dev* **11**, 3157-67.

Liu, N., Fine, R. E. and Johnson, R. J. (1993). Comparison of cDNAs from bovine brain coding for two isoforms of calreticulin. *Biochim Biophys Acta* **1202**, 70-6.

Liu, X., Sun, Y., Constantinescu, S. N., Karam, E., Weinberg, R. A. and Lodish, H. F. (1997b). Transforming growth factor beta-induced phosphorylation of Smad3 is required for growth inhibition and transcriptional induction in epithelial cells. *Proc Natl Acad Sci U S A* **94**, 10669-74.

Lohr, J. L., Danos, M. C. and Yost, H. J. (1997). Left-right asymmetry of a nodal-related gene is regulated by dorsoanterior midline structures during Xenopus development. *Development* **124**, 1465-72.

Lowe, T. M. and Eddy, S. R. (1997). tRNAscan-SE: a program for improved detection of transfer RNA genes in genomic sequence. *Nucleic Acids Res* **25**, 955-64.

Lu, H., Kuang, Y. H., Su, J., Chang, J., Wu, L. S., Kanekura, T., Li, D., Chen, M. L. and Chen, X. CD147 is highly expressed on peripheral blood neutrophils from patients with psoriasis and induces neutrophil chemotaxis. *J Dermatol* **37**, 1053-6.

Luster, A. D., Cardiff, R. D., MacLean, J. A., Crowe, K. and Granstein, R. D. (1998). Delayed wound healing and disorganized neovascularization in transgenic mice expressing the IP-10 chemokine. *Proc Assoc Am Physicians* **110**, 183-96.

Macias-Silva, M., Hoodless, P. A., Tang, S. J., Buchwald, M. and Wrana, J. L. (1998). Specific activation of Smad1 signaling pathways by the BMP7 type I receptor, ALK2. *J Biol Chem* **273**, 25628-36.

MacLennan, D. H., Ostwald, T. J. and Stewart, P. S. (1974). Structural components of the sarcoplasmic reticulum membrane. *Ann N Y Acad Sci* **227**, 527-36.

Maecker, H. T., Todd, S. C. and Levy, S. (1997). The tetraspanin superfamily: molecular facilitators. *Faseb J* **11**, 428-42.

Maizel, A., Tassetto, M., Filhol, O., Cochet, C., Prochiantz, A. and Joliot, A. (2002). Engrailed homeoprotein secretion is a regulated process. *Development* **129**, 3545-53.

Malecova, B. and Morris, K. V. (2010). Transcriptional gene silencing through epigenetic changes mediated by non-coding RNAs. *Curr Opin Mol Ther* **12**, 214-22.

Mangold, O. (1929). Experimente zur Analyse der Determination und Induktion der Medullarplatte. *Wilh. Roux Arch. EntwMech. Org* **117**, 586-696.

Marchal, L., Luxardi, G., Thome, V. and Kodjabachian, L. (2009). BMP inhibition initiates neural induction via FGF signaling and Zic genes. *Proc Natl Acad Sci U S A* **106**, 17437-42.

Marin, F. and Charnay, P. (2000a). Hindbrain patterning: FGFs regulate Krox20 and mafB/kr expression in the otic/preotic region. *Development* **127**, 4925-35.

Marin, F. and Charnay, P. (2000b). Positional regulation of Krox-20 and mafB/kr expression in the developing hindbrain: potentialities of prospective rhombomeres. *Dev Biol* **218**, 220-34.

Massague, J. and Chen, Y. G. (2000). Controlling TGF-beta signaling. *Genes Dev* **14**, 627-44.

Massague, J. and Gomis, R. R. (2006). The logic of TGFbeta signaling. *FEBS Lett* **580**, 2811-20.

Mathis, L., Kulesa, P. M. and Fraser, S. E. (2001). FGF receptor signalling is required to maintain neural progenitors during Hensen's node progression. *Nat Cell Biol* **3**, 559-66.

Mattick, J. S. (2005). The functional genomics of noncoding RNA. *Science* **309**, 1527-8.

Mattick, J. S. and Makunin, I. V. (2005). Small regulatory RNAs in mammals. *Hum Mol Genet* **14 Spec No 1**, R121-32.

Mattick, J. S. and Makunin, I. V. (2006). Non-coding RNA. *Hum Mol Genet* **15 Spec No 1**, R17-29.

Matzuk, M. M., Lu, N., Vogel, H., Sellheyer, K., Roop, D. R. and Bradley, A. (1995c). Multiple defects and perinatal death in mice deficient in follistatin. *Nature* **374**, 360-3.

Mazzarella, R. A., Gold, P., Cunningham, M. and Green, M. (1992). Determination of the sequence of an expressible cDNA clone encoding ERp60/calregulin by the use of a novel nested set method. *Gene* **120**, 217-25.

McMahon, J. A., Takada, S., Zimmerman, L. B., Fan, C. M., Harland, R. M. and McMahon, A. P. (1998). Noggin-mediated antagonism of BMP signaling is required for growth and patterning of the neural tube and somite. *Genes Dev* **12**, 1438-52.

Measday, V., Baetz, K., Guzzo, J., Yuen, K., Kwok, T., Sheikh, B., Ding, H., Ueta, R., Hoac, T., Cheng, B. et al. (2005). Systematic yeast synthetic lethal and synthetic dosage lethal screens identify genes required for chromosome segregation. *Proc Natl Acad Sci U S A* **102**, 13956-61.

Meek, D. W. and Hupp, T. R. The regulation of MDM2 by multisite phosphorylation--opportunities for molecular-based intervention to target tumours? *Semin Cancer Biol* **20**, 19-28.

Mery, A., Aimond, F., Menard, C., Mikoshiba, K., Michalak, M. and Puceat, M. (2005). Initiation of embryonic cardiac pacemaker activity by inositol 1,4,5-trisphosphate-dependent calcium signaling. *Mol Biol Cell* **16**, 2414-23.

Mery, L., Mesaeli, N., Michalak, M., Opas, M., Lew, D. P. and Krause, K. H. (1996). Overexpression of calreticulin increases intracellular Ca2+ storage and decreases store-operated Ca2+ influx. *J Biol Chem* **271**, 9332-9.

Mesaeli, N., Nakamura, K., Opas, M. and Michalak, M. (2001). Endoplasmic reticulum in the heart, a forgotten organelle? *Mol Cell Biochem* **225**, 1-6.

Mesaeli, N., Nakamura, K., Zvaritch, E., Dickie, P., Dziak, E., Krause, K. H., Opas, M., MacLennan, D. H. and Michalak, M. (1999). Calreticulin is essential for cardiac development. *J Cell Biol* **144**, 857-68.

Meulemans, D. and Bronner-Fraser, M. (2004). Gene-regulatory interactions in neural crest evolution and development. *Dev Cell* **7**, 291-9.

Michalak, M., Baksh, S. and Opas, M. (1991). Identification and immunolocalization of calreticulin in pancreatic cells: no evidence for "calciosomes". *Exp Cell Res* **197**, 91-9.

Michalak, M., Corbett, E. F., Mesaeli, N., Nakamura, K. and Opas, M. (1999). Calreticulin: one protein, one gene, many functions. *Biochem J* **344 Pt 2**, 281-92.

Michalak, M., Groenendyk, J., Szabo, E., Gold, L. I. and Opas, M. (2009). Calreticulin, a multi-process calcium-buffering chaperone of the endoplasmic reticulum. *Biochem J* **417**, 651-66.

Michalak, M., Milner, R. E., Burns, K. and Opas, M. (1992). Calreticulin. *Biochem J* **285 (Pt 3)**, 681-92.

Michelsen, K., Yuan, H. and Schwappach, B. (2005). Hide and run. Arginine-based endoplasmic-reticulum-sorting motifs in the assembly of heteromultimeric membrane proteins. *EMBO Rep* **6**, 717-22.

Miller, J. D., Bernstein, H. D. and Walter, P. (1994). Interaction of E. coli Ffh/4.5S ribonucleoprotein and FtsY mimics that of mammalian signal recognition particle and its receptor. *Nature* **367**, 657-9.

Mimouni, N. K., Lyngso, R. B., Griffiths-Jones, S. and Hein, J. (2009). An analysis of structural influences on selection in RNA genes. *Mol Biol Evol* **26**, 209-16.

Minokawa, T., Yagi, K., Makabe, K. W. and Nishida, H. (2001). Binary specification of nerve cord and notochord cell fates in ascidian embryos. *Development* **128**, 2007-17.

Miosge, N., Gotz, W., Sasaki, T., Chu, M. L., Timpl, R. and Herken, R. (1996). The extracellular matrix proteins fibulin-1 and fibulin-2 in the early human embryo. *Histochem J* **28**, 109-16.

Miosge, N., Sasaki, T., Chu, M. L., Herken, R. and Timpl, R. (1998). Ultrastructural localization of microfibrillar fibulin-1 and fibulin-2 during heart development indicates a switch in molecular associations. *Cell Mol Life Sci* **54**, 606-13.

Mizuguchi, G., Shen, X., Landry, J., Wu, W. H., Sen, S. and Wu, C. (2004). ATP-driven exchange of histone H2AZ variant catalyzed by SWR1 chromatin remodeling complex. *Science* **303**, 343-8.

Monne, M., Gafvelin, G., Nilsson, R. and von Heijne, G. (1999). N-tail translocation in a eukaryotic polytopic membrane protein: synergy between neighboring transmembrane segments. *Eur J Biochem* **263**, 264-9.

Monteoliva, L., Matas, M. L., Gil, C., Nombela, C. and Pla, J. (2002). Large-scale identification of putative exported proteins in Candida albicans by genetic selection. *Eukaryot Cell* **1**, 514-25.

Moody, S. A. (1987a). Fates of the blastomeres of the 16-cell stage Xenopus embryo. *Dev Biol* **119**, 560-78.

Moody, S. A. (1987b). Fates of the blastomeres of the 32-cell-stage Xenopus embryo. *Dev Biol* **122**, 300-19.

Moon, J., Parry, G. and Estelle, M. (2004). The ubiquitin-proteasome pathway and plant development. *Plant Cell* **16**, 3181-95.

Moore, S. A., Hurt, E., Yoder, E., Sprecher, H. and Spector, A. A. (1995). Docosahexaenoic acid synthesis in human skin fibroblasts involves peroxisomal retroconversion of tetracosahexaenoic acid. *J Lipid Res* **36**, 2433-43.

Moran, T. D., Abdulla, F. A. and Smith, P. A. (2000). Cellular neurophysiological actions of nociceptin/orphanin FQ. *Peptides* **21**, 969-76.

Moreau, M., Leclerc, C., Gualandris-Parisot, L. and Duprat, A. M. (1994). Increased internal Ca2+ mediates neural induction in the amphibian embryo. *Proc Natl Acad Sci U S A* **91**, 12639-43.

Moreau, M., Neant, I., Webb, S. E., Miller, A. L. and Leclerc, C. (2008). Calcium signalling during neural induction in Xenopus laevis embryos. *Philos Trans R Soc Lond B Biol Sci* **363**, 1371-5.

Morris, L. G., Veeriah, S. and Chan, T. A. Genetic determinants at the interface of cancer and neurodegenerative disease. *Oncogene* **29**, 3453-64.

Morrison, A. J., Highland, J., Krogan, N. J., Arbel-Eden, A., Greenblatt, J. F., Haber, J. E. and Shen, X. (2004). INO80 and gamma-H2AX interaction links ATP-dependent chromatin remodeling to DNA damage repair. *Cell* **119**, 767-75.

Morrison, A. J., Kim, J. A., Person, M. D., Highland, J., Xiao, J., Wehr, T. S., Hensley, S., Bao, Y., Shen, J., Collins, S. R. et al. (2007). Mec1/Tel1 phosphorylation of the INO80 chromatin remodeling complex influences DNA damage checkpoint responses. *Cell* **130**, 499-511.

Mueller, D., Garcia-Cuellar, M. P., Bach, C., Buhl, S., Maethner, E. and Slany, R. K. (2009). Misguided transcriptional elongation causes mixed lineage leukemia. *PLoS Biol* **7**, e1000249.

Muesch, A., Hartmann, E., Rohde, K., Rubartelli, A., Sitia, R. and Rapoport, T. A. (1990). A novel pathway for secretory proteins? *Trends Biochem Sci* **15**, 86-8.

Munoz-Sanjuan, I. and Brivanlou, A. H. (2002). Neural induction, the default model and embryonic stem cells. *Nat Rev Neurosci* **3**, 271-80.

Muramatsu, T. and Miyauchi, T. (2003). Basigin (CD147): a multifunctional transmembrane protein involved in reproduction, neural function, inflammation and tumor invasion. *Histol Histopathol* **18**, 981-7.

Muraoka, K., Nabeshima, K., Murayama, T., Biswas, C. and Koono, M. (1993). Enhanced expression of a tumor-cell-derived collagenase-stimulatory factor in urothelial carcinoma: its usefulness as a tumor marker for bladder cancers. *Int J Cancer* **55**, 19-26.

Murphy, D., Dancis, B. and Brown, J. R. (2008). The evolution of core proteins involved in microRNA biogenesis. *BMC Evol Biol* **8**, 92.

Nagata, T., Kishi, H., Liu, Q. L., Yoshino, T., Matsuda, T., Jin, Z. X., Murayama, K., Tsukada, K. and Muraguchi, A. (2000). Possible involvement of cyclophilin B and caspase-activated deoxyribonuclease in the induction of chromosomal DNA degradation in TCR-stimulated thymocytes. *J Immunol* **165**, 4281-9.

Nakamura, K., Bossy-Wetzel, E., Burns, K., Fadel, M. P., Lozyk, M., Goping, I. S., Opas, M., Bleackley, R. C., Green, D. R. and Michalak, M. (2000). Changes in endoplasmic reticulum luminal environment affect cell sensitivity to apoptosis. *J Cell Biol* **150**, 731-40.

Nakamura, T., Lozano, P. R., Ikeda, Y., Iwanaga, Y., Hinek, A., Minamisawa, S., Cheng, C. F., Kobuke, K., Dalton, N., Takada, Y. et al. (2002). Fibulin-5/DANCE is essential for elastogenesis in vivo. *Nature* **415**, 171-5.

Nakamura, T., Ruiz-Lozano, P., Lindner, V., Yabe, D., Taniwaki, M., Furukawa, Y., Kobuke, K., Tashiro, K., Lu, Z., Andon, N. L. et al. (1999). DANCE, a novel secreted RGD protein expressed in developing, atherosclerotic, and balloon-injured arteries. *J Biol Chem* **274**, 22476-83.

Nakao, A., Afrakhte, M., Moren, A., Nakayama, T., Christian, J. L., Heuchel, R., Itoh, S., Kawabata, M., Heldin, N. E., Heldin, C. H. et al. (1997a). Identification of Smad7, a TGFbeta-inducible antagonist of TGF-beta signalling. *Nature* **389**, 631-5.

Nakao, A., Imamura, T., Souchelnytskyi, S., Kawabata, M., Ishisaki, A., Oeda, E., Tamaki, K., Hanai, J., Heldin, C. H., Miyazono, K. et al. (1997b). TGF-beta receptor-mediated signalling through Smad2, Smad3 and Smad4. *Embo J* **16**, 5353-62.

Nakata, K., Nagai, T., Aruga, J. and Mikoshiba, K. (1997). Xenopus Zic3, a primary regulator both in neural and neural crest development. *Proc Natl Acad Sci U S A* **94**, 11980-5.

Nakata, K., Nagai, T., Aruga, J. and Mikoshiba, K. (1998). Xenopus Zic family and its role in neural and neural crest development. *Mech Dev* **75**, 43-51.

Naruhashi, K., Kadomatsu, K., Igakura, T., Fan, Q. W., Kuno, N., Muramatsu, H., Miyauchi, T., Hasegawa, T., Itoh, A., Muramatsu, T. et al. (1997). Abnormalities of sensory and memory functions in mice lacking Bsg gene. *Biochem Biophys Res Commun* **236**, 733-7.

Navazio, L., Nardi, M. C., Pancaldi, S., Dainese, P., Baldan, B., Fitchette-Laine, A. C., Faye, L., Meggio, F., Martin, W. and Mariani, P. (1998). Functional conservation of calreticulin in Euglena gracilis. *J Eukaryot Microbiol* **45**, 307-13.

Neal, C. R., Jr., Mansour, A., Reinscheid, R., Nothacker, H. P., Civelli, O., Akil, H. and Watson, S. J., Jr. (1999a). Opioid receptor-like (ORL1) receptor distribution in the rat central nervous system: comparison of ORL1 receptor mRNA expression with (125)I-[(14)Tyr]-orphanin FQ binding. *J Comp Neurol* **412**, 563-605.

Neal, C. R., Jr., Mansour, A., Reinscheid, R., Nothacker, H. P., Civelli, O. and Watson, S. J., Jr. (1999b). Localization of orphanin FQ (nociceptin) peptide and messenger RNA in the central nervous system of the rat. *J Comp Neurol* **406**, 503-47.

Nickel, W. (2003). The mystery of nonclassical protein secretion. A current view on cargo proteins and potential export routes. *Eur J Biochem* **270**, 2109-19.

Nickel, W. and Seedorf, M. (2008). Unconventional mechanisms of protein transport to the cell surface of eukaryotic cells. *Annu Rev Cell Dev Biol* **24**, 287-308.

Nielsen, H., Engelbrecht, J., Brunak, S. and von Heijne, G. (1997a). A neural network method for identification of prokaryotic and eukaryotic signal peptides and prediction of their cleavage sites. *Int J Neural Syst* **8**, 581-99.

Nielsen, H., Engelbrecht, J., Brunak, S. and von Heijne, G. (1997b). Identification of prokaryotic and eukaryotic signal peptides and prediction of their cleavage sites. *Protein Eng* **10**, 1-6.

Nielsen, H., Engelbrecht, J., von Heijne, G. and Brunak, S. (1996). Defining a similarity threshold for a functional protein sequence pattern: the signal peptide cleavage site. *Proteins* **24**, 165-77.

Nieto, M. A., Sargent, M. G., Wilkinson, D. G. and Cooke, J. (1994). Control of cell behavior during vertebrate development by Slug, a zinc finger gene. *Science* **264**, 835-9.

Nieuwkoop, P. D. (1985). Inductive interactions in early amphibian development and their general nature. *Journal of Embryology and experimental Morphology* **89 (Suppl.)**, 333-347.

Nikcevic, G., Savic, T., Kovacevic-Grujicic, N. and Stevanovic, M. (2008). Up-regulation of the SOX3 gene expression by retinoic acid: characterization of the novel promoter-response element and the retinoid receptors involved. *J Neurochem* **107**, 1206-15.

Noden, D. M. (1993). Spatial integration among cells forming the cranial peripheral nervous system. *J Neurobiol* **24**, 248-61.

Noden, D. M. and Trainor, P. A. (2005). Relations and interactions between cranial mesoderm and neural crest populations. *J Anat* **207**, 575-601.

Nombela, C., Gil, C. and Chaffin, W. L. (2006). Non-conventional protein secretion in yeast. *Trends Microbiol* **14**, 15-21.

O'Rand, M. G., Richardson, R. T., Zimmerman, L. J. and Widgren, E. E. (1992). Sequence and localization of human NASP: conservation of a Xenopus histone-binding protein. *Dev Biol* **154**, 37-44.

Onichtchouk, D., Glinka, A. and Niehrs, C. (1998). Requirement for Xvent-1 and Xvent-2 gene function in dorsoventral patterning of Xenopus mesoderm. *Development* **125**, 1447-56.

Oppenheimer, J. (1936). Transplantation experiments on developing teleosts (Fundulus and Perca). *J. Exp. Zool.* **72**, 409-437.

Osborne, A. R., Rapoport, T. A. and van den Berg, B. (2005). Protein translocation by the Sec61/SecY channel. *Annu Rev Cell Dev Biol* **21**, 529-50.

Ostwald, T. J. and MacLennan, D. H. (1974). Isolation of a high affinity calcium-binding protein from sarcoplasmic reticulum. *J Biol Chem* **249**, 974-9.

Otte, A. P. and Moon, R. T. (1992). Protein kinase C isozymes have distinct roles in neural induction and competence in Xenopus. *Cell* **68**, 1021-9.

Otte, A. P., van Run, P., Heideveld, M., van Driel, R. and Durston, A. J. (1989). Neural induction is mediated by cross-talk between the protein kinase C and cyclic AMP pathways. *Cell* **58**, 641-8.

Pan, T. C., Kluge, M., Zhang, R. Z., Mayer, U., Timpl, R. and Chu, M. L. (1993a). Sequence of extracellular mouse protein BM-90/fibulin and its calcium-dependent binding to other basement-membrane ligands. *Eur J Biochem* **215**, 733-40.

Pan, T. C., Sasaki, T., Zhang, R. Z., Fassler, R., Timpl, R. and Chu, M. L. (1993b). Structure and expression of fibulin-2, a novel extracellular matrix protein with multiple EGF-like repeats and consensus motifs for calcium binding. *J Cell Biol* **123**, 1269-77.

Papamichos-Chronakis, M., Krebs, J. E. and Peterson, C. L. (2006). Interplay between Ino80 and Swr1 chromatin remodeling enzymes regulates cell cycle checkpoint adaptation in response to DNA damage. *Genes Dev* **20**, 2437-49.

Papanayotou, C., Liao, P., Lu, S.-Q., Kougioumtzidou, E., Zhu, L., Shaw, A., Sheng, G., Streit, A., Yu, D., Soong, T. W. et al. (submitted). Calfacilitin: a novel calcium channel modulator essential for initiation of neural plate development.

Papanayotou, C., Mey, A., Birot, A. M., Saka, Y., Boast, S., Smith, J. C., Samarut, J. and Stern, C. D. (2008). A mechanism regulating the onset of Sox2 expression in the embryonic neural plate. *PLoS Biol* **6**, e2.

Parry, G. and Estelle, M. (2004). Regulation of cullin-based ubiquitin ligases by the Nedd8/RUB ubiquitin-like proteins. *Semin Cell Dev Biol* **15**, 221-9.

Pauli, A., Rinn, J. L. and Schier, A. F. (2011). Non-coding RNAs as regulators of embryogenesis. *Nat Rev Genet* **12**, 136-49.

Pearse, B. R. and Hebert, D. N. Lectin chaperones help direct the maturation of glycoproteins in the endoplasmic reticulum. *Biochim Biophys Acta* **1803**, 684-93.

Pera, E. M., Ikeda, A., Eivers, E. and De Robertis, E. M. (2003). Integration of IGF, FGF, and anti-BMP signals via Smad1 phosphorylation in neural induction. *Genes Dev* **17**, 3023-8.

Pera, E. M., Wessely, O., Li, S. Y. and De Robertis, E. M. (2001). Neural and head induction by insulin-like growth factor signals. *Dev Cell* **1**, 655-65.

Perea-Gomez, A., Rhinn, M. and Ang, S. L. (2001). Role of the anterior visceral endoderm in restricting posterior signals in the mouse embryo. *Int J Dev Biol* **45**, 311-20.

Peterson, C. L., Dingwall, A. and Scott, M. P. (1994). Five SWI/SNF gene products are components of a large multisubunit complex required for transcriptional enhancement. *Proc Natl Acad Sci U S A* **91**, 2905-8.

Peterson, J. R., Ora, A., Van, P. N. and Helenius, A. (1995). Transient, lectin-like association of calreticulin with folding intermediates of cellular and viral glycoproteins. *Mol Biol Cell* **6**, 1173-84.

Piccolo, S., Agius, E., Leyns, L., Bhattacharyya, S., Grunz, H., Bouwmeester, T. and De Robertis, E. M. (1999). The head inducer Cerberus is a multifunctional antagonist of Nodal, BMP and Wnt signals. *Nature* **397**, 707-10.

Piccolo, S., Sasai, Y., Lu, B. and De Robertis, E. M. (1996). Dorsoventral Patterning in Xenopus: Inhibition of ventral signals by direct binding of chordin to BMP-4. *Cell* **86**, 589-598.

Pickart, C. M. (2001). Mechanisms underlying ubiquitination. *Annu Rev Biochem* **70**, 503-33.

Pinho, S., Simonsson, P. R., Trevers, K. E., Stower, M. J., Sherlock, W. T., Khan, M., Streit, A., Sheng, G. and Stern, C. D. (2011). Distinct steps of neural induction revealed by Asterix, Obelix and TrkC, genes induced by different signals from the organizer. *PLoS Biol*.

Pituello, F., Medevielle, F., Foulquier, F. and Duprat, A. M. (1999). Activation of Pax6 depends on somitogenesis in the chick embryo cervical spinal cord. *Development* **126**, 587-96.

Pogoda, H. M. and Meyer, D. (2002). Zebrafish Smad7 is regulated by Smad3 and BMP signals. *Dev Dyn* **224**, 334-49.

Polanowska, J., Martin, J. S., Garcia-Muse, T., Petalcorin, M. I. and Boulton, S. J. (2006). A conserved pathway to activate BRCA1-dependent ubiquitylation at DNA damage sites. *Embo J* **25**, 2178-88.

Polette, M., Gilles, C., Marchand, V., Lorenzato, M., Toole, B., Tournier, J. M., Zucker, S. and Birembaut, P. (1997). Tumor collagenase stimulatory factor (TCSF) expression and localization in human lung and breast cancers. *J Histochem Cytochem* **45**, 703-9.

Poppas, D. P., Pavlovich, C. P., Folkman, J., Voest, E. E., Chen, X., Luster, A. D. and O'Donnell, M. A. (1998). Intravesical bacille Calmette-Guerin induces the antiangiogenic chemokine interferon-inducible protein 10. *Urology* **52**, 268-75; discussion 275-6.

Psychoyos, D. and Stern, C. D. (1996). Restoration of the organizer after radical ablation of Hensen's node and the anterior primitive streak in the chick embryo. *Development* **122**, 3263-73.

Pueyo, J. I. and Couso, J. P. (2008). The 11-aminoacid long Tarsal-less peptides trigger a cell signal in Drosophila leg development. *Dev Biol* **324**, 192-201.

Raghunath, M., Tschodrich-Rotter, M., Sasaki, T., Meuli, M., Chu, M. L. and Timpl, R. (1999). Confocal laser scanning analysis of the association of fibulin-2 with fibrillin-1 and fibronectin define different stages of skin regeneration. *J Invest Dermatol* **112**, 97-101.

Rauch, F., Prud'homme, J., Arabian, A., Dedhar, S. and St-Arnaud, R. (2000). Heart, brain, and body wall defects in mice lacking calreticulin. *Exp Cell Res* **256**, 105-11.

Reijntjes, S., Gale, E. and Maden, M. (2004). Generating gradients of retinoic acid in the chick embryo: Cyp26C1 expression and a comparative analysis of the Cyp26 enzymes. *Dev Dyn* **230**, 509-17.

Rex, M., Orme, A., Uwanogho, D., Tointon, K., Wigmore, P. M., Sharpe, P. T. and Scotting, P. J. (1997a). Dynamic expression of chicken Sox2 and Sox3 genes in ectoderm induced to form neural tissue. *Dev Dyn* **209**, 323-32.

Rex, M., Uwanogho, D., Cartwright, E., Pearl, G., Sharpe, P. T. and Scotting, P. J. (1994). Sox gene expression during neuronal development. *Biochem Soc Trans* **22**, 252S.

Rex, M., Uwanogho, D. A., Orme, A., Scotting, P. J. and Sharpe, P. T. (1997b). cSox21 exhibits a complex and dynamic pattern of transcription during embryonic development of the chick central nervous system. *Mech Dev* **66**, 39-53.

Ribisi, S., Jr., Mariani, F. V., Aamar, E., Lamb, T. M., Frank, D. and Harland, R. M. (2000). Ras-mediated FGF signaling is required for the formation of posterior but not anterior neural tissue in Xenopus laevis. *Dev Biol* **227**, 183-96.

Richard, D. J., Bolderson, E., Cubeddu, L., Wadsworth, R. I., Savage, K., Sharma, G. G., Nicolette, M. L., Tsvetanov, S., McIlwraith, M. J., Pandita, R. K. et al. (2008). Single-stranded DNA-binding protein hSSB1 is critical for genomic stability. *Nature* **453**, 677-81.

Richardson, R. T., Alekseev, O. M., Grossman, G., Widgren, E. E., Thresher, R., Wagner, E. J., Sullivan, K. D., Marzluff, W. F. and O'Rand, M. G. (2006). Nuclear autoantigenic sperm protein (NASP), a linker histone chaperone that is required for cell proliferation. *J Biol Chem* **281**, 21526-34.

Richardson, R. T., Batova, I. N., Widgren, E. E., Zheng, L. X., Whitfield, M., Marzluff, W. F. and O'Rand, M. G. (2000). Characterization of the histone H1-binding protein, NASP, as a cell cycle-regulated somatic protein. *J Biol Chem* **275**, 30378-86.

Risau, W., Hallmann, R. and Albrecht, U. (1986a). Differentiation-dependent expression of proteins in brain endothelium during development of the blood-brain barrier. *Dev Biol* **117**, 537-45.

Risau, W., Hallmann, R., Albrecht, U. and Henke-Fahle, S. (1986b). Brain induces the expression of an early cell surface marker for blood-brain barrier-specific endothelium. *Embo J* **5**, 3179-83.

Roberts, C., Platt, N., Streit, A., Schachner, M. and Stern, C. D. (1991). The L5 epitope: an early marker for neural induction in the chick embryo and its involvement in inductive interactions. *Development* **112**, 959-70.

Rosell, R., Wei, J. and Taron, M. (2009). Circulating MicroRNA Signatures of Tumor-Derived Exosomes for Early Diagnosis of Non-Small-Cell Lung Cancer. *Clin Lung Cancer* **10**, 8-9.

Rouillard, J. M., Zeuker, M. and Gulari, E. (2003). OligoArray 2.0: Thermodynamicaly improved oligonucleotide design for microarrays. *Nucleic Acids Res* **31**, 3057-3062.

Rubartelli, A., Cozzolino, F., Talio, M. and Sitia, R. (1990). A novel secretory pathway for interleukin-1 beta, a protein lacking a signal sequence. *Embo J* **9**, 1503-10.

Rubinstein, A. L., Lee, D., Luo, R., Henion, P. D. and Halpern, M. E. (2000). Genes dependent on zebrafish cyclops function identified by AFLP differential gene expression screen. *Genesis* **26**, 86-97.

Ruhl, D. D., Jin, J., Cai, Y., Swanson, S., Florens, L., Washburn, M. P., Conaway, R. C., Conaway, J. W. and Chrivia, J. C. (2006). Purification of a human SRCAP complex that remodels chromatin by incorporating the histone variant H2A.Z into nucleosomes. *Biochemistry* **45**, 5671-7.

Rutten, K., De Vry, J., Bruckmann, W. and Tzschentke, T. M. Effects of the NOP receptor agonist Ro65-6570 on the acquisition of opiate- and psychostimulant-induced conditioned place preference in rats. *Eur J Pharmacol* **645**, 119-26.

Rutten, K., De Vry, J., Bruckmann, W. and Tzschentke, T. M. Pharmacological blockade or genetic knockout of the NOP receptor potentiates the rewarding effect of morphine in rats. *Drug Alcohol Depend*.

Saint-Jeannet, J. P., Foulquier, F., Goridis, C. and Duprat, A. M. (1989). Expression of N-CAM precedes neural induction in Pleurodeles waltl (urodele, amphibian). *Development* **106**, 675-83.

Saint-Jeannet, J. P., Huang, S. and Duprat, A. M. (1990). Modulation of neural commitment by changes in target cell contacts in Pleurodeles waltl. *Dev Biol* **141**, 93-103.

Saint-Jeannet, J. P., Pituello, F., Huang, S., Foulquier, F. and Duprat, A. M. (1993). Experimentally provoked neural induction results in an incomplete expression of neuronal traits. *Exp Cell Res* **207**, 383-7.

Sakisaka, T. and Takai, Y. (2004). Biology and pathology of nectins and nectin-like molecules. *Curr Opin Cell Biol* **16**, 513-21.

Saldivar, J. R., Sechrist, J. W., Krull, C. E., Ruffins, S. and Bronner-Fraser, M. (1997). Dorsal hindbrain ablation results in rerouting of neural crest migration and changes in gene expression, but normal hyoid development. *Development* **124**, 2729-39.

Sambrook, J. L., Fritsch, E. F. and Maniatis, T. (1989). Molecular Cloning: A laboratory manual. NY: Cold Spring Harbour Laboratory Press.

Sameshima, T., Nabeshima, K., Toole, B. P., Yokogami, K., Okada, Y., Goya, T., Koono, M. and Wakisaka, S. (2000). Expression of emmprin (CD147), a cell surface inducer of matrix metalloproteinases, in normal human brain and gliomas. *Int J Cancer* **88**, 21-7.

Sanson, B. (2001). Generating patterns from fields of cells. Examples from Drosophila segmentation. *EMBO Rep* **2**, 1083-8.

Sasai, Y., Lu, B., Piccolo, S. and De Robertis, E. M. (1996). endoderm induction by the organizer-secreted factors chordin and noggin in Xenopus animal caps. *EMBO Journal* **15 (17)**, 4547-4555.

Sasai, Y., Lu, B., Steinbeisser, H. and De Robertis, E. M. (1995). Regulation of neural induction by the Chd and Bmp-4 antagonistic patterning signals in Xenopus. *Nature* **377**, 757.

Sasai, Y., Lu, B., Steinbeisser, H., Geissert, D., Gont, L. K. and De Robertis, E. M. (1994). Xenopus chordin: A novel dorsalizing factor activated by Organizer-specific homeobox genes. *Cell* **79**, 779-790.

Sato, S. M. and Sargent, T. D. (1989). Development of neural inducing capacity in dissociated Xenopus embryos. *Dev Biol* **134**, 263-6.

Saxén, L. and Toivonen, S. (1962). Primary embryonic induction. London: Academic Press.

Schafer, T., Zentgraf, H., Zehe, C., Brugger, B., Bernhagen, J. and Nickel, W. (2004). Unconventional secretion of fibroblast growth factor 2 is mediated by direct translocation across the plasma membrane of mammalian cells. *J Biol Chem* **279**, 6244-51.

Schoenwolf, G. C., Garcia-Martinez, V. and Dias, M. S. (1992). Mesoderm movement and fate during avian gastrulation and neurulation. *Dev Dyn* **193**, 235-48.

Schoenwolf, G. C. and Yuan, S. (1995). Experimental analyses of the rearrangement of ectodermal cells during gastrulation and neurulation in avian embryos. *Cell Tissue Res* **280**, 243-51.

Schrag, J. D., Procopio, D. O., Cygler, M., Thomas, D. Y. and Bergeron, J. J. (2003). Lectin control of protein folding and sorting in the secretory pathway. *Trends Biochem Sci* **28**, 49-57.

Schulte-Merker, S., Lee, K. J., McMahon, A. P. and Hammerschmidt, M. (1997). The zebrafish organizer requires chordino. *Nature* **387**, 862-3.

Schultheiss, T. M., Burch, J. B. and Lassar, A. B. (1997). A role for bone morphogenetic proteins in the induction of cardiac myogenesis. *Genes Dev* **11**, 451-62.

Scott, I. C., Blitz, I. L., Pappano, W. N., Maas, S. A., Cho, K. W. and Greenspan, D. S. (2001). Homologues of Twisted gastrulation are extracellular cofactors in antagonism of BMP signalling. *Nature* **410**, 475-8.

Sechrist, J. and Bronner-Fraser, M. (1991). Birth and differentiation of reticular neurons in the chick hindbrain: ontogeny of the first neuronal population. *Neuron* **7**, 947-63.

Selleck, M. A. and Bronner-Fraser, M. (1995). Origins of the avian neural crest: the role of neural plate-epidermal interactions. *Development* **121**, 525-38.

Servetnick, M. and Grainger, R. M. (1991). Homeogenetic neural induction in Xenopus. *Dev Biol* **147**, 73-82.

Seulberger, H., Lottspeich, F. and Risau, W. (1990). The inducible blood--brain barrier specific molecule HT7 is a novel immunoglobulin-like cell surface glycoprotein. *Embo J* **9**, 2151-8.

Shen, X., Mizuguchi, G., Hamiche, A. and Wu, C. (2000). A chromatin remodelling complex involved in transcription and DNA processing. *Nature* **406**, 541-4.

Sheng, G., dos Reis, M. and Stern, C. D. (2003). Churchill, a zinc finger transcriptional activator, regulates the transition between gastrulation and neurulation. *Cell* **115**, 603-13.

Sheng, H. Z., Bertuzzi, S., Chiang, C., Shawlot, W., Taira, M., Dawid, I. and Westphal, H. (1997). Expression of murine Lhx5 suggests a role in specifying the forebrain. *Dev Dyn* **208**, 266-77.

Sheng, N., Xie, Z., Wang, C., Bai, G., Zhang, K., Zhu, Q., Song, J., Guillemot, F., Chen, Y. G., Lin, A. et al. (2010). Retinoic acid regulates bone morphogenic protein signal duration by promoting the degradation of phosphorylated Smad1. *Proc Natl Acad Sci U S A* **107**, 18886-91.

Sherry, B., Yarlett, N., Strupp, A. and Cerami, A. (1992). Identification of cyclophilin as a proinflammatory secretory product of lipopolysaccharide-activated macrophages. *Proc Natl Acad Sci U S A* **89**, 3511-5.

Shet, A. S. (2008). Characterizing blood microparticles: technical aspects and challenges. *Vasc Health Risk Manag* **4**, 769-74.

Shi, Y. and Massague, J. (2003). Mechanisms of TGF-beta signaling from cell membrane to the nucleus. *Cell* **113**, 685-700.

Shieh, S.-P., Ning, I.L. and Tsung, S.-D. (1963). Studies on the inductive action of the Hensen's node following its transplantation in ovo to the early chick blastoderm. *Acta Biol. Exp. Sinica* **8**, 441-462.

Shimada, K., Oma, Y., Schleker, T., Kugou, K., Ohta, K., Harata, M. and Gasser, S. M. (2008). Ino80 chromatin remodeling complex promotes recovery of stalled replication forks. *Curr Biol* **18**, 566-75.

Shimizu, K. and Takai, Y. (2003). Roles of the intercellular adhesion molecule nectin in intracellular signaling. *J Biochem* **134**, 631-6.

Simpson, E. H., Johnson, D. K., Hunsicker, P., Suffolk, R., Jordan, S. A. and Jackson, I. J. (1999). The mouse Cer1 (Cerberus related or homologue) gene is not required for anterior pattern formation. *Dev Biol* **213**, 202-6.

Sincock, P. M., Fitter, S., Parton, R. G., Berndt, M. C., Gamble, J. R. and Ashman, L. K. (1999). PETA-3/CD151, a member of the transmembrane 4 superfamily, is localised to the plasma membrane and endocytic system of endothelial cells, associates with multiple integrins and modulates cell function. *J Cell Sci* **112 (Pt 6)**, 833-44.

Sincock, P. M., Mayrhofer, G. and Ashman, L. K. (1997). Localization of the transmembrane 4 superfamily (TM4SF) member PETA-3 (CD151) in normal human tissues: comparison with CD9, CD63, and alpha5beta1 integrin. *J Histochem Cytochem* **45**, 515-25.

Skaar, J. R., Richard, D. J., Saraf, A., Toschi, A., Bolderson, E., Florens, L., Washburn, M. P., Khanna, K. K. and Pagano, M. (2009). INTS3 controls the hSSB1-mediated DNA damage response. *J Cell Biol* **187**, 25-32.

Slack, J. (1994a). Role of fibroblast growth factors as inducing agents in early embryonic development. *Mol Reprod Dev* **39**, 118-24; discussion 24-5.

Slack, J. M. (1994b). Inducing factors in Xenopus early embryos. *Curr Biol* **4**, 116-26.

Slack, J. M. and Isaacs, H. V. (1994). The role of fibroblast growth factors in early Xenopus development. *Biochem Soc Trans* **22**, 585-9.

Smith, J. C., Cooke, J., Green, J. B., Howes, G. and Symes, K. (1989). Inducing factors and the control of mesodermal pattern in Xenopus laevis. *Development* **107**, 149-59.

Smith, J. C., Yaqoob, M. and Symes, K. (1988). Purification, partial characterization and biological effects of the XTC mesoderm-inducing factor. *Development* **103**, 591-600.

Smith, W. C. and Harland, R. M. (1992). Expression cloning of noggin, a new dorsalizing factor localized to the Spemann organizer in Xenopus embryos. *Cell* **70**, 829-40.

Smith, W. C., Knecht, A. K., Wu, M. and Harland, R. M. (1993). Secreted noggin protein mimics the Spemann organizer in dorsalizing Xenopus mesoderm. *Nature* **361**, 547-9.

Smith, W. C., McKendry, R., Ribisi, S., Jr. and Harland, R. M. (1995). A nodal-related gene defines a physical and functional domain within the Spemann organizer. *Cell* **82**, 37-46.

Snyder, P. M. (2009). Down-regulating destruction: phosphorylation regulates the E3 ubiquitin ligase Nedd4-2. *Sci Signal* **2**, pe41.

Spann, P., Ginsburg, M., Rangini, Z., Fainsod, A., Eyal-Giladi, H. and Gruenbaum, Y. (1994). The spatial and temporal dynamics of Sax1 (CHox3) homeobox gene expression in the chick's spinal cord. *Development* **120**, 1817-28.

Spemann, H. and Mangold, H. (1924). Uber Induktion von Embryonalanlangen durch Implantation artfremder Organisatoren. *Roux Arch. EntwMech. Org.* **100**, 599-638.

Spence, S. G., Argraves, W. S., Walters, L., Hungerford, J. E. and Little, C. D. (1992). Fibulin is localized at sites of epithelial-mesenchymal transitions in the early avian embryo. *Dev Biol* **151**, 473-84.

Spiro, R. G., Zhu, Q., Bhoyroo, V. and Soling, H. D. (1996). Definition of the lectin-like properties of the molecular chaperone, calreticulin, and demonstration of its copurification with endomannosidase from rat liver Golgi. *J Biol Chem* **271**, 11588-94.

Staunton, D. E., Dustin, M. L. and Springer, T. A. (1989). Functional cloning of ICAM-2, a cell adhesion ligand for LFA-1 homologous to ICAM-1. *Nature* **339**, 61-4.

Stern, C. D. (2005). Neural induction: old problem, new findings, yet more questions. *Development* **132**, 2007-21.

Stern, C. D. (2006). Neural induction: 10 years on since the 'default model'. *Curr Opin Cell Biol* **18**, 692-7.

Stern, C. D. and Ireland, G. W. (1981). An integrated experimental study of endoderm formation in avian embryos. *Anat Embryol* **163**, 245-63.

Stern, C. D., Ireland, G. W., Herrick, S. E., Gherardi, E., Gray, J., Perryman, M. and Stoker, M. (1990). Epithelial scatter factor and development of the chick embryonic axis. *Development* **110**, 1271-84.

Steventon, B., Carmona-Fontaine, C. and Mayor, R. (2005). Genetic network during neural crest induction: from cell specification to cell survival. *Semin Cell Dev Biol* **16**, 647-54.

Storey, K., Goriely, A., Sargent, C. M., Brown, J. M., Burns, H. D., Abud, H. M. and Heath, J. K. (1998). Early posterior neural induction is induced by FGF in the chick embryo.

Storey, K. G., Crossley, J. M., De Robertis, E. M., Norris, W. E. and Stern, C. D. (1992). Neural induction and regionalisation in the chick embryo. *Development* **114**, 729-41.

Storey, K. G., Selleck, M. A. and Stern, C. D. (1995). Neural induction and regionalisation by different subpopulations of cells in Hensen's node. *Development* **121**, 417-28.

Streit, A., Berliner, A., Papanayotou, C., Sirulnik, A. and Stern, C. D. (2000a). Initiation of neural induction by FGF signalling before gastrulation. *Nature* **406**, 74-78.

Streit, A., Berliner, A. J., Papanayotou, C., Sirulnik, A. and Stern, C. D. (2000b). Initiation of neural induction by FGF signalling before gastrulation. *Nature* **406**, 74-8.

Streit, A., Lee, K. J., Woo, I., Roberts, C., Jessell, T. M. and Stern, C. D. (1998). Chordin regulates primitive streak development and the stability of induced neural cells, but is not sufficient for neural induction in the chick embryo. *Development* **125**, 507-19.

Streit, A., Sockanathan, S., Perez, L., Rex, M., Scotting, P. J., Sharpe, P. T., Lovell-Badge, R. and Stern, C. D. (1997b). Preventing the loss of competence for neural induction: HGF/SF, L5 and Sox-2. *Development* **124**, 1191-202.

Streit, A. and Stern, C. D. (1999). Neural induction. A bird's eye view. *Trends Genet* **15**, 20-4.

Streit, A. and Stern, C. D. (1999a). Establishment and maintenance of the border of the neural plate in the chick: involvement of FGF and BMP activity. *Mech Dev* **82**, 51-66.

Streit, A. and Stern, C. D. (1999b). Mesoderm patterning and somite formation during node regression: differential effects of chordin and noggin. *Mech Dev* **85**, 85-96.

Streit, A., Stern, C. D., Thery, C., Ireland, G. W., Aparicio, S., Sharpe, M. J. and Gherardi, E. (1995). A role for HGF/SF in neural induction and its expression in Hensen's node during gastrulation. *Development* **121**, 813-24.

Streit, A., Yuen, C. T., Loveless, R. W., Lawson, A. M., Finne, J., Schmitz, B., Feizi, T. and Stern, C. D. (1996). The Le(x) carbohydrate sequence is recognized by antibody to L5, a functional antigen in early neural development. *J Neurochem* **66**, 834-44.

Streit, A. C. and Stern, C. D. (1997). Competence for neural induction: HGF/SF, HGF1/MSP and the c-Met receptor. *Ciba Found Symp* **212**, 155-65.

Strieter, R. M., Burdick, M. D., Gomperts, B. N., Belperio, J. A. and Keane, M. P. (2005). CXC chemokines in angiogenesis. *Cytokine Growth Factor Rev* **16**, 593-609.

Strieter, R. M., Polverini, P. J., Arenberg, D. A., Walz, A., Opdenakker, G., Van Damme, J. and Kunkel, S. L. (1995a). Role of C-X-C chemokines as regulators of angiogenesis in lung cancer. *J Leukoc Biol* **57**, 752-62.

Strieter, R. M., Polverini, P. J., Kunkel, S. L., Arenberg, D. A., Burdick, M. D., Kasper, J., Dzuiba, J., Van Damme, J., Walz, A., Marriott, D. et al. (1995b). The functional role of the ELR motif in CXC chemokine-mediated angiogenesis. *J Biol Chem* **270**, 27348-57.

Sugiura, T. and Berditchevski, F. (1999). Function of alpha3beta1-tetraspanin protein complexes in tumor cell invasion. Evidence for the role of the complexes in production of matrix metalloproteinase 2 (MMP-2). *J Cell Biol* **146**, 1375-89.

Suzuki, A., Thies, R. S., Yamaji, N., Song, J. J., Wozney, J. M., Murakami, K. and Ueno, N. (1994). A truncated bone morphogenetic protein receptor affects dorsal-ventral patterning in the early Xenopus embryo. *Proceedings of the National Academy of Sciences, USA* **91**, 10255-10259.

Takahashi, K., Nakanishi, H., Miyahara, M., Mandai, K., Satoh, K., Satoh, A., Nishioka, H., Aoki, J., Nomoto, A., Mizoguchi, A. et al. (1999). Nectin/PRR: an immunoglobulin-like cell adhesion molecule recruited to cadherin-based adherens junctions through interaction with Afadin, a PDZ domain-containing protein. *J Cell Biol* **145**, 539-49.

Takai, Y., Irie, K., Shimizu, K., Sakisaka, T. and Ikeda, W. (2003). Nectins and nectin-like molecules: roles in cell adhesion, migration, and polarization. *Cancer Sci* **94**, 655-67.

Takemoto, T., Uchikawa, M., Kamachi, Y. and Kondoh, H. (2006). Convergence of Wnt and FGF signals in the genesis of posterior neural plate through activation of the Sox2 enhancer N-1. *Development* **133**, 297-306.

Taylor, D. D. and Gercel-Taylor, C. (2008). MicroRNA signatures of tumor-derived exosomes as diagnostic biomarkers of ovarian cancer. *Gynecol Oncol* **110**, 13-21.

Tian, D., Sun, S. and Lee, J. T. The long noncoding RNA, Jpx, is a molecular switch for X chromosome inactivation. *Cell* **143**, 390-403.

Tiedemann, H. (1956a). [Experiments on the chemical identification of embryonal induction substances]. *Hoppe Seylers Z Physiol Chem* **306**, 7-32.

Tiedemann, H. (1956b). [Isolation of ribonucleic acids and nucleotides from embryonal extracts and liver, and their inductor behavior]. *Hoppe Seylers Z Physiol Chem* **306**, 132-42.

Timpl, R., Sasaki, T., Kostka, G. and Chu, M. L. (2003). Fibulins: a versatile family of extracellular matrix proteins. *Nat Rev Mol Cell Biol* **4**, 479-89.

Toivonen, S. and Wartiovaara, J. (1976). Mechanisms of cell interaction during primary embryonic induction studied in transfilter experiments. *Differentiation* **5**, 61-6.

Toke, D. A. and Martin, C. E. (1996). Isolation and characterization of a gene affecting fatty acid elongation in Saccharomyces cerevisiae. *J Biol Chem* **271**, 18413-22.

Tran, H., Mattei, M., Godyna, S. and Argraves, W. S. (1997a). Human fibulin-1D: molecular cloning, expression and similarity with S1-5 protein, a new member of the fibulin gene family. *Matrix Biol* **15**, 479-93.

Tran, H., Tanaka, A., Litvinovich, S. V., Medved, L. V., Haudenschild, C. C. and Argraves, W. S. (1995). The interaction of fibulin-1 with fibrinogen. A potential role in hemostasis and thrombosis. *J Biol Chem* **270**, 19458-64.

Tran, H., VanDusen, W. J. and Argraves, W. S. (1997b). The self-association and fibronectin-binding sites of fibulin-1 map to calcium-binding epidermal growth factor-like domains. *J Biol Chem* **272**, 22600-6.

Tribulo, C., Aybar, M. J., Nguyen, V. H., Mullins, M. C. and Mayor, R. (2003). Regulation of Msx genes by a Bmp gradient is essential for neural crest specification. *Development* **130**, 6441-52.

Trindade, M., Tada, M. and Smith, J. C. (1999). DNA-binding specificity and embryological function of Xom (Xvent-2). *Dev Biol* **216**, 442-56.

Trombetta, E. S. and Parodi, A. J. (2003). Quality control and protein folding in the secretory pathway. *Annu Rev Cell Dev Biol* **19**, 649-76.

Tsuda, T., Wang, H., Timpl, R. and Chu, M. L. (2001). Fibulin-2 expression marks transformed mesenchymal cells in developing cardiac valves, aortic arch vessels, and coronary vessels. *Dev Dyn* **222**, 89-100.

Tsung, S. D., Ning, I. L. and Shieh, S. P. (1965). [Studies on the Inductive Action of the Hensen's Node Following Its Transplantation in Ovo to the Early Chick Blastoderm. Ii. Regionally Specific Induction of the Node Region of Different Ages]. *Shi Yan Sheng Wu Xue Bao* **10**, 69-83.

Turner, A. M. and Morris, K. V. Controlling transcription with noncoding RNAs in mammalian cells. *Biotechniques* **48**, ix-xvi.

Tvrdik, P., Westerberg, R., Silve, S., Asadi, A., Jakobsson, A., Cannon, B., Loison, G. and Jacobsson, A. (2000). Role of a new mammalian gene family in the biosynthesis of very long chain fatty acids and sphingolipids. *J Cell Biol* **149**, 707-18.

Uchikawa, M., Ishida, Y., Takemoto, T., Kamachi, Y. and Kondoh, H. (2003). Functional analysis of chicken Sox2 enhancers highlights an array of diverse regulatory elements that are conserved in mammals. *Dev Cell* **4**, 509-19.

Uchikawa, M., Takemoto, T., Kamachi, Y. and Kondoh, H. (2004). Efficient identification of regulatory sequences in the chicken genome by a powerful combination of embryo electroporation and genome comparison. *Mech Dev* **121**, 1145-58.

Umlauf, D., Fraser, P. and Nagano, T. (2008). The role of long non-coding RNAs in chromatin structure and gene regulation: variations on a theme. *Biol Chem* **389**, 323-31.

Uwanogho, D., Rex, M., Cartwright, E. J., Pearl, G., Healy, C., Scotting, P. J. and Sharpe, P. T. (1995). Embryonic expression of the chicken Sox2, Sox3 and Sox11 genes suggests an interactive role in neuronal development. *Mech Dev* **49**, 23-36.

Vakaet, L. (1965). Resultats de la greffe de noeuds de Hensen d'age different sur le blastoderme de poulet. *C. R. Soc Biol* **159**, 232-233.

Valadi, H., Ekstrom, K., Bossios, A., Sjostrand, M., Lee, J. J. and Lotvall, J. O. (2007). Exosome-mediated transfer of mRNAs and microRNAs is a novel mechanism of genetic exchange between cells. *Nat Cell Biol* **9**, 654-9.

van Attikum, H., Fritsch, O. and Gasser, S. M. (2007). Distinct roles for SWR1 and INO80 chromatin remodeling complexes at chromosomal double-strand breaks. *Embo J* **26**, 4113-25.

Van Obberghen, E., Baron, V., Delahaye, L., Emanuelli, B., Filippa, N., Giorgetti-Peraldi, S., Lebrun, P., Mothe-Satney, I., Peraldi, P., Rocchi, S. et al. (2001). Surfing the insulin signaling web. *Eur J Clin Invest* **31**, 966-77.

Vincent, J. A., Kwong, T. J. and Tsukiyama, T. (2008). ATP-dependent chromatin remodeling shapes the DNA replication landscape. *Nat Struct Mol Biol* **15**, 477-84.

Vogel, A., Rodriguez, C. and Izpisua-Belmonte, J. C. (1996). Involvement of FGF-8 in initiation, outgrowth and patterning of the vertebrate limb. *Development* **122**, 1737-50.

Vogel, B. E. and Hedgecock, E. M. (2001). Hemicentin, a conserved extracellular member of the immunoglobulin superfamily, organizes epithelial and other cell attachments into oriented line-shaped junctions. *Development* **128**, 883-94.

Vogel, T. and Gruss, P. (2009). Expression of Leukaemia associated transcription factor Af9/Mllt3 in the cerebral cortex of the mouse. *Gene Expr Patterns* **9**, 83-93.

von Bubnoff, A. and Cho, K. W. (2001). Intracellular BMP signaling regulation in vertebrates: pathway or network? *Dev Biol* **239**, 1-14.

Wada, I., Ou, W. J., Liu, M. C. and Scheele, G. (1994). Chaperone function of calnexin for the folding intermediate of gp80, the major secretory protein in MDCK cells. Regulation by redox state and ATP. *J Biol Chem* **269**, 7464-72.

Wada, I., Rindress, D., Cameron, P. H., Ou, W. J., Doherty, J. J., 2nd, Louvard, D., Bell, A. W., Dignard, D., Thomas, D. Y. and Bergeron, J. J. (1991). SSR alpha and associated calnexin are major calcium binding proteins of the endoplasmic reticulum membrane. *J Biol Chem* **266**, 19599-610.

Wada, J., Zhang, H., Tsuchiyama, Y., Hiragushi, K., Hida, K., Shikata, K., Kanwar, Y. S. and Makino, H. (2001). Gene expression profile in streptozotocin-induced diabetic mice kidneys undergoing glomerulosclerosis. *Kidney Int* **59**, 1363-73.

Waddington, C. H. (1930). Developmental mechanics of chick and duck embryos. *Nature* **125**, 924-925.

Waddington, C. H. (1932). Experiments on the development of chick and duck embryos cultivated in vitro. *Phil. Trans. Roy. Soc. Lond. B* **221**, 179-230.

Waddington, C. H. (1933a). Induction by coagulated organisers in the chick embryo. *Nature (London)* **131**, 275.

Waddington, C. H. (1933b). Induction by the Primitive Streak and its Derivatives in the Chick. *Journal of Experimental Biology* **10**, 38-48.

Waddington, C. H. (1934). Experiments on embryonic induction. *J. exp. Biol.* **11**, 211-227.

Waddington, C. H. (1936). Organizers in Mammalian Development. *Nature* **138**, 125.

Waddington, C. H. (1937). Experiments on determination in the rabbit embryo. *Arch Biol* **48**, 273-290.

Waddington, C. H. and Schmidt, C. A. (1933b). Induction by heteroplastic grafts of the primitive streak in birds. *Roux' Arch EntwMech Org* **128**, 522-563.

Walter, P. and Johnson, A. E. (1994). Signal sequence recognition and protein targeting to the endoplasmic reticulum membrane. *Annu Rev Cell Biol* **10**, 87-119.

Watanabe, Y. and Le Douarin, N. M. (1996). A role for BMP-4 in the development of subcutaneous cartilage. *Mech Dev* **57**, 69-78.

Wawersik, S., Evola, C. and Whitman, M. (2005). Conditional BMP inhibition in Xenopus reveals stage-specific roles for BMPs in neural and neural crest induction. *Dev Biol* **277**, 425-42.

Wawersik, S., Purcell, P., Rauchman, M., Dudley, A. T., Robertson, E. J. and Maas, R. (1999). BMP7 acts in murine lens placode development. *Dev Biol* **207**, 176-88.

Weinstein, D. C. and Hemmati-Brivanlou, A. (1999). Neural induction. *Annu Rev Cell Dev Biol* **15**, 411-33.

Weinstein, D. C., Ruiz i Altaba, A., Chen, W. S., Hoodless, P., Prezioso, V. R., Jessell, T. M. and Darnell, J. E., Jr. (1994). The winged-helix transcription factor HNF-3 beta is required for notochord development in the mouse embryo. *Cell* **78**, 575-88.

Welch, J. E. and O'Rand, M. G. (1990). Characterization of a sperm-specific nuclear autoantigenic protein. II. Expression and localization in the testis. *Biol Reprod* **43**, 569-78.

Welch, J. E., Zimmerman, L. J., Joseph, D. R. and O'Rand, M. G. (1990). Characterization of a sperm-specific nuclear autoantigenic protein. I. Complete sequence and homology with the Xenopus protein, N1/N2. *Biol Reprod* **43**, 559-68.

Weng, W. and Stemple, D. L. (2003). Nodal signaling and vertebrate germ layer formation. *Birth Defects Res C Embryo Today* **69**, 325-32.

White, T. K., Zhu, Q. and Tanzer, M. L. (1995). Cell surface calreticulin is a putative mannoside lectin which triggers mouse melanoma cell spreading. *J Biol Chem* **270**, 15926-9.

Wicks, S. J., Grocott, T., Haros, K., Maillard, M., ten Dijke, P. and Chantry, A. (2006). Reversible ubiquitination regulates the Smad/TGF-beta signalling pathway. *Biochem Soc Trans* **34**, 761-3.

Wilson, L., Gale, E., Chambers, D. and Maden, M. (2004). Retinoic acid and the control of dorsoventral patterning in the avian spinal cord. *Dev Biol* **269**, 433-46.

Wilson, P. A. and Hemmati-Brivanlou, A. (1995). Induction of epidermis and inhibition of neural fate by Bmp-4. *Nature* **376**, 331-3.

Wilson, P. A., Lagna, G., Suzuki, A. and Hemmati-Brivanlou, A. (1997). Concentration-dependent patterning of the Xenopus ectoderm by BMP4 and its signal transducer Smad1. *Development* **124**, 3177-84.

Wilson, S. I. and Edlund, T. (2001). Neural induction: toward a unifying mechanism. *Nat Neurosci* **4 Suppl**, 1161-8.

Wilson, S. I., Graziano, E., Harland, R., Jessell, T. M. and Edlund, T. (2000). An early requirement for FGF signalling in the acquisition of neural cell fate in the chick embryo. *Curr Biol* **10**, 421-429.

Wilson, S. I., Rydstrom, A., Trimborn, T., Willert, K., Nusse, R., Jessell, T. M. and Edlund, T. (2001). The status of Wnt signalling regulates neural and epidermal fates in the chick embryo. *Nature* **411**, 325-30.

Winnier, G., Blessing, M., Labosky, P. A. and Hogan, B. M. (1995). Bone morphogenetic protein-4 is required for mesoderm formation and patterning in the mouse. *Genes and Development* **9**, 2105-2116.

Wong, M. M., Cox, L. K. and Chrivia, J. C. (2007). The chromatin remodeling protein, SRCAP, is critical for deposition of the histone variant H2A.Z at promoters. *J Biol Chem* **282**, 26132-9.

Woodside, J. L. (1937). The influence of the host age on induction in the chick blastoderm. *J. Exp. Zool.* **75**, 259-281.

Wu, S., Shi, Y., Mulligan, P., Gay, F., Landry, J., Liu, H., Lu, J., Qi, H. H., Wang, W., Nickoloff, J. A. et al. (2007). A YY1-INO80 complex regulates genomic stability through homologous recombination-based repair. *Nat Struct Mol Biol* **14**, 1165-72.

Wu, X., Yen, L., Irwin, L., Sweeney, C. and Carraway, K. L., 3rd. (2004). Stabilization of the E3 ubiquitin ligase Nrdp1 by the deubiquitinating enzyme USP8. *Mol Cell Biol* **24**, 7748-57.

Xu, C., Kim, N. G. and Gumbiner, B. M. (2009). Regulation of protein stability by GSK3 mediated phosphorylation. *Cell Cycle* **8**, 4032-9.

Xu, Q., Leiva, M. C., Fischkoff, S. A., Handschumacher, R. E. and Lyttle, C. R. (1992). Leukocyte chemotactic activity of cyclophilin. *J Biol Chem* **267**, 11968-71.

Xuei, X., Flury-Wetherill, L., Almasy, L., Bierut, L., Tischfield, J., Schuckit, M., Nurnberger, J. I., Jr., Foroud, T. and Edenberg, H. J. (2008). Association analysis of genes encoding the nociceptin receptor (OPRL1) and its endogenous ligand (PNOC) with alcohol or illicit drug dependence. *Addict Biol* **13**, 80-7.

Yamada, M., Szendro, P. I., Prokscha, A., Schwartz, R. J. and Eichele, G. (1999). Evidence for a role of Smad6 in chick cardiac development. *Dev Biol* **215**, 48-61.

Yang, T., Bernabeu, R., Xie, Y., Zhang, J. S., Massa, S. M., Rempel, H. C. and Longo, F. M. (2003). Leukocyte antigen-related protein tyrosine phosphatase receptor: a small ectodomain isoform functions as a homophilic ligand and promotes neurite outgrowth. *J Neurosci* **23**, 3353-63.

Yano, Y., Saito, R., Yoshida, N., Yoshiki, A., Wynshaw-Boris, A., Tomita, M. and Hirotsune, S. (2004). A new role for expressed pseudogenes as ncRNA: regulation of mRNA stability of its homologous coding gene. *J Mol Med* **82**, 414-22.

Yoo, J. S., Moyer, B. D., Bannykh, S., Yoo, H. M., Riordan, J. R. and Balch, W. E. (2002). Non-conventional trafficking of the cystic fibrosis transmembrane conductance regulator through the early secretory pathway. *J Biol Chem* **277**, 11401-9.

You, J. and Pickart, C. M. (2001). A HECT domain E3 enzyme assembles novel polyubiquitin chains. *J Biol Chem* **276**, 19871-8.

Yu, E. Y., Steinberg-Neifach, O., Dandjinou, A. T., Kang, F., Morrison, A. J., Shen, X. and Lue, N. F. (2007). Regulation of telomere structure and functions by subunits of the INO80 chromatin remodeling complex. *Mol Cell Biol* **27**, 5639-49.

Yuan, S. and Schoenwolf, G. C. (1998). De novo induction of the organizer and formation of the primitive streak in an experimental model of notochord reconstitution in avian embryos. *Development* **125**, 201-13.

Yuan, S. and Schoenwolf, G. C. (1999). Reconstitution of the organizer is both sufficient and required to re- establish a fully patterned body plan in avian embryos. *Development* **126**, 2461-73.

Zhang, F., Wu, J. and Yu, X. (2009). Integrator3, a partner of single-stranded DNA-binding protein 1, participates in the DNA damage response. *J Biol Chem* **284**, 30408-15.

Zhang, H. and Bradley, A. (1996). Mice deficient for BMP2 are nonviable and have defects in amnion/chorion and cardiac development. *Development* **122**, 2977-86.

Zhang, H. Y., Chu, M. L., Pan, T. C., Sasaki, T., Timpl, R. and Ekblom, P. (1995). Extracellular matrix protein fibulin-2 is expressed in the embryonic endocardial cushion tissue and is a prominent component of valves in adult heart. *Dev Biol* **167**, 18-26.

Zhang, H. Y., Timpl, R., Sasaki, T., Chu, M. L. and Ekblom, P. (1996). Fibulin-1 and fibulin-2 expression during organogenesis in the developing mouse embryo. *Dev Dyn* **205**, 348-64.

Zhang, R. Z., Pan, T. C., Zhang, Z. Y., Mattei, M. G., Timpl, R. and Chu, M. L. (1994). Fibulin-2 (FBLN2): human cDNA sequence, mRNA expression, and mapping of the gene on human and mouse chromosomes. *Genomics* **22**, 425-30.

Zhang, S., Fei, T., Zhang, L., Zhang, R., Chen, F., Ning, Y., Han, Y., Feng, X. H., Meng, A. and Chen, Y. G. (2007). Smad7 antagonizes transforming growth factor beta signaling in the nucleus by interfering with functional Smad-DNA complex formation. *Mol Cell Biol* **27**, 4488-99.

Zhang, X. M., Yang, Z., Karan, G., Hashimoto, T., Baehr, W., Yang, X. J. and Zhang, K. (2003). Elovl4 mRNA distribution in the developing mouse retina and phylogenetic conservation of Elovl4 genes. *Mol Vis* **9**, 301-7.

Zhou, S., Zhou, H., Walian, P. J. and Jap, B. K. (2005). CD147 is a regulatory subunit of the gamma-secretase complex in Alzheimer's disease amyloid beta-peptide production. *Proc Natl Acad Sci U S A* **102**, 7499-504.

Zhou, S., Zhou, H., Walian, P. J. and Jap, B. K. (2007). Regulation of gamma-secretase activity in Alzheimer's disease. *Biochemistry* **46**, 2553-63.

Zhu, L., Marvin, M. J., Gardiner, A., Lassar, A. B., Mercola, M., Stern, C. D. and Levin, M. (1999). Cerberus regulates left-right asymmetry of the embryonic head and heart. *Current Biology* **9**, 931-938.

Zimmerman, L. B., De Jesus-Escobar, J. M. and Harland, R. M. (1996). The Spemann organizer signal noggin binds and inactivates bone morphogenetic protein 4. *Cell* **86**, 599-606.